Addis Ababa University

College of Natural and Computational Sciences

Department of Chemistry

Phytochemical Studies of *Cyperus esculentus*, *Carissa spinarum*, *Melilotus officinalis*, *Rhus glutinosa* and *Rhus natalensis*

By: Melaku Assefa

Advisors

Dr. Estifanos Ele

Prof. Wendimagegn Mammo

September, 2021

Phytochemical Studies of *Cyperus esculentus*, *Carissa spinarum*, *Melilotus officinalis*, *Rhus glutinosa* and *Rhus natalensis*

A THESIS SUBMITTED TO THE SCHOOL OF GRADUATE STUDIES

ADDIS ABABA UNIVERSITY

By Melaku Assefa

In Partial Fulfillment of the Requirements for the Degree of Doctor of Philosophy in Chemistry

September, 2021

The work described herein was conducted at the Department of Chemistry, College of Natural and Computational Sciences, Addis Ababa University, Ethiopia, between September 2016 and July 2021 under the guidance of Dr Estifanos Ele and Prof. Wendimagegn Mammo.

ADDIS ABABA UNIVERITY

COLLEGE OF NATURAL AND COMPUTATIONAL SCIENCES

DEPARTMENT OF CHEMISTRY

This is to certify that the thesis prepared by Melaku Assefa, entitled: *Phytochemical Studies of Cyperus esculentus, Carissa spinarum, Melilotus officinalis, Rhus glutinosa and Rhus natalensis* and submitted in partial fulfillment of the requirements for the Degree of Doctor of Philosophy (Organic Chemistry) complies with the regulations of the University and meets the accepted standards with respect to originality and quality.

Signed by Examining Committee

Name	**Signature**	**Date**
Dr. Estifanos Ele (Advisor)	_____	_____
Prof. Wendimagegn Mammo (Advisor)	_____	_____
Prof. Abiy Yenesew (Examiner)	_____	_____
Dr. Kibrom G/Hiwot (Examiner)	_____	_____
Dr. Mekonnen Abebayehu (Examiner)	_____	_____
Dr. Negash Getachew (Chairman, Department of Chemistry)	_____	_____

DECLARATION

I, the undersigned, declare that this PhD dissertation is my original work and has not been presented for any degree in any other university and that all sources of materials used for this dissertation have been duly acknowledged.

Name: _____

Signature: _____

Date: _____

This thesis has been submitted for examination with our approval as university advisors.

Name: Dr. Estifanos Ele

Signature: _____

Name: Prof. Wendimagegn Mammo

Signature: _____

Acknowledgements

First, I would like to thank the almighty God for the gift of good health, courage, and support throughout my life. I would like to extend my sincere thanks and regards to my advisors Dr. Estifanos Ele and Prof. Wendimagegn Mammo, for giving me the opportunity to work on this study. They have provided me with extensive support and guidance while working on my study and during the entire time I am in Addis Ababa University (AAU). I would also like to thank all my friends in AAU and my family for all their help and understanding throughout my study. I thank all staff of the Department of Chemistry (AAU) for all the support and help. Finally, Wollo University is gratefully acknowledged for sponsoring my PhD studies.

Phytochemical Studies of *Cyperus esculentus*, *Carissa spinarum*, *Melilotus officinalis*, *Rhus glutinosa* and *Rhus natalensis*

Melaku Assefa Sisay

Department of Chemistry, Addis Ababa University

Abstract

In this study, the essential oils obtained from the rhizomes of *Cyperus esculentus* L. and the roots of *Carissa spinarum* Linn. together with medicinal smoke obtained from burnt roots of *Carissa spinarum* were analyzed by GC-MS. The major components of the essential oil of *Cyperus esculentus* were pinocarveol (11.42%), humulene epoxide II (10.18%), caryophyllene oxide (9.38%) and β-pinene (8.95%). On the other hand, the essential oil obtained from the roots of *Carissa spinarum* was predominantly 2-hydroxyacetophenone (**16**, 82.97%). The dominant components of the *n*-hexane- and MeOH-soluble fractions of the smoke derived from the roots of *Carissa spinarum* were found to be 2,6-dimethoxyphenol, 2-methoxyphenol and 2-hydroxyacetophenone. The radical scavenging activities of the EtOAc extract of the rhizomes of *Cyperus esculentus*, the MeOH-soluble fraction of the smoke derived from the roots of *Carissa spinarum*, the MeOH extract of the seeds of *Melilotus officinalis* and the EtOAc extracts of the fresh leaves of *Rhus glutinosa* and *Rhus natalensis* were also evaluated using the diphenylpicrylhydrazyl (DPPH) method. The smoke derived from the roots of *Carissa spinarum* and the MeOH-soluble fraction of the seeds of *M. officinalis* showed 88.48 ± 0.31% and 26.35 ± 0.54% DPPH inhibition at concentration of 50.00 µg/mL, respectively. On the other hand, the EtOAc-soluble fractions of the rhizomes of *Cyperus esculentus* and

the leaves of *R. glutinosa* and *R. natalensis* reduced DPPH radical by 24.53 ± 0.36%, 94.89 ± 0.10% and 94.94 ± 0.29% at 50.00 µg/mL, respectively. At the same concentration, standard ascorbic acid (a known antioxidant) scavenged the DPPH radical by 96.29 ± 0.06%. The seed fatty acid composition of *M. officinalis* was determined in this study by GC-MS analysis. Hence, the *n*-hexane extract of the seeds of *M. officinalis* unveiled twelve compounds with a combined area percentage of 98.33%, the major constituents being (9*Z*,12*Z*)-octadecadienoic acid (20.22%, 366.08 ppm), 14-methylpentadecanoic acid (19.52%, 353.45 ppm) and (9*E*)-octadecenoic acid (15.94%, 288.66 ppm). Four sesquiterpenes, namely, caryophyllene oxide (**113**), cyperotundone (**12**), corymbolone (**114**) and tricyclohumuladiol (**115**), were also isolated from the EtOAc extract of the rhizomes of *Cyperus esculentus*. Furthermore, two compounds, namely, *cis*-coumaric acid-2-*O*-β-glucopyranoside (*cis*-melilotoside, **116**) and 1,2-benzopyrone (coumarin, **65**), were isolated from the MeOH extract of the seeds of *M. officinalis*. Twelve compounds, namely, pentacosanol (**119**), acacetin (**120**), kaempferol (**38**), rhusflavanone (**121**), rhusflavone (**122**), avicularin (**123**), quercetin (**1**), myricetin (**2**), quercitrin (**124**), shikimic acid (**125**), hyperoside (**126**), and myricetin-3-*O*-β-galactopyranoside (**127**) were obtained from *R. glutinosa* leaves and three compounds, namely, quercetin (**1**), guaijaverin (**131**) and vitexin (**132**) were isolated and characterized from the leaves *R. natalensis*. Spectroscopic techniques such as NMR, UV-Vis, FTIR, HRESIMS and single X-ray crystallography were used to characterize the isolated compounds.

Table of Contents

Acknowledgements I

Abstract II

List of Figures IX

List of Tables X

List of Appendices XIII

List of Abbreviations and Acronyms XIX

1. Introduction 1

1.1. Background 1

1.2. Statement of the Problem 3

1.3. Objectives of the Work 4

1.3.1. General Objective 4

1.3.2. Specific Objectives 4

2. Literature Review 5

2.1. Chemical and Biological Studies on *Cyperus esculentus* 5

2.2. The Bioactivity and Phytochemistry of *Carissa spinarum* 8

2.3. The Bioactivity and Phytochemistry of *Melilotus officinalis* 13

2.4. The Bioactivity and Phytochemistry of the Genus *Rhus* 21

3. Results and Discussion 24

3.1. Phytochemical Studies on the Rhizomes of *Cyperus esculentus* 24

3.1.1. Extraction and Characterization of Compounds from the Essential Oil of *Cyperus esculentus*.....24

3.1.2. DPPH Radical Scavenging Assay of the Rhizomes of *Cyperus esculentus* 29

3.1.3. Fractionation of the Ethyl Acetate Extract of the Rhizomes of *Cyperus esculentus* 29

3.1.4. Characterization of Compounds Isolated from the Rhizomes of *Cyperus esculentus* 30

3.2. Chemical Studies on the Roots of *Carissa spinarum*.....44

3.2.1. Extraction and Characterization of Compounds from the Essential Oil and the Smoke Derived from the Roots of *Carissa spinarum*.....45

3.2.2. The DPPH Radical Scavenging Assay of the Methanol-Soluble Fraction of the Smoke Derived from the Roots of *Carissa spinarum*.....48

3.3. Phytochemical Studies on Extracts of the Seeds of *Melilotus officinalis* 49

3.3.1. Extraction and Characterization of the Seed Fatty Acids of *Melilotus officinalis* 49

3.3.2. DPPH Assay of the Methanol Extract of the Seeds of *Melilotus officinalis*....54

3.3.3. Fractionation of the Methanol Extract of the Seeds of *Melilotus officinalis* ...55

3.3.4. Characterization of Compounds Isolated from the Seeds of *Melilotus officinalis* 56

3.4. Phytochemical Investigation on the Fresh Leaves of *Rhus glutinosa*.....60

3.4.1. DPPH Radical Scavenging Assay of the Ethyl Acetate Fraction of *Rhus glutinosa* 61

3.4.2. Fractionation of the Crude Ethyl Acetate-Soluble Fraction of the DCM:MeOH

Extract of the Leaves of *Rhus glutinosa*.....62

3.4.3. Characterization of Compounds Isolated from the Leaves of *Rhus glutinosa* 63

3.5. Phytochemical Investigation on the Leaves of *Rhus natalensis*.....96

3.5.1. The DPPH Radical Scavenging Assay of the Ethyl Acetate-Soluble Fraction of the Leaves of *Rhus natalensis* 96

3.5.2. Fractionation of the Ethyl Acetate-Soluble Portion of the DCM:MeOH Extract of the Leaves of *Rhus natalensis* 97

3.5.3. Characterization of Compounds Isolated from the EtOAc-Soluble Portion of the DCM:MeOH Extract of the Leaves of *Rhus natalensis*.....98

4. Experimental Section.....105

4.1. General Experimental Procedures.....105

4.2. Plant Material.....106

4.3. Extraction and Characterization.....107

4.3.1. Extraction and Characterization of Compounds from the Rhizomes of *Cyperus esculentus* 107

4.3.1.1. Extraction of Essential Oil by Hydrodistillation.....107

4.3.1.2. Characterization of the Essential Oil from the Rhizomes of *Cyperus esculentus* 108

4.3.1.3. Solvent Extraction of the Rhizomes of *Cyperus esculentus*.....109

4.3.1.4. DPPH Radical Scavenging Assay of the Ethyl Acetate Extract of the Rhizomes of *Cyperus esculentus*.....109

4.3.1.5. Fractionation of the Ethyl Acetate Extract of the Rhizomes of *Cyperus*

esculentus 110

4.3.1.6. Physical and Spectroscopic Data of Compounds Isolated from the Ethyl Acetate Extract of the Rhizomes of *Cyperus esculentus*.....112

4.3.2. Extraction and Characterization of Compounds from the Roots of *Carissa spinarum*.....114

4.3.2.1. Extraction of Essential Oil from the Roots of *Carissa spinarum* by Hydrodistillation 114

4.3.2.2. Collection of the Smoke from Burnt Roots of *Carissa spinarum* and DPPH Radical Scavenging Assay 114

4.3.2.3. GC-MS Characterization of the Essential Oil and Smoke Derived from the Roots of *Carissa spinarum*.....115

4.3.3. Extraction and Characterization of the Seeds of *Melilotus officinalis*.....116

4.3.3.1. Solvent Extraction and DPPH Radical Scavenging Assay of the Seeds of *Melilotus officinalis*.....116

4.3.3.2. Preparation of Fatty Acid Methyl Esters (FAMEs).....117

4.3.3.3. Preparation of Methyl Palmitate Standard.....117

4.3.3.4.aracterization of Fatty Acids from the Seeds of *Melilotus officinalis* 118

4.3.3.5. Fractionation of the MeOH Extract of the Seeds of *Melilotus officinalis* 118

4.3.3.6. Physical and Spectroscopic Data of Compounds **65** and **116**.....119

4.3.4. Extraction and Characterization of Compounds from the Fresh Leaves of *Rhus glutinosa*.....120

4.3.4.1. Extraction of the Fresh Leaves of *Rhus glutinosa* and DPPH Radical Scavenging Assay 120

4.3.4.2. Fractionation of Ethyl Acetate Fraction of the Fresh Leaves of *Rhus glutinosa* 120

4.3.4.3. Physical and Spectroscopic Data of Compounds Isolated from the Leaves of *Rhus glutinosa* 124

4.3.5. Extraction and Characterization of Compounds from the Fresh Leaves of *Rhus natalensis* 130

4.3.5.1. Extraction and DPPH Radical Scavenging Assay of the Fresh Leaves of *Rhus natalensis* 130

4.3.5.2. Fractionation of the EtOAc-Soluble Portion of the DCM:MeOH Extract of the Fresh Leaves of *Rhus natalensis* 130

4.3.5.3. Physical and Spectroscopic Data of Compounds Isolated from EtOAc-Soluble Portion of the DCM:MeOH Extract of the Leaves of *Rhus natalensis* 131

5. Conclusion 133

6. References 135

7. Appendices 151

List of Figures

Figure 1: *Melilotus officinalis* (Photo by Prof. Wendimagegn Mammo).....14

Figure 2: The GC-MS chromatogram of the essential oil from the rhizomes of *Cyperus esculentus*.....25

Figure 3: The GC-MS chromatogram of the methanol and *n*-hexane fractions of the essential oil from the rhizomes of *Cyperus esculentus*.....28

Figure 4: Structures of compounds isolated from the rhizomes of *Cyperus esculentus*.30

Figure 5: The ^{13}C- and DEPT-135 NMR spectra of **113** in $CDCl_3$.....31

Figure 6: The ^{1}H-NMR spectrum of **113** in $CDCl_3$.....32

Figure 7: Selected 2D NMR correlations of compounds **12**, **113, 114** and **115** 40

Figure 8: X-ray crystal structure of **115** 44

Figure 9: The GC-MS chromatogram of the essential oil from the roots of *Carissa spinarum* 45

Figure 10: The GC-MS chromatogram of *n*-hexane- and methanol-soluble fractions of the smoke derived from the roots of *Carissa spinarum*.....46

Figure 11: Calibration curve of methyl palmitate standard. 51

Figure 12: The GC-MS chromatogram of the esterified *n*-hexane extract of the seeds of *M. officinalis* 51

Figure 13: The GC-MS chromatogram of the esterified *n*-hexane extract of the seeds of *M. officinalis* after partitioning with methanol. 54

Figure 14: Compounds isolated from the MeOH extract of the seeds of *M. officinalis*...55

Figure 15: Proposed biosynthetic pathway of coumarin (**65**). 60

Figure 16: Compounds isolated from the leaves of *R. glutinosa*.....63

Figure 17: Partially characterized compounds isolated from the leaves of *R. glutinosa*. 93

Figure 18: Compounds isolated from the leaves *R. natalensis*.....98

Figure 19: Smoke trapping setup (Photo by Melaku Assefa).....115

List of Tables

Table 1: Compounds identified from the essential oil of the rhizomes of *Cyperus esculentus* by GC-MS analysis. 26

Table 2: Radical scavenging activities of the EtOAc extract of the rhizomes of *Cyperus esculentus* and ascorbic acid standards determined using the DPPH assay 29

Table 3: The ^{1}H-NMR data (δ_{ppm}) of compound **113** 33

Table 4: The ^{13}C-NMR data (δ_{ppm}) of compound **113** 34

Table 5: The ^{1}H-NMR data (δ_{ppm}) of compound **12** 36

Table 6: The ^{13}C-NMR data (δ_{ppm}) of compound **12** 36

Table 7: The ^{1}H-NMR data (δ_{ppm}) of compound **114** 38

Table 8: The ^{13}C-NMR data (δ_{ppm}) of compound **114** 39

Table 9: The ^{1}H-NMR data (δ_{ppm}) of compound **115** 42

Table 10: The ^{13}C-NMR data (δ_{ppm}) of compound **115** 43

Table 11: Major compounds identified from the *n*-hexane-soluble fraction of the smoke derived from the roots of *Carissa spinarum* by GC-MS analysis. 47

Table 12: Radical scavenging activities of the MeOH-soluble fraction of the smoke derived from *Carissa spinarum* and ascorbic acid standards. 49

Table 13: Methyl palmitate standard solutions and their corresponding areas. 50

Table 14: Major compounds identified from the *n*-hexane extract of the seeds of *M. officinalis* by GC-MS analysis 52

Table 15: Radical scavenging activities of the methanol extract of the seeds of *M. officinalis* and ascorbic acid standards. 55

Table 16: The ^{1}H-NMR data (δ_{ppm}) of compound **116** 57

Table 17: The ^{13}C-NMR data (δ_{ppm}) of compound **116** 58

Table 18: The ^{1}H-NMR data (δ_{ppm}) of compound **65** 59

Table 19: The ^{13}C-NMR data (δ_{ppm}) of compound **65** 60

Table 20: Radical scavenging activities of the EtOAc-soluble portion of the DCM:MeOH extract of the leaves of *R. glutinosa* and ascorbic acid standards. 62

Table 21: The ^{1}H-NMR data (δ_{ppm}) of compound **120** 65

Table 22: The ^{13}C-NMR data (δ_{ppm}) of compound **120** 65

Table 23: The ^{1}H-NMR data (δ_{ppm}) of compound **38** 68

Table 24: The ^{13}C-NMR data (δ_{ppm}) of compound **38** 68

Table 25: The ^{1}H-NMR data (δ_{ppm}) of compound **121** 70

Table 26: The ^{13}C-NMR data (δ_{ppm}) of compound **121** 71

Table 27: The ^{1}H-NMR data (δ_{ppm}) of compound **122** 73

Table 28: The ^{13}C-NMR data (δ_{ppm}) of compound **122** 74

Table 29: The ^{1}H-NMR data (δ_{ppm}) of compound **123** 76

Table 30: The ^{13}C-NMR data (δ_{ppm}) of compound **123** 77

Table 31: The ^{1}H-NMR data (δ_{ppm}) of compound **1** 79

Table 32: The ^{13}C-NMR data (δ_{ppm}) of compound **1** 80

Table 33: The ^{1}H-NMR data (δ_{ppm}) of compound **2** 82

Table 34: The ^{13}C-NMR data (δ_{ppm}) of compound **2** 82

Table 35: The ^{1}H-NMR data (δ_{ppm}) of compound **124** 84

Table 36: The ^{13}C-NMR data (δ_{ppm}) of compound **124** 85

Table 37: The ^{1}H-NMR data (δ_{ppm}) of compound **125** 86

Table 38: The ^{13}C-NMR data (δ_{ppm}) of compound **125** 87

Table 39: The ^{1}H-NMR data (δ_{ppm}) of compound **126** 89

Table 40: The ^{13}C-NMR data (δ_{ppm}) of compound **126** 89

Table 41: The ^{1}H-NMR data (δ_{ppm}) of compound **127** 91

Table 42: The ^{13}C-NMR data (δ_{ppm}) of compound **127** 92

Table 43: The ^{1}H-NMR data (δ_{ppm}) of compound **128** 94

Table 44: The ^{1}H-NMR data (δ_{ppm}) of compound **129** 95

Table 45: The ^{1}H-NMR data (δ_{ppm}) of compound **130** 96

Table 46: Radical scavenging activities of the EtOAc-soluble portion of the DCM:MeOH extract of the leaves of *R. natalensis* and ascorbic acid standards.....97

Table 47: The ^{1}H-NMR data (δ_{ppm}) of compound **131** 100

Table 48: The ^{13}C-NMR data (δ_{ppm}) of compound **131** 101

Table 49: The ^{1}H-NMR data (δ_{ppm}) of compound **132** 103

Table 50: The ^{13}C-NMR data (δ_{ppm}) of compound **132** 104

List of Appendices

Appendix 1: The $^{1}H–^{1}H$ COSY Spectrum of **113** in $CDCl_3$ 151

Appendix 2: The HSQC Spectrum of **113** in $CDCl_3$ 152

Appendix 3: The HMBC Spectrum of **113** in $CDCl_3$ 153

Appendix 4: The IR Spectrum of **113** 154

Appendix 5: The ^{1}H-NMR Spectrum of **12** in $CDCl_3$ 155

Appendix 6: The ^{13}C-NMR Spectrum of **12** in $CDCl_3$ 156

Appendix 7: The DEPT-135 NMR Spectrum of **12** in $CDCl_3$ 157

Appendix 8: The $^{1}H–^{1}H$ COSY Spectrum of **12** in $CDCl_3$ 158

Appendix 9: The HSQC Spectrum of **12** in $CDCl_3$ 159

Appendix 10: The HMBC Spectrum of **12** in $CDCl_3$ 160

Appendix 11: The IR Spectrum of **12** 161

Appendix 12: The UV Spectrum of **12** in Methanol 161

Appendix 13: The ^{1}H-NMR Spectrum of **114** in $CDCl_3$ 162

Appendix 14: The ^{13}C-NMR Spectrum of **114** in $CDCl_3$ 163

Appendix 15: The DEPT-135 NMR Spectrum of **114** in $CDCl_3$ 164

Appendix 16: The $^{1}H–^{1}H$ COSY Spectrum of **114** in $CDCl_3$ 165

Appendix 17: The HSQC Spectrum of **114** in $CDCl_3$ 166

Appendix 18: The HMBC Spectrum of **114** in $CDCl_3$ 167

Appendix 19: The IR Spectrum of **114** 168

Appendix 20: The ^{1}H-NMR Spectrum of **115** in $CDCl_3$ 169

Appendix 21: The ^{13}C-NMR Spectrum of **115** in $CDCl_3$ 170

Appendix 22: The DEPT-135 NMR Spectrum of **115** in $CDCl_3$ 171

Appendix 23: The $^{1}H–^{1}H$ COSY Spectrum of **115** in $CDCl_3$ 172

Appendix 24: The HSQC Spectrum of **115** in $CDCl_3$ 173

Appendix 25: The HMBC Spectrum of **115** in $CDCl_3$ 174

Appendix 26: The IR Spectrum of **115** 175

Appendix 27: The HRESIMS of Compound **115** 176

Appendix 28: The ^{1}H-NMR Spectrum of **16** in $CDCl_3$ 177

Appendix 29: The ^{13}C-NMR Spectrum of **16** in $CDCl_3$ 178

Appendix 30: The DEPT-135 NMR Spectrum of **16** in $CDCl_3$ 179

Appendix 31: The IR Spectrum of **16** 180

Appendix 32: The UV Spectrum of **16** in Methanol 180

Appendix 33: The ^{1}H-NMR Spectrum of **116** in D_2O 181

Appendix 34: The ^{13}C-NMR Spectrum of **116** in D_2O 182

Appendix 35: The DEPT-135 NMR Spectrum of **116** in D_2O 183

Appendix 36: The ^{1}H–^{1}H COSY Spectrum of **116** in D_2O 184

Appendix 37: The HSQC Spectrum of **116** in D_2O 185

Appendix 38: The HMBC Spectrum of **116** in D_2O 186

Appendix 39: The IR Spectrum of **116** 187

Appendix 40: The UV Spectrum of **116** in Methanol 187

Appendix 41: The ^{1}H-NMR Spectrum of **65** in $CDCl_3$ 188

Appendix 42: The ^{13}C-NMR Spectrum of **65** in $CDCl_3$ 189

Appendix 43: The DEPT-135 NMR Spectrum of **65** in $CDCl_3$ 190

Appendix 44: The IR Spectrum of **65** 191

Appendix 45: The UV Spectrum of **65** in Methanol 191

Appendix 46: The ^{1}H-NMR Spectrum of **119** in $CDCl_3$ 192

Appendix 47: The ^{13}C-NMR Spectrum of **119** in $CDCl_3$ 193

Appendix 48: The DEPT-135 NMR Spectrum of **119** in $CDCl_3$ 194

Appendix 49: The IR Spectrum of **119** 195

Appendix 50: The HRESIMS of Compound **119** 196

Appendix 51: The ^{1}H-NMR Spectrum of **120** in Acetone-d_6 197

Appendix 52: The ^{13}C-NMR Spectrum of **120** in Acetone-d_6 198

Appendix 53: The DEPT-135 NMR Spectrum of **120** in Acetone-d_6 199

Appendix 54: The IR Spectrum of **120** 200

Appendix 55: The UV Spectrum of **120** in Methanol 200

Appendix 56: The HRESIMS of Compound **120** 201

Appendix 57: The ^{1}H-NMR Spectrum of **38** in Acetone-d_6 202

Appendix 58: The ^{13}C-NMR Spectrum of **38** in Acetone-d_6 203

Appendix 59: The DEPT-135 NMR Spectrum of **38** in Acetone-d_6 204

Appendix 60: The IR Spectrum of **38** 205

Appendix 61: The UV Spectrum of **38** in Methanol 205

Appendix 62: The HRESIMS of Compound **38** 206

Appendix 63: The ^{1}H-NMR Spectrum of **121** in MeOD-d_4 207

Appendix 64: The ^{13}C-NMR Spectrum of **121** in MeOD-d_4 208

Appendix 65: The DEPT-135 NMR Spectrum of **121** in MeOD-d_4 209

Appendix 66: The IR Spectrum of **121** 210

Appendix 67: The UV Spectrum of **121** in Methanol 210

Appendix 68: The HRESIMS of Compound **121** 211

Appendix 69: The ^{1}H-NMR Spectrum of **122** in Acetone-d_6 212

Appendix 70: The ^{13}C-NMR Spectrum of **122** in Acetone-d_6 213

Appendix 71: The DEPT-135 NMR Spectrum of **122** in Acetone-d_6 214

Appendix 72: The ^{1}H–^{1}H COSY Spectrum of **122** in Acetone-d_6 215

Appendix 73: The HSQC Spectrum of **122** in Acetone-d_6 216

Appendix 74: The HMBC Spectrum of **122** in Acetone-d_6 217

Appendix 75: The IR Spectrum of **122** 218

Appendix 76: The UV Spectrum of **122** in Methanol 218

Appendix 77: The HRESIMS of Compound **122** 219

Appendix 78: The ^{1}H-NMR Spectrum of **123** in MeOD-d_4 220

Appendix 79: The ^{13}C-NMR Spectrum of **123** in MeOD-d_4 221

Appendix 80: The DEPT-135 NMR Spectrum of **123** in MeOD-d_4 222

Appendix 81: The IR Spectrum of **123** 223

Appendix 82: The UV Spectrum of **123** in Methanol 223

Appendix 83: The HRESIMS of Compound **123** 224

Appendix 84: The ^{1}H-NMR Spectrum of **1** in Acetone-d_6 225

Appendix 85: The ^{13}C-NMR Spectrum of **1** in Acetone-d_6 226

Appendix 86: The DEPT-135 NMR Spectrum of **1** in Acetone-d_6 227

Appendix 87: The IR Spectrum of **1** 228

Appendix 88: The UV Spectrum of **1** in Methanol 228

Appendix 89: The HRESIMS of Compound **1** 229

Appendix 90: The ^{1}H-NMR Spectrum of **2** in Acetone-d_6 230

Appendix 91: The ^{13}C-NMR Spectrum of **2** in Acetone-d_6 231

Appendix 92: The DEPT-135 NMR Spectrum of **2** in Acetone-d_6 232

Appendix 93: The IR Spectrum of **2** 233

Appendix 94: The UV Spectrum of **2** in Methanol 233

Appendix 95: The HRESIMS of Compound **2** 234

Appendix 96: The ^{1}H-NMR Spectrum of **124** in MeOD-d_4 235

Appendix 97: The ^{13}C-NMR Spectrum of **124** in MeOD-d_4 236

Appendix 98: The DEPT-135 NMR Spectrum of **124** in MeOD-d_4 237

Appendix 99: The IR Spectrum of **124** 238

Appendix 100: The UV Spectrum of **124** in Methanol 238

Appendix 101: The HRESIMS of Compound **124** 239

Appendix 102: The ^{1}H-NMR Spectrum of **125** in D_2O 240

Appendix 103: The ^{13}C-NMR Spectrum of **125** in D_2O 241

Appendix 104: The DEPT-135 NMR Spectrum of **125** in D_2O 242

Appendix 105: The IR Spectrum of **125** 243

Appendix 106: The UV Spectrum of **125** in Methanol 243

Appendix 107: The HRESIMS of Compound **125** 244

Appendix 108: The ^{1}H-NMR Spectrum of **126** in MeOD-d_4 245

Appendix 109: The ^{13}C-NMR Spectrum of **126** in MeOD-d_4 246

Appendix 110: The DEPT-135 NMR Spectrum of **126** in MeOD-d_4 247

Appendix 111: The IR Spectrum of **126** 248

Appendix 112: The UV Spectrum of **126** in Methanol 248

Appendix 113: The HRESIMS of Compound **126** 249

Appendix 114: The ^{1}H-NMR Spectrum of **127** in MeOD-d_4 250

Appendix 115: The ^{13}C-NMR Spectrum of **127** in MeOD-d_4 251

Appendix 116: The DEPT-135 NMR Spectrum of **127** in MeOD-d_4 252

Appendix 117: The IR Spectrum of **127** 253

Appendix 118: The UV Spectrum of **127** in Methanol 253

Appendix 119: The HRESIMS of Compound **127** 254

Appendix 120: The ^{1}H-NMR Spectrum of **128** in Acetone-d_6 255

Appendix 121: The ^{1}H-NMR Spectrum of **129** in MeOD-d_4 256

Appendix 122: The ^{1}H-NMR Spectrum of **130** in Acetone-d_6 257

Appendix 123: The HPLC Chromatogram of the Crude Ethyl Acetate-Soluble Fraction of the DCM:MeOH Extract of the Leaves of *R. natalensis* and Compounds Isolated from the Fraction 258

Appendix 124: The ^{1}H-NMR Spectrum of **131** in DMSO-d_6 259

Appendix 125: The ^{13}C-NMR Spectrum of **131** in DMSO-d_6 260

Appendix 126: The DEPT-135 NMR Spectrum of **131** in DMSO-d_6 261

Appendix 127: The IR Spectrum of **131** 262

Appendix 128: The UV Spectrum of **131** in Methanol 262

Appendix 129: The ^{1}H-NMR Spectrum of **132** in DMSO-d_6 263

Appendix 130: The ^{13}C-NMR Spectrum of **132** in DMSO-d_6 264

Appendix 131: The DEPT-135 NMR Spectrum of **132** in DMSO-d_6 265

Appendix 132: The HSQC Spectrum of **132** in DMSO-d_6 266

Appendix 133: The HMBC Spectrum of **132** in DMSO-d_6 267

Appendix 134: The IR Spectrum of **132** 268

Appendix 135: The UV Spectrum of **132** in Methanol 268

List of Abbreviations and Acronyms

NMR	Nuclear Magnetic Resonance
^{1}H-NMR	Proton Nuclear Magnetic Resonance
^{13}C-NMR	Carbon Nuclear Magnetic Resonance
UV-Vis	Ultraviolet-visible
FTIR	Fourier Transform Infrared Spectroscopy
IR	Infrared Spectroscopy
HRESIMS	High Resolution Electron Spray Ionization Mass Spectroscopy
HPLC	High Performance Liquid Chromatography
TLC	Thin Layer Chromatography
PTLC	Preparative Thin Layer Chromatography
CC	Column Chromatography
GC-MS	Gas Chromatography-Mass Spectroscopy
MSD	Mass Selective Detector
NIST	National Institute of Standards and Technology
FAME	Fatty Acid Methyl Ester
h	hours
L	Liter
g	Gram
ppm	Parts Per Million
DCM	Dichloromethane
EtOAc	Ethyl acetate
MeOH	Methanol
D_2O	Deuterium oxide
DMSO	Dimethyl sulfoxide
anh	Anhydrous
DPPH	2,2-diphenyl-1-picrylhydrazyl
mmu	Milli Mass Unit
SD	Standard Deviation
Ag	Agewgna
Amh	Amharigna
Orm	Oromigna
Som	Somaligna
Tig	Tigrinya

1. Introduction

1.1. Background

Plants are one of the rich sources of small molecules that benefit the producer and other living organisms. These small molecules, in broader sense, are defined as natural products which are organic compounds that are produced by a living organism and are not essential for the survival of the producer but provide an evolutionary advantage for the organism within its environment.[1] These group of compounds are also called secondary metabolites. Unlike primary metabolites, secondary metabolites are unique to one organism or common to a small number of closely related organisms. Chemicals of plant origin which may not be required as essential nutrients, but may enhance health status of organisms are called phytochemicals.[2] Phytochemicals obtained from plants include terpenes, alkaloids, and phenolics.[3] They have been associated with protection from and/or treatment of chronic diseases. Natural products have high structural diversity and unique biological activities.[1] Thus, natural products have been utilized in both traditional and modern medicines for treating diseases. In addition to their medicinal values, natural products are commonly used as poisons, perfumes, flavoring agents, insecticides etc.

Traditional medicinal plants have been used to treat numerous diseases for many centuries and are gaining more and more attention due to their reliable therapeutic efficiency.[4] Plant-based drugs remain an important source of therapeutic agents, because of the availability, relatively cheaper cost and non-toxic nature when compared to modern medicine.[4] In Ethiopia about 80 % of the population, relying on the indigenous knowledge, use plant-based traditional medicine as their major primary health care system.[5]

Bioactive compounds occurring in plant materials consist of multi-component mixtures. Their extraction, identification and determination still need further studies. Secondary metabolites from plant materials can be extracted by various techniques such as Soxhlet extraction, maceration, hydrodistillation, etc. These extraction methods are mainly dependent on the type of material to be extracted and the nature of solvents to be used.[6] The isolation and purification of secondary metabolites has gone through innovative developments.[7] Modern techniques offer the capability to parallel the isolation and purification of secondary metabolites. For isolation and purification of phytochemicals, column chromatography and thin-layer chromatography are basic and crucial techniques. Both of these chromatographic techniques are frequently used due to their low cost, suitability, and accessibility in different stationary phases.[8] When it comes to structural elucidation of the secondary metabolites, different advanced spectroscopic techniques like UV-Vis, NMR, IR and mass spectrometry are applicable.[8]

Traditional medicines have been administrated through various methods, application of essential oil and medicinal smoke are the two common ways. The term essential oil is sometimes used as a general term to include all natural, aromatic, and volatile plant oils. Different parts of plants such as flowers, leaves, seeds, roots, stems, barks, and wood have been used to obtain essential oil.[9] Essential oils have a wide range of application in food flavoring, fragrances, perfumes and traditional medicine.[9] The essential oil of a plant can be investigated by using hydrodistillation to extract the oil and GC-MS to characterize the chemical composition.[10] Direct fumigation and inhalation of plant derived medicinal smoke is another widely used methodology to treat different types of diseases. Medicinal

smoke from plant materials can be investigated by burning the plant and collecting the smoke in different solvents. Compounds in the smoke can be characterized using GC-MS.

1.2. Statement of the Problem

Ethiopia is endowed with rich plant biodiversity. It possesses *ca* 6000 species of higher plants of which 10% are endemic. Many of these plants have found applications in the traditional medicinal practices of the country.

Incense plants, which release fragrant smoke when burned, are very common in many parts of Ethiopia. They are used during coffee ceremonies and in special occasions such as rituals and religious functions. They are also burnt as perfumes to give fragrance to the hair, skin and clothing. The present study will focus on extraction, isolation, and structural elucidation of secondary metabolites and biological activity evaluations of two traditionally used incense plants namely, *Cyperus esculentus* (Cyperaceae) and *Carissa spinarum* (Apocynaceae). The study will also focus on plants that are widely used traditionally for treatment of inflammation. Thus, three plants namely, *Melilotus officinalis* (Leguminosae/Fabaceae), *Rhus glutinosa* and *Rhus natalensis* (Anacardiaceae) have been selected for phytochemical investigation. The five plants in this study were selected because of the special place the plants have in the traditional medicine of Ethiopia, although the plants do not all belong to the same family.

1.3. Objectives of the Work

1.3.1. General Objective

The main objective of this research work has been to characterize the chemical composition and establish the antioxidant activities of extracts of *Cyperus esculentus*, *Carissa spinarum*, *M. officinalis*, *R. glutinosa* and *R. natalensis*.

1.3.2. Specific Objectives

1) To determine the chemical constituents of essential oils from the rhizomes of *Cyperus esculentus* and the roots of *Carissa spinarum*,

2) To characterize the smoke from burnt roots of *Carissa spinarum* and the seed fatty acids of *M. officinalis* using GC-MS,

3) To establish the radical scavenging activities of the rhizomes of *Cyperus esculentus*, the roots of *Carissa spinarum*, the seeds of *M. officinalis*, and the fresh leaves of *R. glutinosa* and *R. natalensis*.

4) To isolate secondary metabolites from the rhizomes of *Cyperus esculentus*, the seeds of *M. officinalis*, and the fresh leaves of *R. glutinosa* and *R. natalensis*.

2. Literature Review

2.1. Chemical and Biological Studies on *Cyperus esculentus*

Cyperus esculentus L. (Synonyms: *Chlorocyperus aureus*, *Cyperus aureus*, *Cyperus bahiensis*, *Cyperus buchananii* Boeckeler, *Cyperus bulamensis* Steud., *Cyperus callistus* Ridl., *Cyperus chrysostachys* Boeckeler, *Cyperus damiettensis* A. Dietr., *Cyperus fulvescens* Liebm, *Cyperus gracilescens* Schult., *Cyperus heermannii* Buckley, *Cyperus helodes* Schrad. ex Nees, *Cyperus hydra* Kunth, nom. illeg., *Cyperus lutescens* Torr. & Hook., *Cyperus melanorhizus* Delile, *Cyperus nervosus* Bertol., *Cyperus officinalis* T. Nees, *Cyperus pallidus* Savi, nom. illeg., *Cyperus phymatodes* Muhl., *Cyperus phymatodes* var. heermannii (Buckley) S. Watson, *Cyperus repens* Elliott, *Cyperus ruficomus* Buckley, *Cyperus sieberianus* Link, *Cyperus tenoreanus* Schult. & Schult. f., *Cyperus tenorei* C. Presl, *Cyperus tuberosus* Pursh, nom. illeg., *Cyperus variabilis* Salzm. ex Steud., *Pterocyperus esculentus* (L.) Opiz, *Pycreus esculentus* (L.), Family: Cyperaceae, Local names: *go ondo* (Som); *quunnii* (Orm)) is an erect perennial grass-like and sweet-scented plant with slender and bright green leaves growing from small, brown tuber-bearing rhizomes below the ground.

Cyperus esculentus is a weed plant belonging to the genus *Cyperus* of the family Cyperaceae (sedge family), widespread in many parts of the world and prefers wet grassland and swamps.[11] The family Cyperaceae, which has about 5000 species under 104 genera, is one of the largest families of flowering plants and the genus *Cyperus* is the second largest genus in this family with more than 600 species.[12] *Cyperus esculentus* has brownish flowers and it is indigenous to western Asia and Africa.[11] It is also known by

various other names as tiger nut, chufa, earth nut, yellow nut sedge, groundnut, rush nut, and edible galingale.[13]

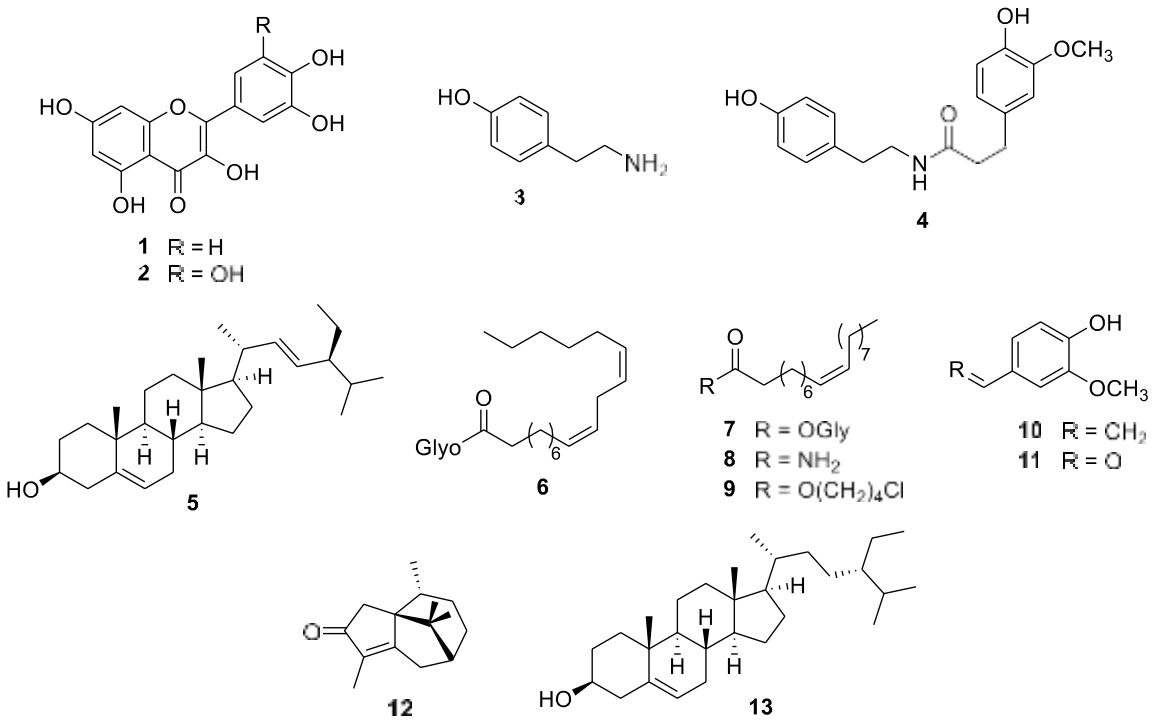
Cyperus esculentus had been cultivated in many parts of the world for its edible tubers.[12] It is one of the lesser known and underutilized crops which are potentially valuable as animal feed and human consumption. *Cyperus esculentus* had been reported to be a "health" food, since its tubers have high fat, carbohydrate, fiber and energy contents.[14] The fatty acid composition of the tubers of *Cyperus esculentus* indicated high unsaturated fatty acid composition, and oleic acid was present in the highest concentration followed by palmitic and linoleic acids.[14b-e,15] The tubers of *Cyperus esculentus* were also found to be rich in some minerals such as potassium, phosphorus, calcium, sodium and zinc as well as vitamins C and E.[14a-c,14e,15a,16] In Spain, the tubers are mainly used to make a refreshing and nonalcoholic milk-like beverage called *horchata de chufa* (tiger nut milk or orgeat) which is usually consumed in summertime.[17] The properties of *Cyperus esculentus* have been exploited in a number of studies including its suitability as biodiesel.[18]

Cyperus esculentus was shown to exhibit hepatoprotective[19], antioxidant and antibacterial activities.[15b,15d,20] It also stimulated sexual motivation and improved sexual performance in rats.[16,21] The use of *Cyperus esculentus* to heal stomach pain, promote normal menstruation, heal mouth and gum ulcers and treat breast lumps and cancer has also been documented.[22] The tubers of the plant were reported to be high in dietary fiber content, which could be effective in the treatment and prevention of many diseases including colon cancer, coronary hearth diseases, obesity, diabetics, blood pressure, constipation, hemorrhoids and gastrointestinal disorders.[23] *Cyperus esculentus* has also been reported to be used in the treatment of flatulence, indigestion, diarrhea, dysentery and excessive

thirst.[19c,24] The rhizomes of *Cyperus esculentus* are widely used for skincare and as a fragrance among the tribes living in Borena, Oromia region, Ethiopia. The bioactive compounds from this plant may be responsible for the clean skin of children and women in remote rural areas of Borana, Ethiopia.

GC-MS analysis of volatile components derived from raw and roasted tubers of *Cyperus esculentus* revealed the main flavor compounds in the raw tubers were alcohols, whereas pyrazines were the main volatiles identified in the roasted tubers.[25] The presence of alkaloids, cyanogenic glycosides, resins, tannins, sterols and saponins in raw tubers of *Cyperus esculentus* and only alkaloids, sterols and resins in roasted tubers was indicated by preliminary phytochemical analysis.[26] Moreover, HPLC characterization of the aqueous extract of *Cyperus esculentus* revealed the presence of flavonoids and polyphenols.[21] Phenolic acids, *p*-hydroxybenzoic acid, vanillic acid, syringic acid, ferulic acid and *p*-coumaric acid, were identified in the MeOH extract of the tubers of *Cyperus esculentus* using paper chromatography and TLC techniques.[27] Several compounds were also identified by GC-MS analysis of the essential oil of *Cyperus esculentus*.[19a,28]

Quercetin (**1**), myricetin (**2**), tyramine (**3**), *N*-feruloyltyramine (**4**), stigmasterol (**5**), linoleic acid and oleic acid glycerol esters (**6** and **7**), together with oleamide (**8**) and 4-chlorobutyl oleate (**9**) were isolated and quantified in the ethanol extract of the rhizomes of *Cyperus esculentus*.[29] The phenolic compounds, *p*-vinylguaiacol (**10**) and *p*-vanillin (**11**), the sesquiterpene, cyprotundone (**12**), and β-sitosterol (**13**) were also reported from the rhizomes of *Cyperus esculentus*.[30]



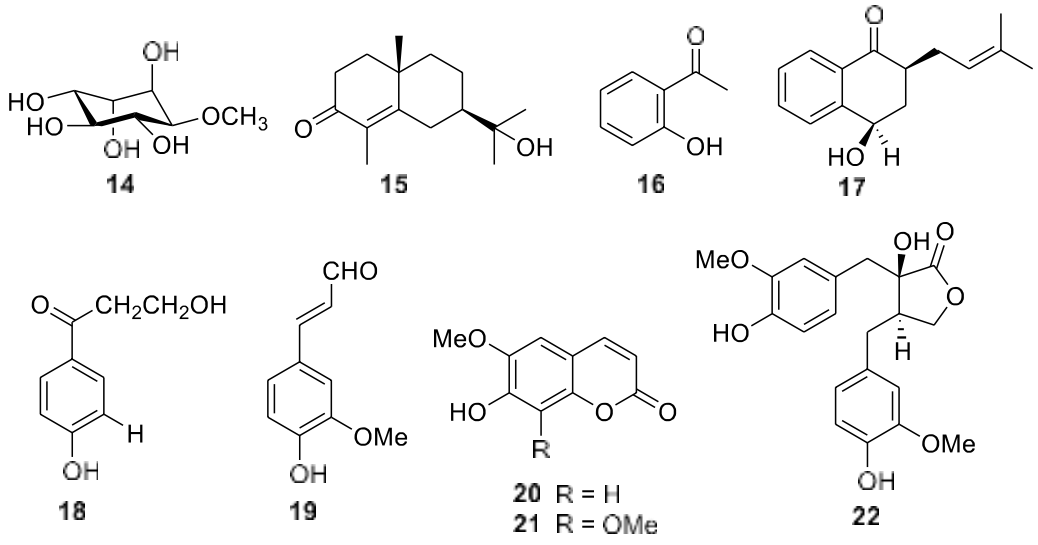
2.2. The Bioactivity and Phytochemistry of *Carissa spinarum*

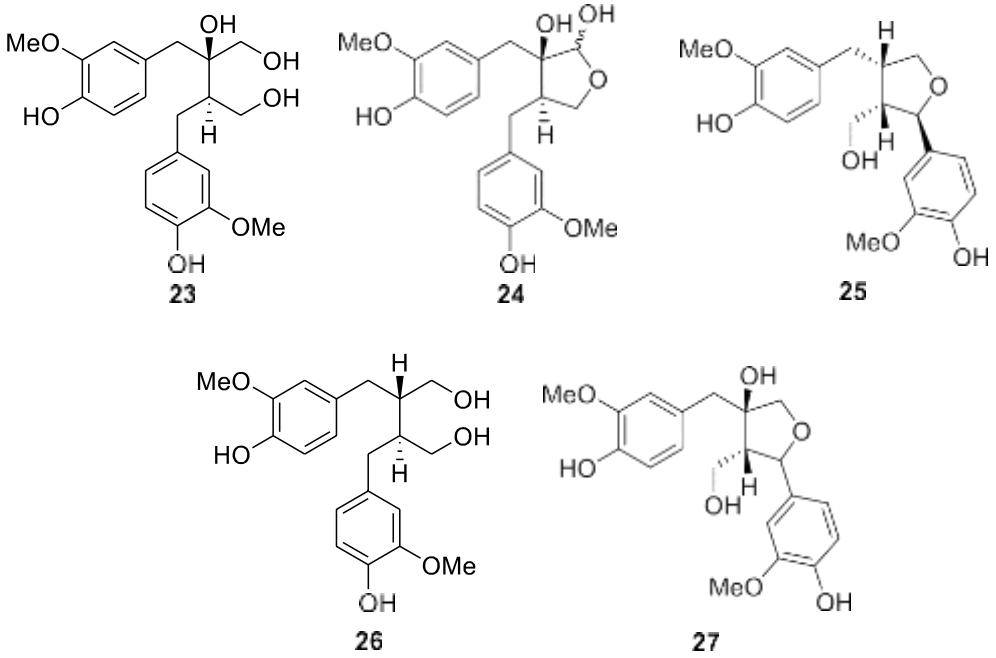
Carissa spinarum Linn. (Synonyms: *Carissa edulis, Carissa tomentosa*, *Carissa richardiana*, *Carissa candolleana* and *Carissa cornifolia*) Family: Apocynaceae, Local names: *Agam* (Amh), *Hagmasa*, *Agamsa* (Orm), *Orgabat*, *Or-gabat* (Som) is a thorny, much-branched shrub or climber growing to 5 m high. It is widely distributed in mountain bushland, at forest margins, along roadsides, riverbanks and rocky slopes at altitudes from 550 – 2500 m.[31]

Carissa spinarum is used as a traditional remedy for treatment of headache, chest complains, rheumatism, oedema, gonorrhoea, syphilis, rabies and it is also used as a remedy for fever, sickle cell anemia, cough, ulcer, toothache, and worm infestation.[32] In pharmacological studies *Carissa spinarum* exhibited antiviral,[33] anticonvulsant,[34] anti-

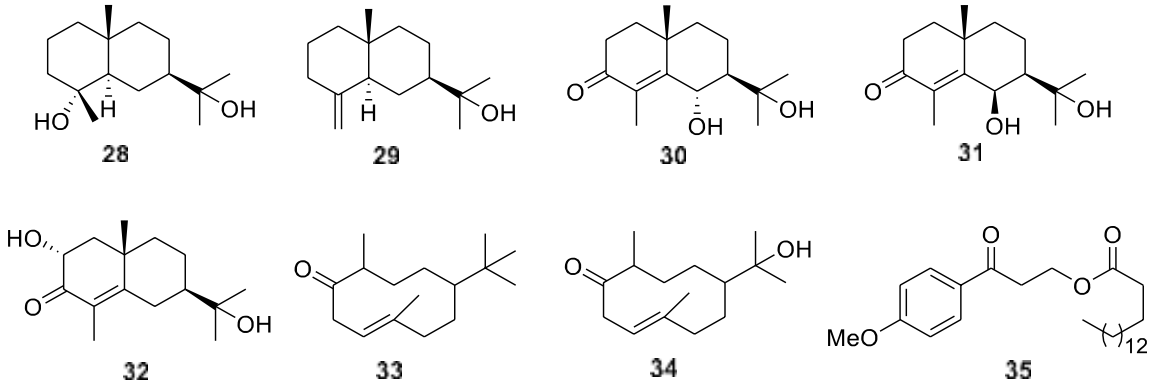
cancer,[35] antiplasmodial,[36] antimicrobial,[37] analgesic,[38] antipyretic,[39] diuretic,[40] hypoglycaemic,[41] as well as wound healing activities.[42] It is also used as a source of dye.[43]

The genus *Carissa* is a rich source of different natural classes of compounds. A literature search for the phytoconstituents of *Carissa spinarum* indicated the isolation of lignans,[44] phenolic compounds,[44a,45] sesquiterpenes,[44b,46] chlorogenic acid derivatives,[32,47] flavonoids and their glycosides,[32,47] cumarins,[44a] triterpenes,[32,48] and cardiac glycosides.[49] The inosit derivative quebrachitol (**14**) was isolated from the twigs of *Carissa spinarum*. Chemical studies on the MeOH extract of the roots of *Carissa spinarum* resulted in the isolation of a sesquiterpene, carissone (**15**), seven aromatic compounds, *O*-hydroxyacetophenone (**16**), catalponol (**17**), vanillin (**11**), 4-hydroxy-(3-hydroxypropionyl)benzene (**18**), coniferaldehyde (**19**), scopoletin (**20**), and isofraxidin (**21**) and six lignans, (–)-nortrachelogenin (**22**), carinol (**23**), carissanol (**24**), (+)-lariciresinol (**25**), (–)-secoisolariciresinol (**26**), and (–)-olivil (**27**).[44a] Compound **16** was also found to be the major component (99.9%) of the DCM extract of the steam distillate of the fresh root bark of *Carissa spinarum* by capillary GC-MS and spectroscopic methods.[45]

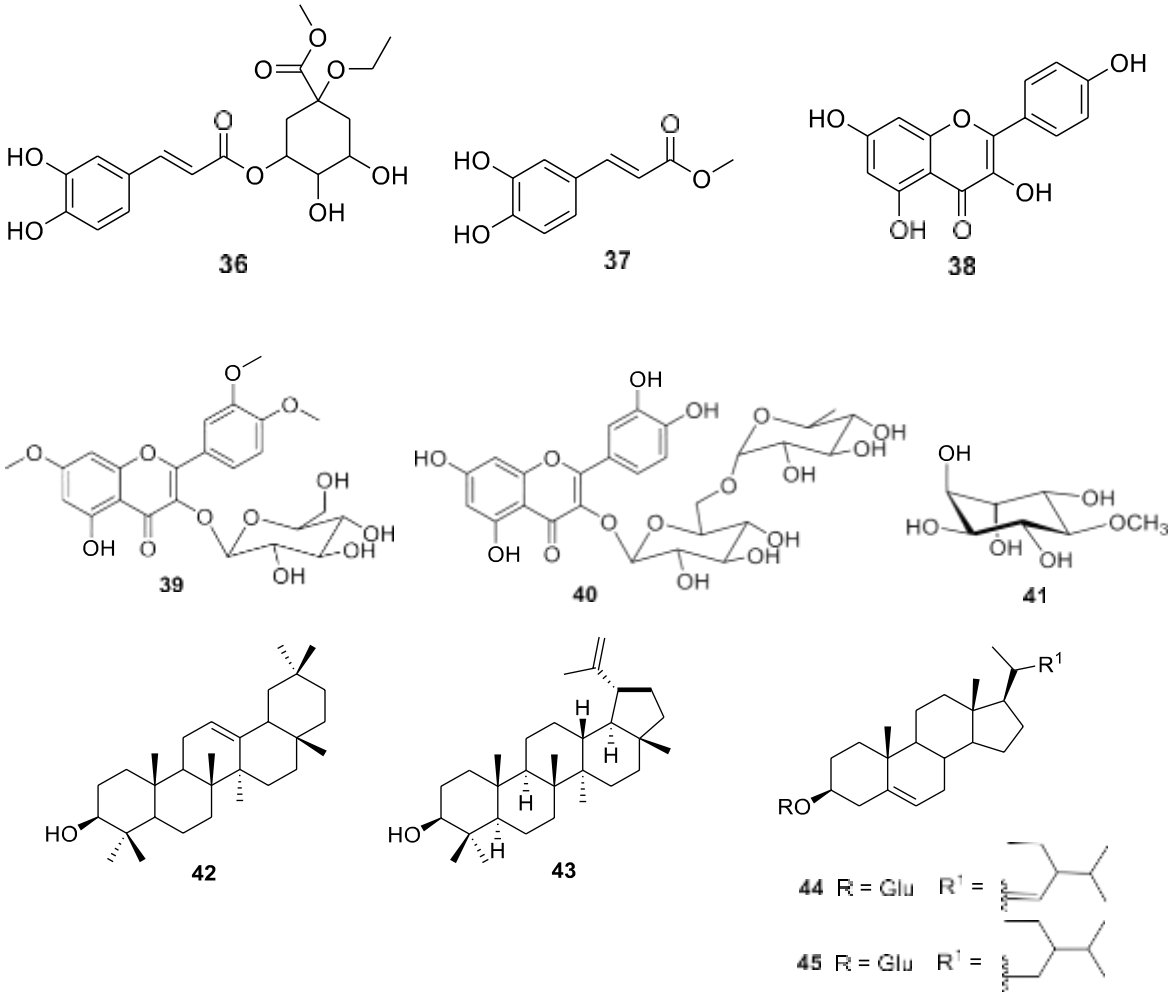




Phytochemical investigation of the petrol- and tetrachloromethane-soluble fractions of the MeOH extract of the roots of *Carissa spinarum* resulted in the isolation of seven sesquiterpenes, namely, carissone (**17**), cryptomeridiol (**28**), β-eudesmol (**29**), 6α-carissanol (**30**), 6β-carissanol (**31**), α-carissanol (**32**), and germacrenone (**33**).[44b] From the stems of *Carissa spinarum*, the germacrane derivative, carenone (**34**), together with 3′-(4″-methoxyphenyl)-3′-oxopropionyl hexadecanoate (**35**) were also isolated.[46]

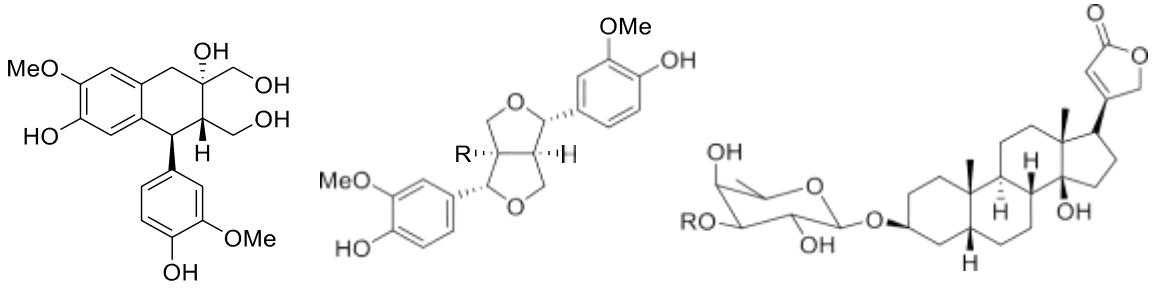


Eleven compounds, namely, chlorogenic acid-1-ethyl ether-1-methyl ester (**36**), caffeic acid methyl ester (**37**), kaempferol (**38**), quercetin-3-*O*-D-glucoside-7,3′,4′-trimethyl ether (**39**), rutin (**40**), pinitol (**41**), *β*-amyrin (**42**), lupeol (**43**), stigmasterol glucoside (**44**), *β*-sitosterol (**13**) and *β*-sitosterol glucoside (**45**), were isolated from the ethanol extract of the aerial parts of *Carissa spinarum*.[32]

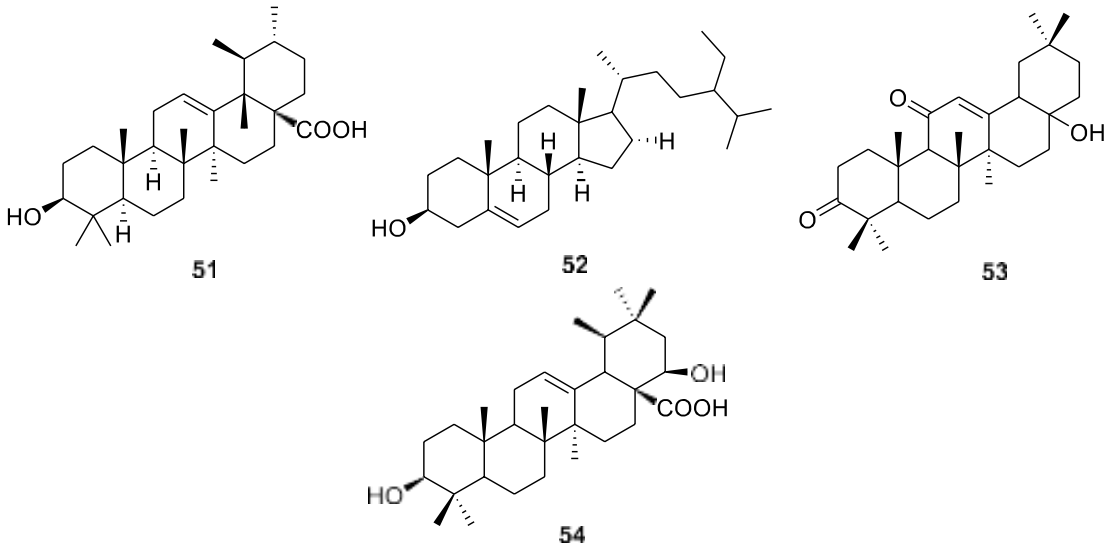


Three lignans, (+)-cycloolivil (**46**), (+)-8-hydroxypinoresinol (**47**), and (+)-pinoresinol (**48**), and two cardiac glycosides, digitoxigenin-3-*O*-β-D-digitalopyranoside (**49**) and evomonoside (**50**), together with carissone (**15**), scopoletin (**20**), (–)-nortrachelogenin (**22**),

carinol (**23**), carissanol (**24**), (–)-secoisolariciresinol (**26**), and (–)-olivil (**27**), were isolated from the MeOH extract of the stem of *Carissa spinarum*.[49]

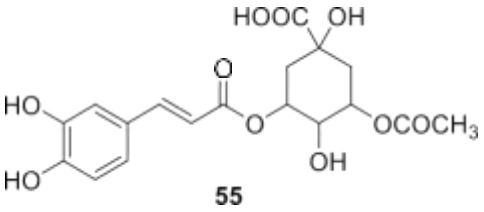


Phytochemical studies on the pet ether extract of the roots of *Carissa spinarum* resulted in the isolation of six compounds, namely, stigmasterol (**5**), ursolic acid (**51**), lupeol (**43**), campesterol (**52**), 17-hydroxy-11-oxo-nor-β-amyrone (**53**) and urs-12-ene-3β,22β-diol-17-carboxylic acid (**54**).[48]

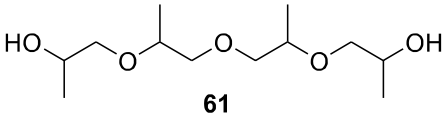


Investigation of the EtOAc and butanol fractions from the ethanol extract of the aerial parts of *Carissa spinarum* afforded 3-*O*-acetyl chlorogenic acid (**55**), along with five flavonol

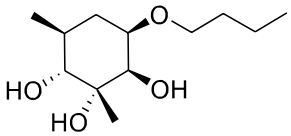
glucosides, namely, kaempferol 3-*O*-*β*-D-glucopyranoside (**56**), quercetin-3-*O*-*β*-D-glucopyranoside (**57**), rhamnetin-3-*O*-*β*-D-glucopyranoside (**58**), isorhamnetin-3-*O*-*β*-D-glucopyranoside (**59**) and isorhamnetin-3-*O*-*β*-D-glucopyranoside-(2″→1‴)-rhamnopyranoside (**60**), together with caredulis (**61**) and (+) butyl-*O*-α-L-rhamnoside (**62**).[47]



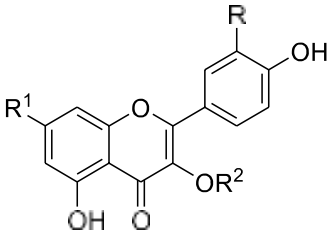
55



61



62



56 R = H, R^1 = OH, R^2 = Glu
57 R = OH, R^1 = OH, R^2 = Glu
58 R = OH, R^1 = OMe, R^2 = Glu
59 R = OMe, R^1 = OH, R^2 = Glu
60 R = OMe, R^1 = OH, R^2 = Glu(2→1)Rha

2.3. The Bioactivity and Phytochemistry of *Melilotus officinalis*

Melilotus officinalis (Figure 1, Synonyms: *Melilotus suaveolens, Medicago officinalis, Melilotus arenarius, Melilotus arvensis, Melilotus neglectus, Melilotus pallidus, Melilotus petitpierreanus, Trifolium officinale*) Local name: *Titako* (Orm)) belongs to the genus *Melilotus* of the Leguminosae (Fabaceae) family, and is an annual, erect herb often more than 1 m tall with small yellow flowers.[50] It is also known as yellow sweet clover or medicinal sweet clover[51] and is widely distributed around the world. It occurs in most parts of Ethiopia, Tanzania, North Asia and India.[50] The flowering stems or just the flowers of

the plant are used medicinally. When dry they have a bitter taste and hay-like smell due to coumarin (**65**).



Figure 1: *Melilotus officinalis* (Photo by Prof. Wendimagegn Mammo)

M. officinalis is used not only as food and forage but also as medicine. It has been used for the treatment of arthritis, brachialgia, bronchitis, hemorrhoids, rheumatism, painful menstruation, palpitations and kidney stones.[52] European Medicines Agency (EMEA) reported that *M. officinalis* is used orally against stomachache, gastric ulcer, disorders of the liver and uterus in folk medicine. Furthermore, it was reported to be used for ulcers of the eyes, earache, hardening and swelling of the uterus.[53] This plant showed anti-inflammatory,[54] antioxidant[55] and antiproliferative effects[56] and has also been reported to

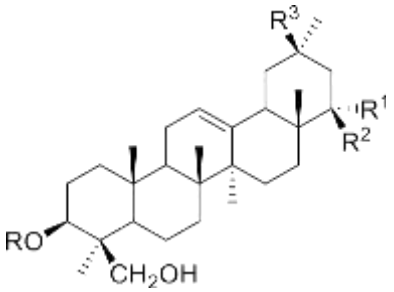
promote tissue regeneration, prevent skin aging, and reduce fat deposition.[57] Phenolic compounds, flavonoids, and coumarins could be responsible for these activities.[56]

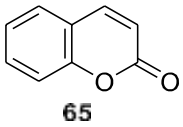
It was reported that saponin and the flavonoid mixture from the BuOH-soluble fraction of *M. officinalis* showed potent inhibitory activity on leucocyte migration.[58] Coumarin (**65**) which originated from this plant species is used in the pharmaceutical industry as an ingredient of anticoagulant drugs.[59] Extracts of *M. officinalis* are used to treat the symptoms of venous and lymphatic insufficiency and capillary fragility.[53] The herb has aromatic, emollient and carminative properties. It was formerly much esteemed in medicine as an emollient and digestive and is recommended for many complaints.[60]

It has been reported that *M. officinalis* is used as nervine tonic, anti-convulsant and also for treatment of insomnia.[52a,61] A scientific study validated the traditional use of the aerial parts of *M. officinalis* as an anxiolytic and resulted in the isolation of kaempferol (**38**) which was found to be responsible for the anxiolytic effect of the plant.[62] In folk medicine, *M. officinalis* is also used for treating jaundice and liver diseases[63] and a bioactivity study revealed that the MeOH extract of the aerial parts of *M. officinalis* showed strong hepatoprotective activity.[64] Examination of the water, acetone, diethyl ether and ethanol extracts of the aerial parts of *M. officinalis* showed that all extracts, especially the acetone extract, exhibited antimicrobial activity and inhibitory activity on biofilm formation.[65] It was also reported that cattle and horses show anemia and hemorrhage when exposed to *M. officinalis.*[66]

M. officinalis was reported to contain uric acid, coumarin, flavonoids and their glycosides, steroids and saponins, fatty acids, triterpenes, oleanane-type triterpene glucuronides,

phenolic acids, and volatile components.[51,52b,58,67] Soyasapogenol B (**63**) and E (**64**) together with coumarin (**65**) and kaempferol (**38**) were isolated and identified from the MeOH extract of the aerial parts of *M. officinalis*.[52b] Phytochemical investigation for compounds with inhibitory effect on leukocyte migration from the BuOH fraction of the MeOH extract of the aerial parts of *M. officinalis* led to the isolation and characterization of azukisaponin V (**66**).[58] A sapogenin, melilotigenin (**67**), was also isolated from the MeOH extract of the dried leaves and flowers of *M. officinalis*.[67f]

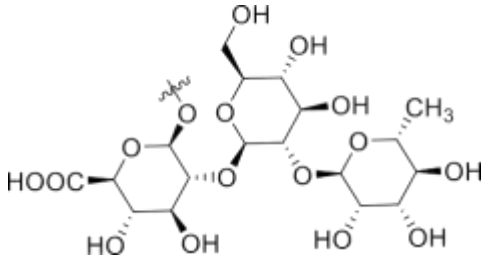




65

63 R = R^1 = H, R^2 = OH, R^3 = CH_3

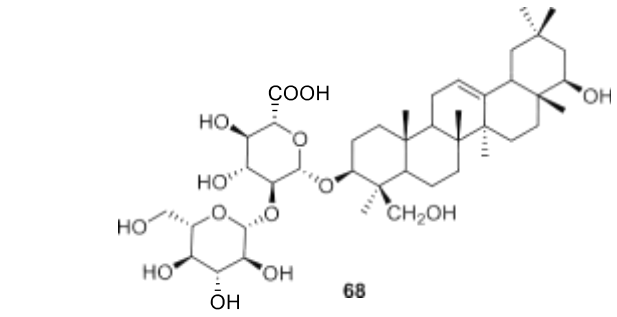
64 R = H, R^1, R^2 = O, R^3 = CH_3



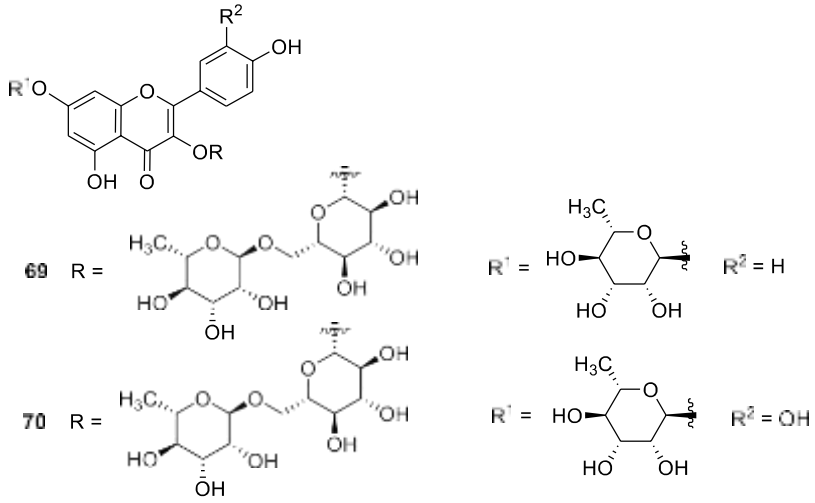
66 R = R^1 = H, R^2 = OH, R^3 = CH_3

67 R = H, R^1, R^2 = O, R^3 = COOH

Further investigation of the BuOH-soluble fraction from the MeOH extract of the aerial parts of *M. officinalis* led to the isolation of two saponins, azukisaponin V (**66**) as the carboxylate form and azukisaponin II (**68**), as well as two flavonoid glycosides, robinin (**69**) and clovin (**70**).[67e]



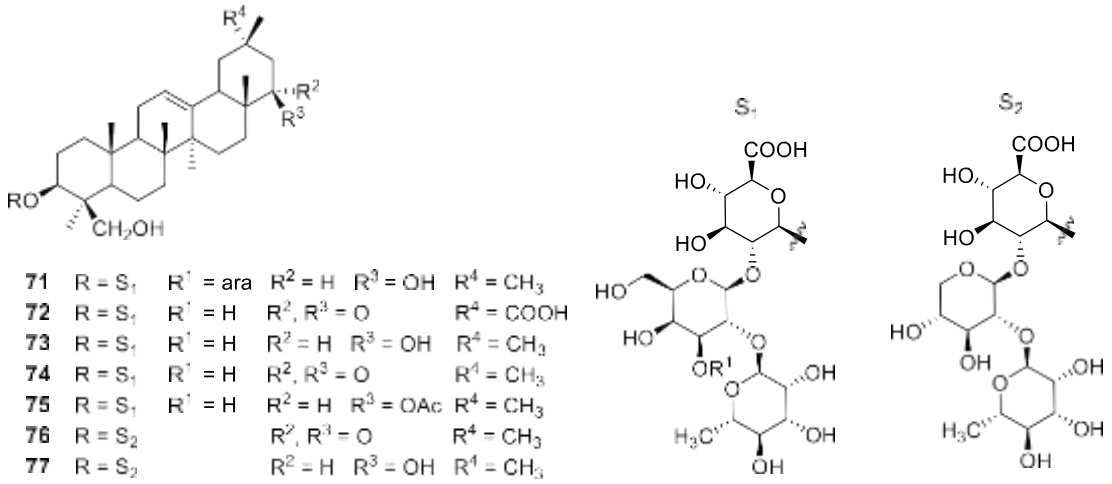
68



69 R =

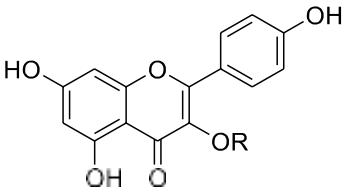
70 R =

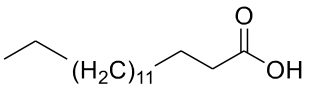
Nohara and Kinjo isolated two oleanene glucuronides, melilotus-saponin O_1 (**71**) and melilotus-saponin O_2 (**72**), together with soyasaponin I (**73**), dehydrosoyasaponin I (**74**), acetyl-soyasaponin I (**75**), wistariasaponin D (**76**) and astragaloside VIII (**77**), from the MeOH extracts of the roots and aerial parts of *M. officinalis.*[51,67c]



71	R = S_1	R^1 = ara	R^2 = H	R^3 = OH	R^4 = CH_3
72	R = S_1	R^1 = H	R^2, R^3 = O		R^4 = COOH
73	R = S_1	R^1 = H	R^2 = H	R^3 = OH	R^4 = CH_3
74	R = S_1	R^1 = H	R^2, R^3 = O		R^4 = CH_3
75	R = S_1	R^1 = H	R^2 = H	R^3 = OAc	R^4 = CH_3
76	R = S_2		R^2, R^3 = O		R^4 = CH_3
77	R = S_2		R^2 = H	R^3 = OH	R^4 = CH_3

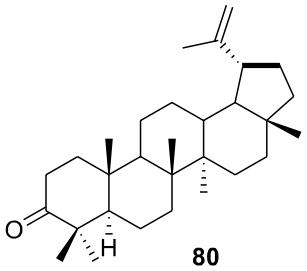
Two flavonoids, robinin (**69**) and kaempferol-3-*O*-[D-galacto-D-gluco-L-arabino-L-rhamnoside] (**78**) were isolated from the leaves and flowers of *M. officinalis*.[67j] Chemical investigation of the MeOH extract of the whole plant material resulted in the isolation of hexadecanoic acid (**79**), kaempferol-3-*O*-*β*-glucopyranoside (**56**) and four triterpenes (lupanone (**80**), lupeol (**43**), betulinic acid (**81**), and oleanolic acid (**82**)).[67i] Three triterpene oleanane glycosides (melilotosides A_1, B_1, and C_1, (**83** – **85**)) and non-glycosylated soyasapogenol B (**65**) were also isolated from the roots of *M. officinalis*.[67g]



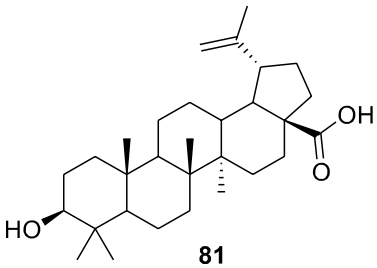


79

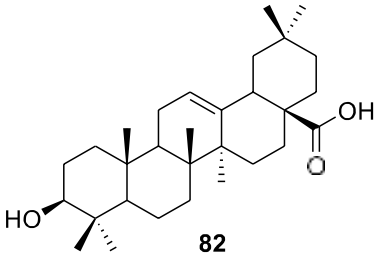
78 R = 3-*O*-[D-galacto-D-gluco-L-arabino-L-rhamnoside]



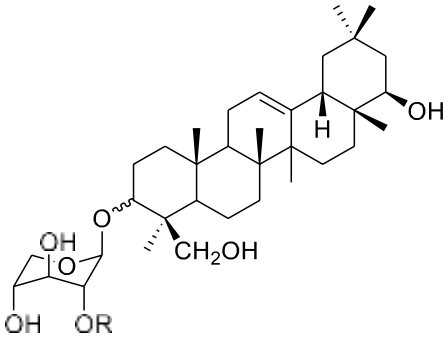
80



81

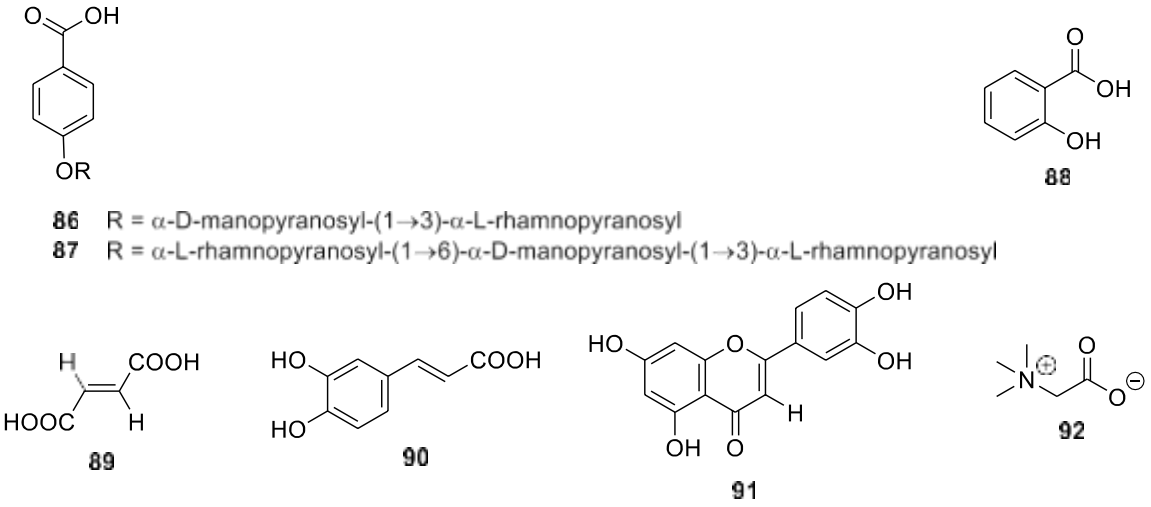


82

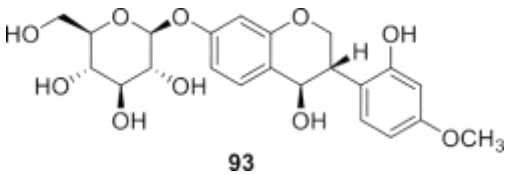


83 R = H
84 R = β-D-galactopyranosyl
85 R = α-L-rhamnopyranosyl-(1→2)-β-D-galactopyranosyl

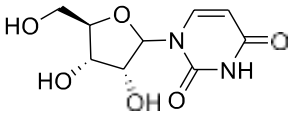
Two *p*-hydroxybenzoic acid glycosides (*p*-hydroxybenzoic acid-4-*O*-α-D-manopyranosyl-(1→3)-α-L-rhamnopyranoside (**86**) and 4-*O*-α-L-rhamnopyranosyl-(1→6)-α-D-manopyranosyl-(1→3)-α-L-rhamnopyranoside (**87**)), three acids (salicylic acid (**88**), fumaric acid (**89**), and caffeic acid (**90**)), two flavonoids (luteolin (**91**), and quercetin (**1**)), together with coumarin (**65**) and betaine (**92**) were isolated from the 70% aqueous ethanol extract of the aerial parts of *M. officinalis*.[67h]



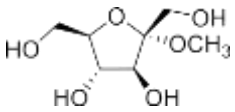
A more recent chemical study on the MeOH extract of the aerial parts of *M. officinalis* resulted in the isolation of the isoflavane derivative melilofficinaside (**93**), together with seven other metabolites, namely, coumarin (**65**), uridine (**94**), methyl-α-D-fructofuranoside (**95**), kaempferol-3-*O*-β-D-glucopyranosyl-7-*O*-α-L-rhamnopyranoside (**96**), quercetin-3-*O*-β-D-glucopyranosyl-7-*O*-α-L-rhamnopyranoside (**97**), robinin (**69**), and kaempferol 3-*O*-α-L-rhamnopyranosyl-(1→2)-[α-rhamnopyranosyl-(1→6)]-β-galactopyranosyl-7-*O*-α-rhamnopyranoside (**98**).[67d]



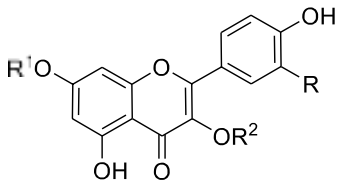
93



94



95

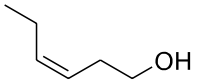


96 R = H, R^1 = α-L-rhamnopyranosyl, R^2 = β-D-glucopyranosyl

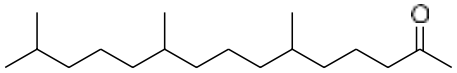
97 R = OH, R^1 = α-L-rhamnopyranosyl, R^2 = β-D-glucopyranosyl

98 R = H, R^1 = α-L-rhamnopyranosyl, R^2 = α-L-rhamnopyranosyl-(1→2)-[α-rhamnopyranosyl-(1→6)]-β-galactopyranosyl

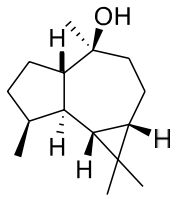
Thirty five volatile compounds were identified with coumarin (**65**, 35.3%) and (*Z*)-3-hexen-1-ol (**99**, 25.9%) being the most prominent by GC-MS analysis of the leaf oil of *M. officinalis*.[67a] However, hexahydrofarnesylacetone (**100**, 16.64%), β-eudesmol (**29**, 11.49%) and globulol (**101**, 8.65%) were found to be the main constituents of the essential oil from the dried aerial parts by GC-MS analysis.[67b] HPLC analysis of the leaves of the plant showed the presence of 18 phenolic compounds including coumarins, flavonoids, and derivatives of phenolic carboxylic acids.[67k] The presence of high amount of unsaturated fatty acids in the seeds of *M. officinalis* was determined by using gas chromatography with flame ionization detection.[67m]



99



100



101

2.4. The Bioactivity and Phytochemistry of the Genus *Rhus*

Anacardiaceae is a family of flowering plants with about 70 genera and 600 species. The genus *Rhus* (sumac) includes about 250 species, which occur mainly in the tropics, subtropics and temperate areas of the world, especially in North America and Africa.[68] *Rhus* species have been used for medicinal and other purposes. They were traditionally used for human consumption[69], wound healing[70], treatment of dysentery[71], diarrhea, menorrhogia, fever, bleeding disorders and inflammation.[70b] Pharmacological studies on extracts of *Rhus* indicated antimicrobial, antifungal, antiviral, antimalarial[72], antioxidant, anti-inflammatory and several other activities.[70b,73] Plants belonging to genus *Rhus* were found to contain biflavonoids[72,74], flavonoids[72,75], phenolic compounds[74j,76], urushiol congeners[77], triterpenes[76c,78], and bichalcones[74j,79]. However, not all *Rhus* species have been adequately investigated for potential bioactive components and their bioactivities.

Rhus glutinosa (Synonyms: *Searsia glutinosa*, *Toxicodendron glutinosum*) Family: Anacardiaceae, Local names: *Kumini* (Ag), *Embus, Qamo* (Amh), *Akessa*, *Tatessa* (Orm), *Shemut* (Tig)) is a spreading or upright shrub or tree 3 – 10 m. This species is named for the new shoots which exude a shiny, sticky liquid (glutinous). This plant has three subspecies, *R. glutinosa subsp. abyssinica, R. glutinosa subsp. unifoliolate* and *R. glutinosa subsp. neoglutinosa*. *R. glutinosa* is endemic to Ethiopia and Eritrea.[80] A literature search on chemical studies of *R. glutinosa* showed that the plant has never been characterized chemically.

Rhus natalensis (Synonyms: *R. glaucescens* var. *macrocarpa* Schweinf., *R. macrocarpa* Engl., *R. abyssinica* Oliv. var, *glabrata, R. crenulate*, *Toxicodendron macrocarpum* (Engl.)

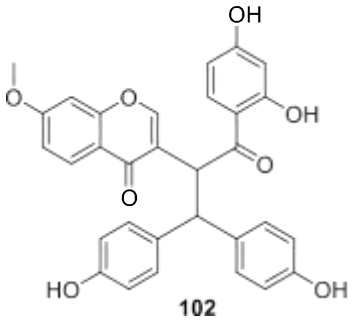
Kuntze, *Toxicodendron natalense* (Bernh. ex Krauss) Kuntze) Family: Anacardiaceae, Local names: *Mstt Aybelash*, *Fatuqa*, *Taquma*, *Ttaquma* (Amh) densely branched shrub, sometimes scandent, or small tree.[81] Several traditional medicinal uses were reported for different parts of *R. natalensis*.[82]

The twigs of *R. natalensis* are used as chewing sticks. Aqueous extract of the twigs possesses inhibitory components to interfere with the virulence and growth of periodontopathic bacteria which in turn reduce the rate of dental plaque formation.[83] The leaves of *R. natalensis* are used traditionally as antimalarial therapy in Kenya and evaluation of the cytotoxicity and efficacy of the plant confirmed its antimalarial activity.[82d,84]

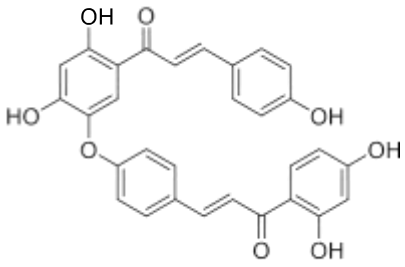
The ethanol extract of the leaves of *R. natalensis* showed affinity to the *N*-methyl-D-aspartic acid (NMDA) receptor indicating its potential for treating epilepsy.[85] The acetone/water (70/30%) extract of the leaves of *R. natalensis* showed anthelmintic property against *Haemonchus contortus*, larval inhibition resulting from the presence of phenolic and non-phenolic compounds.[86] *R. natalensis* also exhibited antiviral[87], antinociceptive,[88] antimicrobial[74j,82e,89], cytotoxic and antioxidant activities[75d,76b].

HPLC and TLC examination of aqueous acetone extract of the leaves of *R. natalensis* resulted in identification of flavonoids, tannins, catechin, proanthocyanidins, *trans*- and *cis*-*p*-coumaric and *trans*-ferulic acids, in addition to gallic, ellagic and chlorogenic acids.[90] The analysis of flavonoids in 80% aqueous MeOH extract of *R. natalensis* using two-dimensional paper chromatography revealed eleven flavonoids, many of which were flavonol glycosides of myricetin and quercetin.[91]

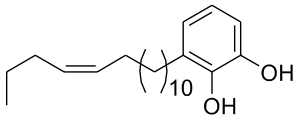
A biflavonoid, rhuschromone (**102**), together with rhuschalcone II (**103**) and 3-((*Z*)-heptadec-13-enyl) benzene-1,2-diol (**104**) were isolated from the hexane and EtOAc extracts of the root bark of *R. natalensis*.[74j] Phytochemical investigation of the DCM extract of the aerial parts of *R. natalensis* resulted in the isolation of four flavanones, 7-*O*-methyl hesperetin (**105**), 7-*O*-methyl naringenin (**106**), (-)-homoeriodictyol (**107**) and eriodictyol-7-methyl ether (**108**), and two flavones, 7-*O*-methyl isokaemferide (**109**) and genkwanin (**110**), in addition to β-amyrin (**42**) and β-sitosterol glucoside (**45**).[75d] Five compounds, epicatechin (**111**), β-sitosterol (**13**), β-sitosterol glucoside (**45**), stigmasterol (**5**) and lupeol (**43**) were also isolated and characterized from the root bark of *R. natalensis*.[76c] Analysis of the EtOAc extract of the roots of *R. natalensis* resulted in the isolation of 3-((*Z*)-heptadec-14-enyl) benzene -1-ol (**112**).[76b]



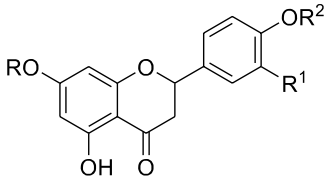
102



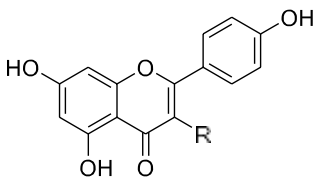
103



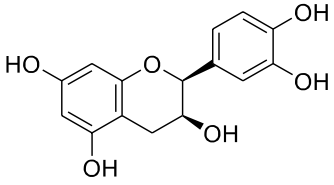
104



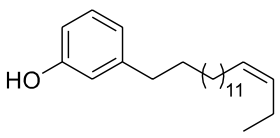
105 R=CH_3 R^1=OH R^2=CH_3
106 R=CH_3 R^1=H R^2=H
107 R=H R^1=OH R^2=CH_3
108 R=CH_3 R^1=OH R^2=H



109 R=OCH_3
110 R=H



111



112

3. Results and Discussion

In this study, essential oils from *Cyperus esculentus* and *Carissa spinarum* and fatty acids from *M. officinalis* were extracted and analyzed by GC-MS. In addition, the smoke obtained from burning the roots of *Carissa spinarum* was trapped in organic solvents and analyzed by GC-MS. The radical scavenging activities of the MeOH-soluble fraction of the smoke derived from *Carissa spinarum*, MeOH extract of *M. officinalis* and the EtOAc extracts of *Cyperus esculentus*, *R. glutinosa* and *R. natalensis* were determined using the DPPH assay. Solvent extracts of *Cyperus esculentus*, *M. officinalis*, *R. glutinosa* and *R. natalensis* were also phytochemically investigated as described in the following sections.

3.1. Phytochemical Studies on the Rhizomes of *Cyperus esculentus*

The aim of this study is to determine the phytochemical composition and bioactivity of essential oil and solvent extract of the rhizomes of *Cyperus esculentus*. The extracts of the plant were subjected to phytochemical analysis as described in the following sections.

3.1.1. Extraction and Characterization of Compounds from the Essential Oil of *Cyperus esculentus*

The dried rhizomes of *Cyperus esculentus* were ground and subjected to hydrodistillation following the procedure described in **Section 4.3.1.1**. The essential oil was then analyzed by GC-MS using the method described in **Section 4.3.1.2**. GC-MS analysis of the essential oil revealed the presence of 25 compounds (Figure 2). Sixteen compounds with qualities greater than 80% and area percentage greater than one were identified by using NIST 2014 mass spectral library search and retention index (*I*). The names of identified compounds

with their respective retention times, area percentages, structures, qualities, and retention indices are given in Table 1. As shown in the table, the major components identified from the essential oil of the rhizomes of *Cyperus esculentus* were pinocarveol (11.42%), humulene epoxide II (10.18%), caryophyllene oxide (9.38%) and β-pinene (8.95%).

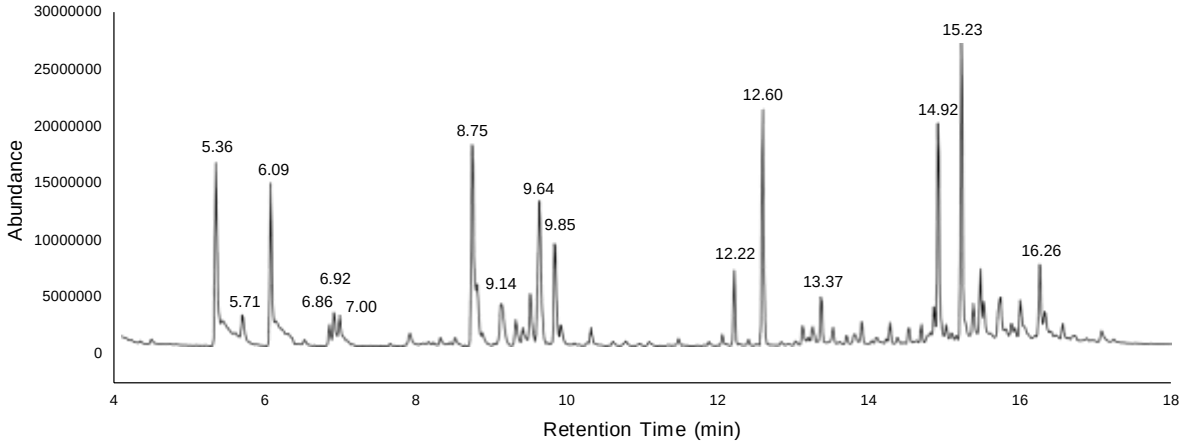


Figure 2: The GC-MS chromatogram of the essential oil from the rhizomes of *Cyperus esculentus.*

Table 1: Compounds identified from the essential oil of the rhizomes of *Cyperus esculentus* by GC-MS analysis.

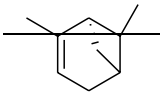
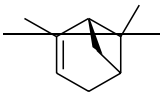
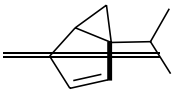
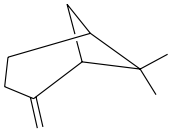
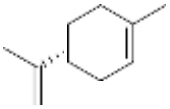
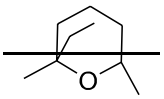
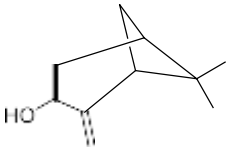
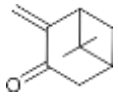
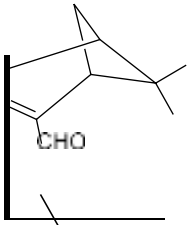
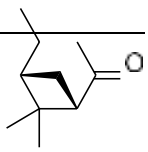
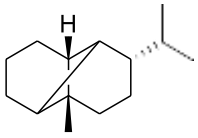
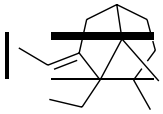
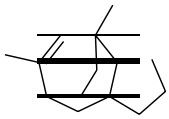
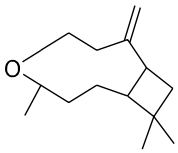
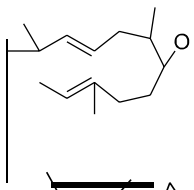
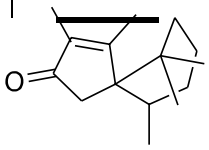
Pk	*Rt*	Area Pct.	Compound	Structure	Q	*I*
1	5.36	6.85	(1*S*)-α-Pinene		97	966.51
2	5.45	3.82	(1*R*)-α-Pinene		94	972.30
3	5.71	1.88	Dehydrosabinene		95	989.43
4	6.09	8.95	β-Pinene		94	1013.55
5	6.92	1.38	Limonene		99	1067.97
6	7.00	1.94	Eucalyptol		95	1072.94
7	8.75	11.42	Pinocarveol		90	1188.12
8	9.14	2.91	Pinocarvone		95	1214.18
9	9.64	7.29	Myrtenal		98	1249.32
10	9.85	3.53	Verbenone		98	1263.67

Table 1 continued

Pk	*Rt*	Area Pct.	Compound	Structure	Q	*I*
11	12.22	2.18	β-Copaene		99	1437.57
12	12.60	7.01	Cyperene		99	1466.78
13	13.37	1.68	Rottundene		98	1528.81
14	14.92	9.38	Caryophyllene oxide		83	1660.37
15	15.23	10.18	Humulene epoxide II		93	1687.25
16	16.26	2.69	Cyperotundone		99	1781.61

Pk = peak number, *Rt* = retention time (min), Area Pct. = area percentage, Q = quality, *I* = retention index

The essential oil of *Cyperus esculentus* was partitioned between MeOH and *n*-hexane, and both the MeOH and *n*-hexane fractions were analyzed by GC-MS. The major compounds identified in the MeOH fraction were verbenone (15.34%), cyperotundone (12.04%) and

pinocarveol (10.19%). On the other hand, cyperene (14.95%) and cyperotundone (9.13%) were found to be the major compounds in the *n*-hexane fraction (Figure 3).

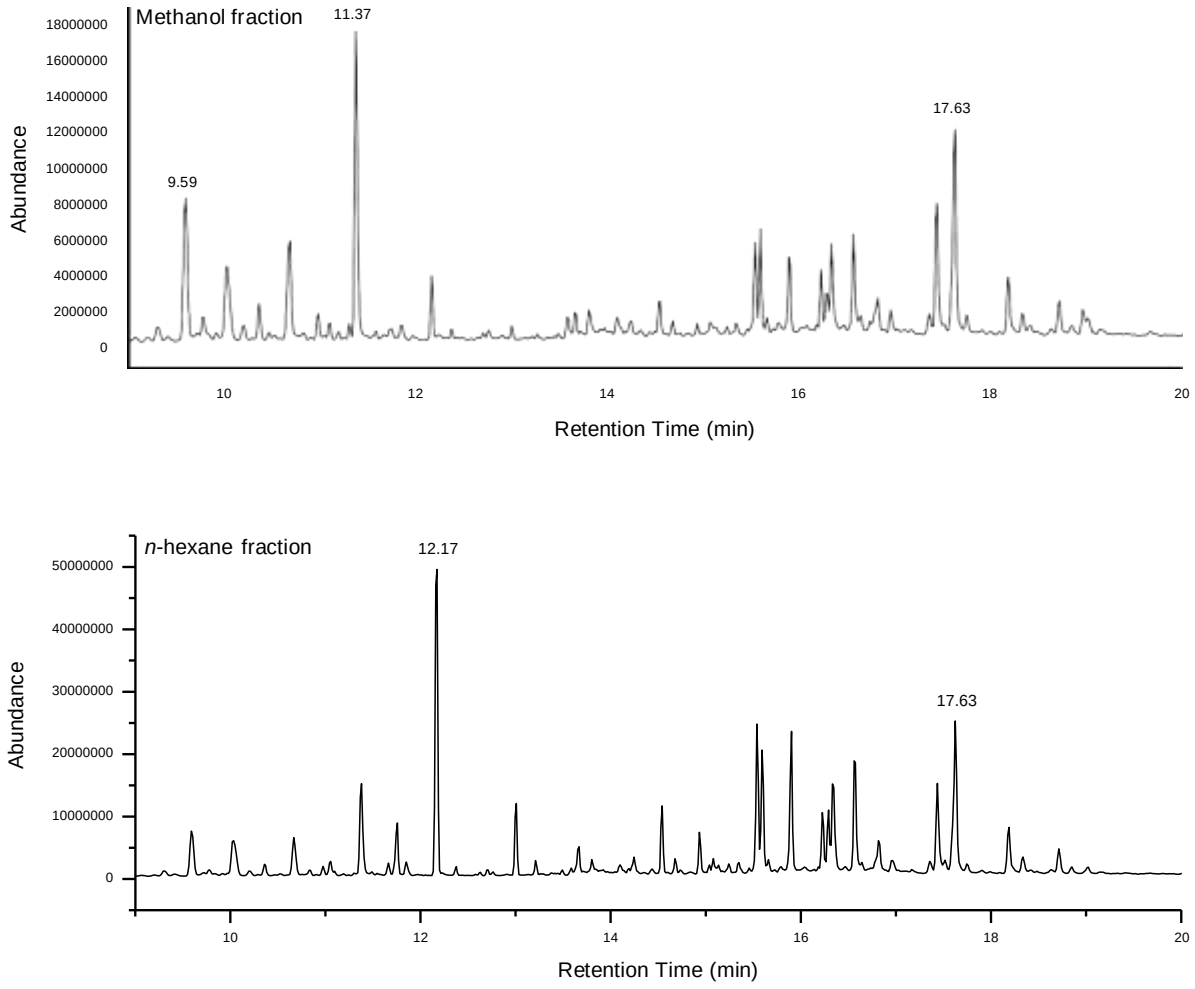


Figure 3: The GC-MS chromatogram of the methanol and *n*-hexane fractions of the essential oil from the rhizomes of *Cyperus esculentus*.

3.1.2. DPPH Radical Scavenging Assay of the Rhizomes of *Cyperus esculentus*

The dried and ground rhizomes of *Cyperus esculentus* were first extracted with *n*-hexane then with EtOAc and finally with MeOH (see **Section 4.3.1.3**). The radical scavenging activity of the EtOAc extract of the rhizomes of *Cyperus esculentus* was assessed using DPPH according to the procedure described in **Section 4.3.1.4**. The extract showed a 27.62% DPPH inhibition at concentration of 100.00 µg/mL and at the same concentration ascorbic acid standard exhibited a 96.09% DPPH inhibition (Table 2).

Table 2: Radical scavenging activities of the EtOAc extract of the rhizomes of *Cyperus esculentus* and ascorbic acid standards determined using the DPPH assay

Concentration (µg/mL)	**% DPPH Inhibition**	
	EtOAc extract of *Cyperus esculentus*	**Ascorbic acid standard**
100.00	27.62 ± 0.33	96.09 ± 0.16
50.00	24.53 ± 0.36	96.29 ± 0.06
25.00	23.22 ± 0.65	96.26 ± 0.06
12.50	22.01 ± 0.37	96.06 ± 0.12
6.25	21.68 ± 0.47	91.30 ± 0.31
3.13	21.45 ± 0.36	54.06 ± 1.27
1.56	20.57 ± 0.31	35.00 ± 0.52

The results are reported as mean ± SD of three replicates.

3.1.2. Fractionation of the Ethyl Acetate Extract of the Rhizomes of *Cyperus esculentus*

In the course of this study, attempts were made to isolate and characterize secondary metabolites from the EtOAc extract of the rhizomes of *Cyperus esculentus* as shown in **Section 4.3.1.5**. Thus, four compounds, caryophyllene oxide (**113**), cyperotundone (**12**),

corymbolone (**114**) and tricyclohumuladiol (**115**) (Figure 4), were isolated by using silica gel and Sephadex LH-20 column chromatography and PTLC techniques. The isolated compounds were then characterized by spectroscopic techniques such as UV-Vis, FTIR, HRESIMS, NMR and single-crystal X-ray crystallography as described in the following section.

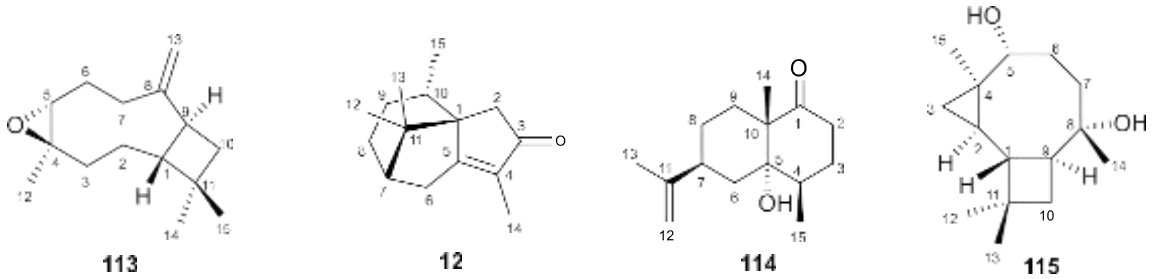
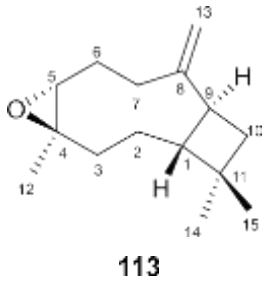


Figure 4: Structures of compounds isolated from the rhizomes of *Cyperus esculentus*.

3.1.4. Characterization of Compounds Isolated from the Rhizomes of *Cyperus esculentus*

3.1.4.1. Characterization of Compound 113



Compound **113** was isolated as colorless crystals and has a melting point of 62.5 – 63.9 °C. The UV-Vis spectrum of **113** did not show any absorption band. The IR spectrum of **113** (Appendix 4) revealed terminal methylene =C–H stretching absorption band at 3430 cm^{-1},

C–H stretching absorption band at 2926 and 2855 cm^{-1}, and terminal methylene C=C stretching absorption at 1737 cm^{-1}. The ^{13}C-NMR spectrum (Figure 5) revealed 15 carbon resonances which are due to three quaternary carbons (δ 34.04, 59.86 and 151.85), three methine carbons (δ 48.75, 50.71 and 63.78), one exocyclic methylene group (δ 121.78), five aliphatic methylene carbons (δ 27.21, 29.77, 30.21, 39.14 and 39.75) and three methyl groups (δ 17.01, 21.62 and 29.90) as evidenced by the DEPT-135 (Figure 5) and HSQC spectra (Appendix 2).

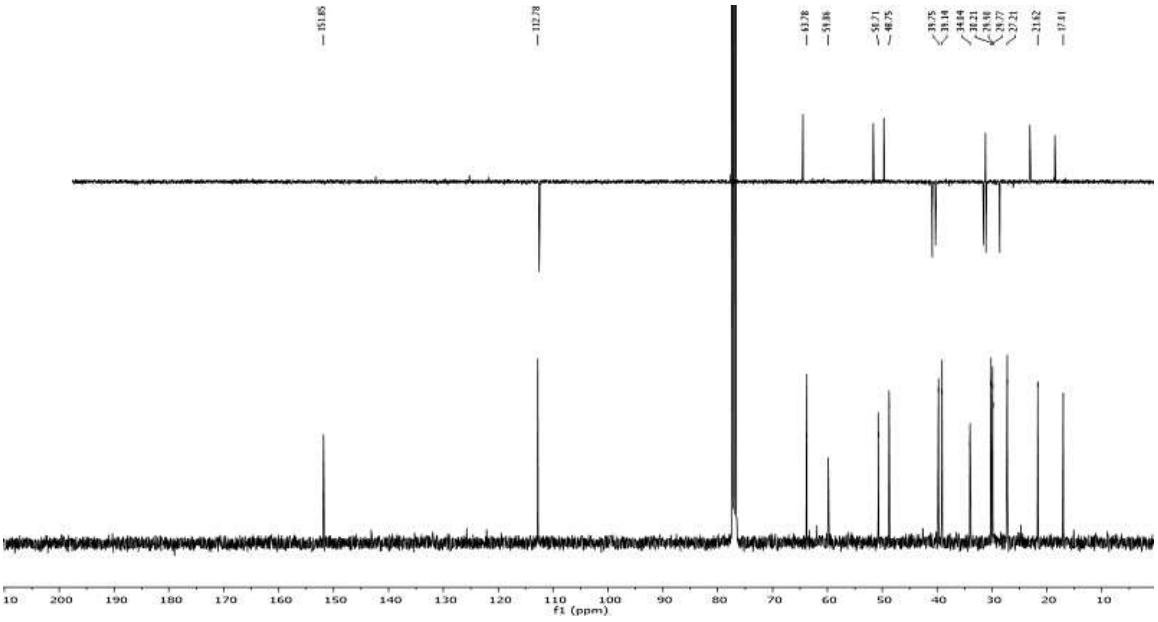


Figure 5: The ^{13}C- and DEPT-135 NMR spectra of **113** in $CDCl_3$.

The ^{1}H-NMR spectrum of **113** (Figure 6) indicated resonances for the exocyclic methylene group at δ 4.88 (1H, *d*, *J* = 1.80 Hz, H-13a) and 4.99 (1H, *d*, *J* = 2.00 Hz, H-13b), one oxygenated methine at δ 2.90 (1H, *dd*, *J* = 10.60, 4.04 Hz, H-5) and three methyl groups at δ 1.00 (3H, *s*, Me-15), 1.02 (3H, *s*, Me-14) and 1.22 (3H, *s*, Me-12) (Table 3). The ^{1}H-^{1}H

COSY NMR spectrum of **113** (Appendix 1) showed correlations for two spin systems, H_2-10/H-9/H-1/H_2-2/H_2-3 and H-5/H_2-6/H_2-7 (Figure 7).

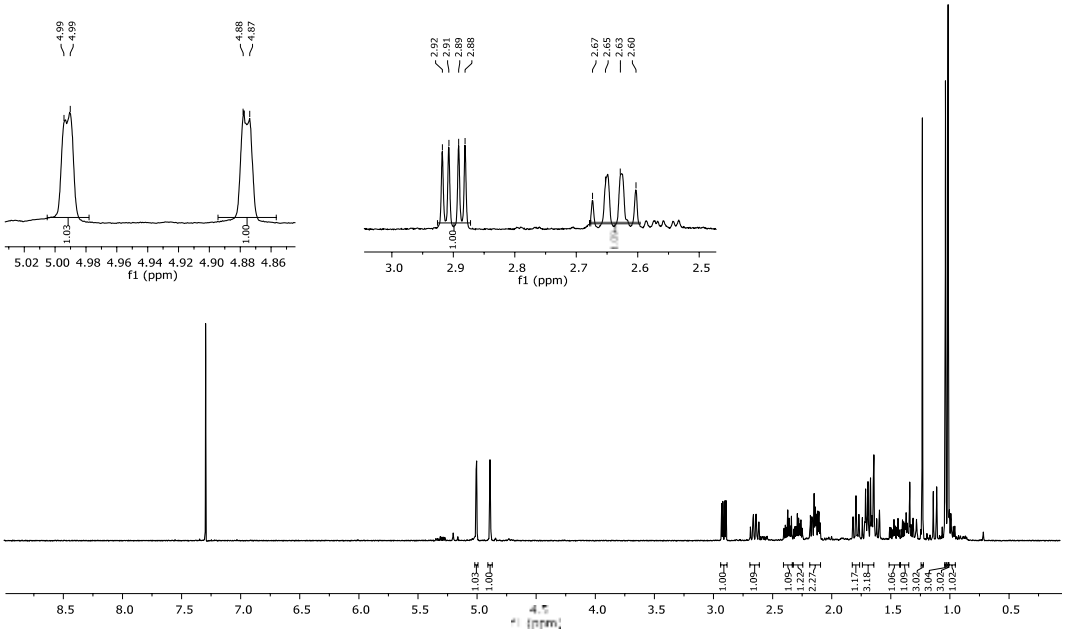


Figure 6: The ^{1}H-NMR spectrum of **113** in $CDCl_3$.

The HMBC (Appendix 3) correlations of H-13 (δ 4.88 and 4.99) with C-7 (δ 29.77) and C-9 (δ 48.75) and correlations of both H-7 (δ 2.13 and 2.36) and H-9 (δ 2.64) with C-8 (δ 151.85) clearly showed that the exocyclic double bond must be located between C-7 and C-9. HMBC correlations of H-1 (δ 1.78) and H-10 (δ 1.68) with C-11 (δ 34.04), Me-14 (δ 21.62), and Me-15 (δ 29.90) and correlations of both Me-14 (δ 1.02) and Me-15 (δ 1.00) with C-11 (δ 34.04) together with correlations between Me-14 and Me-15 indicated the two methyl groups, Me-14 and Me-15, are attached to C-11. The remaining methyl group, Me-12, must be attached to C-4 because of the correlations of H-3 (δ 0.97 and 2.13) with

Me-12 (δ 17.01), and Me-12 (δ 1.22) with both C-4 (δ 59.86) and C-5 (δ 63.78). Furthermore, HMBC correlations of H-1 (δ 1.78) to C-3 (δ 39.14), C-8 (δ 151.85) and C-9 (δ 48.75); H-5 (δ 2.90) to C-3 (δ 39.14), C-4 (δ 59.86) and C-7 (δ 29.77); H-6 (δ 1.37 and 2.27) to C-4 (δ 59.86), and H-9 (δ 2.64) to C-2 (δ 27.21) and C-7 (δ 29.77) were used to elucidate the structure of compound **113** (Figure 4). However, it was not possible to rule out the different configurations of compound **113** based on the above spectroscopic data alone. The NMR data of **113** are in agreement with published data for caryophyllene oxide[92] which was previously reported from the essential oil of another *Cyperus* species *Cyperus bulbosus*.[93]

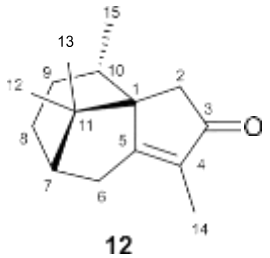
Table 3: The ^{1}H-NMR data (δ_{ppm}) of compound **113**.

113 ($CDCl_3$, 400 MHz)	Lit.[92] ($CDCl_3$, 400 MHz)
1.78 (1H, *t*, *J* = 9.72 Hz, H-1)	1.74 (1H, *t*, *J* = 10.0 Hz, H-1)
1.68 (1H, *m*, H-2)	1.65 (1H, *m*, H-2)
1.46 (1H, *m*, H-2)	1.42 (1H, *m*, H-2)
2.13 (1H, *m*, H-3)	2.09 (1H, *m*, H-3)
0.97 (1H, *m*, H-3)	0.93 (1H, *m*, H-3)
2.90 (1H, *dd*, *J* = 10.60, 4.04 Hz, H-5)	2.85 (1H, *dd*, *J* = 10.6, 4.2 Hz, H-5)
2.27 (1H, *m*, H-6)	2.23 (1H, *m*, H-6)
1.37 (1H, *m*, H-6)	1.32 (1H, *m*, H-6)
2.36 (1H, *m*, H-7)	2.32 (1H, *ddd*, *J* = 12.6, 8.0, 4.3 Hz, H-7)
2.13 (1H, *m*, H-7)	2.11 (1H, *m*, H-7)
2.64 (1H, *q*, *J* = 9.41 Hz, H-9)	2.59 (1H, *q*, *J* = 7.4 Hz, H-9)
1.68 (2H, *m*, H-10)	1.69 (1H, *m*, H-10) 1.62 (1H, *m*, H-10)
1.22 (3H, *s*, H-12)	1.18 (3H, *s*, H-12)
4.99 (1H, *d*, *J* = 2.00 Hz, H-13)	4.95 (1H, *brs*, H-13)
4.88 (1H, *d*, *J* = 1.80 Hz, H-13)	4.83 (1H, *brs*, H-13)
1.02 (3H, *s*, H-14)	0.98 (3H, *s*, H-14)
1.00 (3H, *s*, H-15)	0.96 (3H, *s*, H-15)

Table 4: The ^{13}C-NMR data (δ_{ppm}) of compound **113**.

C	**113** ($CDCl_3$, 100 MHz)	Lit.[92] ($CDCl_3$, 100 MHz)
1	50.71	50.8
2	27.21	27.2
3	39.14	39.2
4	59.86	59.8
5	63.78	63.7
6	30.21	30.3
7	29.77	29.8
8	151.85	151.8
9	48.75	48.7
10	39.75	39.8
11	34.04	34.1
12	17.01	17.0
13	112.78	112.8
14	21.62	21.7
15	29.90	29.9

3.1.4.2. Characterization of Compound 12



12

Compound **12** was isolated as colorless crystals with a melting point of 36.0 – 38.0 °C. The UV-Vis spectrum (Appendix 12) in MeOH of **12** showed an absorption maximum at 246 nm which indicated the presence a conjugated carbonyl group in the molecule. The IR spectrum of **12** (Appendix 11) revealed the C-H stretching absorption bands at 2928 and 2873 cm^{-1}, and the α-β-unsaturated ketone absorption bands at 1707 and 1666 cm^{-1}.

Analysis of the ^{13}C-NMR (Appendix 6) and HSQC (Appendix 9) spectra of **12** revealed the presence of 15 carbons, including one carbonyl carbon (δ 211.06), two olefinic carbons (δ 133.38 and 181.81), two quaternary carbons (δ 41.62 and 58.70), four methylene carbons

(δ 27.00, 28.37, 30.49 and 41.16), two methine carbons (δ 33.72 and 45.35), and four methyl groups (δ 8.35, 16.83, 19.58 and 24.84), which characterized a sesquiterpene skeleton. The ^{1}H-NMR spectrum of **12** (Appendix 5) exhibited signals due to four methyl groups at δ 0.62 (*d, J* = 6.32 Hz), 0.75 (*s*), 1.11 (*s*) and 1.73 (*s*), of which the signal at δ 1.73 was due to a methyl group attached to an olefinic carbon atom (Table 5).

The ^{1}H-^{1}H COSY (Appendix 8) correlations between H-6 (δ 2.31 and 2.60) and H-7 (δ 1.98) and correlation of H-8 (δ 1.42 and 1.98) with H-9 (δ 1.06 and 1.61); H-9 (δ 1.02 and 1.60) with H-10 (δ 2.18); and H-10 (δ 2.18) with Me-15 (δ 0.62) established the connectivity of C-6 to C-7; C-8 to C-9; C-9 to C-10; and C-10 to Me-15. HMBC correlation (Appendix 10) of Me-12 (δ 1.11) with C-7 (δ 45.35), C-11 (δ 41.62) and Me-13 (δ 24.84); correlation of Me-13 (δ 0.75) with C-1 (δ 58.70), C-7 (δ 45.35), C-11 (δ 41.62) and Me-12 (δ 19.58); correlation of Me-14 (δ 1.73) with C-3 (δ 211.06), C-4 (δ 133.38) and C-5 (δ 181.81); and correlation of Me-15 (δ 0.62) with C-1 (δ 58.70), C-9 (δ 28.37) and C-10 (δ 33.72), indicated that Me-12 and Me-13 must be attached to C-11 (δ 41.62) and Me-14 and Me-15 are attached to C-4 (δ 133.38) and C-10 (δ 33.72), respectively. Furthermore, HMBC correlation of H-2 (δ 1.98 and 2.18) with C-3 (δ 211.06), C-4 (δ 133.38), C-5 (δ 181.81), C-10 (δ 33.72) and C-11 (δ 41.62) was used to establish the structure of **12** (Figure 4). However, the different configurations of compound **12** were not ruled out based on the above spectroscopic data. Compound **12** was determined to be cyperotundone by comparing its spectral data with the data reported in the literature[94]. Cyperotundone was previously identified in the MeOH fraction of the smoke from burnt rhizomes of *Cyperus esculentus* using GC-MS analysis.[30b] It was isolated from the rhizomes and tubers of another *Cyperus* species *Cyperus rotundus*.[94-95]

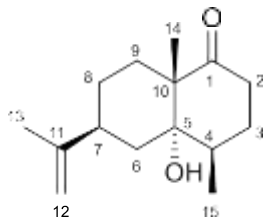
Table 5: The ^{1}H-NMR data (δ_{ppm}) of compound **12**.

12 ($CDCl_3$, 400 MHz)	Lit.[94] ($CDCl_3$, 500 MHz)
1.98 (1H, *m*, H-2)	2.00 (1H, *d*, *J* = 17.5 Hz, H-2)
2.18 (1H, *m*, H-2)	2.14 (1H, *d*, *J* = 17.5 Hz, H-2)
2.60 (1H, *dd*, *J* = 18.92, 7.32 Hz, H-6)	2.60 (1H, *dd*, *J* = 19.0, 6.5 Hz, H-6)
2.31 (1H, *d*, *J* = 18.96 Hz, H-6)	2.29 (1H, *d*, *J* = 19.0 Hz, H-6)
1.98 (1H, *m*, H-7)	1.96 (1H, *ddd*, *J* = 6.5, 3.5, 2.5 Hz, H-7)
1.98 (1H, *m*, H-8)	1.95 (1H, *ddd*, *J* = 13.0, 13.0, 2.5 Hz, H-8)
1.42 (1H, *m*, H-8)	1.41 (1H, *ddd*, *J* = 13.0, 6.5, 3.5 Hz, H-8)
1.60 (1H, *dt*, *J* = 15.16, 6.32 Hz, H-9)	1.59 (1H, *dt*, *J* = 15.0, 6.5 Hz, H-9)
1.02 (1H, *m*, H-9)	1.01 (1H, *dddd*, *J* = 15.0, 13.0, 13.0, 6.5 Hz, H-9)
2.18 (1H, *m*, H-10)	2.17 (3H, *d penta*, *J* = 13.0, 6.5 Hz, H-10)
1.11 (3H, *s*, H-12)	1.10 (3H, *s*, H-12)
0.75 (3H, *s*, H-13)	0.74 (3H, *s*, H-13)
1.73 (3H, *s*, H-14)	1.72 (3H, *s*, H-14)
0.62 (3H, *d*, *J* = 6.32 Hz, H-15)	0.67 (3H, *d*, *J* = 6.5 Hz, H-15)

Table 6: The ^{13}C-NMR data (δ_{ppm}) of compound **12**.

C	**12** ($CDCl_3$, 100 MHz)	Lit.[94] ($CDCl_3$, 125 MHz)
1	58.70	58.7
2	41.16	41.1
3	211.06	210.9
4	133.38	133.4
5	181.81	181.6
6	30.49	30.5
7	45.35	45.4
8	27.00	27.0
9	28.37	28.4
10	33.72	33.7
11	41.62	41.7
12	19.58	19.6
13	24.84	24.8
14	8.35	8.3
15	16.83	16.8

3.1.4.3. Characterization of Compound 114



114

Compound **114** was obtained as colorless crystals and is found to have a melting point of 135.0 – 136.8 °C. The IR spectrum of **114** (Appendix 19) showed the presence of hydroxy group (3435 cm^{-1}), a carbon-carbon double bond (1644 cm^{-1}) and a carbonyl group (1709 cm^{-1}). The ^{13}C-NMR spectrum of **114** (Appendix 14) revealed fifteen carbon resonances assigned with the help of its DEPT-135 (Appendix 15) and HSQC spectra (Appendix 17) to one double bond typical of an isopropenyl group (δ 108.88 and 149.57), one carbonyl carbon (δ 216.17), one oxygenated quaternary carbon (δ 78.64), one quaternary carbon (δ 51.26), five methylene carbons (δ 25.47, 28.02, 30.17, 34.26 and 37.20), two methine carbons (δ 39.32 and 40.55) and three methyl groups (δ 17.77, 20.40 and 21.15).

The ^{1}H-NMR spectrum of **114** (Appendix 13) showed the signal to the methylene protons of the isopropenyl group at δ 4.75 (2H, *s*, H-12). The spectrum also indicated that the signals at δ 1.25 (3H, *s*, Me-14) and 1.76 (3H, *s*, Me-13) are due to methyl groups attached to a quaternary carbon while the third methyl group resonance at δ 1.20 (3H, *d*, J = 7.56 Hz, Me-15) is attached to a methine carbon. ^{1}H-^{1}H COSY correlation (Appendix 16) of H-15 (δ 1.20) with H-4 (δ 1.90) indicated that Me-15 is attached to C-4. The connectivity between C-2 and C-3; C-3 and C-4; C-7 and C-8, and C-8 and C-9 was established by using the ^{1}H-^{1}H COSY correlations between the protons attached to these carbon atoms.

Table 7: The ^{1}H-NMR data (δ_{ppm}) of compound **114**.

114 ($CDCl_3$, 400 MHz)	Lit.[96] ($CDCl_3$, 360 MHz)
2.69 (1H, *m*, H-2)	2.68 (1H, *ddd*, *J* = 15.9, 9.9, 6.1 Hz, H-2)
2.38 (1H, *m*, H-2)	2.42 (1H, *ddd*, *J* = 15.9, 6.6, 5.2 Hz, H-2)
1.90 (1H, *m*, H-3)	1.69 (1H, *dddd*[a], *J* = 9.4, 9.9, 6.6, 5.9 Hz, H-3)
1.60 (1H, *m*, H-3)	2.39 (1H, *dddd*, *J* = 9.4, 6.1, 5.2, 6.2 Hz, H-3)
1.90 (1H, *m*, H-4)	1.86 (1H, *ddq*, *J* = 5.9, 6.2, 7.4 Hz, H-4)
2.38 (1H, *m*, H-6)	1.89 (1H, *dd*, *J* = 13.8, 12.8 Hz, H-6)
1.69 (1H, *m*, H-6)	1.44 (1H, *ddd*, *J* = 13.8, 3.9, 2.0 Hz, H-6)
2.38 (1H, *m*, H-7)	2.32 (1H, *dddd*, *J* = 12.8, 3.9, 13.2, 3.9 Hz, H-7)
1.38 (1H, *dd*, *J* = 12.76, 3.92 Hz, H-8)	1.38 (1H, *dddd*, *J* = 14.3, 13.2, 13.1, 3.8 Hz, H-8)
1.69 (1H, *m*, H-8)	1.69 (1H, *ddddd*[b], *J* = 14.3, 3.9, 4.8, 3.0, 2.0 Hz, H-8)
1.90 (1H, *m*, H-9)	1.90 (1H, *dddd*, *J* = 13.9, 13.1, 4.8, 1.2 Hz, H-9)
1.45 (1H, *ddd*, *J* = 13.83, 3.85, 2.09 Hz, H-9)	1.60 (1H, *ddd*, *J* = 13.9, 3.8, 3.0 Hz, H-9)
4.75 (2H, *s*, H-12)	4.74 (2H, *s*, H-12)
1.76 (3H, *s*, H-13)	1.75 (3H, *s*, H-13)
1.25 (3H, *s*, H-14)	1.24 (3H, *s*, H-14)
1.20 (3H, *d*, *J* = 7.56 Hz, H-15)	1.20 (3H, *d*, *J* = 7.4 Hz, H-15)

[a]Obtained by iterative simulation of the five-spin system and [b]obtained by iterative simulation of the seven-spin system.

The HMBC correlation (Appendix 18) between H-8 (δ 1.38 and 1.69) and C-11 (δ 149.57); H-13 (δ 1.76) and C-7 (δ 39.32); and between H-12 (δ 4.75) and C-7 (δ 39.32), C-11 (δ 149.57) and Me-13 (δ 21.15) indicated that the isopropenyl group is attached to C-7 (δ 39.32). The position of the carbonyl carbon was determined using HMBC correlation of H-2 (δ 2.38 and 2.69) and H-14 (δ 1.25) with C-1 (δ 216.17). Furthermore, HMBC correlation of H-2 with C-4 (δ 40.55), correlation of H-9 (δ 1.45 and 1.90) with C-5 (δ 78.64) and C-7 (δ 39.32) and correlation of H-14 (δ 1.25) with C-5 (δ 78.46) and C-10 (δ 51.26) were used to establish the structure of **114** (Figure 4). It was not possible to

determine the configuration at the stereocenters of compound **114** using the above spectroscopic data alone. Comparison of the spectroscopic data of **114** with those reported in the literature[96] for the sesquiterpenic keto-alcohol corymbolone, revealed a very close resemblance. Corymbolone (**114**) was first isolated in 1985 from the rhizomes of *Cyperus corymbosus* Rottboll.[96] It was also isolated from *Cyperus articulates*.[97]

Table 8: The ^{13}C-NMR data (δ_{ppm}) of compound **114**.

C	**114** ($CDCl_3$, 100 MHz)	Lit.[96] ($CDCl_3$, 90.5 MHz)
1	216.20	214.0
2	34.26	34.4
3	30.17	30.3
4	40.55	40.8
5	78.65	78.7
6	28.02	28.2
7	39.32	39.6
8	25.47	25.7
9	37.20	37.5
10	51.26	51.4
11	149.59	149.6
12	108.89	109.0
13	21.15	21.1
14	20.40	17.8
15	17.77	20.4

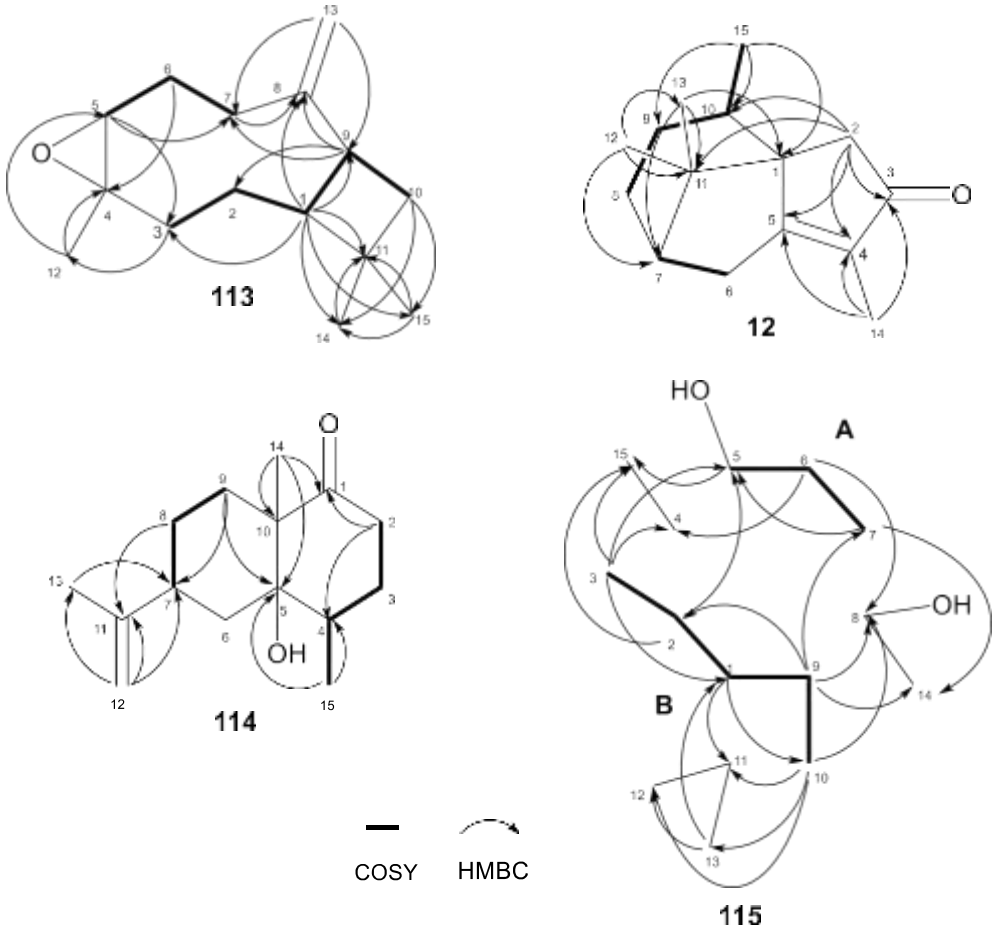
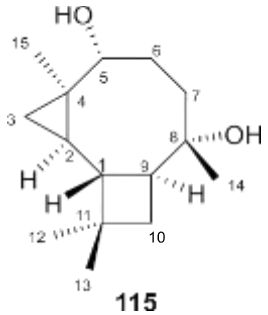


Figure 7: Selected 2D NMR correlations of compounds **12**, **113, 114** and **115**.

3.1.4.4. Characterization of Compound 115



Compound **115** was obtained as a white crystalline powder and had the molecular formula $C_{15}H_{26}O_2$ (degree of unsaturation = 3), as deduced from its HRESIMS that showed a

fragment ion peak at *m/z* 221.1918 $[M - H_2O + H]^+$ (Appendix 27) The IR spectrum of **115** (Appendix 26) unveiled absorption bands due to OH stretching (3326 cm^{-1}), an aliphatic C–H stretching (2947 cm^{-1}) and O–C stretching and bending bands (1459 and 1383 cm^{-1}, respectively). Compound **115** had a melting point of 159.0 – 161.0 °C. The UV-Vis spectrum of **115** in MeOH did not show any absorption band which indicated that there are no chromophores in the molecule.

The ^{1}H-NMR spectrum of **115** (Appendix 20) clearly indicated the existence of four methyl groups and one oxygen-bearing methine carbon atom. The ^{13}C-NMR spectrum of **115** (Appendix 21) showed a total of 15 carbon resonances and together with the DEPT-135 spectrum (Appendix 22) further confirmed the presence of one oxygenated methine, four aliphatic methylene, four methyl, three aliphatic methine, and three quaternary carbon atoms. Since there are no unsaturated carbon atoms in the molecule, **115** was inferred to possess three rings because of the three degrees of unsaturation implied by the molecular formula.

The ^{1}H-^{1}H COSY (Appendix 23) correlations of H-1 (δ 1.08) with H-2 (δ 0.70) and H-9 (δ 1.98); H-2 (δ 0.70) with H-3 (δ 0.23 and 0.49); H-5 (δ 3.25) with H-6 (δ 1.65 and 1.89); H-6 (δ 1.65 and 1.89) with H-7 (δ 1.81); and H-9 (δ 1.98) with H-10 (δ 1.39 and 1.57) were used to assemble two substructures **A** and **B** (Figure 7). HMBC correlations (Appendix 25) of both H-2 (δ 0.70) and H-3 (δ 0.23 and 0.49) with C-5 (δ 74.40) and correlations of H-3 (δ 0.23 and 0.49) and H-6 (δ 1.65 and 1.89) to C-4 (δ 19.99), and correlation of H-9 (δ 1.98) to both C-7 (δ 39.83) and C-8 (δ 73.57) revealed the connectivity between substructures **A** and **B** (Figure 7).

Table 9: The ^{1}H-NMR data (δ_{ppm}) of compound **115**.

115 ($CDCl_3$, 400 MHz)	Lit.[98] ($CDCl_3$, 400 MHz)
1.08 (1H, *d*, *J* = 10.80 Hz, H-1)	1.30 (1H, *t*, *J* = 11.1 Hz, H-1)
0.70 (1H, *ddd*, *J* = 10.80, 8.00, 5.20 Hz, H-2)	0.73 (1H, *m*, H-2)
0.23 (1H, *t*, *J* = 5.00 Hz, H-3)	0.44 (1H, *t*, *J* = 4.5 Hz, H-3)
0.49 (1H, *dd*, *J* = 4.60, 7.80 Hz, H-3)	0.52 (1H, *dd*, *J* = 4.5, 7.8 Hz, H-3)
3.25 (1H, *dd*, *J* = 5.20, 11.20 Hz, H-5)	3.62 (1H, *dd*, *J* = 4.8, 10.6 Hz, H-5)
1.65 (1H, *m*, H-6)	1.99 (1H, *m*, H-6)
1.89 (1H, *m*, H-6)	2.18 (1H, *m*, H-6)
1.81 (2H, *m*, H-7)	2.18 (2H, *m*, H-7)
1.98 (1H, *dt*, *J* = 8.00, 2.80 Hz, H-9)	2.32 (1H, *m*, H-9)
1.39 (1H, *t*, *J* = 10.40 Hz, H-10)	1.59 (1H, *t*, *J* = 10.0 Hz, H-10)
1.57 (1H, *dd*, *J* = 8.00, 10.00 Hz, H-10)	1.77 (1H, *dd*, *J* = 7.8, 10.0 Hz, H-10)
1.05 (3H, *s*, H-12)	1.14 (3H, *s*, H-12)
1.02 (3H, *s*, H-13)	1.04 (3H, *s*, H-13)
1.14 (3H, *s*, H-14)	1.35 (3H, *s*, H-14)
1.13 (3H, *s*, H-15)	1.22 (3H, *s*, H-15)

In addition, the HMBC correlation of H-1 (δ 1.08) to C-10 (δ 33.98) and C-11 (δ 33.56), correlations H-2 (δ 0.70) and H-5 (δ 3.25) to C-15 (δ 17.30), correlation of H-3 (δ 0.23 and 0.49) to C-1 (δ 48.20) and C-15 (δ 17.30), correlation of H-6 (δ 1.65 and 1.89) to C-8 (δ 73.57), correlation of H-7 (δ 1.81) to C-5 (δ 74.40) and C-14 (δ 19.90), correlation of H-9 (δ 1.98) to C-2 (δ 24.16) and C-14 (δ 19.90), correlation of H-10 (δ 1.39 and 1.57) to C-8 (δ 73.57), C-11 (δ 33.56), C-12 (δ 22.14) and C-13 (δ 30.38) and correlation of H-13 (δ 1.02) to C-1 (δ 48.20) and C-12 (δ 22.14) were used to establish the structure of compound **115** as shown in Figure 4.

Table 10: The ^{13}C-NMR data (δ_{ppm}) of compound **115**.

C	**115** ($CDCl_3$, 100 MHz)	Lit.[98] ($CDCl_3$, 100 MHz)
1	48.20	48.4
2	24.16	24.4
3	18.44	19.3
4	19.99	20.5
5	74.40	73.5
6	30.44	32.2
7	39.83	41.5
8	73.57	72.4
9	49.03	50.1
10	33.98	34.9
11	33.56	34.0
12	22.14	22.5
13	30.38	30.6
14	19.90	20.3
15	17.30	18.2

In order to confirm the proposed structure of **115**, single crystal X-ray analysis was done which is reported herein for the first time. Suitable crystals of **115** were obtained from DCM-MeOH (1:1) mixture. Figure 8 shows the X-ray crystal structure of **115**, which confirmed the elucidated structure and gave the absolute configuration of the compound. A comparison of the NMR data of **115** with those reported in the literature for tricyclohumuladiol (Table 9 and Table 10),[98] revealed a very close agreement. Therefore, compound **115** was identified as tricyclohumuladiol which was previously isolated from *Cyperus longus*[99] and *Schisandra plena*.[98]

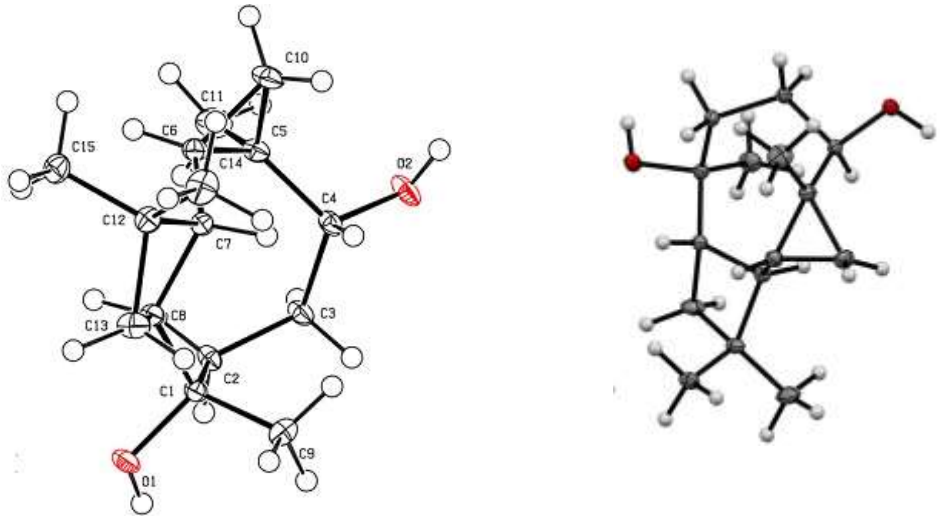


Figure 8: X-ray crystal structure of **115**.

3.2. Chemical Studies on the Roots of *Carissa spinarum*

Carissa spinarum is widely used traditionally as incense plant in South Wollo and for the treatment of numerous diseases. Although the plant is widely used in traditional medicine in Ethiopia and other parts of Africa, there was no prior scientific report on the chemical composition and bioactivity of the essential oil and smoke from the roots of this plant. Therefore, this study was undertaken to evaluate the antioxidant activity and phytochemical constituents of the essential oil and medicinal smoke from the roots of this plant. The roots of *Carissa spinarum* were dried, powdered and extracted by hydrodistillation to obtain essential oil and burned using an electrical stove to collect the smoke. Both the essential oil and medicinal smoke were analyzed by GC-MS and the smoke was tested for its antioxidant activity using the DPPH assay as described below.

3.2.1. Extraction and Characterization of Compounds from the Essential Oil and the Smoke Derived from the Roots of *Carissa spinarum*

The dried and powdered roots of *Carissa spinarum* were extracted by hydrodistillation according to the method described in **Section 4.3.2.1** and then analyzed by GCMS (**Section 4.3.2.3**). The essential oil was found to be predominantly composed of 2-hydroxyacetophenone (**16**, 82.97%) by GC-MS analysis (Figure 9) as well as its UV-Vis, FTIR, ^{1}H-, ^{13}C- and DEPT-NMR (Appendix 28 to Appendix 32) spectra.

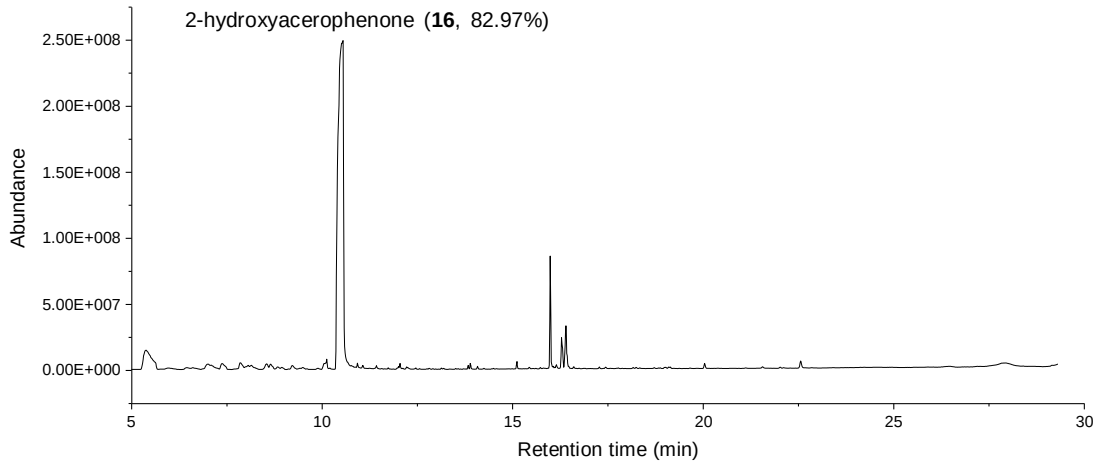


Figure 9: The GC-MS chromatogram of the essential oil from the roots of *Carissa spinarum*.

The smoke from burnt roots of *Carissa spinarum* was collected and analyzed by GC-MS as described in **Section 4.3.2.2** and **Section 4.3.2.3**. A total of 31, compounds, 16 from the *n*-hexane fraction and 15 from the MeOH-soluble portion of the smoke obtained from burnt roots of *Carissa spinarum,* with qualities greater than 72% and area percentage greater than 2, were identified (Figure 10). The different components were characterized by matching

their mass spectra with those of reference compounds recorded in NIST 2014 mass spectral library and confirmed by the retention indices obtained from a series of *n*-alkanes. Table 11 shows that phenolic compounds, namely, 2,6-dimethoxyphenol (14.16%), 2-methoxyphenol (10.34%) and 2-hydroxyacetophenone (9.51%), are the dominant components of the *n*-hexane fraction of the smoke derived from the roots of *Carissa spinarum*.

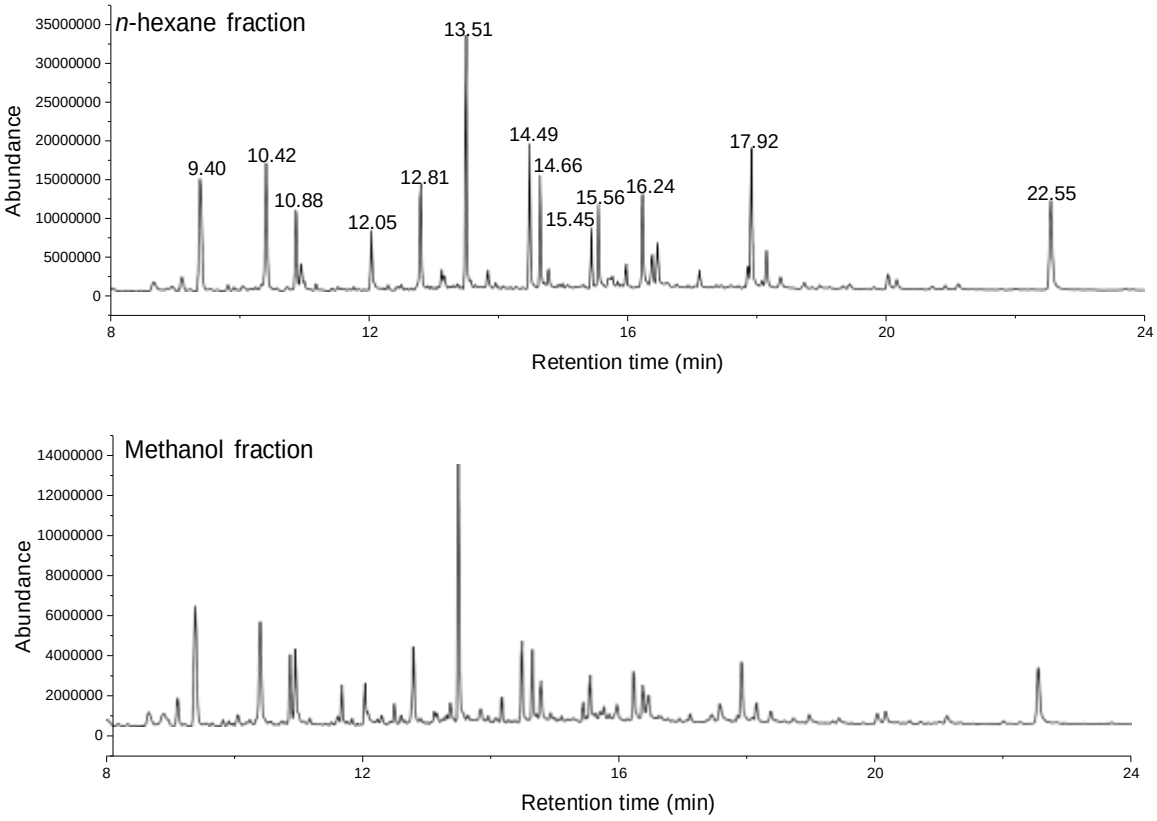


Figure 10: The GC-MS chromatogram of *n*-hexane- and methanol-soluble fractions of the smoke derived from the roots of *Carissa spinarum*.

Table 11: Major compounds identified from the *n*-hexane-soluble fraction of the smoke derived from the roots of *Carissa spinarum* by GC-MS analysis.

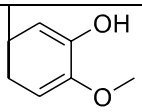
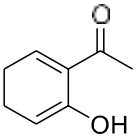
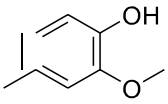
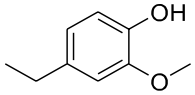
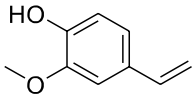
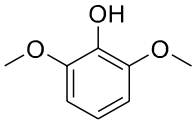
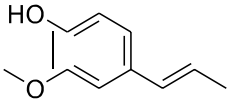
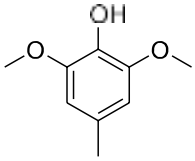
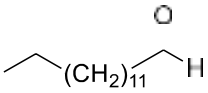
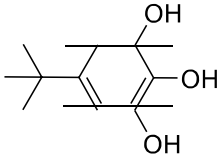
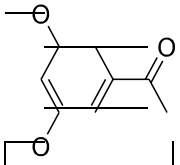
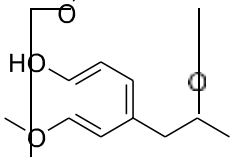
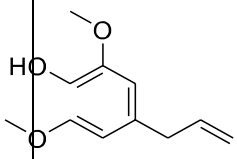
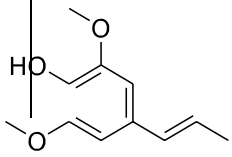
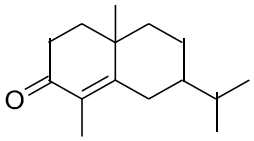
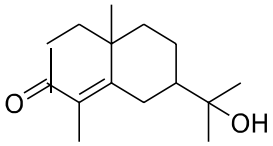
PK	Rt	Area Pct.	Compound	Structure	Q	*I*
1	9.40	10.34	2-Methoxyphenol		95	1232.52
2	10.42	9.51	2-Hydroxyacetophenone		95	1303.73
3	10.88	4.54	Creosol		97	1337.5
4	12.05	3.71	4-Ethyl-2-methoxyphenol		91	1424.05
5	12.81	6.98	2-Methoxy-4-vinylphenol		91	1483.24
6	13.51	14.16	2,6-Dimethoxyphenol		97	1540.37
7	14.49	7.36	*trans*-Isoeugenol		98	1623.50
8	14.66	5.18	3,5-Dimethoxy-4-hydroxytoluene		97	1637.68
9	15.45	2.71	Tetradecanal		99	1706.98
10	15.56	4.37	5-*tert*-Butylpyrogallol		79.9	1717.08

Table 11 continued

PK	Rt	Area Pct.	Compound	Structure	Q	*I*
11	16.24	6.05	3′,5′-Dimethoxy acetophenone		77.7	1779.61
12	16.39	2.21	Guaiacylacetone		80.4	1793.11
13	16.47	2.69	Methoxyeugenol		93	1800.90
14	17.92	8.79	4-Propenylsyringol		98	1917.92
15	18.16	2.64	α-Cyperone		99	1935.24
16	22.55	8.77	Carissone		87.7	2220.94

Pk = peak number, Rt = retention time (min), Area Pct. = area percentage, Q = quality, *I* = retention index

3.2.2. The DPPH Radical Scavenging Assay of the Methanol-Soluble Fraction of the Smoke Derived from the Roots of *Carissa spinarum*

The radical scavenging activity of the MeOH-soluble fraction of the smoke derived from the roots of *Carissa spinarum* was assessed following the procedure described in **Section 4.3.1.4**. The MeOH-soluble fraction showed a 92.60% DPPH inhibition at concentration of 100.00 µg/mL which is comparable to that of ascorbic acid standard that exhibited a

96.09% DPPH inhibition at the same concentration (Table 12). The phenolic compounds in the smoke may be responsible for the observed antioxidant activity.

Table 12: Radical scavenging activities of the MeOH-soluble fraction of the smoke derived from *Carissa spinarum* and ascorbic acid standards.

Concentration (µg/mL)	% DPPH Inhibition	
	MeOH fraction of the smoke from *Carissa spinarum*	Ascorbic acid standard
100.00	92.60 ± 0.34	96.09 ± 0.16
50.00	88.48 ± 0.31	96.29 ± 0.06
25.00	66.06 ± 0.71	96.26 ± 0.06
12.50	47.62 ± 0.11	96.06 ± 0.12
6.25	37.32 ± 0.81	91.30 ± 0.31
3.13	30.97 ± 0.95	54.06 ± 1.27
1.56	26.09 ± 0.15	35.00 ± 0.52

The results are reported as mean ± SD of three replicates.

3.3. Phytochemical Studies on Extracts of the Seeds of *Melilotus officinalis*

The dried and ground seeds of *M. officinalis* were Soxhlet-extracted and then subjected to GC-MS analysis. Phytochemical studies were also conducted on the MeOH extract of the seeds as outlined in the following sections.

3.3.1. Extraction and Characterization of the Seed Fatty Acids of *Melilotus officinalis*

The dried and ground seeds of *M. officinalis* were subjected to Soxhlet extraction with *n*-hexane and the crude oil was esterified using 2% KOH in MeOH. The fatty acid methyl esters were then subjected to GC-MS analysis. Quantifications of components in the *n*-hexane extract were made by using their relative area percentages. Methyl palmitate

external standards were also used to determine the concentrations (ppm) of the components. Thus, standard solutions of methyl palmitate were prepared and analyzed by GC-MS in triplicates at different concentrations (Table 13). The calibration curve shown in Figure 11 was constructed using the mean area of each concentration and then used to calculate the concentrations of the different components.

Table 13: Methyl palmitate standard solutions and their corresponding areas.

Concentration (ppm)	Rt (min)	Area	Average area
1	14.946	37468273.30	
1	14.946	37468273.33	36486414.85
1	14.946	34522697.93	
10	14.960	199432023.00	
10	14.946	205708666.30	201524237.50
10	14.946	199432023.20	
25	14.960	364137351.00	
25	14.960	364137351.00	367682432.90
25	14.959	374772596.80	
50	14.986	644456871.10	
50	14.973	603905108.30	632297810.80
50	14.987	648531452.90	
100	15.013	1137443228.00	
100	15.000	1170868871.00	1157940017.00
100	15.014	1165507951.00	

Rt = retention time (min), ppm = parts per million

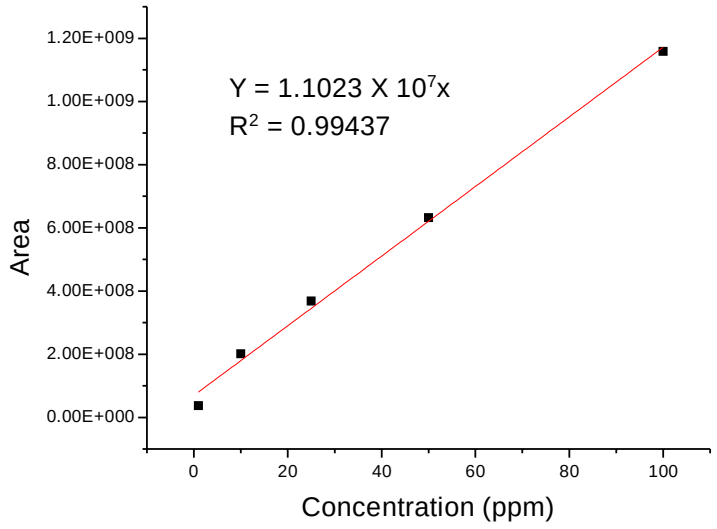


Figure 11: Calibration curve of methyl palmitate standard.

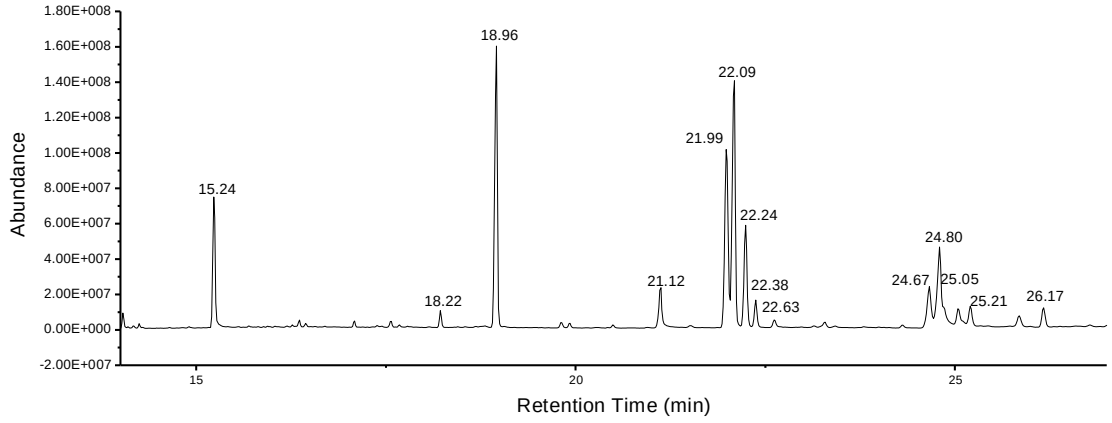


Figure 12: The GC-MS chromatogram of the esterified *n*-hexane extract of the seeds of *M. officinalis.*

GC-MS analysis revealed the presence of 12 compounds with a combined area percentage of 98.33% (Figure 12) including coumarin (8.40%), 10 fatty acids (87.74%), and 5-dodecyldihydrofuran-2(3*H*)-one (2.19%) with qualities greater than 90% and area

percentage greater than one. The NIST 2014 mass spectral library search was used for the identification of individual components in the extract. The names of identified compounds with their respective retention times, area percentages, qualities and concentrations are given in Table 14.

Table 14: Major compounds identified from the *n*-hexane extract of the seeds of *M. officinalis* by GC-MS analysis

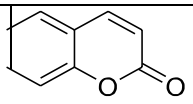
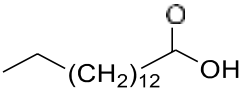
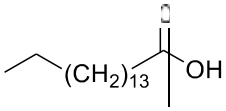
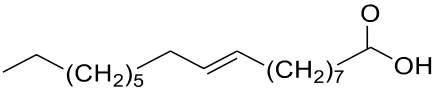
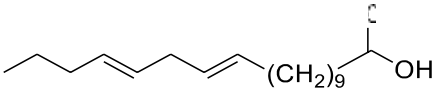
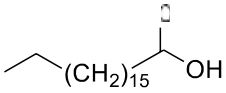
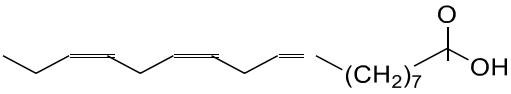
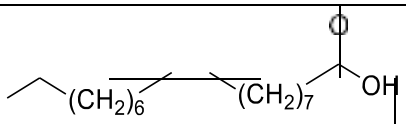
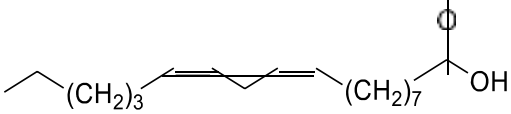
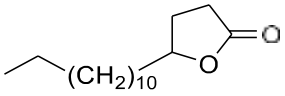
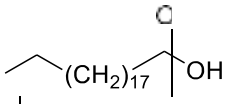
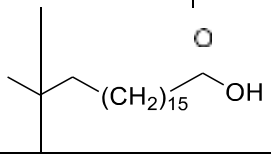
Pk	Rt	Area Pct.	Compound	Structure	Q	C (ppm)
1	15.24	8.40	Coumarin		95	152.19
2	18.96	19.52	14-Methyl pentadecanoic acid		95	353.45
3	21.12	3.41	Palmitic acid		99	61.83
4	21.99	15.94	(9*E*)-Octadecenoic acid		99	288.66
5	22.09	20.22	(9*Z*,12*Z*)-Octadecadienoic acid		99	366.08
6	22.24	8.24	Stearic acid		99	149.26
7	22.38	1.95	Linolenic acid		99	35.36

Table 14 continued

Pk	Rt	Area Pct.	Compound	Structure	Q	C (ppm)
8	24.67	4.39	Oleic acid		99	79.49
9	24.80	10.50	Linoleic acid		99	190.16
10	25.05	2.19	5-Dodecyldihydro furan-2(3*H*)-one		94	39.61
11	25.21	1.85	Eicosanoic acid		99	33.44
12	26.17	1.72	18-Methyl nonadecanoic acid		99	31.20

Pk = peak number, Rt = retention time (min), Area Pct. = area percentage, Q = quality, C = concentration, ppm = parts per million

It is apparent from Table 14 that the *n*-hexane extract of the seeds of *M. officinalis* is mainly composed of unsaturated and polyunsaturated fatty acids. In addition, the extract was found to be rich in (9*Z*,12*Z*)-octadecadienoic acid (20.22%), 14-methylpentadecanoic acid (19.52%) and (9*E*)-octadecenoic acid (15.94%). The presence of unsaturated fatty acids in the seeds *M. officinalis* and *M. alba* was previously reported using gas chromatography and flame ionization analysis.[67m]

The esterified *n*-hexane extract was partitioned between *n*-hexane and MeOH to determine if the amount of the hepatotoxic coumarin[100] can be reduced. GC-MS analysis of the *n*-hexane portion showed a decrease in the amount of coumarin to 1.10% (33.43 ppm) (Figure

13). The above result indicates, the oil from the seeds of *M. officinalis* may not be suitable for cooking purposes but can be used for other applications such as preparation of soap. Further fractionations can be applied to remove all the coumarin and use the oil for cooking.

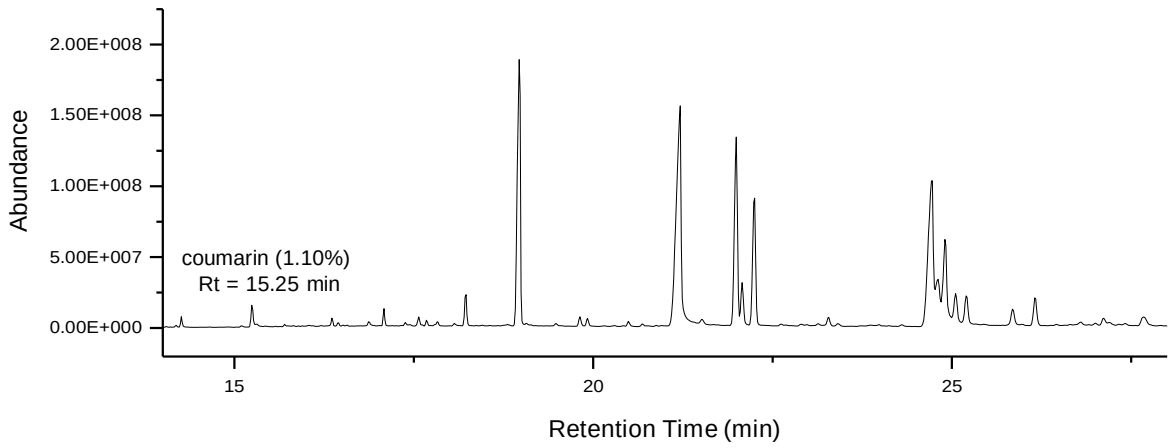


Figure 13: The GC-MS chromatogram of the esterified *n*-hexane extract of the seeds of *M. officinalis* after partitioning with methanol.

3.3.2. DPPH Assay of the Methanol Extract of the Seeds of *Melilotus officinalis*

The marc left after extraction (**Section 3.3.1**) of the seeds of *M. officinalis* with *n*-hexane was further extracted with MeOH in a Soxhlet apparatus to give a brown crude extract (**Section 4.3.3.1**). Radical scavenging activity of the MeOH extract was quantified following the procedure described in **Section 4.3.1.4**. The extract showed a 29.87% DPPH inhibition at concentration of 100.00 µg/mL (Table 15).

Table 15: Radical scavenging activities of the methanol extract of the seeds of *M. officinalis* and ascorbic acid standards.

Concentration (µg/mL)	% DPPH Inhibition	
	MeOH extract of *M. officinalis*	**Ascorbic acid standard**
100.00	29.87 ± 0.49	96.09 ± 0.16
50.00	26.35 ± 0.54	96.29 ± 0.06
25.00	24.82 ± 0.23	96.26 ± 0.06
12.50	24.16 ± 0.16	96.06 ± 0.12
6.25	22.12 ± 0.91	91.30 ± 0.31
3.13	21.62 ± 0.13	54.06 ± 1.27
1.56	21.53 ± 0.12	35.00 ± 0.52

The results are reported as mean ± SD of three replicates.

3.3.3. Fractionation of the Methanol Extract of the Seeds of *Melilotus officinalis*

Attempts were also made to isolate and characterize compounds from the MeOH extract of the seeds of *M. officinalis* as described in **Section 4.3.3.5**. Thus, two compounds, *cis*-coumaric acid-2-*O*-*β*-glucopyranoside (*cis*-melilotoside, **116**) and 1,2-benzopyrone (coumarin, **65**) (Figure 14), were isolated by using Sephadex LH-20 column chromatography and preparative TLC techniques. The structures of the isolated compounds were determined by spectroscopic techniques, UV-Vis, FTIR, and NMR, as described below.

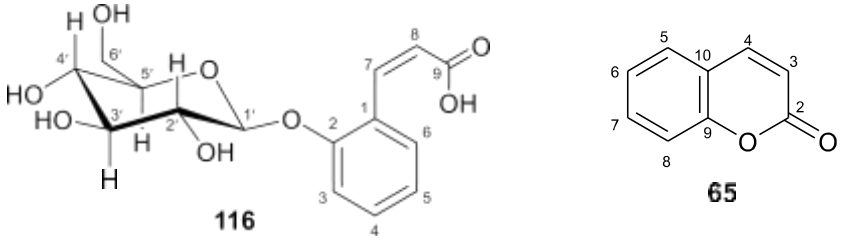
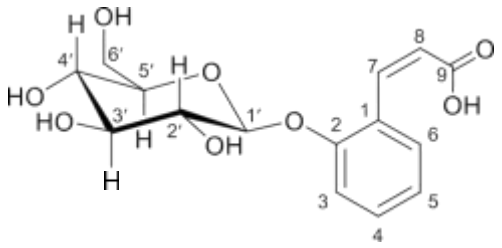


Figure 14: Compounds isolated from the MeOH extract of the seeds of *M. officinalis*

3.3.4. Characterization of Compounds Isolated from the Seeds of *Melilotus officinalis*

3.3.4.1. Characterization of Compound 116



116

Compound **116** was obtained as white crystals and had a melting point of 126.0 – 127.0 °C. The UV-Vis spectrum of **116** in MeOH displayed an absorption maximum (λ_{max}) at 261 nm which is characteristic of a phenolic moiety (Appendix 40). The IR spectrum (Appendix 39) indicated the presence of a carbonyl (1691 cm^{-1}), aromatic (1636, 1240 cm^{-1}) and hydroxy (3391 cm^{-1}) functionalities.

The ^{1}H-NMR spectrum of **116** (Table 16 and Appendix 33) showed two olefinic proton signals at δ 7.09 (1H, *d*, *J* = 12.00 Hz, H-7) and 6.05 (1H, *d*, *J* = 12.00 Hz, H-8), which indicated the presence a *cis* double bond.[101] Besides, the coupling patterns of the aromatic proton signals at δ 7.12 (1H, *d*, *J* = 8.00 Hz, H-3), 7.30 (1H, *d*, *J* = 8.00 Hz, H-4), 7.03 (1H, *t*, *J* = 8.00 Hz, H-5) and 7.34 (1H, *d*, *J* = 8.00 Hz, H-6) suggested the presence of an *ortho*-disubstituted benzene ring. Additionally, the ^{13}C-NMR spectrum (Table 17 and Appendix 34), indicated the presence of a carbonyl carbon (δ 171.74), six aromatic and two olefinic carbon atoms. The signal at δ 153.81 is due to an oxygenated aromatic carbon atom. The HMBC spectrum of **116** (Appendix 38) revealed a correlation between the signal at δ

125.53 (C-1) and the proton signals at δ 7.09 (H-7) and δ 6.05 (H-8). Thus, the olefinic carbon C-7 (δ 137.14) is attached to C-1.

Table 16: The ^{1}H-NMR data (δ_{ppm}) of compound **116**.

116 (D_2O, 400 MHz)	Lit.[102] (MeOD-d_4, 500 MHz)
7.12 (1H, *d*, *J* = 8.00 Hz, H-3)	7.19 (1H, *d*, *J* = 7.9 Hz, H-3)
7.30 (1H, *d*, *J* = 8.00 Hz, H-4)	7.30 (1H, *t*, *J* = 7.9 Hz, H-4)
7.03 (1H, *t*, *J* = 8.00 Hz, H-5)	6.97 (1H, *t*, *J* = 7.9 Hz, H-5)
7.34 (1H, *d*, *J* = 8.00 Hz, H-6)	7.53 (1H, *d*, *J* = 7.9 Hz, H-6)
7.09 (1H, *d*, *J* = 12.00 Hz, H-7)	7.31 (1H, *d*, *J* = 12.5 Hz, H-7)
6.05 (1H, *d*, *J* = 12.00 Hz, H-8)	5.97 (1H, *d*, *J* = 12.5 Hz, H-8)
5.05 (1H, *d*, *J* = 7.20 Hz, H-1′)	4.94 (1H, *d*, *J* = 7.4 Hz, H-1′)
3.53 (1H, *m*, H-2′)	3.49 (1H, *m*, H-2′)
3.53 (1H, *m*, H-3′)	3.46 (1H, *m*, H-3′)
3.42 (1H, *m*, H-4′)	3.40 (1H, *m*, H-4′)
3.53 (1H, *m*, H-5′)	3.43 (1H, *m*, H-5′)
3.84 (1H, *dd*, *J* = 12.40, 2.30 Hz, H-6′)	3.87 (1H, *m*, H-6′)
3.67 (1H, *dd*, *J* = 12.40, 5.40 Hz, H-6′)	3.70 (1H, *m*, H-6′)

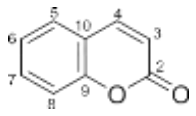
The presence of a glucopyranosyl ring in the structure **116** was indicated by the analysis of its ^{1}H- and ^{13}C-NMR spectra. The glucose moiety, which can be assigned a *β*-configuration on the basis of the coupling constant of the anomeric proton signal at δ 5.05 (1H, *d*, *J* = 7.20 Hz),[103] is attached to the C-2 (δ 153.81) position. Based on the analysis of the spectroscopic data, compound **116** was identified to be *cis*-coumaric acid-2-*O*-β-glucopyranoside (*cis*-melilotoside, Figure 14). Comparison of the spectroscopic data of **116** with those reported in the literature for *cis*-melilotoside showed that the two compounds are identical.[101-102]

Table 17: The ^{13}C-NMR data (δ_{ppm}) of compound **116**.

C	**116** (D_2O, 100 MHz)	Lit.[102] (MeOD-d_4, 125 MHz)
1	125.53	126.9
2	153.81	156.7
3	115.36	116.6
4	130.56	131.5
5	122.85	122.9
6	130.09	131.7
7	137.14	139.7
8	122.02	121.4
9	171.74	170.4
1′	100.41	102.7
2′	72.93	75.0
3′	76.12	78.2
4′	69.44	71.4
5′	75.71	78.3
6′	60.58	62.6

This is the first report on the isolation of *cis*-melilotoside from *M. officinalis*. *cis*-melilotoside has been reported from several plants such as *M. neapolitana*, *Ajuga chamaecistus ssp. tomentella* and *Mikania laevigata*.[101,104]

3.3.4.2. Characterization of Compound 65



65

Compound **65** was isolated as a white powder and had a melting point of 70.0 – 71.0 °C. The UV-Vis spectrum (Appendix 45) of **65** in MeOH revealed an absorption maximum (λ_{max}) at 274 nm and the IR spectrum (Appendix 44) showed absorption band at 1729 due to the α,β-unsaturated carbonyl group of the δ-lactone moiety while the bands at 1288 and 1274 cm^{-1} are due to C-O stretching absorption.

The ^{13}C-NMR spectrum of **65** (Table 19 and Appendix 42) revealed 9 carbon resonances. The signal at δ 160.75 is due to the carbonyl carbon of a δ-lactone. Besides, the two olefinic carbon signals at δ 116.94 and 143.38, and the six aromatic carbon signals at δ 116.76, 118.86, 124.41, 127.84, 131.83 and 154.11 indicated the presence of an aromatic ring and a double bond. In the ^{1}H-NMR spectrum of **65** (Table 18 and Appendix 41), the two olefinic proton doublets at δ 6.46 (J = 9.60 Hz) and 7.74 (J = 9.60 Hz) are attributable to H-3 and H-4 of the lactone nucleus, respectively. The signals at δ 7.34 (2H, *m*, H-5 and H-7) and 7.54 (2H, *m*, H-6 and H-8) revealed the presence of an *ortho*-disubstituted benzene ring. Compound **65** was then identified as 1,2-benzopyrone (coumarin, Figure 14) by comparison of its spectral data with data reported in the literature.[105] Coumarin has previously been isolated from the MeOH extract of the aerial parts of *M. officinalis*.[52b] Coumarin was also found in many plants of the genus *Melilotus*.

Table 18: The ^{1}H-NMR data (δ_{ppm}) of compound **65**.

65 ($CDCl_3$, 400 MHz)	Lit.[105] (DMSO-d_6, 300 MHz)
6.46 (1H, *d*, *J* = 9.60 Hz, H-3)	6.47 (1H, *d*, *J* = 9.6 Hz, H-3)
7.74 (1H, *d*, *J* = 9.60 Hz, H-4)	8.03 (1H, *d*, *J* = 9.9 Hz, H-4)
7.34 (1H, *m*, H-5)	7.29 (1H, *m*, H-5)
7.54 (1H, *m*, H-6)	7.58 (1H, *m*, H-6)
7.34 (1H, *m*, H-7)	7.29 (1H, *m*, H-7)
7.54 (1H, *m*, H-8)	7.58 (1H, *m*, H-8)

Table 19: The ^{13}C-NMR data (δ_{ppm}) of compound **65**.

C	**65** ($CDCl_3$, 100 MHz)	Lit.[105] (DMSO-d_6, 75 MHz)
2	160.75	159.84
3	116.94	116.18
4	143.38	144.10
5	127.84	128.35
6	124.41	124.38
7	131.83	131.84
8	116.76	116.11
9	154.11	153.43
10	118.86	118.6

cis-Melilotoside (**116**) is a biosynthetic precursor of coumarin (**65**) (Figure 15) as shown by ^{14}C feeding experiments.[106] In the biosynthesis of coumarin (**65**), the *trans* isomer of *β*-glucoside-*O*-coumaric acid (**117**) undergoes isomerization to its *cis* isomer (*cis*-melilotoside, **116**), which could then hydrolyze to coumarinic acid (**118**) which in turn lactonizes spontaneously to form coumarin (**65**).

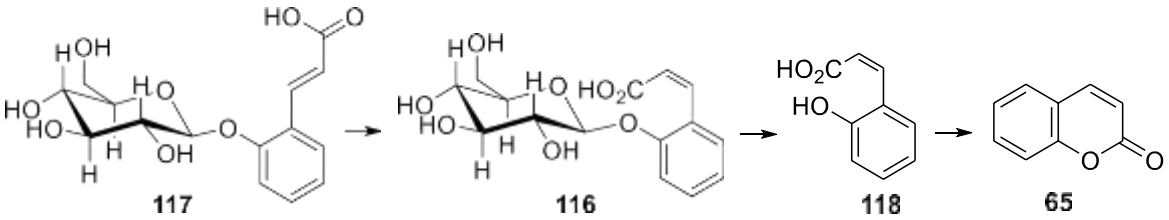


Figure 15: Proposed biosynthetic pathway of coumarin (**65**).[106]

3.4. Phytochemical Investigation on the Fresh Leaves of *Rhus glutinosa*

The fresh leaves of *R. glutinosa* were extracted and subjected to phytochemical studies for the first time to yield a total of twelve compounds, namely, pentacosanol (**119**), 5,7-dihydroxy-4′-methoxyflavone (acacetin, **120**), 3,5,7,4′-tetrahydroxyflavone (kaempferol,

38), 6,8″-binaringenin (rhusflavanone, **121**), 6,8″-naringeninyl apigenin (rhusflavone, **122**), quercetin 3-*O*-α-arabinofuranoside (avicularin, **123**), 3,5,7,3′,4′-pentahydroxyflavone (quercetin, **1**), 3,5,7,3′,4′,5′-hexahydroxyflavone (myricetin, **2**), quercetin-3-*O*-α-rhamnopyranoside (quercitrin, **124**), shikimic acid (**125**), quercetin 3-*O*-β-galactoside (hyperoside, **126**), and myricetin-3-*O*-β-galactopyranoside (**127**) (Figure 16). Acacetin (**120**), avicularin (**123**), and myricetin-3-*O*-β-galactopyranoside (**127**) are reported herein for the first time from the genus *Rhus*. The EtOAc-soluble fraction of the DCM:MeOH (1:1) extract of the leaves of *R. glutinosa* was also tested for its antioxidant activity using the DPPH assay. The extraction and characterization of compounds isolated from the leaves of *R. glutinosa* is discussed in the following sections.

3.4.1. DPPH Radical Scavenging Assay of the Ethyl Acetate Fraction of *Rhus glutinosa*

The grounded fresh leaves of *R. glutinosa* were extracted as described in **Section 4.3.4.1**. The radical scavenging activity of the EtOAc-soluble fraction of the DCM:MeOH (1:1) extract of the leaves of *R. glutinosa* was determined following the procedure described in **Section 4.3.1.4**. The EtOAc-soluble fraction was able to reduce the stable DPPH radical by 94.89% at 50.00 µg/mL to the yellow-colored diphenylpicrylhydrazicine indicating its potential as a radical scavenger. At the same concentration standard ascorbic acid scavenged the DPPH radical by 96.29% (Table 20). The presence of flavonoids (**Section 3.4.3**) could be responsible for the observed high antioxidant activity of the leaves of *R. glutinosa*. This result supports the traditional medicinal use of *Rhus* plants for treatment of inflammation[70b] because of their antioxidant activities.

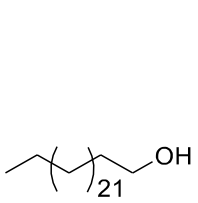
Table 20: Radical scavenging activities of the EtOAc-soluble portion of the DCM:MeOH extract of the leaves of *R. glutinosa* and ascorbic acid standards.

Concentration (µg/mL)	% DPPH Inhibition	
	EtOAc-soluble portion of the extract of *R. glutinosa*	Ascorbic acid standard
50.00	94.89 ± 0.10	96.29 ± 0.06
25.00	94.84 ± 0.17	96.26 ± 0.06
12.50	68.41 ± 0.89	96.06 ± 0.12
6.25	46.74 ± 1.08	91.30 ± 0.31
3.13	32.40 ± 0.72	54.06 ± 1.27
1.56	27.28 ± 0.46	35.00 ± 0.52

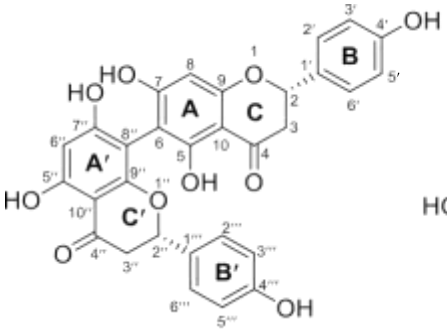
The results are reported as mean ± SD of three replicates.

3.4.2. Fractionation of the Crude Ethyl Acetate-Soluble Fraction of the DCM:MeOH Extract of the Leaves of *Rhus glutinosa*

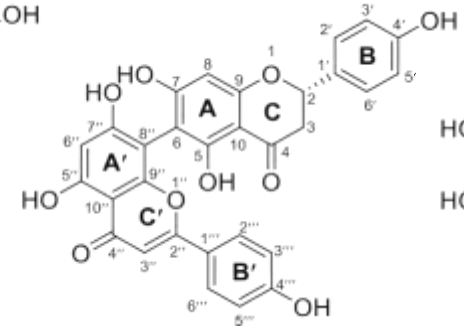
Fractionation of the EtOAc-soluble portion of the DCM:MeOH (1:1) extract of the fresh leaves of *R. glutinosa* (see **Section 4.3.4.2**) resulted in the isolation of twelve compounds (Figure 16). The structural determination of the isolated compounds was based on spectral analysis and by comparison of these with data reported in the literature. The structural elucidation of these compounds is discussed in the following section.



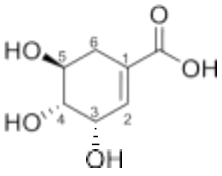
119



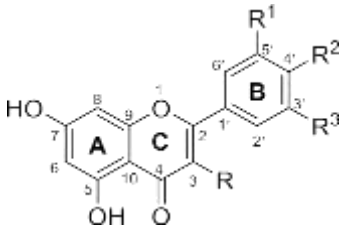
121



122



125



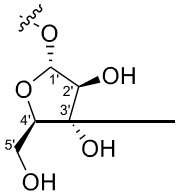
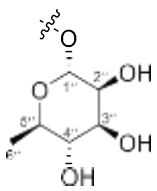
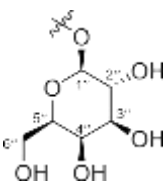
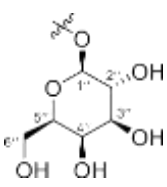
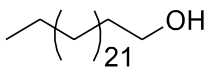
	1	2	38	120	123	124	126	127
R =	OH	OH	OH	H				
R^1 =	OH	OH	H	H	OH	OH	OH	OH
R^2 =	OH	OH	OH	OCH_3	OH	OH	OH	OH
R^3 =	H	OH	H	H	H	H	H	OH

Figure 16: Compounds isolated from the leaves of *R. glutinosa*.

3.4.3. Characterization of Compounds Isolated from the Leaves of *Rhus glutinosa*

3.4.3.1. Characterization of Compound 119



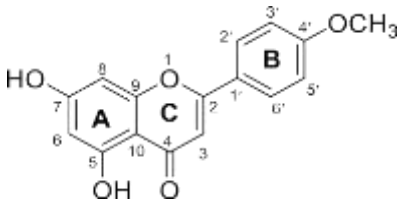
119

Compound **119** was isolated as a white amorphous powder and its positive ion HRESIMS (Appendix 50) gave a molecular ion peak $[M+Na]^+$ at *m/z* 391.3916 which is compatible

with the molecular formula $C_{25}H_{52}O$. The UV-Vis spectrum of **119** in MeOH did not show any absorption band which indicated that there are no chromophores and that it might be a saturated hydrocarbon. In the IR spectrum of **119** (Appendix 49), the absorption band at 3370 cm^{-1} indicated the O–H stretching. The aliphatic C–H stretching bands appeared at 2917 and 2849 cm^{-1} and the C–O stretching band was observed at 1221 cm^{-1}.

The ^{1}H- (Appendix 46) and ^{13}C-NMR (Appendix 47) spectra of **119** showed one oxygenated methylene signal [at δ_H 3.66 (*t*, *J* = 6.60 Hz) and at δ_C 63.12], one terminal methyl signal [at δ_H 0.90 (*t*, *J* = 6.80 Hz) and at δ_C 14.12] and alkyl methylene signals [at δ_H 1.59 (*q*, *J* = 6.80 Hz, 2H), 1.27 (*m*, 44H) and at δ_C 32.82, 31.94, 29.71, 29.63, 29.45, 29.38, 25.75, 22.70]. These spectral data indicated that compound **119** is a straight chain primary alcohol and the structure **119** (pentacosanol, Figure 16) was assigned based on the available spectroscopic data. Pentacosanol (**119**) was previously reported from various plants including *Cayratia trifolia* L., *Stellaria media* and *Crataegus monogyna* Jacq.[107]

3.4.3.2. Characterization of Compound 120



120

Compound **120** was obtained as a light-yellow powder (m. p. 259.0 – 260.0 °C). Its HRESIMS spectrum (Appendix 56) showed a mass fragment peak $[M - CH_3 + H]^+$ at *m/z* 271.0606. The molecular formula of $C_{16}H_{12}O_5$ was deduced based on the analysis of the HRESIMS and NMR spectral data (Table 21 and Table 22) of **120**. The UV-Vis spectrum

of **120** (Appendix 55) showed absorption maxima at 270 and 328 nm while the IR spectrum (Appendix 54) revealed absorption bands at 3411 (hydroxy), 1651 (carbonyl), and 1510 (phenyl) cm^{-1} which suggested the presence of a flavone.[108]

Table 21: The ^{1}H-NMR data (δ_{ppm}) of compound **120**.

120 (Acetone-d_6, 400 MHz)	Lit.[109] ($CDCl_3$ with drops of MeOD, 500 MHz)
6.70 (1H, *s*, H-3)	6.43 (1H, *s*, H-3)
13.00 (1H, *s*, 5-OH)	–
6.28 (1H, *d*, *J* = 2.00 Hz, H-6)	6.15 (1H, *d*, *J* = 2.0 Hz, H-6)
6.58 (1H, *d*, *J* = 2.00 Hz, H-8)	6.32 (1H, *d*, *J* = 2.0 Hz, H-8)
8.05 (2H, *d*, *J* = 9.20 Hz, H-2′/H-6′)	7.72 (2H, *d*, *J* = 9.0 Hz, H-2′/H-6′)
7.15 (2H, *d*, *J* = 9.20 Hz, H-3′/H-5′)	6.89 (2H, *d*, *J* = 9.0 Hz, H-3′/H-5′)
3.93 (3H, *s*, 4′-OCH_3)	3.76 (3H, *s*, 4′-OCH_3)

Table 22: The ^{13}C-NMR data (δ_{ppm}) of compound **120**.

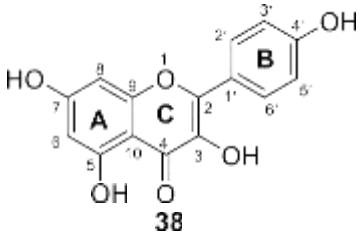
C	**120** (Acetone-d_6, 100 MHz)	Lit.[109] ($CDCl_3$ with drops of MeOD, 125 MHz)
2	164.19	164.0
3	103.67	103.6
4	182.20	182.3
5	162.48	161.4
6	98.90	99.13
7	163.90	163.9
8	93.90	94.1
9	157.94	157.8
10	104.45	104.4
1′	123.48	123.3
2′	128.18	127.9
3′	114.51	114.3
4′	162.84	162.5
OCH_3–4′	55.09	55.3
5′	114.51	114.3
6′	128.18	127.9

The ^{13}C- and DEPT-135 NMR spectra (Appendix 52 and Appendix 53) of **120** showed the presence of 16 carbon signals, which correspond to eight quaternary of which five are oxygenated and one is a conjugated carbonyl, seven methine and one methoxy group. In the ^{1}H-NMR spectrum (Table 21), the two aromatic *meta*-coupled doublets at δ 6.28 (1H, *d*, *J* = 2.00 Hz,) and 6.58 (1H, *d*, *J* = 2.00 Hz,) are assigned to H-6 and H-8 of ring A. The down-field signal at δ 13.00 (1H, *s*) indicated the presence of an intramolecular hydrogen bonded OH group at C-5. The doublets at δ 8.05 (2H, *J* = 9.20 Hz) and 7.15 (2H, *J* = 9.20 Hz), which appeared as a set of AA′XX′ spin system,[110] are assigned to H-2′/H-6′ and H-3′/H-5′, respectively, of the 4′-substituted B-ring. The remaining two singlets at δ 6.70 (1H) and 3.93 (3H) are assigned to the methine proton at C-3 and the methoxy group at C-4′. Comparison of the UV-Vis spectrum of compound **120** (Appendix 55) with those reported in the literature for the C-4′-methoxyflavone (acacetin)[111] and the C-5-methoxyflavone (genkwanin)[112] were used to establish the position of the methoxy group at C-4′. The structure of compound **120** is therefore determined to be 5,7-dihydroxy-4′-methoxyflavone (acacetin, Figure 16) which is reported herein for the first time from a *Rhus* species. Comparison of the spectroscopic data of **120** with those reported for acacetin in the literature revealed a close agreement.[109]

Acacetin (**120**) was previously reported from various plant species, including *Carthamus tinctorius*, *Tanacetum sinaicum*, *Chrozophora tinctoria*, *Wissadula periplocifolia*, *Agastache mexicana* and *Turnera diffusa*.[113] Acacetin possesses diverse biological activities, including neuroprotective, cardioprotective, anti-ageing, anticancer, antimicrobial, anti-viral, anti-inflammatory, anti-oxidant, antimalarial and antidiabetic activities.[113] It also exhibited inhibitory effect towards enzymes, including monoamine

oxidase B, human topoisomerase-I, glutathione reductase, cyclo-oxygenase (COX) I/II, acetylcholinesterase, aromatase, aldose reductase and xanthine oxidase.[113]

3.4.3.3. Characterization of Compound 38



38

Compound **38** was obtained as yellow amorphous powder. Its HRESIMS spectrum (Appendix 62) showed a molecular ion peak $[M+H]^+$ at *m/z* 287.0557 corresponding to the molecular formula $C_{15}H_{10}O_6$. The UV-Vis spectrum of **38** (Appendix 61) showed λ_{max} at 266 and 366 nm, which together with the ^{1}H- (Appendix 57) and ^{13}C-NMR (Appendix 58) spectra suggested the presence of a flavonol structure with hydroxy substituents at C-4′ and C-5 positions.[108] The IR spectrum (Appendix 60) showed absorption bands corresponding to hydroxy (3326 cm^{-1}), double bond (1607 cm^{-1}) and carbonyl (1658 cm^{-1}) groups.

A total of fifteen carbon signals were observed in the ^{13}C-NMR spectrum of **38** (Appendix 58) which were assigned with the help of the DEPT-135 NMR spectrum (Appendix 59) to six aromatic methines, six aromatic and two olefinic quaternary carbons, and a carbonyl carbon. The ^{1}H-NMR spectrum of **38** (Table 23 and Appendix 57) showed signals corresponding to *meta*-coupled aromatic protons at δ 6.29 (1H, *d*, *J* = 1.60 Hz,) and 6.56 (1H, *d*, *J* = 1.60 Hz,) which are attributed to H-6 and H-8 of ring A, respectively. The spectrum also showed two-proton doublets at δ 8.18 (*J* = 8.80 Hz,) and 7.04 (*J* = 8.80 Hz) that appeared as a set of AA′XX′ spin system[110] corresponding to the four aromatic protons,

H-2′/H-6′ and H-3′/H-5′ in ring B, characteristic of a 4′-substituted flavone. Compound **38** (Figure 16) was identified as 3,5,7,4′-tetrahydroxyflavone based on the above spectroscopic data. Comparison of the NMR data of **38** with those reported in the literature[114] for kaempferol revealed a very close agreement (Table 23 and Table 24). Kaempferol is a well-known flavonol which was isolated from various plants[114] including the EtOAc extract of a *Rhus* species, *R. wallichi*.[115]

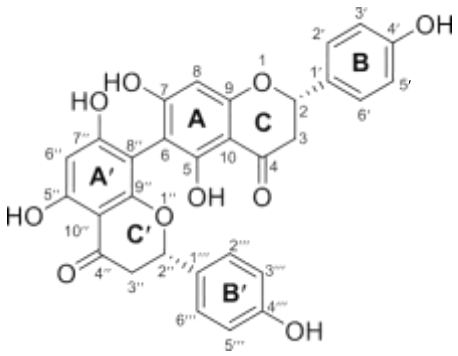
Table 23: The ^{1}H-NMR data (δ_{ppm}) of compound **38**.

38 (Acetone-d_6, 400 MHz)	Lit.[114] (Acetone-d_6, 400 MHz)
12.21 (1H, *s*, 5-OH)	–
6.29 (1H, *d*, *J* = 1.60 Hz, H-6)	6.27 (1H, *d*, *J* = 2.0 Hz, H-6)
6.56 (1H, *d*, *J* = 1.60 Hz, H-8)	6.54 (1H, *d*, *J* = 2.0 Hz, H-8)
8.18 (2H, *d*, *J* = 8.80 Hz, H-2′/H-6′)	8.16 (2H, *d*, *J* = 8.8 Hz, H-2′/H-6′)
7.04 (2H, *d*, *J* = 8.80 Hz, H-3′/H-5′)	7.03 (2H, *d*, *J* = 8.8 Hz, H-3′/H-5′)

Table 24: The ^{13}C-NMR data (δ_{ppm}) of compound **38**.

C	**38** (Acetone-d_6, 100 MHz)	Lit.[114] (Acetone-d_6, 100 MHz)
2	146.13	146.9
3	135.76	136.5
4	175.73	176.5
5	156.91	157.7
6	98.27	98.9
7	164.10	165.0
8	93.61	94.3
9	159.28	160.1
10	103.27	103.9
1′	122.45	123.1
2′	129.58	130.3
3′	115.45	116.1
4′	161.45	161.9
5′	115.45	116.1
6′	129.58	130.3

3.4.3.4. Characterization of Compound 121



121

Compound **121** was isolated as a yellow amorphous powder with m. p. 203.5 – 205.3 °C. The positive ion HRESIMS of **121** (Appendix 68) gave a protonated molecular ion peak $[M+H]^+$ at *m/z* 543.1287 which is compatible with the molecular formula $C_{30}H_{22}O_{10}$. The UV absorption maxima at 224 and 296 nm, in the UV-Vis spectrum of **121** (Appendix 67) indicated the presence of a flavanone skeleton,[108] while the infrared spectrum (Appendix 66) confirmed the presence of hydroxy (3430 cm^{-1}), aromatic (1401 cm^{-1}) and carbonyl (1635 cm^{-1}) functionalities.

The ^{13}C-NMR spectrum of **121** (Appendix 64) showed a total of 26 carbon resonances. The DEPT-135 NMR spectrum (Appendix 65) revealed that six of the signals are due to oxygenated quaternary aromatic carbon atoms and fourteen correspond to aromatic methine carbon atoms with four sets of equivalent carbons. The remaining carbon signals can be attributed to two carbonyl carbons, two aliphatic methylene and two oxygenated methine carbon atoms.

The ^{1}H-NMR spectrum of **121** (Table 25 and Appendix 63) indicated the presence of ten aromatic and six chromanone ring protons. This in combination with the ^{13}C-NMR and

HRESIMS data suggested that **121** is composed of two flavanone units joined by a C–C linkage. The absence of *meta*-coupled protons in the ^{1}H-NMR spectrum suggested interflavanonyl linkage between rings A and A′.[116] The ^{1}H-NMR spectrum also exhibited two sets of AA′XX′ spin system[110] at δ 7.35 (H-2′/H-6′) and 6.83 (H-3′/H-5′) in ring B and 7.20 (H-2‴/H-6‴) and 6.74 (H-3‴/H-5‴) in ring B′, respectively. Furthermore, the ^{1}H-NMR spectrum showed two aromatic proton singlets at δ 6.03 and 6.05 attributed to H-8 and H-6″, respectively. The above spectral evidence suggests the structure of **121** is unsymmetrical and composed of two naringenin units joined by an interflavanonyl linkage between C6 and C8″. Therefore, **121** is assigned the structure of 6-8″-binaringenin (rhusflavanone, Figure 16). Comparison of the above spectral data and specific rotation of **121** with those reported in the literature[74h,74i] for rhusflavanone revealed a very close resemblance. Rhusflavanone (**121**) was first isolated from the ethanol extract of the seed kernels of *R. succedanea*.[74a,116]

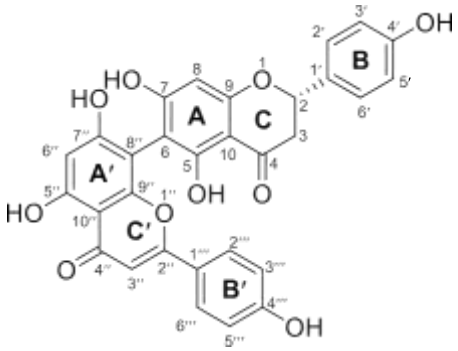
Table 25: The ^{1}H-NMR data (δ_{ppm}) of compound **121**.

121 (MeOD-d_4, 400 MHz)	Lit.[74h,74i] (MeOD-d_4, 400 MHz)
5.37 (1H, *m*, H-2)	5.31 (1H, *dd*, *J* = 12.7, 2.8 Hz, H-2)
3.11 (1H, *m*, H-3)	3.04 (1H, *m*, H-3)
2.73 (1H, *m*, H-3)	2.68 (1H, *m*, H-3)
6.03 (1H, *s*, H-8)	6.14 (1H, *s*, H-8)
7.35 (2H, *d*, *J* = 8.40 Hz, H-2′/H-6′)	7.57 (2H, br. *d*, *J* = 8.8 Hz, H-2′/H-6′)
6.83 (2H, *d*, *J* = 8.40 Hz, H-3′/H-5′)	6.79 (2H, br. *d*, *J* = 8.8 Hz, H-3′/H-5′)
5.37 (1H, *m*, H-2″)	5.37 (1H, *dd*, *J* = 12.7, 2.8 Hz, H-2″)
3.11 (1H, *m*, H-3″)	3.04 (1H, *m*, H-3″)
2.73 (1H, *m*, H-3″)	2.68 (1H, *m*, H-3″)
6.05 (1H, *s*, H-6″)	6.28 (1H, *s*, H-6″)
7.20 (2H, *d*, *J* = 8.40 Hz, H-2‴/H-6‴)	7.01 (2H, *br. d*, *J* = 8.8 Hz, H-2‴/H-6‴)
6.74 (2H, *d*, *J* = 8.40 Hz, H-3‴/H-5‴)	6.58 (2H, *br. d*, *J* = 8.8 Hz, H-3‴/H-5‴)

Table 26: The ^{13}C-NMR data (δ_{ppm}) of compound **121**.

C	**121** (MeOD-d_4, 100 MHz)	Lit.[74h,74i] (MeOD-d_4, 100 MHz)
2	79.15	80.00
3	42.77	44.12
4	196.88	198.20
5	157.14	156.92
6	99.91	100.79
7	165.54	166.70
8	94.41	96.83
9	165.51	165.12
10	101.89	103.79
1′	130.07	130.93
2′	127.68	129.28
3′	114.92	116.88
4′	161.41	162.24
5′	114.92	116.88
6′	127.68	129.28
2″	78.48	79.87
3″	42.49	43.87
4″	196.51	197.91
5″	161.89	162.60
6″	95.38	99.73
7″	163.39	163.94
8″	101.09	100.90
9″	162.69	162.64
10″	102.24	105.43
1‴	129.86	130.93
2‴	127.14	128.52
3‴	114.77	116.16
4‴	157.59	158.57
5‴	114.77	116.16
6‴	127.14	128.52

3.4.3.5. Characterization of Compound 122



122

Compound **122** was obtained as a light-yellow powder with m. p. 238.9 – 240.1 °C. The positive ion HRESIMS of **122** (Appendix 77) showed a molecular ion peak $[M+H]^+$ at *m/z* 541.1135 corresponding to the molecular formula $C_{30}H_{20}O_{10}$. The UV-Vis spectrum of **122** in MeOH (Appendix 76) exhibited four absorption maxima at 228, 276, 297, and 333 nm characteristic of a flavonoid.[108] The IR spectrum (Appendix 75) exhibited a broad OH absorption band at 3419 cm^{-1} and two intramolecular hydrogen bonded carbonyl bands at 1638 and 1610 cm^{-1}, together with the ^{13}C-NMR resonances, at δ_C 196.67 and 182.60 for two carbonyl groups, indicated the presence of a 5-hydroxyflavone and a 5-hydroxyflavanone nucleus in **122**.[117]

The NMR spectra of **122** (Table 27 and Table 28) together with its HRESIMS, UV, and IR spectra suggested that it is composed of a flavanone and a flavone units joined by a C–C linkage. As in that of **121**, the ^{1}H-NMR spectrum of **122** (Table 27 and Appendix 69) did not show *meta*-coupled proton resonances suggesting a linkage between rings A and A′ of the flavanone and flavone units, respectively. The ^{1}H-NMR spectrum also revealed two sets of AA′XX′ spin system[110] at δ 7.45 (H-2′/H-6′) and 6.95 (H-3′/H-5′), attributed to ring B, and 7.68 (H-2‴/H-6‴) and 6.92 (H-3‴/H-5‴) attributed to ring B′.

The two downfield shifted resonances at δ 13.11 (*s*) and 12.64 (*s*) indicated the presence of two hydrogen-bonded hydroxy groups at C-5″ and C-5. This was supported by the HMBC correlation (Appendix 74) of the proton signal at δ_H 13.11 with the C-5″ resonance at δ_C 161.82. The three doublet of doublets at δ_H 5.55 (1H, *J* = 12.80, 3.00 Hz), 3.33 (1H, *J* = 17.00, 12.80 Hz) and 2.83 (1H, *J* = 17.00, 3.00 Hz) were assigned to H-2 and the geminal protons at C-3 of the flavanone unit based on the HSQC spectrum of **122** (Appendix 73). The magnitude of the coupling constant between H-2 and H-3 (12.80, 3.00 Hz) suggested that H-2 is axial and therefore the configuration of ring B is equatorial.[118] The HSQC spectrum also indicated that the remaining three aromatic singlets at δ_H 6.66, 6.42 and 6.23 can be attributed to H-3" and H-6" of the flavone unit and H-8 of the flavanone unit, respectively.

Table 27: The ^{1}H-NMR data (δ_{ppm}) of compound **122**.

122 (Acetone-d_6, 400 MHz)	Lit.[74h,74i] (MeOD-d_4, 400 MHz)
5.55 (1H, *dd*, *J* = 12.80, 3.00 Hz, H-2)	5.35 (1H, *dd*, *J* = 12.4, 2.4 Hz, H-2)
3.33 (1H, *dd*, *J* = 17.00, 12.80 Hz, H-3)	3.17 (1H, *m*, H-3)
2.83 (1H, *dd*, *J* = 17.00, 3.00 Hz, H-3)	2.74 (1H, *m*, H-3)
12.64 (1H, *s*, 5-OH)	–
6.23 (1H, *s*, H-8)	6.15 (1H, *s*, H-8)
7.45 (2H, *d*, *J* = 8.80 Hz, H-2′/H-6′)	7.35 (2H, br. *d*, *J* = 8.4 Hz, H-2′/H-6′)
6.95 (2H, *d*, *J* = 8.80 Hz, H-3′/H-5′)	6.83 (2H, br. *d*, *J* = 8.4 Hz, H-3′/H-5′)
6.66 (1H, *s*, H-3″)	6.54 (1H, *s*, H-3″)
13.11 (1H, *s*, 5″-OH)	–
6.42 (1H, *s*, H-6″)	6.35 (1H, *s*, H-6″)
7.68 (2H, *d*, *J* = 8.80 Hz, H-2‴/H-6‴)	7.52 (2H, br. *d*, *J* = 8.4 Hz, H-2‴/H-6‴)
6.92 (2H, *d*, *J* = 8.80 Hz, H-3‴/H-5‴)	6.76 (2H, br. *d*, *J* = 8.4 Hz, H-3‴/H-5‴)

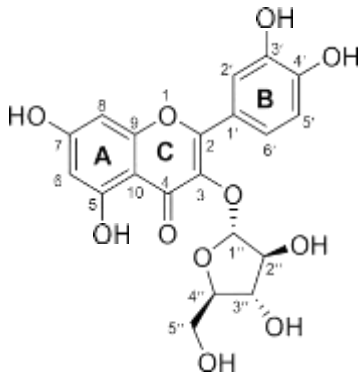
The only significant differences in the ^{13}C-NMR spectra of **122** (Appendix 70) and **121** (Appendix 64) are the upfield shift of the C-4″ resonance to δ_C 182.20 (δ_C 196.51 in **121**)

and the downfield shift of the signal due to C-2″ to δ_C 164.13 (δ_C 78.48 in **121**) and that of C-3″ to δ_C 102.90 (δ_C 42.49 in **121**) suggesting the presence of one flavanone and one flavone units in **122** compared to two flavanone units in **121**. The structure of **122** was then determined to be 6-8″-naringeninyl apigenin (rhusflavone, Figure 16).[74b] The ^{1}H- and ^{13}C-NMR data of **122** agree very well with those reported for rhusflavone in the literature[74h,74i] as shown in Table 27 and Table 28, respectively. Rhusflavone (**122**) was also isolated from the ethanol extract of the seed kernels of *R. succedanea*.[74b]

Table 28: The ^{13}C-NMR data (δ_{ppm}) of compound **122**.

C	**122** (Acetone-d_6, 100 MHz)	Lit.[74h,74i] (MeOD-d_4, 100 MHz)
2	79.16	80.50
3	42.48	43.95
4	196.53	197.89
5	162.67	163.42
6	102.39	103.22
7	165.02	166.66
8	94.91	95.88
9	163.11	164.32
10	99.86	101.05
1′	129.83	130.91
2′	128.21	129.12
3′	115.35	116.45
4′	157.89	158.78
5′	115.35	116.45
6′	128.21	129.12
2″	164.13	165.85
3″	102.90	103.22
4″	182.60	184.06
5″	161.82	162.38
6″	98.81	99.85
7″	162.78	164.06
8″	98.69	100.45
9″	155.73	156.91
10″	104.66	105.40
1‴	122.54	123.26
2‴	128.25	129.55
3‴	115.95	116.76
4‴	160.92	162.27
5‴	115.95	116.76
6‴	128.25	129.55

3.4.3.6. Characterization of Compound 123



123

Compound **123** was obtained as a yellow powder with m. p. 198.7 – 199.6 °C. The molecular formula $C_{20}H_{18}O_{11}$ was assigned for compound **123** based on its HRESIMS (Appendix 83, $[M + H]^+$ at *m/z* 435.0913) coupled with its ^{1}H- and ^{13}C-NMR data (Table 29 and Table 30). Compound **123** displayed characteristic UV absorption maxima at 257, 299, and 354 nm for a flavone skeleton (Appendix 82).[108] The IR spectrum (Appendix 81) showed absorption bands for hydroxy (3410 cm^{-1}), aromatic (1606 cm^{-1}) and a conjugated carbonyl (1654 cm^{-1}) groups in agreement with a flavone moiety in the structure of **123**.

Detailed examination of the NMR data of **123** together with its UV-Vis and IR spectra indicated that it belongs to flavone glycoside class of compounds. The ^{13}C-NMR spectrum (Appendix 79) showed carbon resonances for both the flavone (15 carbons) and pentose (5 carbons) moieties. In addition, the HRESIMS spectrum of compound **123** showed a significant fragment ion peak at *m/z* 303.0494 [M − 132.0419 (pentose unit) + H]$^+$ supporting the presence of a monosaccharide in compound **123**.

The presence of a quercetin (**1**) moiety[119] was determined by careful examination of the ^{1}H-NMR spectrum of **123** (Table 29). The observation of two *meta*-coupled proton resonances at δ 6.23 (*d*, *J* = 2.00 Hz, H-6) and 6.42 (*d*, *J* = 2.00 Hz, H-8) indicated ring A is 5,7-disubstituted. The ^{1}H-NMR spectrum also exhibited a characteristic resonance of an ABX spin system[120] for ring B protons at δ 7.55 (*d*, *J* = 2.00 Hz, H-2′), 7.52 (*dd*, *J* = 8.40, 2.00 Hz, H-6′) and 6.92 (*d*, *J* = 8.40 Hz, H-5′) suggesting a 3′,4′-disubstituted ring B.

Table 29: The ^{1}H-NMR data (δ_{ppm}) of compound **123**.

123 (MeOD-d_4, 400 MHz)	Lit.[121] (MeOD-d_4, 500 MHz)
6.23 (1H, *d*, *J* = 2.00 Hz, H-6)	6.20 (1H, *d*, *J* = 2.0 Hz, H-6)
6.42 (1H, *d*, *J* = 2.00 Hz, H-8)	6.39 (1H, *d*, *J* = 2.0 Hz, H-8)
7.55 (1H, *d*, *J* = 2.00 Hz, H-2′)	7.52 (1H, *d*, *J* = 2.0 Hz, H-2′)
6.92 (1H, *d*, *J* = 8.40 Hz, H-5′)	6.90 (1H, *d*, *J* = 8.3 Hz, H-5′)
7.52 (1H, *dd*, *J* = 8.40, 2.00 Hz, H-6′)	7.48 (1H, *dd*, *J* = 2.0, 8.3 Hz, H-6′)
5.49 (1H, br. *s*, H-1″)	5.46 (1H, br. *s*, H-1″)
4.35 (1H, *dd*, *J* = 3.00, 1.00 Hz, H-2″)	4.32 (1H, br. *d*, *J* = 2.9 Hz, H-2″)
3.93 (1H, *dd*, *J* = 5.20, 3.20 Hz, H-3″)	3.90 (1H, *dd*, *J* = 2.9, 4.9 Hz, H-3″)
3.88 (1H, *q*, *J* = 4.50 Hz, H-4″)	3.86 (1H, br. *q*, *J* = 4.9 Hz, H-4″)
3.52 (2H, *dd*, *J* = 4.20, 2.20 Hz, H-5″)	3.51 (1H, *dd*, *J* = 3.4, 11.7 Hz, H-5″) 3.48 (1H, *dd*, *J* = 4.4, 11.7 Hz, H-5″)

The presence of quercetin-3-*O*-glycosidic linkage was determined from the corresponding anomeric proton signal at δ 5.49 (br. *s*, 1H) as well as the ^{13}C-NMR spectrum. The position of glycosylation was established from the ^{13}C-NMR chemical shifts of **123** in comparison with the corresponding carbon resonances of the aglycone quercetin (**1**). Thus, the signals due to C-2, C-4, C-5 and C-10 showed downfield shifts by 10.49, 2.91, 0.29 and 1.0 ppm, respectively, while the signal corresponding to C-3 showed an upfield shift of 2.34 ppm, compared to the corresponding signals in quercetin (**1**, Table 32).[122] The above

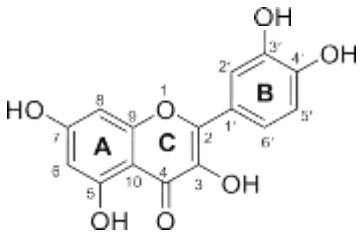
spectroscopic data allowed for the identification of compound **123** as quercetin 3-*O*-*α*-arabinofuranoside (avicularin, Figure 16). Comparison of the NMR spectral data of **123** with those reported in the literature for avicularin[114,121,123] revealed a very close agreement.

Table 30: The ^{13}C-NMR data (δ_{ppm}) of compound **123**.

C	**123** (MeOD-d_4, 100 MHz)	Lit.[121] (MeOD-d_4, 125 MHz)
2	157.95	159.4
3	133.52	134.9
4	178.59	180.0
5	161.70	163.1
6	98.49	99.9
7	164.65	166.0
8	93.36	94.8
9	157.17	158.6
10	104.23	105.6
1′	121.69	123.1
2′	115.44	116.9
3′	144.96	146.4
4′	148.46	149.8
5′	115.04	116.5
6′	121.57	123.0
1″	108.13	109.6
2″	81.91	83.3
3″	77.29	78.7
4″	86.61	88.0
5″	61.13	62.6

Avicularin (**123**) was previously isolated from the butanol extract of the aerial parts of *Polygonum equisetiforme*,[123] the MeOH extract of the leaves of *Psidium guajava*[121] and the ethanol extract of *Rosa rugosa*[114]. However, this is the first report of avicularin from a *Rhus* species.

3.4.3.7. Characterization of Compound 1



1

Compound **1** was obtained as a yellow powder and had a melting point of 309.0 – 310.0 °C. The positive ion HRESIMS of **1** (Appendix 89) exhibited a molecular ion peak $[M+H]^+$ at *m/z* 303.0503 in accordance with the molecular formula $C_{15}H_{10}O_7$. Comparison of the HRESIMS spectra of **1** (Appendix 89) and **123** (Appendix 83) indicated that **1** ($[M+H]^+$ at *m/z* 303.0503) has a similar mass spectral fragmentation pattern with the aglycon part of **123** (*m/z* 303.0494 $[M - 132.0419 + H]^+$). The UV-Vis spectrum (Appendix 88, λ_{max}, 255 and 371 nm) also suggested **1** to be a flavonol with an unsubstituted 3-hydroxy group.[108] In addition, the IR spectrum of **1** (Appendix 87) revealed the presence of a hydroxy (3410 cm^{-1}), carbonyl (1656) and aromatic (1616 cm^{-1}) functionalities in agreement with a flavonol skeleton.

The NMR data of **1** (Table 31 and Table 32) is very similar to that of **123** (Table 29 and Table 30) except that **1** lacks the signals due to the arabinose moiety in the spectrum of **123**. The ^{13}C-NMR spectrum of **1** (Appendix 85) showed the presence of 15 carbon signals of which one is due to a conjugated carbonyl (δ 175.68), 12 are due to aromatic carbons (six quaternary carbons with five being oxygenated at δ 103.23, 164.14, 161.41, 156.87, 146.08, 144.98, and six methines at δ 122.85, 120.55, 115.36, 114.89, 98.27, 93.57) and

the remaining two carbon resonances correspond to oxygenated olefinic carbons (δ 147.49 and 135.86).

Table 31: The ^{1}H-NMR data (δ_{ppm}) of compound **1**.

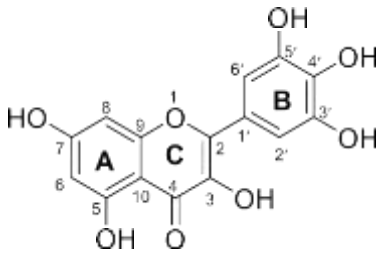
1 (Acetone-d_6, 400 MHz)	Lit.[119] (DMSO-d_6, 500 MHz)
12.20 (1H, *s*, 5-OH)	12.48 (1H, *s*, 5-OH)
6.28 (1H, *d*, *J* = 2.00 Hz, H-6)	6.17 (1H, *d*, *J* = 2.0 Hz, H-6)
6.54 (1H, *d*, *J* = 2.00 Hz, H-8)	6.39 (1H, *d*, *J* = 2.0 Hz, H-8)
7.84 (1H, *d*, *J* = 2.20 Hz, H-2′)	7.66 (1H, *d*, *J* = 2.0 Hz, H-2′)
7.01 (1H, *d*, *J* = 8.50 Hz, H-5′)	6.87 (1H, *d*, *J* = 8.5 Hz, H-5′)
7.71 (1H, *dd*, *J* = 8.50, 2.20 Hz, H-6′)	7.53 (1H, *dd*, *J* = 2.0, 8.0 Hz, H-6′)

The ABX spin system[120] in the aromatic region of the ^{1}H-NMR spectrum of compound **1** (Table 31) at δ 7.84 (1H, *d*, *J* = 2.20 Hz, H-2′), 7.71 (1H, *dd*, *J* = 8.50, 2.20 Hz, H-6′) and 7.01 (1H, *d*, *J* = 8.50 Hz, H-5′) suggested a 3′,4′-disubstituted ring B. The two *meta*-coupled proton resonances at δ 6.28 (1H, *d*, *J* = 2.00 Hz, H-6) and 6.54 (1H, *d*, *J* = 2.00 Hz, H-8), were also observed in the ^{1}H-NMR spectrum of **1** which suggested that ring A is 5,7-disubstituted. The downfield signal at δ 12.20 (1H, *s*) is assigned to the chelated OH group at C-5. Based on the above spectral data and comparison with the data reported in the literature, the structure of **1** was identified as 3,5,7,3′,4′-pentahydroxyflavone (quercetin, Figure 16).[119]Quercetin (**1**) is a well-known natural product which has many beneficial health effects such as antiviral, anti-inflammatory, antibacterial, antioxidant and muscle-relaxing properties. Furthermore, it improves normal cell survival and prevents tumor proliferation.[124] Quercetin (**1**) was previously isolated from the EtOAc extract of *R. wallichi*.[115]

Table 32: The ^{13}C-NMR data (δ_{ppm}) of compound **1**.

C	**1** (Acetone-d_6, 100 MHz)	Lit.[119] (DMSO-d_6, 125 MHz)
2	147.49	147.9
3	135.86	135.9
4	175.68	176.0
5	161.41	160.9
6	98.27	98.4
7	164.14	164.1
8	93.57	93.8
9	156.87	156.3
10	103.23	103.2
1′	122.85	122.1
2′	114.89	115.2
3′	144.98	145.2
4′	146.08	147.0
5′	115.36	115.8
6′	120.55	120.2

3.4.3.8. Characterization of Compound 2



2

Compound **2** was obtained as a light-yellow powder and had a melting point of 320.2 – 321.9 °C. The positive ion HRESIMS of **2** (Appendix 95) gave a molecular ion peak $[M+H]^+$ at *m/z* 319.0458, which is 16 mass units higher than that of compound **1** ($[M+H]^+$ at *m/z* 303.0503). The molecular formula $C_{15}H_{10}O_8$ was then deduced for compound **2**. On the basis of IR (Appendix 93, 3392, 1660, 1610 cm^{-1}) and UV-Vis (Appendix 94, λ_{max}, 254, 305 and 374 nm) spectral data of compound **2** and in comparison with the spectral data of **1**, the presence of a 3,5,7,3',4',5'-hexahydroxyl flavone system was suggested.[108]

The only difference between the ^{1}H-NMR spectra of **2** (Table 33 and Appendix 90) and **1** (Table 31 and Appendix 84) is the absence of the ABX spin system[120] corresponding to ring B proton resonances in the spectrum of **2**. Instead, the spectrum of **2** displayed a two-proton singlet at δ 7.44 (H-2′/H-6′) suggesting ring B is 3′,4′,5′-trisubstituted. Like that of **1**, the ^{1}H-NMR spectrum of **2** displayed *meta*-coupled proton signals at δ 6.27 (*d, J* = 2.00 Hz, H-6) and 6.53 (*d, J* = 2.00 Hz, H-8) due to the 5,7-dihydroxy substituted A ring. The signal due to the intramolecular hydrogen bonded OH group at C-5 is also observed at δ 12.18 (1H, *s*).

The ^{13}C-NMR spectrum of **2** (Table 34 and Appendix 91) showed 15 carbon resonances. In conjunction with the DEPT-135 NMR spectrum (Appendix 92), the signals were attributed to one conjugated carbonyl carbon [δ 175.63 (C-4)], six oxygenated quaternary aromatic carbons [δ 164.09 (C-2), 161.41 (C-9), 156.83 (C-5), 145.52 (C-3′/5′) and 136.02 (C-4′)], four aromatic methine carbons [δ 107.42 (C-2′/6′), 98.24 (C-6) and 93.51 (C-8)], two aromatic quaternary carbons [δ 121.86 (C-1′) and 103.22 (C-10)] and two oxygenated olefinic quaternary carbon atoms [δ 146.07 (C-2) and 135.53 (C-3)]. Based on the above spectral data compound **2** was identified as 3,5,7,3′,4′,5′-hexahydroxyflavone (myricetin, Figure 16). The NMR data of **2** agreed very well with those reported in the literature[125] for myricetin which was previously isolated from the MeOH extracts of the flowers of *Rhododendron mucronulatum*[125] and the EtOAc extract of *R. wallichi*.[115]

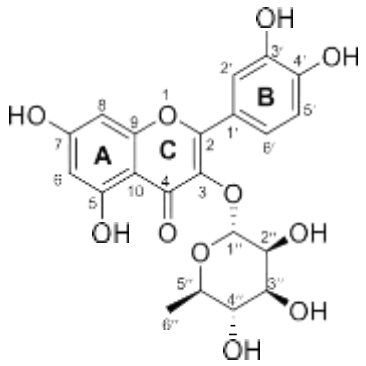
Table 33: The ^{1}H-NMR data (δ_{ppm}) of compound **2**.

2 (Acetone-d_6, 400 MHz)	Lit.[125] (MeOD-d_4, 500 MHz)
12.18 (1H, *s*, 5-OH)	–
6.27 (1H, *d*, *J* = 2.00 Hz, H-6)	6.18 (1H, *d*, *J* = 1.7 Hz, H-6)
6.53 (1H, *d*, *J* = 2.00 Hz, H-8)	6.37 (1H, *d*, *J* = 1.8 Hz, H-8)
7.44 (2H, *s*, H-2′/H-6′)	7.35 (2H, *s*, H-2′/H-6′)

Table 34: The ^{13}C-NMR data (δ_{ppm}) of compound **2**.

C	**2** (Acetone-d_6, 100 MHz)	Lit.[125] (MeOD-d_4, 125 MHz)
2	146.07	148.3
3	135.53	137.2
4	175.63	177.5
5	156.83	158.4
6	98.24	99.5
7	164.09	165.8
8	93.51	94.7
9	161.41	162.7
10	103.22	104.8
1′	121.86	123.4
2′	107.42	108.8
3′	145.52	147.0
4′	136.02	137.6
5′	145.52	147.0
6′	107.42	108.8

5.4.3.9. Characterization of Compound 124



124

Compound **124** (m. p. 237.8 – 240.2 °C) was obtained as a yellow amorphous powder. It showed a molecular ion peak $[M+H]^+$ at *m/z* 449.1077 in its HRESIMS corresponding to the molecular formula $C_{21}H_{20}O_{11}$ (Appendix 101). The spectrum also revealed a prominent fragment ion peak at *m/z* 303.0500 [M − 146.0577 (methyl pentose unit) + H]$^+$ indicating that compound **124** is a flavonol monosaccharide. The IR spectrum of **124** (Appendix 99) showed absorption bands corresponding to hydroxy (3411 cm^{-1}), carbonyl (1655 cm^{-1}), conjugated diene (1608 cm^{-1}) and phenyl (1500 cm^{-1}) moieties. The UV-Vis spectrum (Appendix 100) exhibited the characteristic absorption bands for a flavonol.[108]

In the ^{1}H-NMR spectrum of **124** (Table 35 and Appendix 96), two *meta*-coupled doublets of a 5,7-dihydroxylated A ring system appeared at δ 6.22 (*J* = 2.00 Hz, H-6) and 6.39 (*J* = 2.00 Hz, H-8). The ABX spin system[120] due to three aromatic protons at δ 7.36 (*d*, *J* = 2.00 Hz, H-2′), 7.33 (*dd*, *J* = 8.40, 2.00 Hz, H-6′) and 6.93 (*d*, *J* = 8.40 Hz, H-5′) can be attributed to the 3′,4′-dihydroxylated B ring in a flavonol skeleton. The ^{1}H-NMR spectrum clearly showed that the aglycone of compound **124** is quercetin (**1,** Figure 16).[119] The spectrum further showed characteristic signals due to a rhamonpyranose moiety. The fact that

compound **124** is a 3-*O*-substituted quercetin rhamnopyranoside was indicated by the downfield shifts of the signals due to C-2, C-4, C-5 and C-10 by 9.65, 2.58, 0.42 and 1.28 ppm, respectively, and the upfield shift of the signal due to C-3 by 1.01 ppm in the ^{13}C-NMR spectrum of **124** (Table 36) compared to the corresponding signals in the spectrum of the aglycone, quercetin (**1**, Table 32).[122,126] Compound **124** was then characterized as quercetin-3-*O*-α-rhamnopyranoside (quercitrin, Figure 16) based on the above spectroscopic data. Comparison of the NMR spectral data of **124** with those reported in the literature[125] for quercitrin revealed a close agreement.

Table 35: The ^{1}H-NMR data (δ_{ppm}) of compound **124**.

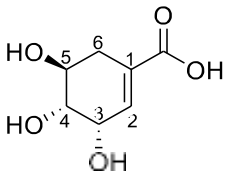
124 (MeOD-d_4, 400 MHz)	Lit.[125] (MeOD-d_4, 500 MHz)
6.22 (1H, *d*, *J* = 2.00 Hz, H-6)	6.22 (1H, *d*, *J* = 1.7 Hz, H-6)
6.39 (1H, *d*, *J* = 2.00 Hz, H-8)	6.38 (1H, *d*, *J* = 1.7 Hz, H-8)
6.93 (1H, *d*, *J* = 8.40 Hz, H-5′)	6.94 (1H, *d*, *J* = 8.3 Hz, H-5′)
7.33 (1H, *dd*, *J* = 8.40, 2.00 Hz, H-6′)	7.34 (1H, *dd*, *J* = 1.9, 8.3 Hz, H-6′)
5.37 (1H, *d*, *J* = 1.60 Hz, H-1″)	5.39 (1H, *d*, *J* = 1.7 Hz, H-1″)
4.24 (1H, *dd*, *J* = 1.60, 3.20 Hz, H-2″)	4.26 (1H, *dd*, *J* = 1.7, 3.2 Hz, H-2″)
3.77 (1H, *dd*, *J* = 3.40, 9.40 Hz, H-3″)	3.75 (1H, *dd*, *J* = 3.2, 9.3 Hz, H-3″)
3.41 (1H, *m*, H-4″)	3.45 – 3.44 (1H, *m*, H-4″)
3.41 (1H, *m*, H-5″)	3.39 – 3.35 (1H, *m*, H-5″)
0.96 (3H, *d*, *J* = 6.40 Hz, H-6″)	0.98 (3H, *d*, *J* = 5.9 Hz, H-6″)

Quercitrin (**124**) was previously isolated from the MeOH extracts of the flowers of *Rhododendron mucronulatum*[125] and the fruits of *R. parviflora*.[127]

Table 36: The ^{13}C-NMR data (δ_{ppm}) of compound **124**.

C	**124** (MeOD-d_4, 100 MHz)	Lit.[125] (MeOD-d_4, 125 MHz)
2	157.14	158.1
3	134.85	136.5
4	178.27	179.4
5	161.83	162.9
6	98.42	100.5
7	164.49	165.7
8	93.31	95.4
9	157.92	158.7
10	104.52	106.1
1′	121.60	122.4
2′	114.98	116.7
3′	145.03	146.8
4′	148.40	149.0
5′	115.56	117.2
6′	121.46	122.4
1″	102.16	103.8
2″	70.63	72.3
3″	70.75	72.4
4″	71.88	73.6
5″	70.51	72.0
6″	16.25	18.0

3.4.3.10. Characterization of Compound 125



125

Compound **125** was isolated as a white crystalline powder with m. p. 186.5 – 187.2 °C. The UV-Vis spectrum of **125** (Appendix 106) showed λ_{max} at 355 nm and the IR spectrum (Appendix 105) showed absorption bands for hydroxy (3482 and 3385 cm^{-1}) and conjugated carbonyl (1682 and 1648 cm^{-1}) groups. The molecular formula $C_7H_{10}O_5$ was determined for compound **125** by analysis of its positive ion HRESIMS spectrum (Appendix 107) which showed a molecular ion peak $[M+Na]^+$ at *m*/*z* 197.0422. The ^{13}C-

NMR spectrum of **125** (Appendix 103) showed seven carbon resonances which were assigned with the help of the DEPT-135 NMR spectrum (Appendix 104) to one carboxylic acid group (δ_C 170.15), two olefinic methine carbon atoms (δ_C 129.71 for C-1 and 137.12 for C-2), three oxygenated aliphatic methine carbon atoms (δ_C 65.69 for C-3, 66.51 for C-4, and 70.96 for C-5) and one aliphatic methylene carbo atom (δ_C 30.25 for C-6).

The ^{1}H-NMR spectral data of **125** (Table 37 and Appendix 102) strengthened the information provided by the ^{13}C- and DEPT-135 NMR spectra. Thus, the ^{1}H-NMR clearly showed signals corresponding to one olefinic proton at δ 6.68 (*dt*, *J* = 4.00, 2.00 Hz, H-2), and three oxygen-bearing methine protons at δ 4.30 (*t*, *J* = 4.00 Hz, H-3), 3.63 (*dd*, *J* = 8.20, 4.20 Hz, H-4) and 3.88 (*dt*, *J* = 8.00, 5.80 Hz, H-5). The remaining two signals at δ 2.08 (1H, *ddt*, *J* = 18.20, 6.20, 1.80 Hz) and 2.59 (1H, *ddt*, *J* = 18.20, 5.40, 1.40 Hz) were assigned to the methylene protons at C-6. Compound **125** was identified as 3,4,5-trihydroxycyclohex-1-ene-1-carboxylic acid (shikimic acid, Figure 16) based on the above spectroscopic data and by comparison of these with those reported in the literature[128] for shikimic acid.

Table 37: The ^{1}H-NMR data (δ_{ppm}) of compound **125**.

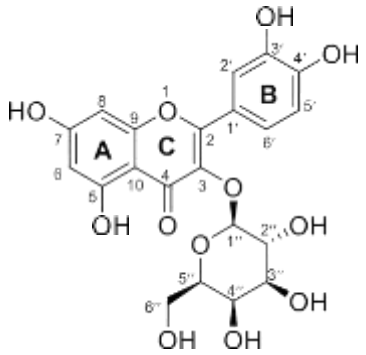
125 (D_2O, 400 MHz)	Lit.[128] (MeOD-d_4, 500 MHz)
6.68 (1H, *dt*, *J* = 4.00, 2.00 Hz, H-2)	6.79 (1H, *dt*, *J* = 3.5, 2.0 Hz, H-2)
4.30 (1H, *t*, *J* = 4.00 Hz, H-3)	4.36 (1H, *ddd*, *J* = 5.5, 4.0, 2.0 Hz, H-3)
3.63 (1H, *dd*, *J* = 8.20, 4.20 Hz, H-4)	3.66 (1H, *dd*, *J* = 7.5, 4.0 Hz, H-4)
3.88 (1H, *dt*, *J* = 8.00, 5.80 Hz, H-5)	3.98 (1H, *dt*, *J* = 7.5, 5.5 Hz, H-5)
2.08 (1H, *ddt*, *J* = 18.20, 6.20, 1.80 Hz, H-5)	2.12 (1H, *ddt*, *J* = 18.5, 5.5, 2.0 Hz, H-5)
2.59 (1H, *ddt*, *J* = 18.20, 5.40, 1.40 Hz, H-6)	2.69 (1H, *ddt*, *J* = 18.5, 5.0, 2.0 Hz, H-6)

Table 38: The ^{13}C-NMR data (δ_{ppm}) of compound **125**.

C	**125** (D_2O, 100 MHz)	Lit.[128] (MeOD-d_4, 125 MHz)
1	129.71	130.8
2	137.12	138.8
3	65.69	67.3
4	66.51	68.4
5	70.96	72.8
6	30.25	31.7
COOH	170.15	170.1

Shikimic acid (**125**) was first isolated in 1885 from *Illicium religiosum*.[129] It is found in a variety of plants and is a metabolite involved in the shikimate pathway responsible for the biosynthesis of aromatic amino acids in plants and microorganisms.[129]

3.4.3.11. Characterization of Compound 126



126

Compound **126** was obtained as a yellow powder with m. p. 232.6 – 233.4 °C. It was shown to possess the molecular formula $C_{21}H_{20}O_{12}$ by HRESIMS (Appendix 113) that revealed a $[M + Na]^+$ ion at *m/z* 487.0861. The IR (Appendix 111) and UV-Vis (Appendix 112) spectra of **126** exhibited characteristic signals for a flavonol skeleton.[108] The fact that compound **126** is a glycoside of quercetin (**1**)[119] was apparent from its ^{1}H-NMR spectrum

(Table 39 and Appendix 108). Thus, two *meta*-coupled proton resonances appeared at δ 6.23 (*d, J* = 2.00 Hz, H-6) and 6.43 (*d, J* = 2.00 Hz, H-8) due to the 5,7-disubstituted A-ring. The ABX spin system[120] due to the three aromatic protons in the 3′,4′-disubstituted B-ring appeared at δ 7.86 (*d, J* = 2.00 Hz, H-2′), 7.61 (*dd, J* = 8.50, 2.00 Hz, H-6′) and 6.89 (*d, J* = 8.60 Hz, H-5′).

The sugar moiety was identified as β-galactose by comparison of the ^{1}H- and ^{13}C-NMR spectral data of **126** with those reported in the literature (Table 39 and Table 40).[121] In addition, the ^{1}H-NMR spectrum showed signals at δ 5.15 (1H, *d, J* = 8.00 Hz), 3.67 (1H, *dd, J* = 6.00, 10.80 Hz) and 3.50 (1H, *m*) due to the anomeric proton and the diastereotopic geminal protons of the CH_2OH group, respectively. The ^{13}C-NMR signals at δ 104.08 and 60.57 are due to the anomeric carbon (C-1″) and the CH_2OH (C-6″), respectively.[122] The coupling constant of the anomeric proton of **126** (*J* = 8.00 Hz) revealed *β*-configuration for the galactose moiety.[103]

The site of glycosylation was confirmed by the downfield shifts of the signals due to C-2, C-4, C-5 and C-10 and the upfield shift of the signal due to C-3 in the ^{13}C-NMR spectrum of **126** as compared to the corresponding signals in the spectrum of the aglycone, quercetin (**1**, Table 32).[122] Compound **126** was identified as quercetin 3-*O*-*β*-galactoside (hyperoside, Figure 16) based on the above spectral data and by comparison of these with the data reported for hyperoside in the literature[121]. Hyperoside (**126**) was previously isolated from the MeOH extract of the leaves of *Psidium guajava*,[121] the EtOAc extract of the leaves of *R. wallichi*[115] and the MeOH extract of the fruits of *R. parviflora*.[127]

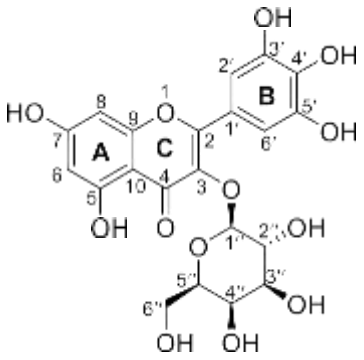
Table 39: The ^{1}H-NMR data (δ_{ppm}) of compound **126**.

126 (MeOD-d_4, 400 MHz)	Lit.[121] (DMSO-d_6, 500 MHz)
6.23 (1H, *d*, *J* = 2.00 Hz, H-6)	6.19 (1H, *d*, *J* = 1.5 Hz, H-6)
6.43 (1H, *d*, *J* = 2.00 Hz, H-8)	6.39 (1H, *d*, *J* = 1.5 Hz, H-8)
7.86 (1H, *d*, *J* = 2.00 Hz, H-2′)	7.52 (1H, *d*, *J* = 2.0 Hz, H-2′)
6.89 (1H, *d*, *J* = 8.60 Hz, H-5′)	6.81 (1H, *d*, *J* = 8.3 Hz, H-5′)
7.61 (1H, *dd*, *J* = 8.50, 2.00 Hz, H-6′)	7.66 (1H, *dd*, *J* = 2.0, 8.3 Hz, H-6′)
5.15 (1H, *d*, *J* = 8.00 Hz, H-1″)	5.36 (1H, *d*, *J* = 7.8 Hz, H-1″)
3.85 (1H, *dd*, *J* = 7.80, 9.40 Hz, H-2″)	3.56 (1H, *dd*, *J* = 7.8, 9.3 Hz, H-2″)
3.58 (1H, *m*, H-3″)	3.36 (1H, *dd*, *J* = 3.4, 9.3 Hz, H-3″)
3.88 (1H, *d*, *J* = 3.20 Hz, H-4″)	3.64 (1H, br. *d*, *J* = 3.4 Hz, H-4″)
3.58 (1H, *m*, H-5″)	3.31 (1H, *m*, H-5″)
3.67 (1H, *dd*, *J* = 6.00, 10.80 Hz, H-6″)	3.45 (1H, *dd*, *J* = 5.4, 10.2 Hz, H-6″)
3.50 (1H, *m*, H-6″)	3.28 (1H, *m*, H-6″)

Table 40: The ^{13}C-NMR data (δ_{ppm}) of compound **126**.

C	**126** (MeOD-d_4, 100 MHz)	Lit.[121] (DMSO-d_6, 125 MHz)
2	157.52	156.4
3	134.44	133.6
4	178.16	177.4
5	161.62	161.0
6	98.57	98.8
7	164.72	164.6
8	93.34	93.6
9	157.08	156.2
10	104.26	103.8
1′	121.61	122.0
2′	114.70	115.2
3′	144.43	144.8
4′	148.57	148.4
5′	116.38	116.0
6′	121.48	121.2
1″	104.08	102.0
2″	71.74	71.2
3″	73.69	73.2
4″	68.66	67.9
5″	75.75	75.8
6″	60.57	60.1

3.4.3.12. Characterization of Compound 127



127

Compound **127** was obtained as a light-yellow amorphous powder and had a melting point of 194.0 – 196.0 °C. The IR spectrum (Appendix 117) showed absorption bands for hydroxy (3326 cm^{-1}), and carbonyl (1650 cm^{-1}) groups and the UV-Vis spectrum (Appendix 118) showed absorption maxima at 257 and 365 nm indicating the presence of a flavone moiety.[108] Compound **127** showed a molecular ion peak $[M+H]^+$ at *m/z* 481.0974 in its HRESIMS (Appendix 119) suggesting the molecular formula $C_{21}H_{20}O_{13}$. The HRESIMS also showed a prominent fragment ion peak at *m/z* 319.0455 [M − 162.0519 (hexose unit) + H]$^+$ indicating compound **127** as a flavonol monosaccharide.

The ^{13}C-NMR coupled with the DEPT-135 NMR spectra of compound **127** (Appendix 115 and Appendix 116) revealed signals for one conjugated carbonyl carbon (δ 178.00 (C-4)), six oxygenated quaternary aromatic carbons (δ 164.76 (C-7), 161.60 (C-5), 156.99 (C-9), 144.99 (C-3′, 5′) and 136.75 (C-4′)), four aromatic methine carbons (δ 108.52 (C-2′, 6′), 98.50 (C-6) and 93.27 (C-8)), two aromatic quaternary carbons (δ 120.27 (C-1′) and 104.17 (C-10)), two oxygenated olefinic quaternary carbons (δ 157.26 (C-2) and 134.58 (C-3)),

and signals due to a sugar moiety (δ 104.14 (C-1″), 75.82 (C-5″), 73.72 (C-3″), 71.88 (C-2″), 68.63 (C-4″), and 60.52 (C-6″)).

The ^{1}H-NMR spectrum of compound **127** revealed the presence of two *meta*-coupled proton resonances at δ 6.22 (*d*, *J* = 2.00 Hz, H-6) and 6.41 (*d*, *J* = 2.00 Hz, H-8) indicating that ring A is 5,7-disubstituted. The two-proton singlet at δ 7.40 (H-2′/H-6′) suggested that ring B is 3′,4′,5′-trisubstituted (Table 41 and Appendix 114). The presence of a myricetin (**2**, Figure 16) moiety was evident from the ^{1}H-NMR spectrum.[125] The spectrum also showed signals between δ 3.90 and 5.22 due to a sugar moiety. Comparison of the NMR data of **127** with literature[130] suggested that **127** is a myricetin-*O*-β-glycoside.

Table 41: The ^{1}H-NMR data (δ_{ppm}) of compound **127**.

127 (MeOD-d_4, 400 MHz)	Lit.[130] (MeOD-d_4, 400 MHz)
6.22 (1H, *d*, *J* = 2.00 Hz, H-6)	6.20 (1H, *d*, *J* = 2.12 Hz, H-6)
6.41 (1H, *d*, *J* = 2.00 Hz, H-8)	6.40 (1H, *d*, *J* = 2.08 Hz, H-8)
7.40 (2H, *s*, H-2′/H-6′)	7.40 (2H, *s*, H-2′/H-6′)
5.22 (1H, *d*, *J* = 7.60 Hz, H-1″)	5.21 (1H, *d*, *J* = 7.8 Hz, H-1″)
3.86 (1H, *dd*, *J* = 9.60, 7.84 Hz, H-2″)	3.84 (1H, *dd*, *J* = 9.6, 7.8 Hz, H-2″)
3.60 (1H, *m*, H-3″)	3.60 (1H, *dd*, *J* = 9.5, 3.2 Hz, H-3″)
3.90 (1H, *d*, *J* = 3.52 Hz, H-4″)	3.89 (1H, *d*, *J* = 3.1 Hz, H-4″)
3.53 (1H, *m*, H-5″)	3.54 (1H, *d*, *J* = 5.8 Hz, H-5″)
3.60 (1H, *m*, H-6″)	3.63 (1H, *m*, H-6″)
3.68 (1H, *dd*, *J* = 11.26, 6.18 Hz, H-6″)	3.67 (1H, *dd*, *J* = 11.1, 6.0 Hz, H-6″)

The downfield shifts of the signals due to C-2, C-4, C-5 and C-10 by 11.19, 2.37, 4.77 and 0.95 ppm, respectively, and the upfield shift of the signal due to C-3 by 0.95 ppm in the ^{13}C-NMR spectrum of **127** as compared to the corresponding signals in the aglycone,

myricetin (**2**, Table 34), were used to establish the site of glycosylation.[122] Compound **127** was therefore identified as myricetin-3-*O*-β-galactopyranoside (Figure 16). Comparison of the NMR spectral data of **127** with those reported for myricetin-3-*O*-β-galactopyranoside in the literature revealed a very close agreement.[130-131] This is the first report of compound **127** from a *Rhus* species. However, compound **127** was previously isolated from *Cistus salviifolius*[130], *Davilla elliptica*[132], *Erica andevalensis*[133], and *Myrtus communis*.[134] It showed antinociceptive[132], antiulcerogenic[133], antioxidant and antigenotoxic activities.[134]

Table 42: The ^{13}C-NMR data (δ_{ppm}) of compound **127**.

C	**127** (MeOD-d_4, 100 MHz)	Lit.[130] (MeOD-d_4, 100 MHz)
2	157.26	157.33
3	134.58	134.62
4	178.00	178.00
5	161.60	161.53
6	98.50	98.51
7	164.78	164.62
8	93.27	93.30
9	156.99	156.96
10	104.17	104.23
1′	120.27	120.33
2′	108.52	108.63
3′	144.99	145.01
4′	136.75	136.74
5′	144.99	145.01
6′	108.52	108.63
1″	104.14	104.23
2″	71.88	71.91
3″	73.72	73.74
4″	68.63	68.66
5″	75.82	75.82
6″	60.52	60.59

Three more flavonoids (**128**, **129**, and **130** (Figure 17)) were also isolated from the EtOAc-soluble fraction of the DCM:MeOH (1:1) extract of the leaves of *R. glutinosa* and were partially characterized only based on their ^{1}H-NMR data due to paucity of material. Elucidation of the structures of the compounds is discussed below.

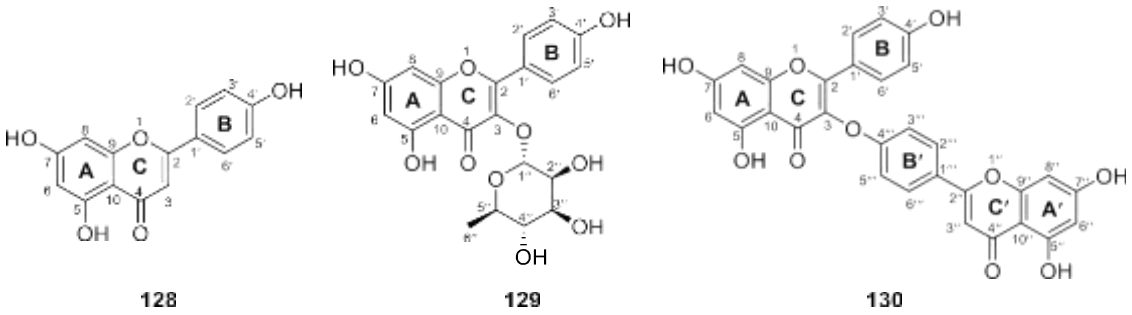


Figure 17: Partially characterized compounds isolated from the leaves of *R. glutinosa*.

Compound **128** was obtained as a yellow amorphous powder. The ^{1}H-NMR spectrum of **128** (Appendix 120) revealed two *meta*-coupled aromatic proton resonances at δ 6.23 (*J* = 2.20 Hz) and 6.56 (*J* = 2.20 Hz) due to H-6 and H-8, respectively. The spectrum also showed a set of AA′XX′ spin system[110] at δ 7.96 (2H, *d*, *J* = 8.00 Hz, H-2′/H-6′) and 7.04 (2H, *d*, *J* = 8.00 Hz, H-3′/H-5′) corresponding to the protons on the 4′-substituted B-ring. The two singlets at δ 6.65 and 13.04 are assigned to the methine proton at C-3 and the intramolecular hydrogen bonded hydroxy group at C-5. The ^{1}H-NMR data of compound **128** (Table 43) is very similar to those of acacetin (**120**, Table 21) except that the spectrum of **128** is devoid of the signal due to a methoxy group suggesting the presence of hydroxy group instead. The structure of compound **128** was therefore determined to be 4′,5,7-trihydroxyflavone (apigenin, Figure 17). Comparison of the ^{1}H-NMR data of **128** with those reported for apigenin in the literature revealed a close agreement.[135] Apigenin was previously isolated from the fruits of *R. typhina*.[136]

Table 43: The ^{1}H-NMR data (δ_{ppm}) of compound **128**.

128 (Acetone-d_6, 400 MHz)	Lit.[135] (DMSO-d_6, 500 MHz)
6.65 (1H, *s*, H-3)	6.78 (1H, *s*, H-3)
13.04 (1H, *s*, 5-OH)	12.97 (1H, *s*, 5-OH)
6.23 (1H, *d*, *J* = 2.20 Hz, H-6)	6.19 (1H, *d*, *J* = 2.0 Hz, H-6)
6.56 (1H, *d*, *J* = 2.20 Hz, H-8)	6.48 (1H, *d*, *J* = 2.0 Hz, H-8)
7.96 (2H, *d*, *J* = 8.00 Hz, H-2′/H-6′)	7.93 (2H, *d*, *J* = 8.8 Hz, H-2′/H-6′)
7.04 (2H, *d*, *J* = 8.00 Hz, H-3′/H-5′)	6.93 (2H, *d*, *J* = 8.8 Hz, H-3′/H-5′)

Compound **129** was obtained as a yellow powder. In the ^{1}H-NMR spectrum of compound **129** (Appendix 121), two *meta*-coupled doublets were observed at δ 6.21 (*J* = 2.00 Hz) and 6.38 (*J* = 2.00 Hz) due to H-6 and H-8, respectively, of ring A. Two sets of signals at δ 7.79 (2H, *J* = 8.80 Hz, H-2′/H-6′) and 6.96 (2H, *J* = 8.80 Hz, H-3′/H-5′) with AA′XX′ spin system[110] are due to the protons of the 4′-substituted B-ring suggesting the presence of a kaempferol (**38**) moiety.[114] The ^{1}H-NMR data also revealed the presence of a rhamnose moiety attached to kaempferol. Thus, the ^{1}H-NMR spectrum of **129** showed the anomeric proton resonance at δ 5.40 (1H, *d*, *J* = 1.60 Hz, H-1″) indicating the α-configuration of the sugar. The methyl protons resonance of the rhamnose appeared at δ 0.94 (3H, *d*, *J* = 5.60 Hz, H-6″) and the remaining four proton resonances were observed at δ 3.60 (2H, *m*, H-4″, H-5″), 3.73 (1H, *m*, H-3″) and 4.24 (1H, *dd*, *J* = 3.20, 1.60 Hz, H-2″). Compound **129** was therefore identified as kaempferol-3-*O*-α-rhamnopyranoside (afzelin, Figure 17) based on the above spectroscopic data. Comparison of the ^{1}H-NMR data of **129** with those reported in the literature[125] for afzelin revealed a very close agreement (Table 44). Afzelin was previously identified in the leaves of *R. verniciflua* by LC-MS analysis.[137]

Table 44: The ^{1}H-NMR data (δ_{ppm}) of compound **129**.

129 (MeOD-d_4, 400 MHz)	Lit.[125] (MeOD-d_4, 500 MHz)
6.21 (1H, *d*, *J* = 2.00 Hz, H-6)	6.22 (1H, *d*, *J* = 1.8 Hz, H-6)
6.38 (1H, *d*, *J* = 2.00 Hz, H-8)	6.40 (1H, *d*, *J* = 1.9 Hz, H-8))
7.79 (2H, *d*, *J* = 8.80 Hz, H-2′/H-6′)	7.78 (2H, *d*, *J* = 8.5 Hz, H-2′/H-6′)
6.96 (2H, *d*, *J* = 8.80 Hz, H-3′/H-5′)	6.95 (2H, *d*, *J* = 8.7 Hz, H-3′/H-5′)
5.40 (1H, *d*, *J* = 1.60 Hz, H-1″)	5.40 (1H, *d*, *J* = 1.7 Hz, H-1″)
4.24 (1H, *dd*, *J* = 3.20, 1.60 Hz, H-2″)	4.28 (1H, *dd*, *J* = 3.2, 1.7 Hz, H-2″)
3.73 (1H, *m*, H-3″)	3.75 (1H, *dd*, *J* = 3.2, 9.3 Hz, H-3″)
3.60 (2H, *m*, H-4″, H-5″)	3.36 (2H, *m*, H-4″, H-5″)
0.94 (3H, *d*, *J* = 5.60 Hz, H-6″)	0.96 (3H, *d*, *J* = 6.1 Hz, H-6″)

Compound **130** was obtained as a light-yellow amorphous powder. The fact that this compound is dimeric flavonoid was evident from its ^{1}H-NMR spectrum (Appendix 122). Thus, the spectrum exhibited two sets of AA′XX′ spin system[110] at δ 7.87 (2H, H-2′/H-6′), 6.93 (2H, H-3′/H-5′), 8.11 (2H, H-2‴/H-6‴), and 6.95 (2H, H-3‴/H-5‴) indicating rings B and B′ are disubstituted. The spectrum also showed signals corresponding to four *meta*-coupled aromatic protons at δ 6.23 (1H, *d*, *J* = 2.00 Hz), 6.48 (1H, *d*, *J* = 2.00 Hz), 6.20 (1H, *d*, *J* = 2.00 Hz), and 6.42 (1H, *d*, *J* = 2.00 Hz) which are attributed to H-6 and H-8 of ring A and H-6″ and H-8″ of ring A′, respectively. Furthermore, the spectrum revealed one olefinic proton singlet at δ 6.61 (1H, *s*) due to H-3″. The above spectral data allowed for the assignment of structure for **130.** Comparison of the ^{1}H-NMR data of **130** with those reported in the literature[138] (Table 45) for delicaflavone revealed a very close agreement. There are no previous reports on the isolation of delicaflavone from a *Rhus* species.

Table 45: The ^{1}H-NMR data (δ_{ppm}) of compound **130**.

130 (Acetone-d_6, 400 MHz)	Lit.[138] (DMSO-d_6, 500 MHz)
6.23 (1H, *d*, *J* = 2.00 Hz, H-6)	6.24 (1H, *d*, *J* = 2.0 Hz, H-6)
6.48 (1H, *d*, *J* = 2.00 Hz, H-8)	6.53 (1H, *d*, *J* = 2.0 Hz, H-8)
7.87 (2H, *d*, *J* = 9.20 Hz, H-2′/H-6′)	7.82 (2H, *d*, *J* = 8.5 Hz, H-2′/H-6′)
6.93 (2H, *d*, *J* = 9.20 Hz, H-3′/H-5′)	6.88 (2H, *d*, *J* = 8.5 Hz, H-3′/H-5′)
6.61 (1H, *s*, H-3″)	6.85 (1H, *s*, H-3″)
6.20 (1H, *d*, *J* = 2.00 Hz, H-6″)	6.19 (1H, *d*, *J* = 2.2 Hz, H-6″)
6.42 (1H, *d*, *J* = 2.00 Hz, H-8″)	6.47 (1H, *d*, *J* = 2.2 Hz, H-8″)
8.11 (2H, *d*, *J* = 9.20 Hz, H-2‴/H-6‴)	7.98 (2H, *d*, *J* = 9.0 Hz, H-2‴/H-6‴)
6.95 (2H, *d*, *J* = 9.02 Hz, H-3‴/H-5‴)	7.23 (2H, *d*, *J* = 9.0 Hz, H-3‴/H-5‴)

3.5. Phytochemical Investigation on the Leaves of *Rhus natalensis*

Phytochemical analysis on the leaves of *R. natalensis* resulted in the isolation of three compounds, namely, 3,5,7,3′,4′-pentahydroxyflavone (quercetin, **1**), quercetin 3-*O*-α-arabinopyranoside (guaijaverin, **131**) and apigenin 8-*C*-β-glucopyranoside (vitexin, **132**) (Figure 18). DPPH radical scavenging activity of the plant extract was also determined in this study. The phytochemical investigation on the leaves *R. natalensis* is discussed in the following sections.

3.5.1. The DPPH Radical Scavenging Assay of the Ethyl Acetate-Soluble Fraction of the Leaves of *Rhus natalensis*

The ground fresh leaves of *R. natalensis* were extracted as described in **Section 4.3.5.1**. The DPPH radical scavenging activity of the EtOAc-soluble portion of the DCM:MeOH (1:1) extract of the leaves of *R. natalensis* was determined following the procedure described in **Section 4.3.1.4**. The EtOAc portion showed a 94.94% DPPH inhibition at a

concentration of 50.00 µg/mL (Table 46). The standard ascorbic acid showed 96.29% DPPH inhibition at the same concentration. The flavonoids in the leaves of *R. natalensis* (**Section 3.5.3**) could be responsible for the observed DPPH inhibition.

Table 46: Radical scavenging activities of the EtOAc-soluble portion of the DCM:MeOH extract of the leaves of *R. natalensis* and ascorbic acid standards.

Concentration (µg/mL)	% DPPH Inhibition	
	EtOAc-soluble portion of the extract of *R. natalensis*	Ascorbic acid standard
50.00	94.94 ± 0.29	96.29 ± 0.06
25.00	88.30 ± 0.20	96.26 ± 0.06
12.50	61.45 ± 1.15	96.06 ± 0.12
6.25	47.19 ± 1.91	91.30 ± 0.31
3.13	30.85 ± 1.20	54.06 ± 1.27
1.56	27.54 ± 0.84	35.00 ± 0.52

The results are reported as mean ± SD of three replicates.

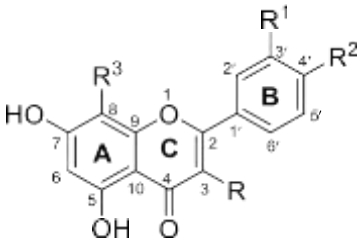
3.5.2. Fractionation of the Ethyl Acetate-Soluble Portion of the DCM:MeOH Extract of the Leaves of *Rhus natalensis*

The fractionation of the EtOAc-soluble portion of the DCM:MeOH (1:1) extract of the leaves of *R. natalensis* is described in **Section 4.3.5.2**. Three compounds, namely, quercetin (**1**), guaijaverin (**131**) and vitexin (**132**) (Figure 18) were isolated from the EtOAc-soluble portion. The crude EtOAc fraction of the DCM:MeOH extract of the leaves of *R. natalensis* and a mixture of the three isolated compounds, **1**, **131** and **132**, were also analyzed by HPLC. HPLC chromatogram of the EtOAc fraction showed the three compounds **1**, **131**, and **132** (Appendix 123). The HPLC chromatogram also indicated the presence of highly

polar compounds which are very difficult to isolate using silica gel column chromatography. Characterizations of the isolated compounds is discussed in the following section.

3.5.3. Characterization of Compounds Isolated from the EtOAc-Soluble Portion of the DCM:MeOH Extract of the Leaves of *Rhus natalensis*

Compound **1** was identified as the common flavonoid quercetin[119] based on its spectral data. Quercetin was also obtained from the leaves *R. glutinosa* as described in **Section 3.4.3**.



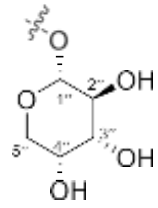
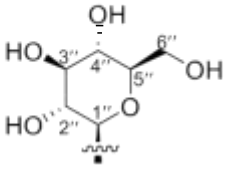
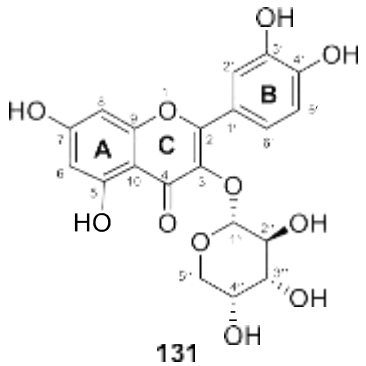
	R	R^1	R^2	R^3
1	OH	OH	OH	H
131		OH	OH	H
132	H	H	OH	

Figure 18: Compounds isolated from the leaves *R. natalensis*.

3.5.3.1. Characterization of Compound 131



131

Compound **131** was obtained as a light-yellow powder with melting point 238.0 – 240.0 °C. The UV-Vis spectrum in MeOH (Appendix 128) displayed characteristic absorption maximum for a flavone moiety (λ_{max}, 257 and 359 nm).[108] Furthermore, the IR spectrum (Appendix 127) in KBr of **131** indicated the presence of hydroxy (3475 cm^{-1}), carbonyl (1656 cm^{-1}), conjugated diene (1599 cm^{-1}) and phenyl (1509 cm^{-1}) functionalities.

The ^{13}C-NMR (Appendix 125) of **131** showed 20 carbon resonances which are attributed to ten quaternary (seven of which are oxygenated and one is a conjugated carbonyl), nine methine and one methylene carbon atoms based on the DEPT-135 NMR spectrum (Appendix 126). The ^{1}H-NMR spectrum of **131** (Table 47 and Appendix 124) revealed two *meta*-coupled aromatic protons of the 5,7-disubstituted ring A at δ 6.21 (*d*, *J* = 2.00 Hz, H-6) and 6.41 (*d*, *J* = 2.00 Hz, H-8); an ABX[120] pattern corresponding to three aromatic protons of the 3′,4′-disubstituted B ring at δ 7.51 (*d*, *J* = 2.28 Hz, H-2′), 7.67 (*dd*, *J* = 8.44, 2.16 Hz, H-6′) and 6.84 (*d*, *J* = 8.60 Hz, H-5′), and one chelated OH group at δ 12.66 (*s*, 5-OH). The above ^{1}H-NMR data indicates the presence of a quercetin (**1**) moiety.[119] The ^{1}H-NMR data also revealed the presence of a sugar moiety attached to quercetin (**1**). The anomeric proton resonance at δ 5.28 (*d*, *J* = 5.32 Hz, H-1″) indicates the α-configuration

of the sugar. The remaining five aliphatic proton resonances appeared in the range of δ 3.22 – 3.76 due to H-2″ to H-5″ of the sugar unit.

The 3-*O*-glycosidic nature of **131** was determined from its ^{13}C-NMR data. The spectrum revealed downfield shifts of the signals corresponding to C-2, C-4, C-5 and C-10 by 9.24, 2.31, 0.27, and 1.14 ppm, respectively, and an upfield shift of the signal due to C-3 by 1.66 ppm corresponding to the spectrum of the aglycone, quercetin (**1**, Table 32).[122] Thus, compound **131** was identified as quercetin 3-*O*-α-arabinopyranoside (guaijaverin, Figure 18) based on the above spectroscopic data and is reported herein for the first time from a *Rhus* species. Comparison of the NMR data of **131** with those reported in the literature for guaijaverin[121] revealed a very close agreement.

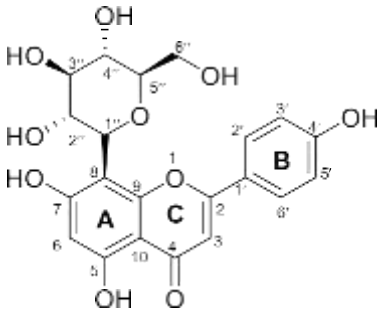
Table 47: The ^{1}H-NMR data (δ_{ppm}) of compound **131**.

131 (DMSO-d_6, 400 MHz)	Lit.[121] (MeOD-d_4, 500 MHz)
12.66 (1H, *s*, 5-OH)	–
6.21 (1H, *d*, *J* = 2.00 Hz, H-6)	6.20 (1H, *d*, *J* = 2.0 Hz, H-6)
6.41 (1H, *d*, *J* = 2.00 Hz, H-8)	6.39 (1H, *d*, *J* = 2.0 Hz, H-8)
7.51 (1H, *d*, *J* = 2.28 Hz, H-2′)	7.73 (1H, *d*, *J* = 2.0 Hz, H-2′)
6.84 (1H, *d*, *J* = 8.60 Hz, H-5′)	6.86 (1H, *d*, *J* = 8.4 Hz, H-5′)
7.67 (1H, *dd*, *J* = 8.44, 2.16 Hz, H-2′)	7.57 (1H, *dd*, *J* = 8.4, 2.0 Hz, H-2′)
5.28 (1H, *d*, *J* = 5.32 Hz, H-1″)	5.15 (1H, *d*, *J* = 6.4 Hz, H-1″)
3.76 (1H, *dd*, *J* = 7.20, 5.16 Hz, H-2″)	3.89 (1H, *dd*, *J* = 8.2, 6.4 Hz, H-2″)
3.51 (1H, *dd*, *J* = 7.20, 3.40 Hz, H-3″)	3.64 (1H, *dd*, *J* = 8.2, 3.1 Hz, H-3″)
3.62 (1H, *m*, H-4″)	3.81 (1H, *m*, H-4″)
3.62 (1H, *m*, H-5″)	3.81 (1H, *m*, H-5″)
3.22 (*dd*, *J* = 11.36, 2.52 Hz, 1H, H-5″)	3.43 (1H, *dd*, *J* = 13.5, 3.1 Hz, H-5″)

Table 48: The ^{13}C-NMR data (δ_{ppm}) of compound **131**.

C	**131** (DMSO-d_6, 100 MHz)	Lit.[121] (MeOD-d_4, 125 MHz)
2	156.73	158.7
3	134.20	135.7
4	177.99	179.5
5	161.68	163.1
6	99.12	99.9
7	164.63	166.0
8	93.96	94.7
9	156.73	158.4
10	104.37	105.7
1′	121.35	123.1
2′	116.19	117.5
3′	145.45	146.0
4′	149.05	150.0
5′	115.82	116.2
6′	122.56	122.9
1″	101.84	104.6
2″	72.09	74.1
3″	71.17	72.9
4″	66.52	69.1
5″	64.74	66.9

3.5.3.2. Characterization of Compound 132



132

Compound **132** was isolated as a yellow powder (m. p. 257.8 – 259.5 °C). The UV-Vis spectrum (Appendix 135) in MeOH showed two absorption maxima at 270 and 339 nm

characteristic of a flavone moiety, while the IR spectrum (Appendix 134) showed the hydroxy (3414 cm^{-1}) and carbonyl (1655 cm^{-1}) functionalities in the molecule.[108]

A total of 21 carbon signals were observed in the ^{13}C-NMR spectrum of **132** (Appendix 130). Based on the DEPT-135 and HSQC spectra (Appendix 131 and Appendix 132) the signals were attributed to one conjugated carbonyl (δ 182.57 (C-4)), seven quaternary aromatic carbons (δ 104.49 (C-10), 105.08 (C-8), 122.07 (C-1′), 156.47 (C-9), 160.86 (C-5), 161.62 (C-4′), and 163.08 (C-7)), two olefinic carbons (δ 102.91 (C-3) and 164.41 (C-2)), five aromatic methine carbons (δ 98.61 (C-6), 116.28 (C-3′, 5′) and 129.44 (C-2′, 6′)), one anomeric methine carbon (δ 73.37 (C-1″)) typical of a C-glucopyranosyl moiety,[122] and five sugar carbon atoms (δ 61.74 (C-6″), 70.99 (C-4″), 71.96 (C-2″), 78.65 (C-3″) and 82.31 (C-5″)).

The ^{1}H-NMR data of compound **132** (Table 49 and Appendix 129) showed a down-field signal at δ 13.18 (*s*) indicating a chelated OH group at C-5, four aromatic proton resonances of an AA′XX′ spin system[110] of the 4′-substituted B-ring at δ 8.03 (2H, *d*, *J* = 8.84 Hz, H-2′/H-6′) and 6.89 (2H, *d*, *J* = 8.84 Hz, H-3′/H-5′), two aromatic proton singlets at δ 6.79 (*s*, 1H, H-3) and 6.28 (*s*, 1H, H-6), and the signal due to the anomeric proton of the C-glycoside at δ 4.69 (*d*, *J* = 9.84 Hz, 1H). The remaining six proton resonances in the range between δ 3.25 and 3.84 were assigned to the glycoside unit as shown in Table 49.

The HMBC correlations (Appendix 133) of H-3 (δ 6.79) to C-1' (δ 122.07), C-2 (δ 164.41), C-4 (δ 182.57) and C-10 (δ 104.49), and correlations of H-6 (δ 6.28) to C-5 (δ 160.86), C-7 (δ 163.08), C-8 (δ 105.08) and C-10 (δ 104.49) were used to confirm that the signals at δ 6.79 and 6.28 are due to the protons at C-3 and C-6, respectively. The fact that the B-ring

hydroxy group is attached to C-4′ was confirmed by using the HMBC correlations of H-2′ (δ 8.03) and H-3′ (δ 6.89) to C-4′ (δ 161.62). In addition, the HMBC correlations of H-1″ (δ 4.69) to C-7 (δ 163.08), C-8 (δ 105.08) and C-9 (δ 156.47) were used to establish the position of the C-glucopyranosyl unit at C-8. The above spectroscopic data allowed for the identification of **132** as apigenin 8-*C*-β-glucopyranoside (vitexin, Figure 18). Comparison of the NMR data of **132** with those reported in the literature for vitexin[139] revealed a very close agreement as depicted in Table 49 and Table 50. This is the first report of vitexin (**132**) from a *Rhus* species. However, vitexin (**132**) was reported from various plant species, including *Trollius ledebouri*, *Colocasia esculenta*, and *Antidesma ghaesembilla*.[139-140]

Table 49: The ^{1}H-NMR data (δ_{ppm}) of compound **132**.

132 (DMSO-d_6, 400 MHz)	Lit.[139] (DMSO-d_6, 500 MHz)
6.79 (1H, *s*, H-3)	6.77 (1H, *s*, H-3)
13.18 (1H, *s*, 5-OH)	–
6.28 (1H, *s*, H-6)	6.27 (1H, *s*, H-6)
8.03 (2H, *d*, *J* = 8.84 Hz, H-2′/H-6′)	8.02 (2H, *d*, *J* = 8.0 Hz, H-2′/H-6′)
6.89 (2H, *d*, *J* = 8.84 Hz, H-3′/H-5′)	6.89 (2H, *d*, *J* = 8.0 Hz, H-3′/H-5′)
4.69 (1H, *d*, *J* = 9.84 Hz, H-1″)	4.69 (1H, *d*, *J* = 10.0 Hz, H-1″)
3.84 (1H, *t*, *J* = 9.34 Hz, H-2″)	3.84 (1H, *dd*, *J* = 9.0, 10.0 Hz, H-2″)
3.25 (1H, *m*, H-3″)	3.29 (1H, *m*, H-3″)
3.53 (1H, *m*, H-4″)	3.34 (1H, *m*, H-4″)
3.25 (1H, *m*, H-5″)	3.26 (1H, *m*, H-5″)
3.53 (1H, *m*, H-6″)	3.52 (1H, *dd*, *J* = 5.5, 11.0 Hz, H-6″)
3.77 (1H, *dd*, *J* = 5.56, 11.54 Hz, H-6″)	3.76 (1H, *br. d*, *J* = 11.0 Hz, H-6″)

Table 50: The ^{13}C-NMR data (δ_{ppm}) of compound **132**.

C	**132** (DMSO-d_6, 100 MHz)	Lit.[139] (DMSO-d_6, 125 MHz)
2	164.41	163.91
3	102.91	102.41
4	182.57	182.04
5	160.86	160.38
6	98.61	98.14
7	163.08	162.68
8	105.08	104.59
9	156.47	155.98
10	104.49	104.00
1′	122.07	121.59
2′	129.44	128.92
3′	116.28	115.80
4′	161.62	161.12
5′	116.28	115.80
6′	129.44	128.92
1″	73.37	73.36
2″	71.96	70.84
3″	78.65	78.65
4″	70.99	70.54
5″	82.31	81.80
6″	61.74	61.28

4. Experimental Section

4.1. General Experimental Procedures

All chemicals, reagents and solvents used in this study were analytical/HPLC grade and purchased from Sigma-Aldrich, Germany. All other chemicals were purchased from Fisher Scientific, UK. Optical rotations were determined with a AUTOPOL IV automatic polarimeter. UV-vis and FT-IR spectra were determined using a UV-T60 spectrophotometer and a Perkin-Elmer Spectrum 65 instrument in the range 4000 – 200 cm^{-1}, respectively. Melting point was recorded using a METTLER TOLEDO FP82HT hot stage coupled with a METTLER TOLEDO FP90 central processor. Gas chromatography-mass spectrometry (GC-MS) experiments were conducted on Agilent Technologies 7820A GC system coupled with Agilent Technologies 5977E MSD, USA. Chromatographic peaks were identified by using NIST 2014 mass spectral library search and retention index (*I*) calculation. ^{1}H- and ^{13}C-NMR spectra were recorded on a Bruker Avance 400 NMR spectrometer at 400.13 and 100.60 MHz, respectively. High-resolution electrospray ionization mass spectra (HRESIMS) were carried out in the positive ion mode on Agilent G6520A Q-TOF LC-MS and the samples were run with 90% MeOH with 0.04% formic acid and 10% water with 0.04% formic acid at 0.3 mL/minute. X-ray crystal structure analysis was performed using a Bruker D8 VENTURE area detector diffractometer. Column chromatography was performed using silica gel 60 (Merck), particle size 0.063 – 0.200 (70 – 230 mesh ASTM) and Sephadex LH-20 (GE Healthcare Bio-Sciences AB, Sweden). Preparative thin-layer chromatography (PTLC) was carried out on acid-washed silica gel with 254 nm fluorescent indicator (Sigma-Aldrich, Germany) pre-coated on glass (20 × 20 cm). Thin-layer chromatography (TLC) was performed with Merck Kieselgel 60

F254 precoated plates which were visualized under UV light and by spraying with vanillin (1.0 g vanillin with 5% H_2SO_4 in MeOH) and cerium molybdate stain (ammonium molybdate (12.0 g), ceric ammonium molybdate (0.5 g), and conc. H_2SO_4 (15.0 mL) in distilled water (235.0 mL)) followed by heating for a few seconds.

4.2. Plant Material

Cyperus esculentus

The rhizomes of *Cyperus esculentus L.* were collected from Yabelo city, Borena Zone, Oromia regional state, Ethiopia. The plant specimen was identified by the Department of Plant Sciences, Addis Ababa University, Addis Ababa, Ethiopia. A voucher specimen (No. Mel-001) was deposited at the National Herbarium, Addis Ababa University, Addis Ababa, Ethiopia.

Carissa spinarum

The roots of *Carissa spinarum* were collected from Harbu city, Wollo, Ethiopia. The plant specimen was identified by the Department of Plant Sciences, Addis Ababa University, Addis Ababa, Ethiopia. A voucher specimen (No. Mel-004) was deposited at the National Herbarium, Addis Ababa University, Addis Ababa, Ethiopia.

Melilotus officinalis

M. officinalis was grown in the garden of Chemistry Department, Addis Ababa University, Addis Ababa, Ethiopia. A voucher specimen (No. Mel-003) was identified and deposited at the National Herbarium, Addis Ababa University, Addis Ababa, Ethiopia.

Rhus glutinosa

The leaves of *R. glutinosa* were collected from Gulele Botanical Garden, Addis Ababa, Ethiopia, on October 27, 2018. A voucher specimen (No. Mel-002) was identified by the Department of Plant Sciences, Addis Ababa University, Addis Ababa, Ethiopia, and deposited at the National Herbarium, Addis Ababa University, Addis Ababa, Ethiopia. The plant material was stored in a freezer until extraction.

Rhus natalensis

The leaves of *R. natalensis* were collected from Yabelo area, Borena Zone, Oromia regional state, Ethiopia. A voucher specimen (No. Mel-005) was identified and deposited at the National Herbarium, Addis Ababa University, Addis Ababa, Ethiopia.

4.3. Extraction and Characterization

4.3.1. Extraction and Characterization of Compounds from the Rhizomes of *Cyperus esculentus*

4.3.1.1. Extraction of Essential Oil by Hydrodistillation

The dried rhizomes of *Cyperus esculentus* were ground and subjected to hydrodistillation following the method described by Costa *et. al.*[10] Thus, the powdered plant material (1.0 kg) was placed in a distillation flask containing distilled water (2.0 L) and the flask was then attached to a Clevenger apparatus which was connected to a condenser. The contents of the flask were heated to boiling on a heating mantle and hydrodistillation continued for 8 h after initial boiling. The essential oil (5.6 mL) was collected, dried over anh Na_2SO_4, filtered, and then stored until analysis by GC-MS. The essential oil (1.0 mL) was

partitioned between MeOH (2.0 mL) and *n*-hexane (2.0 mL) and both the MeOH and *n*-hexane fractions were analyzed by GC-MS.

Retention index (*I*) was calculated for the different components in the essential oil of *Cyperus esculentus*. For retention index calculation, a mixture of *n*-alkanes ($C_9 - C_{23}$) was injected and analyzed using the same experimental condition as that of the essential oil analysis. The retention indices of the different components were then calculated according to the van den Dool and Kratz relationship (Equation 1).[141]

$$I = 100n + 100\left(\frac{R_{t(unknown)} - R_{t(n)}}{R_{t(n+1)} - R_{t(n)}}\right) \quad \text{---------- Equation 1}$$

where *I* is retention index of the analyte, *n* is the number of carbon atoms of the *n*-alkane eluting immediately before the analyte, $R_{t(unknown)}$ is the retention time of the analyte, $R_{t(n)}$ and $R_{t(n+1)}$ are the retention times of the reference *n*-alkanes eluting immediately before and after the analyte, respectively.

4.3.1.2. Characterization of the Essential Oil from the Rhizomes of *Cyperus esculentus*

The mixture of *n*-alkanes and the essential oil obtained from the rhizomes of *Cyperus esculentus* were analyzed by using an Agilent Technology 7820A GC system coupled with an Agilent Technology 5977E MSD system equipped with an autosampler. The chromatographic separation was done on a column 30 m in length and 0.25 µm in thickness coated with HP-5MS, (5%-phenyl)-methylpolysiloxane, at a pressure of 8 psi and a flow rate of 0.97989 mL/min. Ultra-high pure helium (99.999%) was used as carrier gas at constant flow mode. An Agilent G4567A autosampler was used to inject 1 µL of the sample

with a splitless injection mode into the inlet heated to 275 ºC with a total run time of 29.33 min. Oven temperature was programmed with the initial column temperature of 60 ºC and hold-time 2 min. The column temperature was increased at a rate of 10 ºC/min until the temperature reached 200 ºC and then heated again at the rate of 3 ºC/min until the temperature reached 240 ºC. No mass spectra were collected during the first 4 min of the solvent delay. The transfer line and the ion source temperatures were 280 ºC and 230 ºC, respectively. The detector voltage was 1600 V and the electron energy was 70 eV. Mass spectral data were collected from 40 – 650 *m*/*z*. The names, structures, and qualities of peaks were determined through National Institute of Standards and Technology (NIST) 2014 library search and retention index (*I*) calculation.

4.3.1.3. Solvent Extraction of the Rhizomes of *Cyperus esculentus*

The dried rhizomes of *Cyperus esculentus* L. (1.0 kg) were pulverized and extracted first with *n*-hexane (3.5 L) for 24 h, and the *n*-hexane was removed under reduced pressure to yield a crude extract (11.3 g). The marc left after extraction with *n*-hexane was further extracted with EtOAc (3.5 L) for another 24 h, and the EtOAc was removed to yield a crude extract (19.7 g). The marc left after removal of the EtOAc was finally extracted with MeOH (3.5 L) for 24 h, and then the MeOH was removed under reduced pressure to yield a crude extract (50.9 g).

4.3.1.4. DPPH Radical Scavenging Assay of the Ethyl Acetate Extract of the Rhizomes of *Cyperus esculentus*

The DPPH radical scavenging assay is a simple method for quantifying antioxidants by measuring absorbance at 517 nm due to the stable 2,2-diphenyl-1-picrylhydrazyl (DPPH)

radical.[142] The radical scavenging activity of the EtOAc extract of the rhizomes of *Cyperus esculentus* was assessed using DPPH according to the procedure described by Hoque *et. al*.[143] The extract was first dissolved in MeOH to afford 1.0 mg/mL solution. It was then serially diluted in MeOH to give concentrations of 500.00, 250.00, 125.00, 62.50, 31.25, 15.63 and 7.81 µg/mL. To 1.0 mL of each solution, 4.0 mL of 0.004% DPPH solution in MeOH was added to make 100.00, 50.00, 25.00, 12.50, 6.25, 3.13 and 1.56 µg/mL solutions. The mixtures were shaken vigorously and left to stand in the dark for 30 min. The absorbance of the samples was then recorded at 517 nm using a UV-Vis spectrophotometer. The radical scavenging activity of the extract was measured in relation to ascorbic acid (a known antioxidant) standards. All measurements were performed in triplicates and the percentage DPPH inhibition of the extract and ascorbic acid standards were calculated using Equation 2.

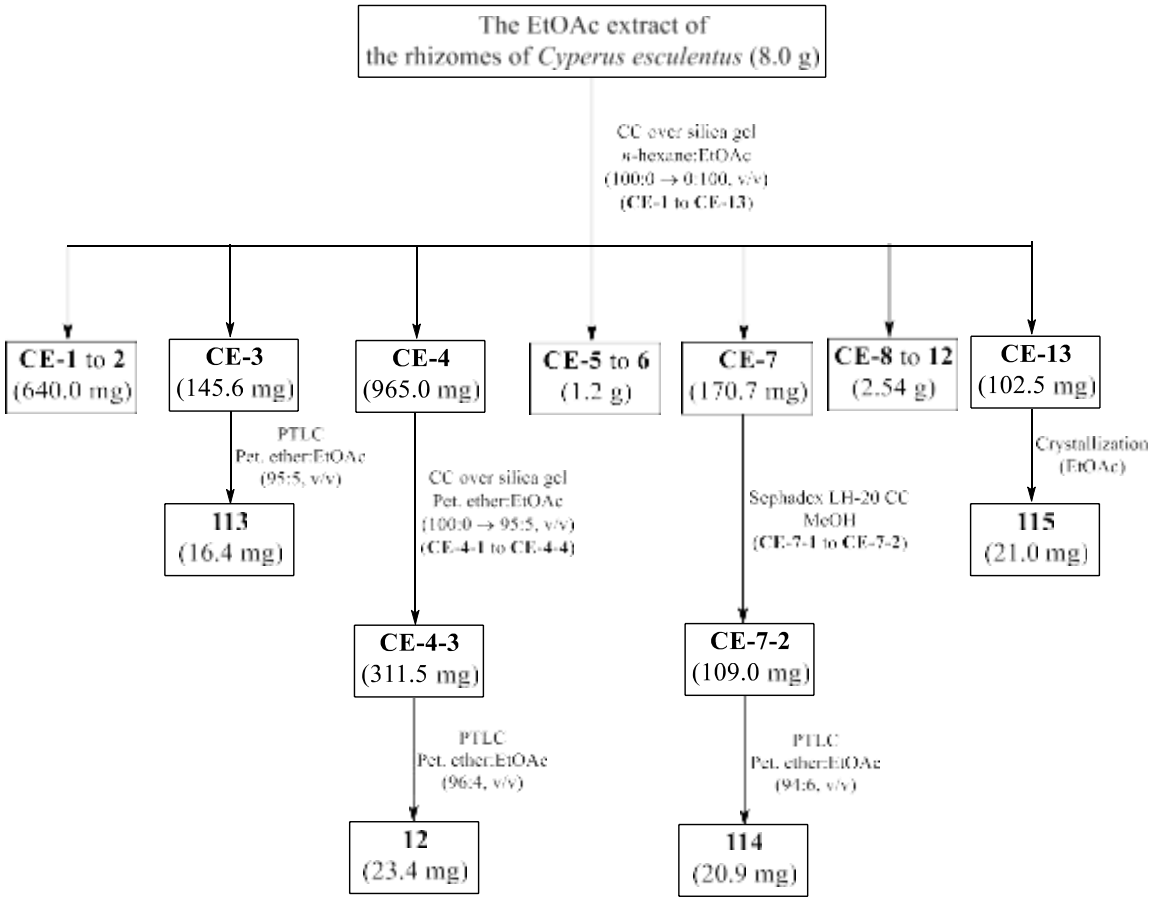
$$\%\ \text{DPPH inhibition} = \frac{A_{control} - A_{extract}}{A_{control}} \times 100 \quad \text{---------- Equation 2}$$

where $A_{control}$ is the absorbance of DPPH solution in MeOH and $A_{extract}$ is the absorbance of the test sample plus DPPH solution.

4.3.1.5. Fractionation of the Ethyl Acetate Extract of the Rhizomes of *Cyperus esculentus*

The EtOAc crude extract (8.0 g) was fractionated over a column of silica gel (80.0 g) using a gradient of EtOAc in *n*-hexane (0:100 → 100:0, v/v) to furnish a total of 111 fractions. The fractions were combined based on their TLC profiles into thirteen fractions (**CE-1** to **CE-13**). Purification of fraction **CE-3** (145.6 mg) by PTLC using pet ether:EtOAc (95:5,

v/v) as eluent gave compound **113** (16.4 mg). Fraction **CE-4** (965.0 mg) was subjected to column chromatography over silica gel (40.0 g) using a gradient of EtOAc in pet ether (0:100 → 5:95, v/v) to give 72 subfraction which were combined into four groups (**CE-4-1** to **CE-4-4**) based on their TLC profiles. Subfraction **CE-4-3** (311.5 mg) was further fractionated by PTLC using pet ether:EtOAc (96:4, v/v) as eluent to give compound **12** (23.4 mg). Fraction **CE-7** (170.7 mg) was subjected to column chromatography over Sephadex LH-20 using MeOH as eluent to yield two subfractions (**CE-7-1** to **CE-7-2**). Purification of subfraction **CE-7-2** (109.0 mg) by PTLC using pet ether:EtOAc (94:6, v/v) as eluent gave compound **114** (20.9 mg). Crystallization of fraction **CE-13** (102.5 mg) from EtOAc afforded compound **115** (21.0 mg) as white crystals.



4.3.1.6. Physical and Spectroscopic Data of Compounds Isolated from the Ethyl Acetate Extract of the Rhizomes of *Cyperus esculentus*

Caryophyllene Oxide (**113**): Colorless crystals, m. p. 62.5 – 63.9 °C, Lit.[93] m. p. 64.0 °C; IR_v (KBr, cm^{-1}): 3430, 2926, 2855, 1737, 1463, 1384; ^{1}H-NMR (400 MHz, $CDCl_3$, δ, ppm): 4.99 (1H, *d*, *J* = 2.00 Hz, H-13a), 4.88 (1H, *d*, *J* = 1.80 Hz, H-13b), 2.90 (1H, *dd*, *J* = 10.60, 4.04 Hz, H-5), 2.64 (1H, *q*, *J* = 9.41 Hz, H-9), 2.36 (1H, *m*, H-7a), 2.27 (1H, *m*, H-6a), 2.13 (2H, *m*, H-3a, H-7b), 1.78 (1H, *t*, *J* = 9.72 Hz, H-1), 1.68 (3H, *m*, H-2a, H-10), 1.46 (1H, *m*, H-2b), 1.37 (1H, *m*, H-6b), 1.22 (3H, *s*, Me-12), 1.02 (3H, *s*, Me-14), 1.00 (3H, *s*, Me-15), 0.97 (1H, *m*, H-3b). ^{13}C-NMR (100 MHz, $CDCl_3$, δ, ppm): 151.85 (C-8), 112.78 (C-13), 63.78 (C-5), 59.86 (C-4), 50.71 (C-1), 48.75 (C-9), 39.75 (C-10), 39.14 (C-3), 34.04 (C-11), 30.21 (C-6), 29.90 (Me-15), 29.77 (C-7), 27.21 (C-2), 21.62 (Me-14), 17.01 (Me-12).[92]

Cyperotundone (**12**): Colorless crystals, m. p. 36.0 – 38.0 °C, Lit.[94] m. p. 38.0 – 40.0 °C; $[\alpha]_D^{25} - 2.35^0$ (*c* 0.085, MeOH); UV (MeOH, λ_{max}, nm): 246; IR_v (KBr, cm^{-1}): 2928, 2873, 1707, 1666, 1464, 1371, 1277, 1168, 1056; ^{1}H-NMR (400 MHz, $CDCl_3$, δ, ppm): 2.60 (1H, *dd*, *J* = 18.92, 7.32 Hz, H-6a), 2.31 (1H, *d*, *J* = 18.96 Hz, H-6b), 2.18 (2H, *m*, H-2a, H-10), 1.98 (3H, *m*, H-2b, H-7, H-8a), 1.73 (3H, *s*, Me-14), 1.60 (1H, *dt*, *J* = 15.16, 6.32 Hz, H-9a), 1.42 (1H, *m*, H-8b), 1.11 (3H, *s*, Me-12), 1.02 (1H, *m*, H-9b), 0.75 (3H, *s*, Me-13), 0.62 (3H, *d*, *J* = 6.44 Hz, Me-15). ^{13}C-NMR (100 MHz, $CDCl_3$, δ, ppm): 211.06 (C-3), 181.81 (C-5), 133.38 (C-4), 58.70 (C-1), 45.35 (C-7), 41.63 (C-11), 41.16 (C-2), 33.72 (C-10), 30.49 (C-6), 28.37 (C-9), 27.00 (C-8), 24.84 (Me-13), 19.58 (Me-12), 16.83 (Me-15), 8.35 (Me-14).[94]

Corymbolone (**114**): Colorless crystals, m. p. 135.0 – 136.8 °C, Lit.[96] m. p. 136.5 – 137.0 °C; $[\alpha]_D^{25} + 17.48^0$ (*c* 0.88, MeOH); IR_v (KBr, cm^{-1}): 3435, 2927, 2857, 1737, 1709, 1644, 1456, 1384, 1279, 1260, 1172, 1087, 1044, 1028, 887; ^{1}H-NMR (400 MHz, $CDCl_3$, δ, ppm): 4.75 (2H, *s*, H-12), 2.69 (1H, *m*, H-2a), 2.38 (3H, *m*, H-2b, H-6, H-7), 1.90 (3H, *m*, H-3a, H-4, H-9a), 1.76 (3H, *s*, Me-13), 1.69 (2H, *m*, H-6b, H-8b), 1.60 (1H, *m*, H-3b), 1.45 (1H, *ddd*, *J* = 13.83, 3.85, 2.09 Hz, H-9b), 1.38 (1H, *dd*, *J* = 12.76, 3.92 Hz, H-8a), 1.25 (3H, *s*, Me-14), 1.20 (3H, *d*, *J* = 7.56 Hz, Me-15). ^{13}C-NMR (100 MHz, $CDCl_3$, δ, ppm): 216.20 (C-1), 149.59 (C-11), 108.89 (C-12), 78.65 (C-5), 51.26 (C-10), 40.55 (C-4), 39.32 (C-7), 37.20 (C-9), 34.26 (C-2), 30.17 (C-3), 28.02 (C-6), 25.47 (C-8), 21.15 (C-13), 20.4 (C-14), 17.77 (C-15).[96-97]

Tricyclohumuladiol (115): White crystalline powder, m. p. 159.0 – 161.0 °C, Lit.[98] m. p. 160.0 – 162.0 °C; IR_v (KBr, cm^{-1}): 3326, 2947, 1459, 1383, 1135, 1075, 1013, 964, 897; HRESIMS *m/z* 221.1918 $[M - H_2O + H]^+$ (calculated for $C_{15}H_{25}O$, 221.1905, Δ 0.0013 mmu); ^{1}H-NMR (400 MHz, $CDCl_3$, δ, ppm): 3.25 (1H, *dd*, *J* = 5.20, 11.20 Hz, H-5), 1.98 (1H, *dt*, *J* = 8.00, 2.80 Hz, H-9), 1.89 (1H, *m*, H-6a), 1.81 (2H, *m*, H-7), 1.65 (1H, *m*, H-6b), 1.57 (1H, *dd*, *J* = 8.00, 10.00 Hz, H-10a), 1.39 (1H, *t*, *J* = 10.40 Hz, H-10b), 1.14 (3H, *s*, Me-14), 1.13 (3H, *s*, Me-15), 1.08 (1H, *d*, *J* = 10.80 Hz, H-1), 1.05 (3H, *s*, Me-12), 1.02 (3H, *s*, Me-13), 0.70 (1H, *ddd*, *J* = 10.90, 7.90, 5.30 Hz, H-2), 0.49 (1H, *dd*, *J* = 4.60, 7.80 Hz, H-3a), 0.23 (1H, *t*, *J* = 5.00 Hz, H-3b). ^{13}C-NMR (100 MHz, $CDCl_3$, δ, ppm): 74.40 (C-5), 73.57 (C-8), 49.03 (C-9), 48.20 (C-1), 39.83 (C-7), 33.98 (C-10), 33.56 (C-11), 30.44 (C-6), 30.38 (C-13), 24.16 (C-2), 22.14 (C-12), 19.99 (C-4), 19.90 (C-14), 18.44 (C-3), 17.30 (C-15).[98]

4.3.2. Extraction and Characterization of Compounds from the Roots of *Carissa spinarum*

4.3.2.1. Extraction of Essential Oil from the Roots of *Carissa spinarum* by Hydrodistillation

The essential oil of the roots of *Carissa spinarum* was extracted by hydrodistillation following the procedure described by Costa *et. al*.[10] Thus, powdered roots of *Carissa spinarum* (300.0 g) and distilled water (500.0 mL) were placed in a distillation flask which was attached to a Clevenger apparatus and a condenser and the mixture was heated to boiling. After 8 h, the essential oil (1.5 mL) was collected, dried over anh Na_2SO_4, filtered and then analyzed by GC-MS.

4.3.2.2. Collection of the Smoke from Burnt Roots of *Carissa spinarum* and DPPH Radical Scavenging Assay

Dried and powdered roots of *Carissa spinarum* (300.0 g) were burned using an electrical stove (Figure 19) and the smoke was collected using an inverted funnel fitted with a rubber tube. The smoke was allowed to pass thorough a suction flask (250.0 mL) containing MeOH (100.0 mL) which in turn was connected to another 250.0 mL suction flask that contained *n*-hexane (100.0 mL). The side arm of the *n*-hexane-containing flask was attached to a water aspirator in order to help draw the smoke from the smoker into the solvents. The MeOH and *n*-hexane solutions were dried over anh Na_2SO_4, filtered and the solvents were removed under reduced pressure to yield methanol (2.5 g) and *n*-hexane (441.4 mg) residues which were then analyzed by GC-MS.



Figure 19: Smoke trapping setup (Photo by Melaku Assefa)

The retention index (*I*) of the different components in the smoke derived from the roots of *Carissa spinarum* was calculated by analyzing a mixture of *n*-alkanes under the same experimental condition as that of the smoke analysis and using the van den Dool and Kratz relationship (Equation 1, **Section 4.3.1.1**).[141] The radical scavenging activity of the MeOH-soluble fraction of the smoke derived from the roots of *Carissa spinarum* was assessed using DPPH according to the procedure described in **Section 4.3.1.4**.

4.3.2.3. GC-MS Characterization of the Essential Oil and Smoke Derived from the Roots of *Carissa spinarum*

The essential oil and smoke obtained by burning the roots of *Carissa spinarum* were analyzed by using an Agilent Technology 7820A GC system coupled with an Agilent

Technology 5977E MSD equipped with an autosampler. The chromatographic separation was done on a DB-1701, (14%-cyanopropyl-phenyl)-methylpolysiloxane, column (30 × 0.25 µm) at a pressure of 8 psi and a flow rate 0.97989 mL/min. Ultra-high pure helium (99.999%) was used as carrier gas at constant flow mode. An Agilent G4567A autosampler was used to inject 1 µL of the sample with a splitless injection mode into the inlet heated to 275 ºC with a total run time of 29.33 min. Oven temperature was programmed with the initial column temperature of 60 ºC and hold-time of 2 min. The column temperature was increased at a rate of 10 ºC/min until the temperature reached 200 ºC and then heated again at the rate of 3 ºC/min until the temperature reached 240 ºC. No mass spectra were collected during the first 4 min of the solvent delay. The transfer line and the ion source temperatures were 280 ºC and 230 ºC, respectively. The detector voltage was 1600 V and the electron energy was 70 eV. Mass spectral data were collected from 40 – 650 *m*/*z*. The names, structures, and qualities of peaks were determined through NIST 2014 library search and retention index (*I*) calculation.

4.3.3. Extraction and Characterization of the Seeds of *Melilotus officinalis*

4.3.3.1. Solvent Extraction and DPPH Radical Scavenging Assay of the Seeds of *Melilotus officinalis*

The dried and ground seeds of *M. officinalis* (100.0 g) were Soxhlet-extracted with *n*-hexane (300.0 mL) for 8 h. The *n*-hexane was removed under reduced pressure to yield a yellow oil (2.1 g). The marc left after *n*-hexane extraction was further extracted with MeOH (300.0 mL) for another 8 h and the MeOH was removed under reduced pressure to yield a

brown residue (9.3 g). The DPPH radical scavenging activity of the MeOH extract of the seeds of *M. officinalis* was assessed following the procedure described in **Section 4.3.1.4**.

4.3.3.2. Preparation of Fatty Acid Methyl Esters (FAMEs)

The *n*-hexane extract of the seeds of *M. officinalis* (0.5 g) was placed in a 50.0 mL round bottom flask fitted with a condenser and 2% methanolic KOH (3.0 mL) was added. The mixture was heated at 50 °C for 30 min on a water bath with continuous shaking. The reaction mixture was cooled to room temperature and transferred to a separatory funnel. Saturated NaCl (1.0 mL) was added and the mixture was extracted with pet ether (15.0 mL). The organic layer was separated, dried over anh Na_2SO_4, filtered and concentrated to yield the esterified product (150.9 mg) which was analyzed by GC-MS. The esterified *n*-hexane extract was also partitioned between *n*-hexane (2.0 mL) and MeOH (2.0 mL) and the *n*-hexane portion was then analyzed by GC-MS.

4.3.3.3. Preparation of Methyl Palmitate Standard

To determine the concentrations of the different components in the *n*-hexane extract of the seeds of *M. officinalis*, methyl palmitate standards were used. Methyl palmitate was prepared by Fischer esterification[144] of palmitic acid. Thus, in a 50.0 mL round bottom flask equipped with a reflux condenser, palmitic acid (1.0 g) was dissolved in MeOH (10.0 mL) and then conc. H_2SO_4 (1.0 mL) was carefully added. The mixture was heated on a water bath at 50 ºC for 1 h and then cooled to room temperature. Chloroform (30.0 mL) was added and the mixture was transferred to a separatory funnel and washed with deionized water (30.0 mL). The organic layer was then washed with aqueous $NaHCO_3$ (30.0 mL) and water (30.0 mL), dried over anh Na_2SO_4, filtered and concentrated to afford

methyl palmitate. Standard solutions of methyl palmitate were prepared at concentrations of 1, 10, 25, 50 and 100 ppm and analyzed by GC-MS in triplicates.

4.3.3.4. Characterization of Fatty Acids from the Seeds of *Melilotus officinalis*

GC-MS analyses of the fatty acid methyl esters were conducted on an Agilent Technology 7820A GC system coupled with an Agilent Technology 5977E MSD equipped with an autosampler. The chromatographic separation was done on a DB-1701 (14%-cyanopropyl-phenyl-methylpolysiloxane) column (30 m x 0.25 µm) at a pressure of 8 psi and a flow rate of 0.97989 mL/min. Ultra-high pure helium (99.999%) was used as carrier gas at constant flow mode. An Agilent G4567A autosampler was used to inject 1.0 µL of the sample with a splitless injection mode into the inlet heated to 275 ºC with a total run time of 29.3 min. Oven temperature was programmed with the initial column temperature of 60 ºC and hold-time 2.0 min. The column temperature was increased to 200 ºC at a rate of 10 ºC/min and then heated again at a rate of 3 ºC/min until the temperature reached 240 ºC. No mass spectra were collected during the first 4 min. of the solvent delay. The transfer line and the ion source temperatures were 280 ºC and 230 ºC, respectively. The detector voltage was 1600 V and the electron energy was 70 eV. Mass spectral data were collected from 40 – 650 *m*/*z*. The names, structures, and qualities of peaks were determined through NIST mass spectral library search (Table 14).

4.3.3.5. Fractionation of the MeOH Extract of the Seeds of *Melilotus officinalis*

The MeOH extract (2.0 g) of the seeds of *M. officinalis* was first suspended in acetone (100.0 mL) and the acetone-insoluble fraction (125.0 mg) was collected by filtration. The

acetone insoluble material (50.0 mg) was subjected to column chromatography over Sephadex LH-20 using $CHCl_3$:MeOH (2:1) as eluent to yield compound **116** (12.0 mg).

The MeOH extract (2.0 g) was dissolved in MeOH:H_2O (1:1) (200.0 mL) and then extracted with EtOAc (300.0 mL). Removal of the solvent under reduced pressure afforded a gummy residue (650.0 mg). The EtOAc-soluble material (55.0 mg) was purified by PTLC using pet ether:EtOAc (90:10) as eluent to yield compound **65** (15.8 mg).

4.3.3.6. Physical and Spectroscopic Data of Compounds 65 and 116

1,2-Benzopyrone (Coumarin) (65): White powder, m. p. 70 – 71 °C, Lit.[105] m. p. 70.0 – 72.0 °C; UV (MeOH, λ_{max}, nm): 274; IR_v (KBr, cm^{-1}): 2960, 2929, 2858, 1730, 1288, 1274, 1123, 1073, 743; ^{1}H-NMR (400 MHz, $CDCl_3$, δ, ppm): 7.74 (1H, *d*, *J* = 9.60 Hz, H-4), 7.54 (2H, *m*, H-6, H-8), 7.34 (2H, *m*, H-5, H-7), and 6.46 (1H, *d*, *J* = 9.60 Hz, H-3). ^{13}C-NMR (100 MHz, $CDCl_3$, δ, ppm): 160.75 (C-2), 154.11 (C-9), 143.38 (C-4), 131.83 (C-7), 127.84 (C-5), 124.41 (C-6), 118.86 (C-10), 116.94 (C-3), 116.76 (C-8).[105]

***Cis*-Coumaric Acid-2-*O*-β-Glucopyranoside (*cis*-Melilotoside) (116)**: White crystals, m. p. 126.0 – 127.0 °C, Lit.[102] m. p. 126.1 – 127.3 °C; UV (MeOH, λ_{max}, nm): 261; IR_v (KBr, cm^{-1}): 3391, 2926, 2856, 1691, 1636, 1488, 1455, 1240, 1075, 1043, 760; ^{1}H-NMR (400 MHz, D_2O, δ, ppm): 7.34 (1H, *d*, *J* = 8.00 Hz, H-6), 7.30 (1H, *d*, *J* = 8.00 Hz, H-4), 7.12 (1H, *d*, *J* = 8.00 Hz, H-3), 7.09 (1H, *d*, *J* = 12.00 Hz, H-7), 7.03 (1H, *t*, *J* = 8.00 Hz, H-5), 6.05 (1H, *d*, *J* = 12.00 Hz, H-8), 5.05 (1H, *d*, *J* = 7.20 Hz, H-1′), 3.84 (1H, *dd*, *J* = 12.40, 2.30 Hz, H-6′), 3.67 (1H, *dd*, *J* = 12.40, 5.40 Hz, H-6′), 3.53 (3H, *m*, H-2′, H-3′, H-5′), 3.42 (1H, *m*, H-4′). ^{13}C-NMR (100 MHz, D_2O, δ, ppm): 171.74 (C-9), 153.81 (C-2), 137.14 (C-

7), 130.56 (C-4), 130.09 (C-6), 125.53 (C-1), 122.85 (C-5), 122.02 (C-8), 115.36 (C-3), 100.41 (C-1′), 76.12 (C-3′), 75.71 (C-5′), 72.93 (C-2′), 69.44 (C-4′), 60.58 (C-6′).[101-102]

4.3.4. Extraction and Characterization of Compounds from the Fresh Leaves of *Rhus glutinosa*

4.3.4.1. Extraction of the Fresh Leaves of *Rhus glutinosa* and DPPH Radical Scavenging Assay

The fresh leaves of *R. glutinosa* were ground by adding liquid nitrogen and crushing with mortar and pestle. The powdered material (1.0 kg) was extracted with DCM:MeOH (1:1, 2 × 3 L) for 48 h. The combined extract was concentrated under reduced pressure to afford a yellow residue (127.7 g). Part of the crude extract (95.4 g) was first dissolved in MeOH:H_2O (1:1, 200.0 mL) and extracted with *n*-hexane (3 × 200.0 mL) and then with EtOAc (3 × 200.0 mL) to give rise to the EtOAc-soluble fraction (39.5 g). The radical scavenging assay of the EtOAc-soluble fraction of the fresh leaves of *R. glutinosa* was assessed following the procedure described in **Section 4.3.1.4**.

4.3.4.2. Fractionation of Ethyl Acetate Fraction of the Fresh Leaves of *Rhus glutinosa*

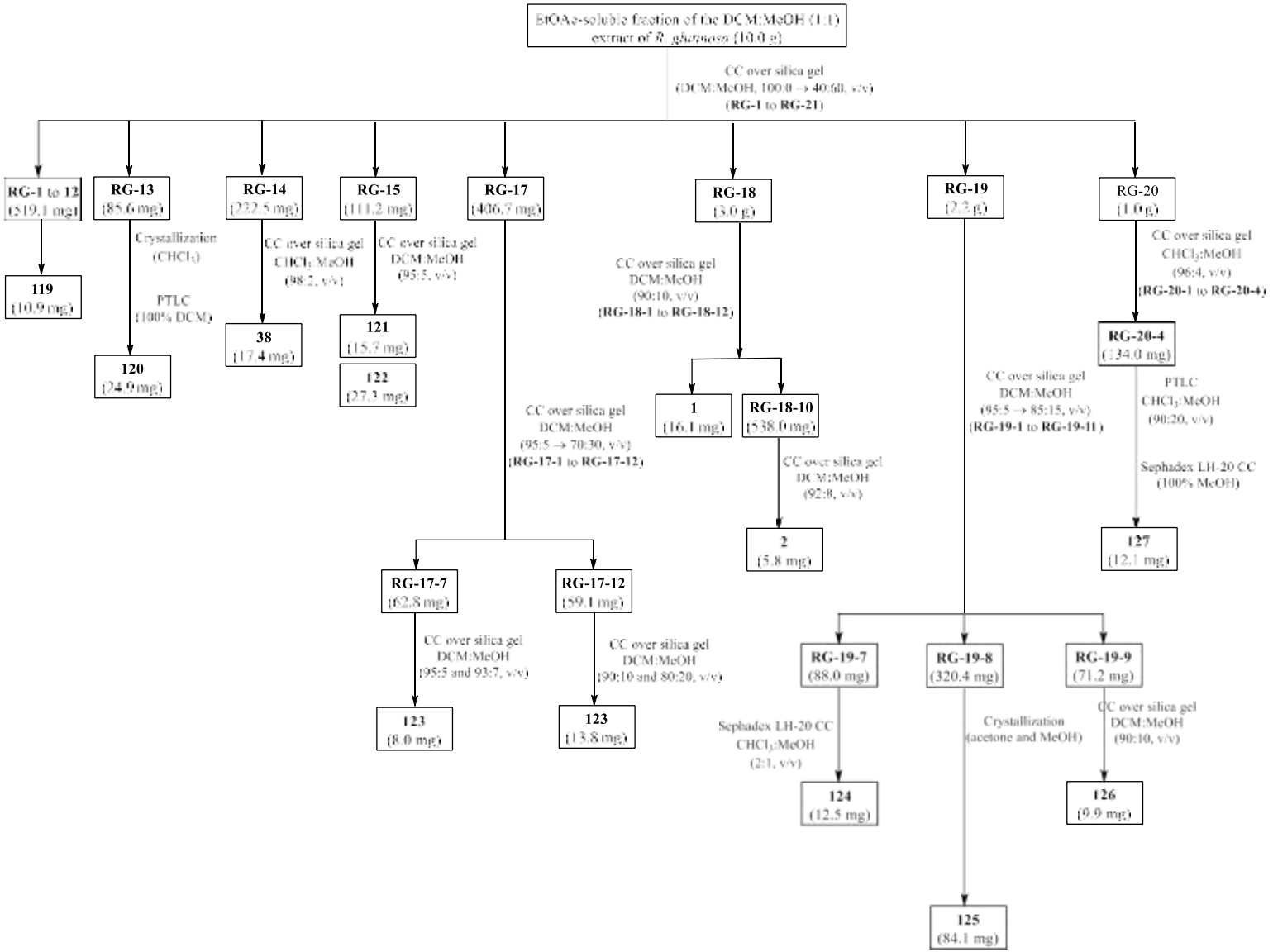
The EtOAc-soluble fraction of the DCM:MeOH (1:1) extract of the leaves *R. glutinosa* (10.0 g) was dissolved in a small quantity of MeOH and mixed with silica gel (10.0 g) to prepare a slurry. The slurry was dried *in vacuo* and loaded on a silica gel (200.0 g) column prepared in DCM. The column was run with a gradient of MeOH in DCM (0:100 → 40:60, v/v) to yield a total of 310 fractions and compound **119** (10.9 mg). The different fractions were combined into 21 groups (**RG–1** to **RG–21**) based on their TLC profiles.

Repeated crystallization of fraction **RG–13** (85.6 mg) from $CHCl_3$ and subsequent purification by PTLC using DCM as eluent yielded compound **120** (24.9 mg). Purification of about 222.5 mg of **RG-14** (1.1 g) by column chromatography over silica gel (30.0 g) using $CHCl_3$:MeOH (98:2, v/v) as eluent resulted in the isolation of compound **38** (17.4 mg). Fraction **RG–15** (111.2 mg) was dissolved in MeOH and adsorbed on silica gel (200.0 mg) and then subjected to column chromatography on silica gel (38.0 g) using DCM:MeOH (95:5, v/v) as eluent to afford compounds **121** (15.7 mg) and **122** (27.3 mg).

About 406.7 mg of fraction **RG–17** (1.3 g) was subjected to column chromatography over silica gel (40.0 g) using a gradient of MeOH in DCM (5:95 → 30:70, v/v) as eluent. A total of 90 subfractions were collected and combined into 12 groups (**RG–17–1** to **RG–17–12**) based on their TLC profiles. Subfraction **RG–17–7** (62.8 mg) was further purified over a short column of silica gel (15.0 g) using DCM:MeOH (95:5 and 93:7, v/v) as eluent to give compound **123** (8.0 mg). Purification of subfraction **RG–17–12** (59.1 mg) by chromatography over a column of silica gel (12.1 g) using DCM:MeOH (90:10 and 80:20, v/v) as eluent also resulted in the isolation of compound **123** (13.8 mg).

Fraction **RG–18** (3.0 g) was dissolved in MeOH and adsorbed on silica gel (3.0 g) and chromatographed over a column of silica gel (83.8 g) using DCM:MeOH (90:10, v/v) as eluent to give 12 subfractions (**RG–18-1** to **RG–18-12**) and pure compound **1** (16.1 mg). Subfraction **RG–18–10** (538.0 mg) was rechromatographed over a column of silica gel (15.0 g) using DCM:MeOH (98:2, v/v) as eluent to yield compound **2** (5.8 mg). Column chromatography of fraction **RG–19** (2.2 g) over silica gel (143.7 g) using DCM:MeOH (95:5 → 85:15, v/v) as eluent afforded 11 subfractions **RG–19-1** to **RG–19-11.** Column chromatography of subfraction **RG–19-7** (88.0 mg) over Sephadex LH-20 using

$CHCl_3$:MeOH (2:1, v/v) as eluent resulted in the isolation of compound **124** (12.5 mg). Repeated crystallization of subfraction **RG-19-8** (320.4 mg) from acetone and then from MeOH afforded compound **125 (**84.1 mg). Purification of subfraction **RG–19-9** (71.2 mg) by column chromatography over silica gel (15.0 g) using DCM:MeOH (90:10, v/v) as eluent gave compound **126** (9.9 mg). Fraction **RG-20** (1.0 g) was chromatographed over silica gel (100.0 g) using $CHCl_3$:MeOH (96:4, v/v) as eluent to furnish four subfractions, **RG-20-1** to **RG-20-4**. Subsequent purification of subfraction **RG-20-4** (134.0 mg) by PTLC ($CHCl_3$:MeOH, 90:20, v/v) and then by column chromatography over Sephadex LH-20 (100% MeOH) resulted in the isolation of compound **127** (12.1 mg).


EtOAc-soluble fraction of the DCM:MeOH (1:1) extract of R. glutinosa (10.0 g)
CC over silica gel (DCM:MeOH, 100:0 → 40:60, v/v) (RG-1 to RG-21)
RG-1 to 12 (519.1 mg)
RG-13 (85.6 mg)
RG-14 (232.5 mg)
RG-15 (111.2 mg)
RG-17 (406.7 mg)
RG-18 (3.0 g)
RG-19 (2.3 g)
RG-20 (1.0 g)
119 (10.9 mg)
Crystallization (CHCl3)
PTLC (100% DCM)
120 (24.9 mg)
CC over silica gel CHCl3:MeOH (98:2, v/v)
38 (17.4 mg)
CC over silica gel DCM:MeOH (95:5, v/v)
121 (15.7 mg)
122 (27.3 mg)
CC over silica gel DCM:MeOH (95:5 → 70:30, v/v) (RG-17-1 to RG-17-12)
CC over silica gel DCM:MeOH (90:10, v/v) (RG-18-1 to RG-18-12)
1 (16.1 mg)
RG-18-10 (538.0 mg)
CC over silica gel DCM:MeOH (92:8, v/v)
2 (5.8 mg)
CC over silica gel DCM:MeOH (95:5 → 85:15, v/v) (RG-19-1 to RG-19-11)
CC over silica gel CHCl3:MeOH (96:4, v/v) (RG-20-1 to RG-20-4)
RG-20-4 (134.0 mg)
PTLC CHCl3:MeOH (90:20, v/v)
Sephadex LH-20 CC (100% MeOH)
127 (12.1 mg)
RG-17-7 (62.8 mg)
RG-17-12 (59.1 mg)
CC over silica gel DCM:MeOH (95:5 and 93:7, v/v)
123 (8.0 mg)
CC over silica gel DCM:MeOH (90:10 and 80:20, v/v)
123 (13.8 mg)
RG-19-7 (88.0 mg)
RG-19-8 (320.4 mg)
RG-19-9 (71.2 mg)
Sephadex LH-20 CC CHCl3:MeOH (2:1, v/v)
124 (12.5 mg)
Crystallization (acetone and MeOH)
125 (84.1 mg)
CC over silica gel DCM:MeOH (90:10, v/v)
126 (9.9 mg)

4.3.4.3. Physical and Spectroscopic Data of Compounds Isolated from the Leaves of *Rhus glutinosa*

Pentacosanol (119): White amorphous powder, m. p. 67.0 – 69.0 °C; IR_v (KBr, cm^{-1}): 3370, 2917, 2849, 1644, 1473, 1463, 1449, 1304, 1245, 1221, 755; HRESIMS *m/z* 391.2906 $[M+Na]^+$ (calculated for $C_{25}H_{52}NaO$, 391.3916, Δ 0.101 mmu); ^{1}H-NMR (400 MHz, $CDCl_3$, δ, ppm): 3.66 (2H, *t*, *J* = 6.60 Hz, H-1), 1.59 (2H, *q*, *J* = 6.80 Hz, H-2), 1.27 (44H, *m*, H-3 – H-24), 0.90 (3H, *t*, *J* = 6.80 Hz, Me-25). ^{13}C-NMR (100 MHz, $CDCl_3$, δ, ppm): 63.12, 32.82, 31.94, 29.71, 29.63, 29.45, 29.38, 25.75, 22.70, 14.13.

5,7-Dihydroxy-4′-methoxyflavone (Acacetin) (120): Light yellow powder, m. p. 259.0 – 260.0 °C, Lit.[111] m. p. 254.6 – 257.5 °C; UV (MeOH, λ_{max}, nm): 270, 328; IR_v (KBr, cm^{-1}): 3411, 2924, 2853, 1651, 1627, 1607, 1564, 1510, 1432, 1384, 1240, 1187, 1166, 839, 825; HRESIMS *m/z* 271.0606 $[M - CH_3 + H]^+$ (calculated for $C_{15}H_{11}O_5$, 271.0606, Δ 0.0000 mmu); ^{1}H-NMR (400 MHz, Acetone-d_6, δ, ppm): 13.00 (1H, *s*, 5-OH), 8.05 (2H, *d*, *J* = 9.20 Hz, H-2′, 6′), 7.15 (2H, *d*, *J* = 9.20 Hz, H-3′, 5′), 6.70 (1H, *s*, H-3), 6.58 (1H, *d*, *J* = 2.00 Hz, H-8), 6.28 (1H, *d*, *J* = 2.00 Hz, H-6), 3.93 (3H, *s*, OCH_3-4′). ^{13}C-NMR (100 MHz, Acetone-d_6, δ, ppm): 182.20 (C-4), 164.19 (C-2), 163.90 (C-7), 162.84 (C-4′), 162.48 (C-5), 157.94 (C-9), 128.18 (C-2′, 6′), 123.48 (C-1′), 114.51 (3′, 5′), 104.45 (C-10), 103.67 (C-3), 98.9 (C-6), 93.9 (C-8), 55.09 (OCH_3-4′).[109]

3,5,7,4′-Tetrahydroxyflavone (Kaempferol) (38): Light yellow powder, m. p. 275.3 – 277.0 °C, Lit.[114] m. p. 278.0 – 279.0 °C; UV (MeOH, λ_{max}, nm): 266, 366; IR_v (KBr, cm^{-1}): 3326, 2924, 2853, 1658, 1607, 1511, 1376, 1168; HRESIMS *m/z* 287.0557 $[M+H]^+$ (calculated for $C_{15}H_{11}O_6$, 287.0556, Δ 0.0001 mmu); ^{1}H-NMR (400 MHz, Acetone-d_6, δ,

ppm): 12.21 (1H, *s*, 5-OH), 8.18 (2H, *d*, *J* = 8.80 Hz, H-2′, 6′), 7.04 (2H, *d*, *J* = 8.80 Hz, H-3′, 5′), 6.56 (1H, *d*, *J* = 1.60 Hz, H-8), 6.29 (1H, *d*, *J* = 1.60 Hz, H-6). ^{13}C-NMR (100 MHz, Acetone-d_6, δ, ppm): 175.73 (C-4), 164.10 (C-7), 161.45 (C-4′), 159.28 (C-9), 156.91 (C-5), 146.13 (C-2), 135.76 (C-3), 129.58 (C-2′, 6′), 122.45 (C-1′), 115.45 (C-3′, 5′), 103.27 (C-10), 98.27 (C-6), 93.61 (C-8).[114]

6-8′′-Binaringenin (Rhusflavanone) (**121**): Yellow amorphous powder, m. p. 203.5 – 205.3 °C, Lit.[74h] m. p. 206.0 – 208.0 °C; $[\alpha]_D^{25} - 69.33^0$ (*c* 0.15, MeOH); UV (MeOH, λ_{max}, nm): 224, 296; IR_v (KBr, cm^{-1}): 3430, 3200, 2924, 2853, 1635, 1618, 1401, 1385, 1170, 1093; HRESIMS *m/z* 543.1287 $[M+H]^+$ (calculated for $C_{30}H_{23}O_{10}$, 543.1291, Δ 0.0004 mmu); ^{1}H-NMR (400 MHz, MeOD-d_4, δ, ppm): 7.35 (2H, *d*, *J* = 8.40 Hz, H-2′, H-6′), 7.20 (2H, *d*, *J* = 8.40 Hz, H-2′′′, H-6′′′′), 6.83 (2H, *d*, *J* = 8.40 Hz, H-3′, H-5′), 6.74 (2H, *d*, *J* = 8.40 Hz, H-3′′′, H-5′′′), 6.05 (1H, *s*, H-6′′), 6.03 (1H, *s*, H-8), 5.37 (2H, *m*, H-2, H-2′′), 3.11 (2H, *m*, H-3, H-3′′), 2.73 (2H, *m*, H-3, H-3′′). ^{13}C-NMR (100 MHz, MeOD-d_4, δ, ppm): 196.88 (C-4), 196.51 (C-4′′), 165.54 (C-7), 165.51 (C-9), 163.39 (C-7′′), 162.69 (C-9′′), 161.89 (C-5′′), 161.41 (C-4′), 157.59 (C-4′′′), 157.14 (C-5), 130.07 (C-1′), 129.86 (C-1′′′), 127.68 (C-2′, 6′), 127.14 (C-2′′′, 6′′′), 114.92 (C-3′, 5′), 114.77 (C-3′′′, 5′′′), 102.24 (C-10′′), 101.89 (C-10), 101.09 (C-8′′), 99.91 (C-6), 95.38 (C-6′′), 94.41 (C-8), 79.15 (C-2), 78.48 (C-2′′), 42.77 (C-3), 42.49 (C-3′′).[74h,74i]

6-8′′-Naringeninyl Apigenin (Rhusflavone) (**122**): Light yellow powder, m. p. 238.9 – 240.1 °C, Lit.[74h] m. p. 230.0 – 232.0 °C; $[\alpha]_D^{25} - 100.00^0$ (*c* 0.13, MeOH); UV (MeOH, λ_{max}, nm): 228, 276, 297, 333; IR_v (KBr, cm^{-1}): 3419, 3236, 2924, 2853, 1638, 1610, 1516, 1450, 1365, 1290, 1239, 1177, 1159, 1090, 833; HRESIMS *m/z* 541.1135 $[M+H]^+$ (calculated for $C_{30}H_{21}O_{10}$: 541.1135, Δ 0.0000 mmu); ^{1}H-NMR (400 MHz, Acetone-d_6, δ,

ppm): 13.11 (1H, *s*, 5-OH), 12.64 (1H, *s*, 5″-OH), 7.68 (2H, *d*, *J* = 8.80 Hz, H-2‴, H-6‴), 7.45 (2H, *d*, *J* = 8.40 Hz, H-2′, H-6′), 6.95 (2H, *d*, *J* = 8.80 Hz, H-3′, H-5′), 6.92 (2H, *d*, *J* = 8.80 Hz, H-3‴, H-5‴), 6.66 (1H, *s*, H-3″), 6.42 (1H, *s*, H-6″), 6.23 (1H, *s*, H-8), 5.55 (1H, *dd*, *J* = 12.80, 3.00 Hz, H-2), 3.33 (1H, *dd*, *J* = 17.00, 12.80 Hz, H-3a), 2.83 (1H, *dd*, *J* = 17.00, 3.00 Hz, H-3b). ^{13}C-NMR (100 MHz, Acetone-d_6, δ, ppm): 196.53 (C-4), 182.60 (C-4″), 165.02 (C-7), 164.13 (C-2″), 163.11 (C-9), 162.78 (C-7″), 162.67 (C-5), 161.82 (C-5″), 160.92 (C-4‴), 157.89 (C-4′), 155.73 (C-9″), 129.83 (C-1′), 128.25 (C-2‴, 6‴), 128.21 (C-2′, 6′), 122.54 (C-1‴), 115.95 (C-3‴, 5‴), 115.35 (C-3′, 5′), 104.66 (C-10″), 102.90 (C-3″), 102.39 (C-6), 99.86 (C-10), 98.81 (C-6″), 98.69 (C-8″), 94.91 (C-8), 79.16 (C-2), 42.48 (C-3).[74h,74i]

Quercetin 3-*O*-*α*-Arabinofuranoside (Avicularin) (123): Yellow powder, m. p. 198.7 – 199.6 °C, Lit.[114] m. p. 200.0 – 201.0 °C; UV (MeOH, λ_{max}, nm): 257, 299, 354; IR$_v$ (KBr, cm^{-1}): 3410, 2959, 2924, 2853, 1654, 1606, 1502, 1384, 1364, 1200, 1113, 948; HRESIMS *m/z* 435.0913 $[M+H]^+$ (calculated for $C_{20}H_{19}O_{11}$: 435.0926, Δ 0.0014 mmu), 303.0449 ([M – 132.0419 (pentose unit) + H]$^+$; ^{1}H-NMR (400 MHz, MeOD-d_4, δ, ppm): 7.55 (1H, *d*, *J* = 2.00 Hz, H-2′), 7.52 (1H, *dd*, *J* = 8.40, 2.00 Hz, H-6′), 6.92 (1H, *d*, *J* = 8.40 Hz, H-5′), 6.42 (1H, *d*, *J* = 2.00 Hz, H-8), 6.23 (1H, *d*, *J* = 2.00 Hz, H-6), 5.49 (1H, br. *s*, H-1″), 4.35 (1H, *dd*, *J* = 3.00, 1.00 Hz, H-2″), 3.93 (1H, *dd*, *J* = 5.20, 3.20 Hz, H-3″), 3.88 (1H, *q*, *J* = 4.50 Hz, H-4″), 3.52 (2H, *dd*, *J* = 4.20, 2.20 Hz, H-5″). ^{13}C-NMR (100 MHz, MeOD-d_4, δ, ppm): 178.59 (C-4), 164.65 (C-7), 161.7 (C-5), 157.95 (C-2), 157.17 (C-9), 148.46 (C-4′), 144.96 (C-3′), 133.52 (C-3), 121.69 (C-1′), 121.57 (C-6′), 115.44 (C-2′), 115.04 (C-5′), 108.13 (C-1″), 104.23 (C-10), 98.49 (C-6), 93.36 (C-8), 86.61 (C-4″), 81.91 (C-2″), 77.29 (C-3″), 61.13 (C-5″).[114,121,123]

3,5,7,3′,4′-Pentahydroxyflavone (Quercetin) (1): Yellow powder, m. p. 309.0 – 310.0 °C, Lit.[125] m. p. 317.0 – 318.0 °C; UV (MeOH, λ_{max}, nm): 255, 371; IR_v (KBr, cm^{-1}): 3410, 2924, 2853, 1656, 1616, 1513, 1384, 1367, 1318, 1245, 1209, 1164, 1093, 819; HRESIMS *m/z* 303.0503 $[M+H]^+$ (calculated for $C_{15}H_{10}O_7$: 303.0499, Δ 0.0002 mmu); ^{1}H-NMR (400 MHz, Acetone-d_6, δ, ppm): 12.20 (1H, *s*, 5-OH), 7.84 (1H, *d*, *J* = 2.20 Hz, H-2′), 7.71 (1H, *dd*, *J* = 8.50, 2.20 Hz, H-6′), 7.01 (1H, *d*, *J* = 8.50 Hz, H-5′), 6.54 (1H, *d*, *J* = 2.00 Hz, H-8), 6.28 (1H, *d*, *J* = 2.00 Hz, H-6). ^{13}C-NMR (100 MHz, Acetone-d_6, δ, ppm): 175.68 (C-4), 164.14 (C-7), 161.41 (C-5), 156.87 (C-9), 147.49 (C-2), 146.08 (C-4′), 144.98 (C-3′), 135.86 (C-3), 122.85 (C-1′), 120.55 (C-6′), 115.36 (C-5′), 114.89 (C-2′), 103.23 (C-10), 98.27 (C-6), 93.57 (C-8).[119]

3,5,7,3′,4′,5′-Hexahydroxyflavone (Myricetin) (2): Light yellow powder, m. p. 320.2 – 321.9 °C, Lit.[125] m. p. 324.0 °C (dec.); UV (MeOH, λ_{max}, nm): 254, 305, 374; IR_v (KBr, cm^{-1}): 3392, 2924, 2853, 1660, 1610, 1514, 1453, 1384, 1319, 1206, 1166, 1028; HRESIMS *m/z* 319.0458 $[M+H]^+$ (calculated for $C_{15}H_{11}O_8$: 319.0454, Δ 0.0004 mmu); ^{1}H-NMR (400 MHz, Acetone-d_6, δ, ppm): 12.18 (1H, *s*, 5-OH), 7.44 (2H, *s*, H-2′, H-6′), 6.53 (1H, *d*, *J* = 2.00 Hz, H-8), 6.27 (1H, *d*, *J* = 2.00 Hz, H-6). ^{13}C-NMR (100 MHz, Acetone-d_6, δ, ppm): 175.63 (C-4), 164.09 (C-7), 161.41 (C-9), 156.83 (C-5), 146.07 (C-2), 145.52 (C-3′, 5′), 136.02 (C-4′), 135.53 (C-3), 121.86 (C-1′), 107.42 (C-2′, 6′), 103.22 (C-10), 98.24 (C-6), 93.51 (C-8).[125]

Quercetin 3-*O*-α-Rhamnoside (Quercitrin) (124): Yellow powder, m. p. 237.8 – 240.2 °C, Lit.[125] m. p. 240.0 °C (dec.); UV (MeOH, λ_{max}, nm): 257, 352; IR_v (KBr, cm^{-1}): 3411, 2924, 2853, 1655, 1608, 1500, 1453, 1361, 1202, 1168, 1088, 1060, 997; HRESIMS *m/z* 449.1077 $[M+H]^+$ (calculated for $C_{21}H_{21}O_{11}$: 449.1084, Δ 0.0007 mmu); ^{1}H-NMR (400

MHz, MeOD-d_4, δ, ppm): 7.36 (1H, *d*, *J* = 2.00 Hz, H-2′), 7.33 (1H, *dd*, *J* = 8.40, 2.00 Hz, H-6′), 6.93 (1H, *d*, *J* = 8.40 Hz, H-5′), 6.39 (1H, *d*, *J* = 2.00 Hz, H-8), 6.22 (1H, *d*, *J* = 2.00 Hz, H-6), 5.37 (1H, *d*, *J* = 1.60 Hz, H-1″), 4.24 (1H, *dd*, *J* = 1.60, 3.20 Hz, H-2″), 3.77 (1H, *dd*, *J* = 3.40, 9.40 Hz, H-3″), 3.41 (2H, *m*, H-4″, 5″), 0.96 (3H, *d*, *J* = 6.40 Hz, H-6″). ^{13}C-NMR (100 MHz, MeOD-d_4, δ, ppm): 178.27 (C-4), 164.49 (C-7), 161.83 (C-5), 157.92 (C-9), 157.14 (C-2), 148.40 (C-4′), 145.03 (C-3′), 134.85 (C-3), 121.60 (C-1′), 121.46 (C-6′), 115.56 (C-5′), 114.98 (C-2′), 104.52 (C-10), 102.16 (C-1″), 98.42 (C-6), 93.31 (C-8), 71.88 (C-4″), 70.75 (C-3″), 70.63 (C-2″), 70.51 (C-5″), 16.25 (C-6″).[125]

3,4,5-Trihydroxy-1-Cyclohexene-Carboxylic Acid (Shikimic Acid) (125): White powder, m. p. 186.5 – 187.2 °C, Lit.[128] m. p. 182.0 – 184.0 °C; UV (MeOH, λ_{max}, nm): 355; IR_v (KBr, cm^{-1}): 3482, 3385, 3220, 1682, 1648, 1455, 1294, 1276, 1091, 1072, 1060, 930; HRESIMS *m/z* 197.0422 $[M+Na]^+$ (calculated for $C_7H_{10}O_5Na$: 197.0426, Δ 0.0004 mmu); ^{1}H-NMR (400 MHz, D_2O, δ, ppm): 6.68 (1H, *dt*, *J* = 4.00, 2.00 Hz, H-2), 4.30 (1H, *t*, *J* = 4.00 Hz, H-3), 3.88 (1H, *dt*, *J* = 8.00, 5.80 Hz, H-5), 3.63 (1H, *dd*, *J* = 8.20, 4.20 Hz, H-4), 2.59 (1H, *ddt*, *J* = 18.20, 5.40, 1.40 Hz, H-6a), 2.08 (1H, *ddt*, *J* = 18.20, 6.20, 1.80 Hz, H-6b). ^{13}C-NMR (100 MHz, D_2O, δ, ppm): 170.15 (COOH), 137.12 (C-2), 129.71 (C-1), 70.96 (C-5), 66.51 (C-4), 65.69 (C-3), 30.25 (C-6).[128]

Quercetin 3-*O*-β-Galactoside (Hyperoside) (126): Yellow powder, m. p. 232.6 – 233.4 °C, Lit.[114] m. p. 234.0 – 236.0 °C; UV (MeOH, λ_{max}, nm): 258, 359; IR_v (KBr, cm^{-1}): 3431, 2923, 2852, 1656, 1608, 1509, 1499, 1454, 1384; HRESIMS *m/z* 487.0861 $[M+Na]^+$ (calculated for $C_{21}H_{20}O_{12}Na$: 487.0852, Δ 0.0009 mmu); ^{1}H-NMR (400 MHz, MeOD-d_4, δ, ppm): 7.86 (1H, *d*, *J* = 2.00 Hz, H-2′), 7.61 (1H, *dd*, *J* = 8.50, 2.00 Hz, H-6′), 6.89 (1H, *d*, *J* = 8.60 Hz, H-5′), 6.43 (1H, *d*, *J* = 2.00 Hz, H-8), 6.23 (1H, *d*, *J* = 2.00 Hz, H-6), 5.15

(1H, *d*, *J* = 8.00 Hz, H-1″), 3.88 (1H, *d*, *J* = 3.20 Hz, H-4″), 3.85 (1H, *dd*, *J* = 7.80, 9.40 Hz, H-2″), 3.67 (1H, *dd*, *J* = 6.00, 10.80 Hz, H-6″), 3.58 (2H, *m*, H-3″, 5″), 3.50 (1H, *m*, H-6″). ^{13}C-NMR (100 MHz, MeOD-d_4, δ, ppm): 178.16 (C-4), 164.72 (C-7), 161.62 (C-5), 157.52 (C-2), 157.08 (C-9), 148.57 (C-4′), 144.43 (C-3′), 134.44 (C-3), 121.61 (C-1′), 121.48 (C-6′), 116.38 (C-5′), 114.70 (C-2′), 104.26 (C-10), 104.08 (C-1″), 98.57 (C-6), 93.34 (C-8), 75.75 (C-5″), 73.69 (C-3″), 71.74 (C-2″), 68.66 (C-4″), 60.57 (C-6″).[121]

Myricetin-3-*O*-β-Galactopyranoside (127): Light yellow amorphous powder, m. p. 194.0 – 196.0 °C, Lit.[131] m. p. 196.0 – 198.0 °C; UV (MeOH, λ_{max}, nm): 257, 365; IR_v (KBr, cm^{-1}): 3326, 2924, 2853, 1658, 1607, 1511, 1376, 1169; HRESIMS *m/z* 481.0974 $[M+H]^+$ (calculated for $C_{21}H_{21}O_{13}$, 481.0982, Δ 0.0008 mmu); ^{1}H-NMR (400 MHz, MeOD-d_4, δ, ppm): 7.40 (2H, *s*, H-2′, 6′), 6.41 (1H, *d*, *J* = 2.00 Hz, H-8), 6.22 (1H, *d*, *J* = 2.00 Hz, H-6), 5.22 (1H, *d*, *J* = 7.60 Hz, H-1″), 3.90 (1H, *d*, *J* = 3.52 Hz, H-4″), 3.86 (1H, *dd*, *J* = 9.60, 7.84 Hz, H-2″), 3.68 (1H, *dd*, *J* = 11.26, 6.18 Hz, H-6″a), 3.60 (2H, *m*, H-3″, H-6″b), 3.53 (1H, *m*, H-5″). ^{13}C-NMR (100 MHz, MeOD-d_4, δ, ppm): 178.00 (C-4), 164.76 (C-7), 161.60 (C-5), 157.26 (C-2), 156.99 (C-9), 144.99 (C-3′, 5′), 136.75 (C-4′), 134.58 (C-3), 120.27 (C-1′), 108.52 (C-2′, 6′), 104.17 (C-10), 104.14 (C-1″), 98.50 (C-6), 93.27 (C-8), 75.82 (C-5″), 73.72 (C-3″), 71.88 (C-2″), 68.63 (C-4″), 60.52 (C-6″).[130-131]

4.3.5. Extraction and Characterization of Compounds from the Fresh Leaves of *Rhus natalensis*

4.3.5.1. Extraction and DPPH Radical Scavenging Assay of the Fresh Leaves of *Rhus natalensis*

The ground fresh leaves of *R. natalensis* (1.0 kg) were extracted with a mixture of DCM:MeOH (1:1, 2 × 3.0 L) for 48 h and the extract was concentrated to give a dark green residue (81.0 g). The crude extract (70.0 g) was first dissolved in a mixture of MeOH:H_2O (1:1, 200.0 mL) and then extracted with *n*-hexane (3 × 200.0 mL) and EtOAc (3 × 200.0 mL) successively. Removal of the solvents afforded *n*-hexane (24.2 g) and EtOAc (21.6 g) residues. The DPPH radical scavenging assay of the EtOAc-soluble portion of the DCM:MeOH extract of fresh leaves of *R. natalensis* was determined according to the procedure described in **Section 4.3.1.4**.

4.3.5.2. Fractionation of the EtOAc-Soluble Portion of the DCM:MeOH Extract of the Fresh Leaves of *Rhus natalensis*

The residue obtained from the EtOAc-soluble portion of the DCM:MeOH (1:1) extract of the fresh leaves of *R. natalensis* (10.0 g) was subjected to column chromatography over silica gel (155.0 g) using a gradient of MeOH in $CHCl_3$ (0:100 → 25:75, v/v) to give 55 fractions which were combined into seven groups (**RN-1** to **RN-7**). Fractionation of **RN-6** (970.0 mg) over a column of silica gel (80.0 g) using $CHCl_3$:MeOH (100:0 → 80:20, v/v) gave five subfractions (**RN-6-1** to **RN-6-5**). Subfraction **RN-6-2** (143.1 mg) was further purified by column chromatography over silica gel (50.0 g) using the solvent $CHCl_3$:MeOH (90:10, v/v) to afford **1** (7.9 mg). Fraction **RN-5** (1.7 g) was chromatographed on a column

of silica gel (82.0 g) using DCM:MeOH (90:10, v/v) and gave eight subfractions (**RN-5-1** to **RN-5-8**). PTLC separation of subfraction **RN-5-6** (79.1 mg) using DCM:MeOH (90:10, v/v) afforded two fractions (**RN-5-6-1** and **RN-5-6-2**). Rechromatography of fraction **RN-5-6-2** (46.5 mg) over silica gel (25.0 g) column using $CHCl_3$:MeOH (96:4, v/v) resulted in the isolation of **131** (15.7 mg). Crystallization of about 100.0 mg of fraction **RN-6** from MeOH yielded compound **132** (13.3 mg). The crude EtOAc fraction of *R. natalensis* and a mixture of the three isolated compounds, **1**, **131** and **132**, were compared by using HPLC.

4.3.5.3. Physical and Spectroscopic Data of Compounds Isolated from EtOAc-Soluble Portion of the DCM:MeOH Extract of the Leaves of *Rhus natalensis*

Quercetin 3-*O*-α-Arabinopyranoside (Guaijaverin) (131): Light yellow powder, m. p. 238.0 – 240.0 °C; Lit.[145] m. p. 240.0 °C; UV (MeOH, λ_{max}, nm): 257, 359; IR_v (KBr, cm^{-1}): 3475, 3373, 2923, 2853, 1656, 1599, 1559, 1509, 1457, 1358, 1292, 1202, 1069, 1026; ^{1}H-NMR (400 MHz, DMSO-d_6, δ, ppm): 7.67 (1H, *dd*, *J* = 8.44, 2.16 Hz, H-6′), 7.51 (1H, *d*, *J* = 2.28 Hz, H-2′), 6.84 (1H, *d*, *J* = 8.60 Hz, H-5′), 6.41 (1H, *d*, *J* = 2.00 Hz, H-8), 6.21 (1H, *d*, *J* = 2.04 Hz, H-6), 5.28 (1H, *d*, *J* = 5.32 Hz, H-1″), 3.76 (1H, *dd*, *J* = 7.20, 5.16 Hz, H-2″), 3.62 (2H, *m*, H-4″, H-5″), 3.51 (1H, *dd*, *J* = 7.20, 3.40 Hz, H-3″), 3.22 (1H, *dd*, *J* = 11.36, 2.52 Hz, H-5″). ^{13}C-NMR (100 MHz, DMSO-d_6, δ, ppm): 177.99 (C-4), 164.63 (C-7), 161.68 (C-5), 156.73 (C-2, C-9), 149.05 (C-4′), 145.45 (C-3′), 134.20 (C-3), 122.56 (C-6′), 121.35 (C-1′), 116.19 (C-2′), 115.82 (C-5′), 104.37 (C-10), 101.84 (C-1″), 99.12 (C-6), 93.96 (C-8), 72.09 (C-2″), 71.17 (C-3″), 66.52 (C-4″), 64.74 (C-5″).[121]

Apigenin 8-*C*-β-Glucopyranoside (Vitexin) (132): Yellow powder, m. p. 257.8 – 259.5 °C; Lit.[139] m. p. 263.0 °C; UV (MeOH, λ_{max}, nm): 270, 339; IR_v (KBr, cm^{-1}): 3414, 2924,

2853, 1738, 1655, 1618, 1510, 1465, 1383, 1039; ^{1}H-NMR (400 MHz, DMSO-d_6, δ, ppm): 13.18 (1H, *s*, 5-OH), 8.03 (2H, *d*, *J* = 8.84 Hz, H-2′, 6′), 6.89 (2H, *d*, *J* = 8.84 Hz, H-3′, 5′), 6.79 (1H, *s*, H-3), 6.28 (1H, *s*, H-6), 4.69 (1H, *d*, *J* = 9.84 Hz, H-1″), 3.84 (1H, *t*, *J* = 9.34 Hz, H-2″), 3.77 (1H, *dd*, *J* = 5.56, 11.54 Hz, H-6a″), 3.53 (2H, *m*, H-4″, 6b″), 3.25 (2H, *m*, H-3″, 5″). ^{13}C-NMR (100 MHz, DMSO-d_6, δ, ppm): 182.57 (C-4), 164.41 (C-2), 163.08 (C-7), 161.62 (C-4′), 160.86 (C-5), 156.47 (C-9), 129.44 (C-2′, 6′), 122.07 (C-1′), 116.28 (3′, 5′), 105.08 (C-8), 104.49 (C-10), 102.91 (C-3), 98.61 (C-6), 82.31 (C-5″), 78.65 (C-3″), 73.37 (C-1″), 71.96 (C-2″), 70.99 (C-4″), 61.74 (C-6″).[139]

5. Conclusion

In this research, essential oils from the rhizomes of *Cyperus esculentus* and the roots of *Carissa spinarum* together with the medicinal smoke obtained from the roots of *Carissa spinarum* were analyzed by GC-MS. The different components were characterized by matching their mass spectra with those of reference compounds recorded in NIST 2014 mass spectral library and confirmed by their retention indices. The antioxidant activity of the EtOAc extract of the rhizomes of *Cyperus esculentus* and the MeOH-soluble fraction of the smoke obtained from the roots of *Carissa spinarum* was also evaluated. The EtOAc extract of the rhizomes of *Cyperus esculentus* showed a 27.62% DPPH inhibition while the MeOH-soluble fraction of the smoke obtained from the roots of *Carissa spinarum* showed a 92.60% DPPH inhibition at concentration of 100.0 μg/mL. Phytochemical investigation of the EtOAc extract of the rhizomes of *Cyperus esculentus* resulted in the isolation of four sesquiterpenes, namely, caryophyllene oxide (**113**), cyperotundone (**12**), corymbolone (**114**) and tricyclohumuladiol (**115**).

The fatty acid composition of the *n*-hexane extract of the seeds of *M. officinalis* was determined by GC-MS analysis. Quantifications of components in the extract were made by using their relative area percentages and methyl palmitate external standards. Coumarin (**65**), which has been grouped among compounds that show hepatotoxicity,[100] was detected in significant amount in the seed oil. Therefore, it may not be suitable to use the oil for cooking purposes. Phytochemical investigation of the seeds of *M. officinalis* resulted in the isolation of *cis*-melilotoside (**116**) and coumarin (**65**) by column chromatography over Sephadex LH-20 and preparative TLC techniques.

The DPPH radical scavenging activities were evaluated for the MeOH fraction of the seeds of *M. officinalis* and the EtOAc-soluble portions of the DCM:MeOH extracts of fresh leaves of *R. glutinosa* and *R. natalensis*. The fractions exhibited 26.35, 94.89 and 94.94% DPPH inhibition at concentration of 50.0 μg/mL, respectively. The fact that both plant extracts showed strong antioxidant activities supports the traditional medicinal use of *Rhus* plants for treatment of inflammation[70b]. The EtOAc-soluble portions of the fresh leaves of *R. glutinosa* and *R. natalensis* were also phytochemically investigated. Thus, 12 compounds, namely, pentacosanol (**119**), acacetin (**120**), kaempferol (**38**), rhusflavanone (**121**), rhusflavone (**122**), avicularin (**123**), quercetin (**1**), myricetin (**2**), quercitrin (**124**), shikimic acid (**125**), hyperoside (**126**), and myricetin-3-*O*-β-galactopyranoside (**127**), were isolated and characterized from the EtOAc fraction of *R. glutinosa* and 3 compounds, namely, quercetin (**1**), guaijaverin (**131**) and vitexin (**132**) were obtained from the EtOAc fraction of *R. natalensis*. The isolated compounds were characterized by spectroscopic techniques including NMR, UV-vis, FTIR, and HRESIMS. The presence of flavonoids in the EtOAc-soluble portions of the fresh leaves of *R. glutinosa* and *R. natalensis* could be responsible for the observed high antioxidant activities of the leaves of *R. glutinosa* and *R. natalensis*. There were indications that very polar compounds existed in the extracts of the leaves of *R. natalensis.* Such compounds might be isolated from the leaves of *R. natalensis* by using reverse phase chromatographic techniques.

6. References

(1) Maplestone, R. A.; Stone, M. J.; Williams, D. H. *Gene* **1992,** *115*, 151-157.

(2) Molyneux, R. J.; Lee, S. T.; Gardner, D. R.; Panter, K. E.; James, L. F. *Phytochemistry* **2007,** *68*, 2973-2985.

(3) Dillard, C. J.; German, J. B. *J. Sci. Food Agric.* **2000,** *80*, 1744-1756.

(4) Yang, Y.; Deng, J. *TrAC, Trends Anal. Chem.* **2016,** *82*, 68-88.

(5) Mesfin, K.; Tekle, G.; Tesfay, T. *J. Med. Plants. Stud.* **2013,** *1*, 32-37.

(6) Azmir, J.; Zaidul, I. S. M.; Rahman, M. M.; Sharif, K. M.; Mohamed, A.; Sahena, F.; Jahurul, M. H. A.; Ghafoor, K.; Norulaini, N. A. N.; Omar, A. K. M. *J. Food Eng.* **2013,** *117*, 426-436.

(7) Altemimi, A.; Watson, D. G.; Kinsel, M.; Lightfoot, D. A. *Chem. Cent. J.* **2015,** *9*, 39-53.

(8) Altemimi, A.; Lakhssassi, N.; Baharlouei, A.; Watson, D. G.; Lightfoot, D. A. *Plants* **2017,** *6*, 42-64.

(9) Dehpour, A.; Babakhani, B.; Khazaei, S.; Asadi, M. *J. Med. Plants Res.* **2011,** *5*, 3667-3672.

(10) Costa, A. V.; Pinheiro, P. F.; de Queiroz, V. T.; Rondelli, V. M.; Marins, A. K.; Valbon, W. R.; Pratissoli, D. *J. Essent. Oil Bear. Pl.* **2015,** *18*, 374-381.

(11) Inga, H.; Sue, E.; Sebsebe, D., *Cyperus esculentus* L. In *Flora of Ethiopia and Eritrea*, The National Herbarium, Biology Department, Addis Ababa University and The Department of Systematic Botany, Uppsala University: Addis Ababa, Ethiopia, 1997; Vol. 6, p 451.

(12) Simpson, D. A.; Inglis, C. A. *Kew Bull.* **2001,** *56*, 257-360.

(13) De Vries, F. T. *Econ. Bot.* **1991,** *45*, 27–37.

(14) (a) Saalia, F. K.; Ellis, W. O.; Oduro, I.; Asante, F. A. *Am. J. Food Nutr.* **2014,** *2*, 49-54. (b) Belewu, M. A.; Belewu, K. Y. *Int. J. Agric. Biol.* **2007,** *5*, 785-787. (c) Sánchez-Zapata, E.; Fernández-López, J.; Angel Pérez-Alvarez, J. *Compr. Rev. Food Sci. Food Saf.* **2012,** *11*, 366-377. (d) Coşkuner, Y.; Ercan, R.; Karababa, E.; Nazlıcan, A. N. *J. Sci. Food Agric.* **2002,** *82*, 625-631. (e) Arafat, S. M.; Gaafar, A. M.; Basuny, A. M.; Nassef, S. L. *World Appl. Sci. J.* **2009,** *7*, 151-156.

(15) (a) Ozcan, M.; Gumuscu, A.; Er, F.; Arslan, D.; Ozkalp, B. *Chem. Nat. Compd.* **2010,** *46*, 276-276. (b) Jing, S.; Ouyang, W.; Ren, Z.; Xiang, H.; Ma, Z. *J. Sci. Food Agric.* **2013,** *93*, 1505-1509. (c) Eteshola, E.; Oraedu, A. C. I. *J. Am. Oil Chem.' Soc.* **1996,** *73*, 255-257. (d) Abdel, K. M.; Fath El-Rahman, A. *Int. J. Adv. Res.* **2016,** *4*, 1712-1718.

(16) Allouh, M. Z.; Daradka, H. M.; Ghaida, J. H. A. *BMC Complement. Altern. Med.* **2015,** *15*, 331-337.

(17) Mosquera, L. A.; Sims, C. A.; Bates, R. P.; O'keefe, S. F. *J. Food Sci.* **1996,** *61*, 856-861.

(18) (a) Barminas, J. T.; Maina, H. M.; Tahir, S.; Kubmarawa, D.; Tsware, K. *Bioresour. Technol.* **2001,** *79*, 87-89. (b) Zhang, H. Y.; Hanna, M. A.; Ali, Y.; Nan, L. *Ind. Crops Prod.* **1996,** *5*, 177-181.

(19) (a) Hassanein, H. D.; Nazif, N. M.; Aboutabl, E. A.; Hammouda, F. M. *J. Appl. Sci. Res.* **2011,** *7*, 2455-2461. (b) Onuoha, N. O.; Ogbusua, N. O.; Okorie, A. N.; Ejike, C. E. C. C. *J. Intercult. Ethnopharmacol.* **2017,** *6*, 290-295. (c) Oyedepo, T. A.; Odoje, O. F. *Res. Rev.: J. Pharm. Toxicol. Stud.* **2014,** *2*, 37-41.

(20) Jing, S.; wang, S.; Li, Q.; Zheng, L.; Yue, L.; Fan, S.; Tao, G. *Food Chem.* **2016,** *192*, 319-327.

(21) Olabiyi, A. A.; Oboh, G.; Akinyemi, A. J.; Ademiluyi, A. O.; Boligon, A. A.; Anraku de Campos, M. M. *J. Funct. Foods* **2017,** *34*, 152-158.

(22) Fabunmi, T. O.; Adigbo, S. O.; Adebayo, O. O. *J. Agric. Res.* **2017,** *55*, 185-196.

(23) (a) Anderson, J. W.; Smith, B. M.; Gustafson, N. J. *Am. J. Clin. Nutr.* **1994,** *59*, 1242S-1247S. (b) Anderson, J. W.; Baird, P.; Davis, R. H., Jr; Ferreri, S.; Knudtson, M.; Koraym, A.; Waters, V.; Williams, C. L. *Nutr. Rev.* **2009,** *67*, 188-205.

(24) (a) Adejuyitan, J. A. *Am. J. food Technol.* **2011,** *6*, 197-201. (b)Chevallier, A., In *The Encyclopedia of Medicinal Plants*, Dorling Kindersley Press: London, 1996; pp 48-51.

(25) Cantalejo, M. J. *J. Agric. Food. Chem.* **1997,** *45*, 1853-1860.

(26) Chukwuma, E. R.; Obioma, N.; Christopher, O. I. *Pak. J. Nutr.* **2010,** *9*, 709-715.

(27) Tames, R. S.; Gesto, M. D. V.; Vieitez, E. *Physiol. Plant.* **1973,** *28*, 195-200.

(28) (a) Kubmarawa, D.; Ogunwande, I. A.; Okorie, D. A.; Olawore, N. O.; Kasali, A. A. *Flavour Fragr. J.* **2005,** *20*, 640-641. (b) Hassanein, H. D.; Nazif, N. M.; Shahat, A. A.; Hammouda, F. M.; Aboutable, E.-S. A.; Saleh, M. A. *J. Essent. Oil Bear. Pl.* **2014,** *17*, 251-264. (c) Ekundayo, O.; Oderinde, R.; Ogundeyin, M.; Stahl-Biskup, E. *Flavour Fragr. J.* **1991,** *6*, 261-264.

(29) Vega-Morales, T.; Mateos-Díaz, C.; Pérez-Machín, R.; Wiebe, J.; Gericke, N. P.; Alarcón, C.; López-Romero, J. M. *Food Chem.* **2019,** *297*, 124896-124901.

(30) (a) Abu-Mustafa, E.; Fayez, M.; Gad, A.; Osman, F. *J. Org. Chem.* **1960,** *25*, 1269-1269. (b) Gugsa, T.; Yaya, E. E. *Am. J. Essent. Oil. Nat. Prod.* **2018,** *6*, 04-12.

(31) (a) Inga, H.; Sue, E.; Sileshi, N., *Carissa spinarum*. In *Flora of Ethiopia and Eritrea*, The National Herbarium, Biology Department, Addis Ababa University and The Department of Systematic Botany, Uppsala University: Addis Ababa, Ethiopia, 2003; Vol. 4, Part 1, p 90. (b) Reinhard, F.; Admasu, A., *Carissa edulis*. In *Honeybee Flora of Ethiopia*, Vier-Turme-Verlag, Benedict Press: Munsterschwarzach, Germany, 1994; pp 29-30.

(32) Al-yuossef, H. M.; Hassan, W. H. B. *Biomed. & Pharmacol. J.* **2012,** *5*, 09-18.

(33) Tolo, F. M.; Rukunga, G. M.; Muli, F. W.; Njagi, E. N. M.; Njue, W.; Kumon, K.; Mungai, G. M.; Muthaura, C. N.; Muli, J. M.; Keter, L. K.; Oishi, E.; Kofi-Tsekpo, M. W. *J. Ethnopharmacol.* **2006,** *104*, 92-99.

(34) (a) Ya'u, J.; Yaro, A. H.; Abubakar, M. S.; Anuka, J. A.; Hussaini, I. M. *J. Ethnopharmacol.* **2008,** *120*, 255-258. (b) Jawaid, T.; Argal, S.; Singh, S. *J. Pharm. Res.* **2011,** *4*, 1138-1140.

(35) Sehar, I.; Pal, H. C.; Shukla, S.; Bhushan, S.; Hamid, A.; Gupta, B. D.; Saxena, A. K. *J. Pharm. Pharmacol.* **2011,** *63*, 1078-1090.

(36) (a) Kirira, P. G.; Rukunga, G. M.; Wanyonyi, A. W.; Muregi, F. M.; Gathirwa, J. W.; Muthaura, C. N.; Omar, S. A.; Tolo, F.; Mungai, G. M.; Ndiege, I. O. *J. Ethnopharmacol.* **2006,** *106*, 403-407. (b) Kebenei, J.; Ndalut, P.; Sabah, A. *Int. J. Appl. Res. Nat. Prod.* **2011,** *4*, 1-5.

(37) Ibrahim, H.; Bolaji, R.; Abdurrahman, E.; Shok, M.; Ilyas, N.; Habib, A. *Chem. Class J.* **2005,** *2*, 15-18.

(38) Ibrahim, H.; Abdulrahman, E. M.; Shok, M.; Ilyas, N.; Musa, K. Y.; Ukandu, I. *Afr. J. Biotechnol.* **2007,** *6*, 1233-1235.

(39) Hegde, K.; Joshi, A. B. *Der Pharm. Lett.* **2010,** *2*, 255-260.

(40) Nedi, T.; Mekonnen, N.; Urga, K. *J. Ethnopharmacol.* **2004,** *95*, 57-61.

(41) El-Fiky, F. K.; Abou-Karam, M. A.; Afify, E. A. *J. Ethnopharmacol.* **1996,** *50*, 43-47.

(42) Sanwal, R.; Chaudhary, A. K. *J. Ethnopharmacol.* **2011,** *135*, 792-796.

(43) Omino, E. A.; Kokwaro, J. O. *J. Ethnopharmacol.* **1993,** *40*, 167-180.

(44) (a) Achenbach, H.; Waibel, R.; Addae-Mensah, I. *Phytochemistry* **1983,** *22*, 749-753. (b) Achenbach, H.; Waibel, R.; Addae-Mensah, I. *Phytochemistry* **1985,** *24*, 2325-2328.

(45) Bentley, M. D.; Brackett, S. R.; Chapya, A. *J. Nat. Prod.* **1984,** *47*, 1056-1057.

(46) Rao, R. J.; Kumar, U. S.; Reddy, S. V.; Tiwari, A. K.; Rao, J. M. *Nat. Prod. Res.* **2005,** *19*, 763-769.

(47) Al-Youssef, H. M.; Hassan, W. H. B. *Arabian J. Chem.* **2017,** *10*, 109-113.

(48) Karunakar, H.; Satyanarayana, D.; Joshi, A. B. *J. Pharm. Sci.* **2012,** *2*, 55-59.

(49) Wangteeraprasert, R.; Lipipun, V.; Gunaratnam, M.; Neidle, S.; Gibbons, S.; Likhitwitayawuid, K. *Phytother. Res.* **2012,** *26*, 1496-1499.

(50) Inga, H.; Sue, E., *Melilotus suaveolens*. In *Flora of Ethiopia*, The National Herbarium, Biology Department, Addis Ababa University and The Department of Systematic Botany, Uppsala University: Addis Ababa, Ethiopia, 1989; Vol. 3, p 245.

(51) Udayama, M.; Kinjo, J.; Yoshida, N.; Nohara, T. *Chem. Pharm. Bull.* **1998,** *46*, 526-527.

(52) (a) Hamid, A.; Raina, A. *Int. J. Sci. Res.* **2014,** *3*, 538-545. (b) Kang, S. S.; Lim, C.-H.; Lee, S. Y. *Arch. Pharm. Res.* **1987,** *10*, 9-13.

(53) *European Union Herbal Monograph on Melilotus officinalis (L.) Lam., Herba* European Medicines Agency: Committee on Herbal Medicinal Products: London, UK, 2008.

(54) Pleşca-Manea, L.; Pârvu, A. E.; Pârvu, M.; Taaˇmaş, M.; Buia, R.; Puia, M. *Phytother. Res.* **2002,** *16*, 316-319.

(55) (a) Pourmorad, F.; Hosseinimehr, S.; Shahabimajd, N. *Afr. J. Biotechnol.* **2006,** *5*, 1142-1145. (b) Miliauskas, G.; Venskutonis, P.; Van Beek, T. *Food Chem.* **2004,** *85*, 231-237.

(56) Trouillas, P.; Calliste, C.-A.; Allais, D.-P.; Simon, A.; Marfak, A.; Delage, C.; Duroux, J.-L. *Food Chem.* **2003,** *80*, 399-407.

(57) Pastorino, G.; Marchetti, C.; Borghesi, B.; Cornara, L.; Ribulla, S.; Burlando, B. *Ind. Crops Prod.* **2017,** *96*, 158-164.

(58) Kang, S. S.; Lee, Y.-S.; Lee, E.-B. *Kor. J. Pharmacogn.* **1987,** *18*, 89-93.

(59) Casley-Smith, J. R.; Morgan, R. G.; Piller, N. B. *N. Engl. J. Med.* **1993,** *329*, 1158-1163.

(60) Grieve, M.; Leyel, C. F., Melilot. In *A Modern Herbal: The Medicinal, Culinary, Cosmetic and Economic Properties, Cultivation and Floklore of Herbs, Grasses, Fungi, Shrubs and Trees with All Their Modern Scientific Uses,* Dover Publications: New York, 1971; Vol. 2, pp 525-527.

(61) Duke, J. A., Yellow Sweet Clover (*Melilotus officinalis* Lam.). In *Handbook of Medicinal Herbs*, 2nd ed.; CRC press: Boca Raton, FL, 2002; pp 806-807.

(62) Kaur, S.; Sharma, A.; Bedi, P. M. S. *JBAPN* **2017,** *7*, 379-390.

(63) (a) Gîrd, C. E.; Duţu, L. E.; Lidia, M.; Popescu, M. P.; Sterie, A. T. *Farmacia* **2009,** *57*, 184-191. (b) Safarpour, A. R.; Kaviyani, F.; Sepehrimanesh, M.; Ahmadi, N.; Koohi Hosseinabadi, O.; Tanideh, N.; Showraki, N. *Ann. Colorectal Res.* **2015,** *3*, 295 - 211.

(64) Alamgeer, Z.; Qaisar, M.; Uttra, A.; Ahsan, H.; Khan, K.; Khan, I.; Saleem, M.; Khadijai, A. H.; Sharif, A.; Younis, W. *Acta. Pol. Pharm. Drug Res.* **2017,** *74*, 903-909.

(65) Mladenović, K.; Muruzović, M.; Stefanović, O.; Vasić, S.; Čomić, R. *J. Anim. Plant Sci.* **2016,** *26*, 1436-1444.

(66) Khan, R. U.; Mehmood, S.; Khan, S. U. *Pak. J. Pharm. Sci.* **2018,** *31*, 57-67.

(67) (a) Quijano-Celis, C. E.; Pino, J. A.; Morales, G. *J. Essent. Oil Bear. Pl.* **2010,** *13*, 313-315. (b) Gudzenko, A. V.; Vinogradov, B. A. *World Appl. Sci. J.* **2014,** *29*, 171-172. (c) Hirakawa, T.; Okawa, M.; Kinjo, J.; Nohara, T. *Chem. Pharm. Bull.* **2000,** *48*, 286-287. (d) Ilhan, M.; Ali, Z.; Khan, I. A.; Küpeli Akkol, E. *Nat. Prod. Res.* **2019,** *33*, 1856-1861. (e) Kang, S. S.; Lee, Y. S.; Lee, E. B. *Arch. Pharm. Res.* **1988,** *11*, 197-202. (f) Kang, S. S.; Woo, W. S. *J. Nat. Prod.* **1988,** *51*, 335-338. (g) Khodakov, G. V. *Chem. Nat. Compd.* **2010,** *46*, 572-575. (h) Liu, Y.-T.; Gong, P.-H.; Xiao, F.-Q.; Shao, S.; Zhao, D.-Q.; Yan, M.-M.; Yang, X.-W. *Molecules* **2018,** *23*, 271-282. (i) Suhail, A. M.; Mohtasheem, M.; Azhar, I.; Hasan, M.; Bano, H. *J. Basic Appl. Sci.* **2008,** *4*, 89-94. (j) Sutiashvili, M. G.; Alaniya, M. D. *Chem. Nat. Compd.* **1999,** *35*, 584-584. (k) Bubenchikova, V. N.; Drozdova, I. L. *Pharm. Chem. J.* **2004,** *38*, 195-196. (l) Dombrowicz, E.; Swiatek, L.; Guryn, R.; Zadernowski, R.

Pharmazie **1991,** *46*, 156-157. (m) Bakoglu, A.; Kiliç, Ö.; Kökten, K. *Anal. Chem. Lett.* **2016,** *6*, 174-180.

(68) Gallant, J. B.; Kemp, J. R.; Lacroix, C. R. *Int. J. Plant Sci.* **1998,** *159*, 539-549.

(69) Bajracharya, D. *Z. Lebensm. Unters. Forsch.* **1980,** *171*, 363-366.

(70) (a) Sezik, E.; Tabata, M.; Yesilada, E.; Honda, G.; Goto, K.; Ikeshiro, Y. *J. Ethnopharmacol.* **1991,** *35*, 191-196. (b) Mossa, J. S.; Rafatullah, S.; Galal, A. M.; Al-Yahya, M. A. *Int. J. Pharmacognos* **1995,** *33*, 242-246.

(71) Bhattarai, N. K. *Int. J. Pharmacognos* **1991,** *29*, 284-295.

(72) Ahmed, M. S.; Galal, A. M.; Ross, S. A.; Ferreira, D.; ElSohly, M. A.; Ibrahim, A.-R. S.; Mossa, J. S.; El-Feraly, F. S. *Phytochemistry* **2001,** *58*, 599-602.

(73) (a) Choi, W.; Jung, H.; Kim, K.; Lee, S.; Yoon, S.; Park, J.; Kim, S.; Cheon, S.; Eo, W.; Lee, S. *J. Biomed. Biotechnol.* **2011,** *2012*, 1-7. (b) Lin, Y.-M.; Anderson, H.; Flavin, M. T.; Pai, Y.-H. S.; Mata-Greenwood, E.; Pengsuparp, T.; Pezzuto, J. M.; Schinazi, R. F.; Hughes, S. H.; Chen, F.-C. *J. Nat. Prod.* **1997,** *60*, 884-888.

(74) (a) Lin, Y.-m.; Chen, F.-c. *Tetrahedron Lett.* **1973,** *14*, 4747-4750. (b) Fa-Ching, C.; Yuh-Meei, L.; Jung-Chung, W. *Phytochemistry* **1974,** *13*, 1571-1574. (c) Lin, Y.-M.; Chen, F.-C.; Lee, K.-H. *Planta Med.* **1989,** *55*, 166-168. (d) Fa-Ching, C.; Yuh-Meei, L.; Chi-Ming, L. *Phytochemistry* **1974,** *13*, 276-278. (e) Yuh-Meei, L.; Fa-Ching, C. *Phytochemistry* **1974,** *13*, 657-658. (f) Chen, F.-C.; Lin, Y.-M. *Phytochemistry* **1975,** *14*, 1644-1647. (g) Lin, Y.-m.; Chen, F.-c. *Phytochemistry* **1974,** *13*, 1617-1619. (h) Shrestha, S.; Park, J.-H.; Lee, D.-Y.; Cho, J.-G.; Cho, S.; Yang, H.-J.; Yong, H.-I.; Yoon, M.-S.; Han, D.-S.; Baek, N.-I. *J. Ethnopharmacol.* **2012,** *142*, 213-220. (i) Shrestha, S.; Park, J.-H.; Lee, D.-Y.; Cho, J.-G.; Seo, W.-

D.; Kang, H. C.; Yoo, K.-H.; Chung, I.-S.; Jeon, Y.-J.; Yeon, S.-W.; Baek, N.-I. *J. Korean Soc. Appl. Biol. Chem.* **2012,** *55*, 557-562. (j) Mwangi, H. M.; Mabusela, W. T.; Abegaz, B. M.; Martin, O. O. *J. Med. Plants Res.* **2013,** *7*, 619-623. (k) Svenningsen, A. B.; Madsen, K. D.; Liljefors, T.; Stafford, G. I.; Staden, J. v.; Jäger, A. K. *J. Ethnopharmacol.* **2006,** *103*, 276-280.

(75) (a) Young, D. A. *Am. J. Bot.* **1979,** *66*, 502-510. (b) Hattori, S.; Matsuda, H. *Arch. Biochem. Biophys.* **1952,** *37*, 85-89. (c) Mossa, J. S.; Sattar, E. A.; Abou-Shoer, M.; Galal, A. M. *Int. J. Pharmacognos* **1996,** *34*, 198-201. (d) Alqasoumi, S. I.; Basudan, O. A.; Alam, P.; Abdel-Kader, M. S. *Pak. J. Pharm. Sci.* **2016,** *29*, 97-103.

(76) (a) Bagchi, A.; Sahai, M.; Ray, A. B. *Planta Med.* **1985,** *51*, 467-468. (b) Matata, D. Z.; Moshi, M. J.; Machumi, F.; Ngassapa, O. D.; Swanepoel, B.; Oosthuizen, K.; Venables, L.; Koekemoer, T.; Heydenreich, M.; Kazyoba, P. E.; van de Venter, M. *Phytochem. Lett.* **2020,** *36*, 120-126. (c) Njoroge, P. W.; Opiyo, S. A. *Am. J. Chem.* **2019,** *9*, 150-158. (d) Wu, P.-L.; Lin, S.-B.; Huang, C.-P.; Chiou, R. Y. Y. *J. Nat. Prod.* **2002,** *65*, 1719-1721.

(77) Du, Y.; Oshima, R.; Iwatsuki, H.; Kumanotani, J. *J. Chromatogr. A* **1984,** *295*, 179-186.

(78) Sung, C.-K.; Akiyama, T.; Sankawa, U.; Iitaka, Y.; Han, D.-S. *J. Chem. Soc., Chem. Commun.* **1980,** *19*, 909-910.

(79) (a) Masesane, I. B.; Yeboah, S. O.; Liebscher, J.; Mügge, C.; Abegaz, B. M. *Phytochemistry* **2000,** *53*, 1005-1008. (b) Mdee, L. K.; Yeboah, S. O.; Abegaz, B. M. *J. Nat. Prod.* **2003,** *66*, 599-604.

(80) Inga, H.; Sue, E., *R. glutlnosa A. Rich.* In *Flora of Ethiopia and Eritrea*, The National Herbarium, Biology Department, Addis Ababa University and The Department of Systematic Botany, Uppsala University: Addis Ababa, Ethiopia, 1989; Vol. 3, p 528.

(81) Inga, H.; Sue, E., *R. natalensis* Krauss. In *Flora of Ethiopia*, The National Herbarium, Biology Department, Addis Ababa University and The Department of Systematic Botany, Uppsala University: Addis Ababa, Ethiopia, 1989; Vol. 3, pp 523-524.

(82) (a) Geissler, P. W.; Harris, S. A.; Prince, R. J.; Olsen, A.; Odhiambo, R. A.; Oketch-Rabah, H.; Madiega, P. A.; Andersen, A.; Mølgaard, P. *J. Ethnopharmacol.* **2002,** *83*, 39-54. (b) Kamuhabwa, A.; Nshimo, C.; de Witte, P. *J. Ethnopharmacol.* **2000,** *70*, 143-149. (c) Jeruto, P.; Lukhoba, C.; Ouma, G.; Otieno, D.; Mutai, C. *J. Ethnopharmacol.* **2008,** *116*, 370-376. (d) Gathirwa, J. W.; Rukunga, G. M.; Mwitari, P. G.; Mwikwabe, N. M.; Kimani, C. W.; Muthaura, C. N.; Kiboi, D. M.; Nyangacha, R. M.; Omar, S. A. *J. Ethnopharmacol.* **2011,** *134*, 434-442. (e) Omwenga, E. O.; Hensel, A.; Shitandi, A.; Goycoolea, F. M. *J. Ethnopharmacol.* **2015,** *176*, 508-514. (f) Ssegawa, P.; Kasenene, J. M. *J. Ethnopharmacol.* **2007,** *113*, 521-540. (g) Stafford, G. I.; Pedersen, M. E.; van Staden, J.; Jäger, A. K. *J. Ethnopharmacol.* **2008,** *119*, 513-537. (h) Chinsembu, K. C.; Hedimbi, M. *J. Ethnobiol. Ethnomed.* **2010,** *6*, 25-33. (i) Mugisha, M. K.; Asiimwe, S.; Namutebi, A.; Borg-Karlson, A.-K.; Kakudidi, E. K. *J. Ethnopharmacol.* **2014,** *155*, 194-202. (j) Kisangau, D. P.; Lyaruu, H. V. M.; Hosea, K. M.; Joseph, C. C. *J. Ethnobiol.*

Ethnomed. **2007,** *3*, 29-36. (k) Orech, F. O.; Schwarz, J. G. *S. Afr. J. Bot.* **2017,** *108*, 278-280.

(83) (a) Homer, K. A.; Manji, F.; Beighton, D. *J. Clin. Periodontol.* **1992,** *19*, 305-310. (b) Homer, K. A.; Manji, F.; Beighton, D. *Arch. Oral Biol.* **1990,** *35*, 421-424.

(84) Gathirwa, J. W.; Rukunga, G. M.; Njagi, E. N. M.; Omar, S. A.; Mwitari, P. G.; Guantai, A. N.; Tolo, F. M.; Kimani, C. W.; Muthaura, C. N.; Kirira, P. G.; Ndunda, T. N.; Amalemba, G.; Mungai, G. M.; Ndiege, I. O. *J. Ethnopharmacol.* **2008,** *115*, 223-231.

(85) Jäger, A. K.; Knap, D. M.; Nielsen, B.; Stafford, G. I.; Van Staden, J. *S. Afr. J. Bot.* **2012,** *78*, 312-314.

(86) Mengistu, G.; Hoste, H.; Karonen, M.; Salminen, J. P.; Hendriks, W. H.; Pellikaan, W. F. *Vet. Parasitol.* **2017,** *237*, 110-116.

(87) Parker, M. E.; Chabot, S.; Ward, B. J.; Johns, T. *J. Ethnopharmacol.* **2007,** *114*, 146-152.

(88) Kariuki, H. N.; Kanui, T. I.; Yenesew, A.; Mbugua, P. M.; Patel, N. B. *Phytopharmacology* **2012,** *2*, 312-317.

(89) Korir, R.; Kimani, C.; Gathirwa, J.; Wambura, M.; Bii, C. *Afr. J. Health Sci.* **2012,** *20*, 4-10.

(90) Mueller-Harvey, I.; Hartley, R. D.; Reed, J. D. *J. Sci. Food Agric.* **1987,** *39*, 1-14.

(91) Furth, D. G.; Young, D. A. *Oecologia* **1988,** *74*, 496-500.

(92) Choudhary, M. I.; Siddiqui, Z. A.; Nawaz, S. A.; Atta ur, R. *J. Nat. Prod.* **2006,** *69*, 1429-1434.

(93) Komai, K.; Shimizu, M.; Tang, C.; Tsutsui, H. *Mem. Fac. Agri. Kinki Univ.* **1994,** *27*, 39-45.

(94) Xu, Y.; Zhang, H.-W.; Wan, X.-C.; Zou, Z.-M. *Magn. Reson. Chem.* **2009,** *47*, 527-531.

(95) (a) Hikino, H.; Aota, K.; Takemoto, T. *Chem. Pharm. Bull.* **1965,** *13*, 628-630. (b) Hikino, H.; Aota, K.; Takemoto, T. *Chem. Pharm. Bull.* **1966,** *14*, 890-896.

(96) Garbarino, J. A.; Gambaro, V.; Chamy, M. C. *J. Nat. Prod.* **1985,** *48*, 323-325.

(97) Nyasse, B.; tih, R. G.; Sondengam, B. L.; Martin, M. T.; Bodo, B. *Phytochemistry* **1988,** *27*, 179-181.

(98) Li, R. T.; Zhao, A. H.; Sheng, Y. H.; Na, Z.; Sun, H. D. *J. Asian Nat. Prod. Res.* **2005,** *7*, 847-852.

(99) Xu, F.; Morikawa, T.; Matsuda, H.; Ninomiya, K.; Yoshikawa, M. *J. Nat. Prod.* **2004,** *67*, 569-576.

(100) Lake, B. G.; Grasso, P. *Fundam. Appl. Toxicol.* **1996,** *34*, 105-117.

(101) Sadati, N.; Jenett-Siems, K.; Siems, K.; Ardekania, M. R. S.; Hadjiakhoondi, A.; Akbarzadeh, T.; Ostad, S. N.; Khanavi, M. *Z. Naturforsch., C* **2012,** *67*, 275-281.

(102) Canuto, K. M.; Silveira, E. R.; Bezerra, A. M. E. *Quim. Nova* **2010,** *33*, 662-666.

(103) Drake, E. N.; Brown, C. E. *J. Chem. Educ.* **1977,** *54*, 124-127.

(104) (a) Ferreira, F. P.; de Oliveira, D. C. R. *Tetrahedron Lett.* **2010,** *51*, 6856-6859. (b) Esposito, A.; Fiorentino, A.; D'Abrosca, B.; Izzo, A.; Cefarelli, G.; Golino, A.; Monaco, P. *J. Plant Interact.* **2008,** *3*, 199-210.

(105) Ghareeb, M. A.; Saad, A. M.; Abdou, A. M.; Refahy, L. A.-G.; Ahmed, W. S. *Orient. J. Chem.* **2016,** *32*, 3053-3061.

(106) (a) Kosuge, T.; Conn, E. E. *J. Biol. Chem.* **1961,** *236*, 1617-1621. (b) Stoker, J.; Bellis, D. *J. Biol. Chem.* **1962,** *237*, 2303-2305.

(107) (a) García, M. D.; Sáenz, M. T.; Ahumada, M. C.; Cert, A. *J. Chromatogr. A* **1997,** *767*, 340-342. (b) Pande, A.; Shukla, Y. N.; Tripathi, A. K. *Phytochemistry* **1995,** *39*, 709-711. (c) Sowmya, S.; Perumal, P. C.; Ravi, S.; Anusooriya, P.; Shanmughavel, P.; Murugesh, E.; Chaithanya, K. K.; Gopalakrishnan, V. K. *Jordan J. Biol. Sci.* **2021,** *14*, 359-365.

(108) Mabry, T. J.; Markham, K. R.; Thomas, M. B., The Ultraviolet Spectra of Flavones and Flavonols. In *The Systematic Identification of Flavonoids*, Springer-Verlag: New York, 1970; pp 41-56.

(109) Gomes, R. A.; Ramirez, R. R. A.; Maciel, J. K. d. S.; Agra, M. d. F.; Souza, M. d. F. V. d.; Falcão-Silva, V. S.; Siqueira-Junior, J. P. *Quim. Nova* **2011,** *34*, 1385-1388.

(110) Silverstein, R. M.; Webster, F. X.; Kiemle, D. J., Magnetic Equivalence (Spin-Coupling Equivalence). In *Spectrometric Identification of Organic Compounds*, 7th ed.; John Wiley & Sons. Inc.: New Jersey, USA, 2005; pp 162-164.

(111) Sakamura, S.; Terayama, Y.; Kawakatsu, S.; Ichihara, A.; Saito, H. *Agric. Biol. Chem.* **1980,** *44*, 2951-2954.

(112) Kumarasamy, Y.; Cox, P. J.; Jaspars, M.; Nahar, L.; Sarker, S. D. *Nat. Prod. Commun.* **2006,** *1*, 641-644.

(113) Semwal, R. B.; Semwal, D. K.; Combrinck, S.; Trill, J.; Gibbons, S.; Viljoen, A. *Phytochem. Lett.* **2019,** *32*, 56-65.

(114) Xiao, Z. P.; Wu, H. K.; Wu, T.; Shi, H.; Hang, B.; Aisa, H. A. *Chem. Nat. Compd.* **2006,** *42*, 736-737.

(115) Sinha, S. C.; Sahai, M.; Ray, A. B. *J. Nat. Prod.* **1986,** *49*, 546-546.

(116) Chen, F.-C.; Lin, Y.-M. *J. Chem. Soc., Perkin Trans. 1* **1976,** *1*, 98-101.

(117) Pelter, A.; Warren, R.; Chexal, K. K.; Handa, B. K.; Rahman, W. *Tetrahedron* **1971,** *27*, 1625-1634.

(118) Clark-Lewis, J. *Aust. J. Chem.* **1968,** *21*, 2059-2075.

(119) Liu, H.; Mou, Y.; Zhao, J.; Wang, J.; Zhou, L.; Wang, M.; Wang, D.; Han, J.; Yu, Z.; Yang, F. *Molecules* **2010,** *15*, 7933-7945.

(120) Silverstein, R. M.; Webster, F. X.; Kiemle, D. J., Pople Notation. In *Spectrometric Identification of Organic Compounds*, 7th ed.; John Wiley & Sons. Inc.: New Jersey, USA, 2005; p 147.

(121) Park, B.-J.; Matsuta, T.; Kanazawa, T.; Park, C.-H.; Chang, K.-J.; Onjo, M. *Chem. Nat. Compd.* **2012,** *48*, 477-479.

(122) Agrawal, P. K.; Bansal, M. C., Flavonoid Glycosides. In *Studies in Organic Chemistry 39: Carbon-13 NMR of Flavonoids*, Agrawal, P. K., Ed. Elsevier: Amsterdam, Netherlands, 1989; Vol. 39, pp 283 - 364.

(123) Dawidar, A.; Abdel-Mogib, M.; El-Naggar, M. E.; Mostafa, M. *Res. J. Pharm. Biol. Chem. Sci.* **2014,** *5*, 140-148.

(124) (a) Boots, A. W.; Haenen, G. R. M. M.; Bast, A. *Eur. J. Pharmacol.* **2008,** *585*, 325-337. (b) Jan, A. T.; Kamli, M. R.; Murtaza, I.; Singh, J. B.; Ali, A.; Haq, Q. M. R. *Food Rev. Int.* **2010,** *26*, 302-317. (c) Kang, J.; Li, Z.; Wu, T.; Jensen, G. S.; Schauss, A. G.; Wu, X. *Food Chem.* **2010,** *122*, 610-617.

(125) Kim, M.; Jones, A. D.; Chung, T.-Y. *Appl. Biol. Chem.* **1996,** *39*, 320-326.

(126) Yasukawa, K.; Sekine, H.; Takido, M. *Phytochemistry* **1989,** *28*, 2215-2216.

(127) Shrestha, S.; Lee, D.-Y.; Park, J.-H.; Cho, J.-G.; Seo, W.-D.; Kang, H. C.; Jeon, Y.-J.; Yeon, S.-W.; Bang, M.-H.; Baek, N.-I. *J. Korean Soc. Appl. Biol. Chem.* **2012,** *55*, 689-693.

(128) Zhang, Y.; DeWitt, D. L.; Murugesan, S.; Nair, M. G. *Chem. Biodivers.* **2004,** *1*, 426-441.

(129) Candeias, N. R.; Assoah, B.; Simeonov, S. P. *Chem. Rev.* **2018,** *118*, 10458-10550.

(130) Gürbüz, P.; Demirezer, L. Ö.; Güvenalp, Z.; Kuruüzüm-Uz, A.; Kazaz, C. *Rec. Nat. Prod.* **2015,** *9*, 175-183.

(131) Ye, G.; Huang, C. *Chem. Nat. Compd.* **2006,** *42*, 232-234.

(132) Campos, J. J.; de Oliveira Azevedo, A.; de Souza Filho, J. D.; Castro Perez, A.; Castro Braga, F. *J. Ethnopharmacol.* **2013,** *150*, 270-274.

(133) Reyes, M.; Martín, C.; Lastra, C. A. d. l.; Trujillo, J.; Toro, M. V.; Ayuso, M. J. *Z. Naturforsch., C* **1996,** *51*, 563-569.

(134) Hayder, N.; Bouhlel, I.; Skandrani, I.; Kadri, M.; Steiman, R.; Guiraud, P.; Mariotte, A.-M.; Ghedira, K.; Dijoux-Franca, M.-G.; Chekir-Ghedira, L. *Toxicol. in Vitro* **2008,** *22*, 567-581.

(135) Alwahsh, M.; Khairuddean, M.; Chong, W. *Rec. Nat. Prod.* **2015,** *9*, 159-163.

(136) Qiu, D.-R.; Wang, D.-C.; Yang, S.-X.; Zhang, Y.-M.; Wei, D.-S.; Zhang, M.-Z.; Sun, J.-Z.; Cong, J.; Guo, J.; He, S.-L.; Qin, J.-C. *Biochem. Syst. Ecol.* **2016,** *69*, 261-265.

(137) Suruga, K.; Tomita, T.; Kadokura, K.; Arai, T. *Food Nutr. Res.* **2019,** *63*, 3601-3609.

(138) Lin, L.-C.; Chou, C.-J. *Chin. Pharm. J.* **2000,** *52*, 211-218.

(139) Cuc, N. T.; Nhiem, N. X.; Yen, P. H.; Anh, H. L. T.; Van Minh, C.; Van Kiem, P. *Vietnam J. Chem.* **2015,** *53*, 94-97.

(140) Zhou, X.; Peng, J.; Fan, G.; Wu, Y. *J. Chromatogr. A* **2005,** *1092*, 216-221.

(141) van Den Dool, H.; Kratz, P. C. *J. Chromatogr. A* **1963,** *11*, 463-471.

(142) Blois, M. S. *Nature* **1958,** *181*, 1199-1200.

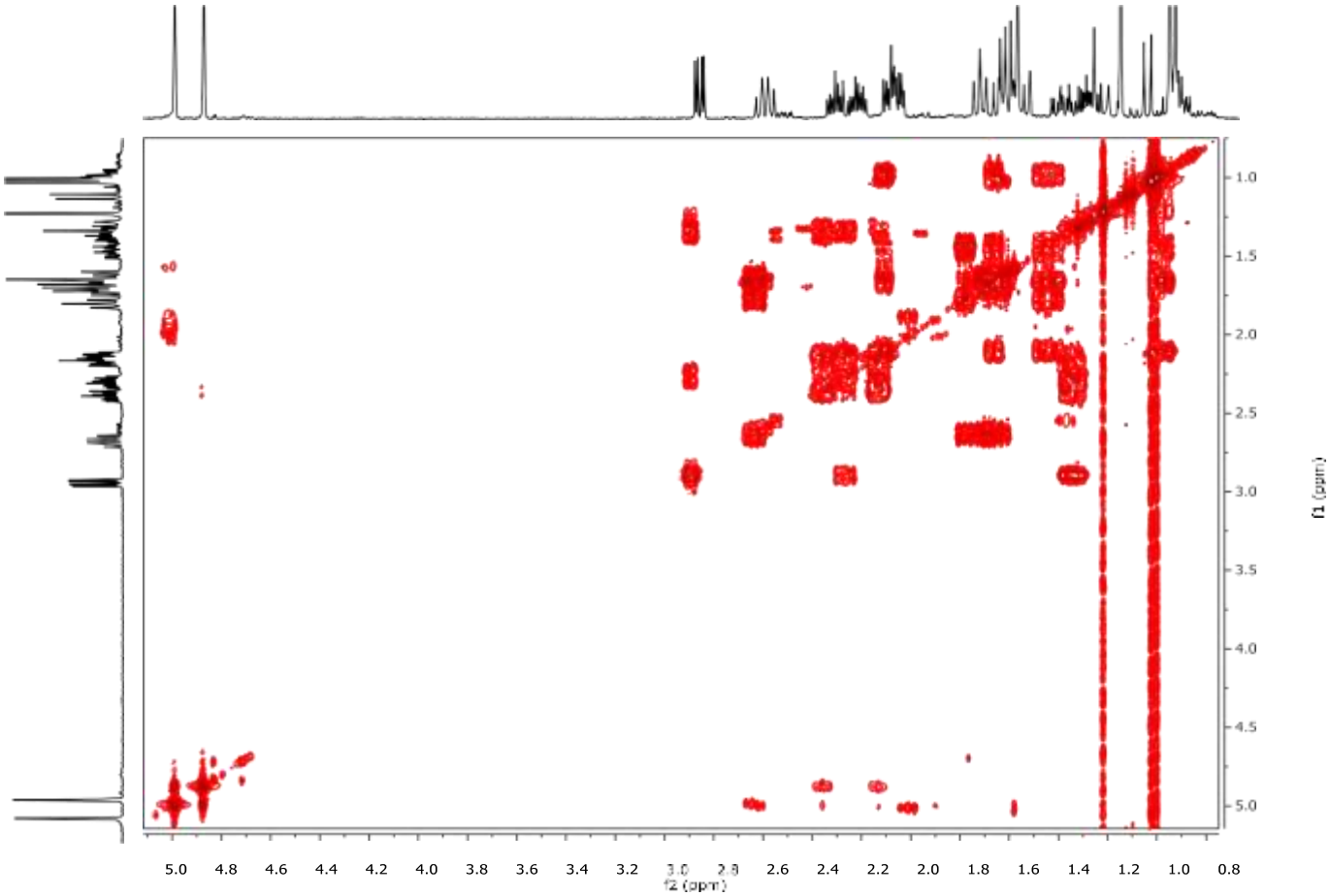
(143) Bhuiyan, M. A. R.; Hoque, M. Z.; Hossain, S. J. *World J. Agric. Sci.* **2009,** *5*, 318-322.

(144) Christie, W. W., Preparation of Ester Derivatives of Fatty Acids for Chromatographic Analysis. In *Advances in Lipid Methodology* Oily Press: Dundee, 1993; Vol. 2, pp 69 - 111.

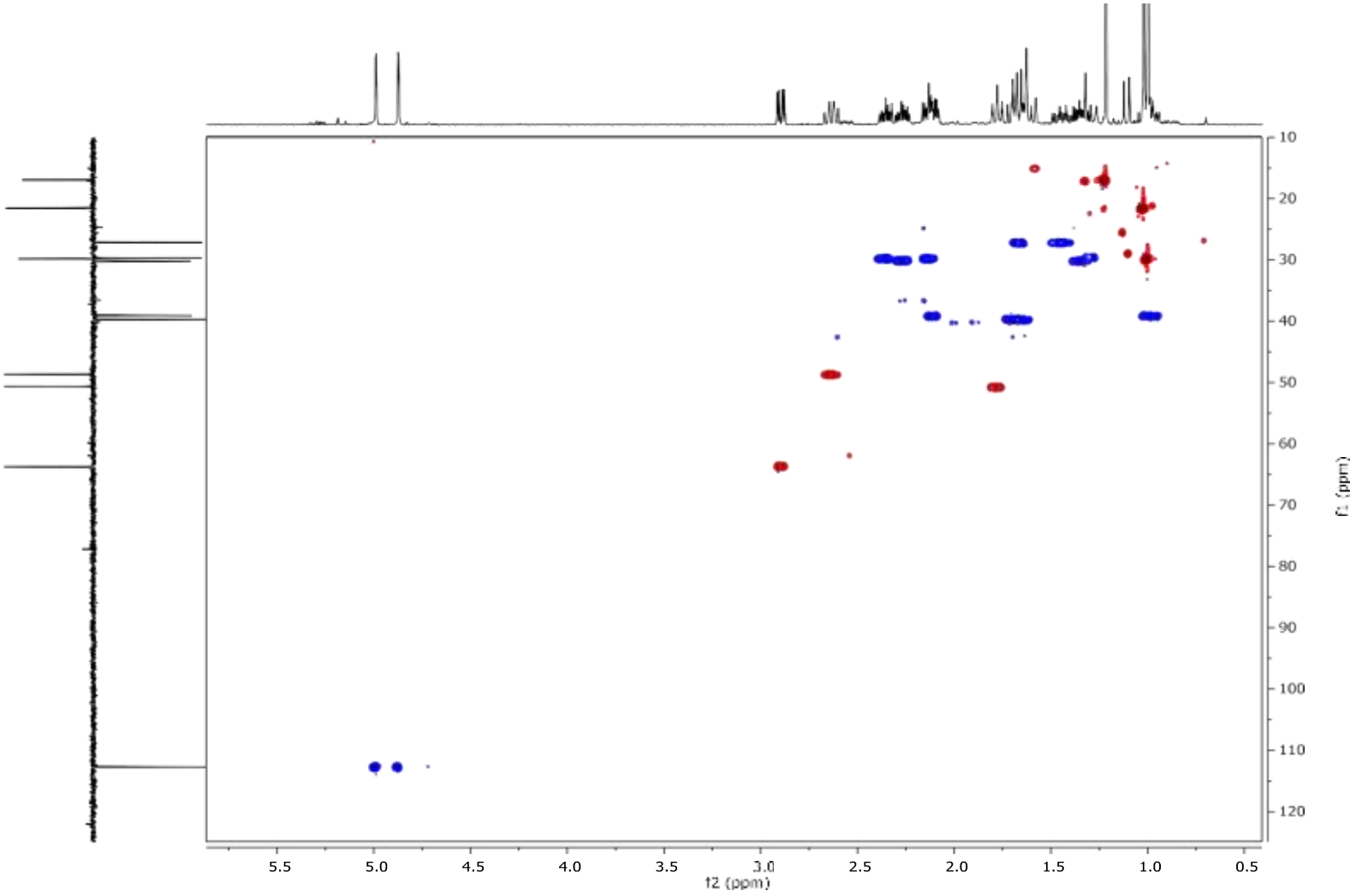
(145) Fraisse, D.; Heitz, A.; Carnat, A.; Carnat, A. P.; Lamaison, J. L. *Fitoterapia* **2000,** *71*, 463-464.

7. Appendices

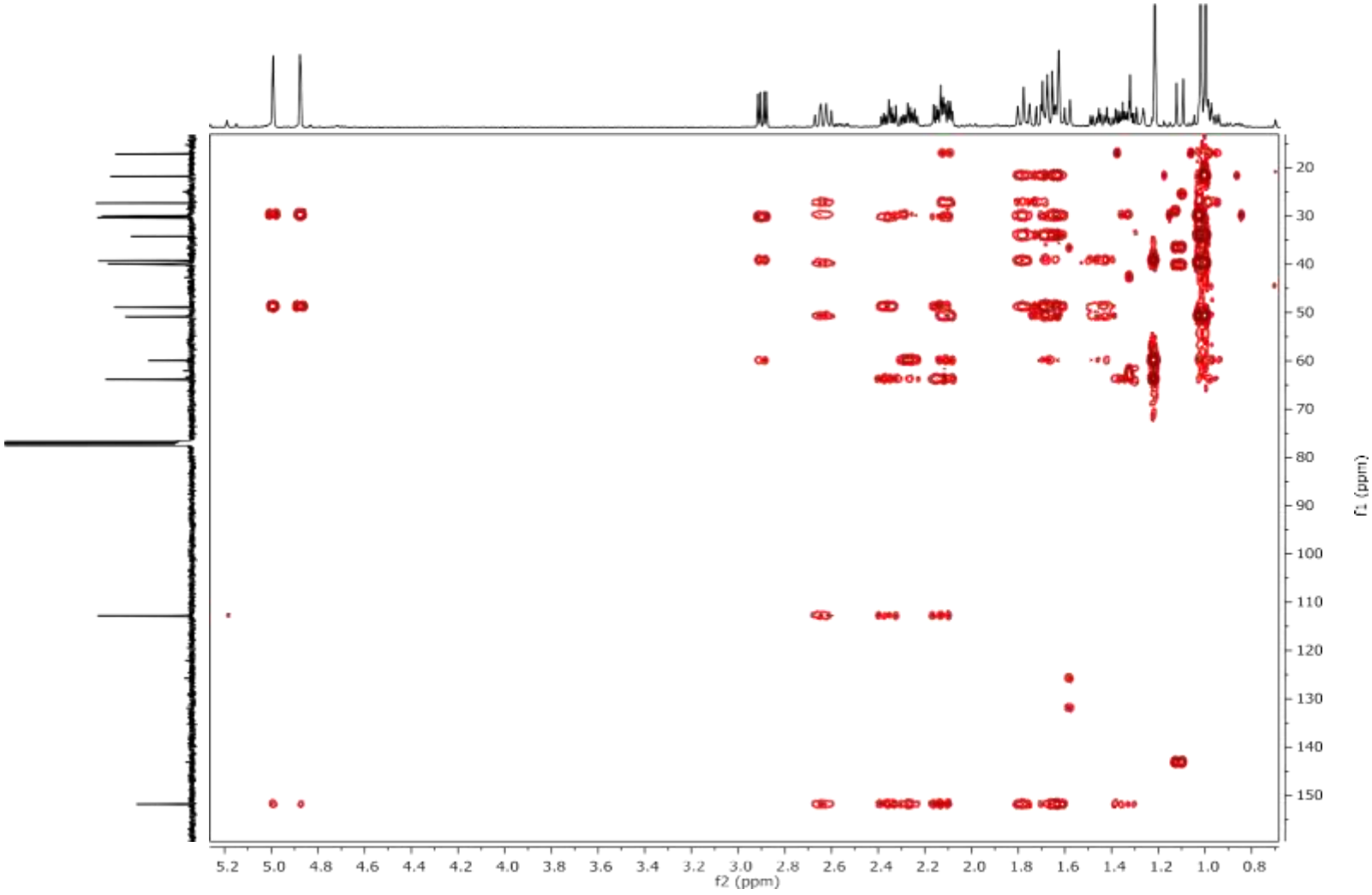
Appendix 1: The ^{1}H–^{1}H COSY Spectrum of **113** in $CDCl_3$.



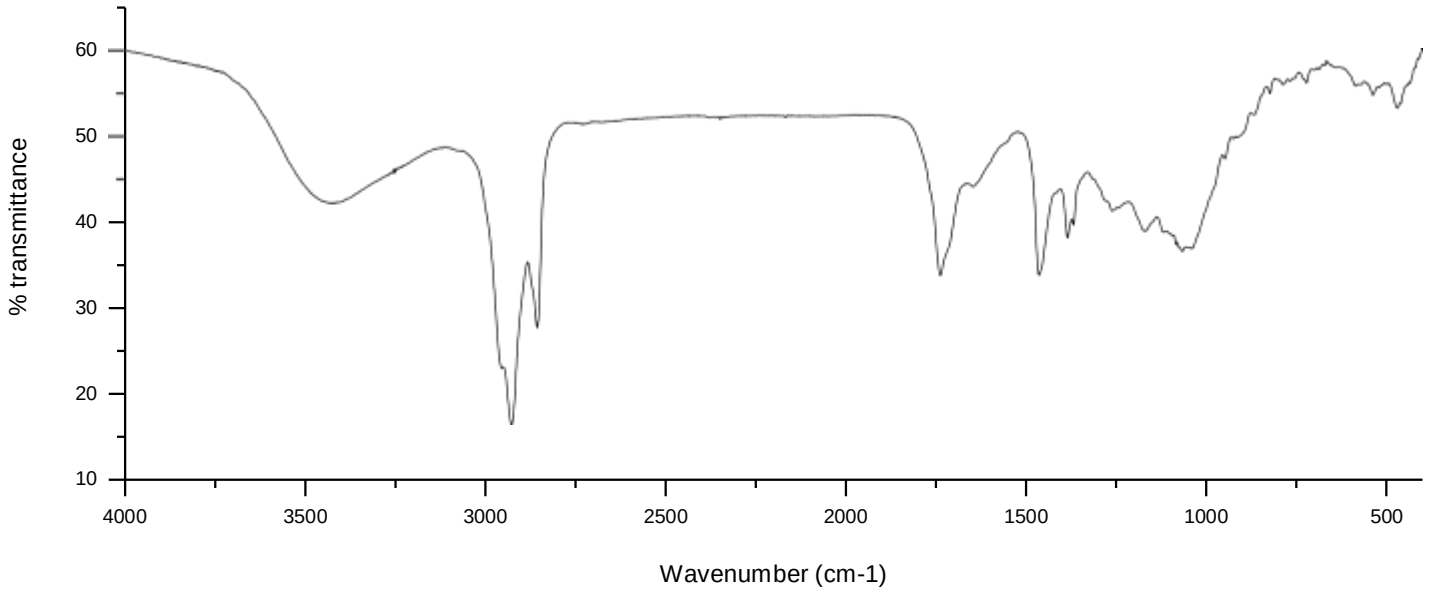
Appendix 2: The HSQC Spectrum of **113** in $CDCl_3$.



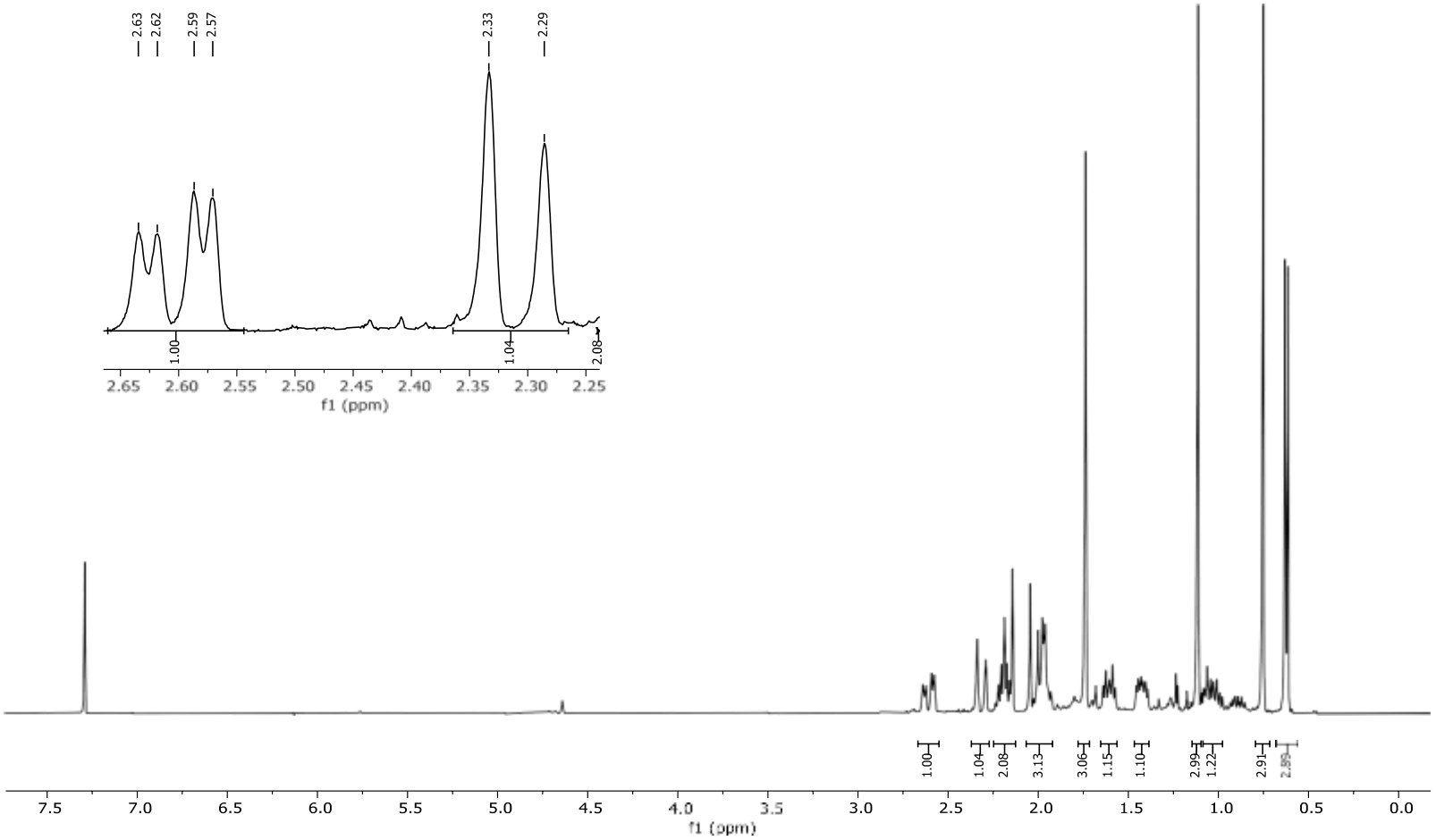
Appendix 3: The HMBC Spectrum of **113** in $CDCl_3$.



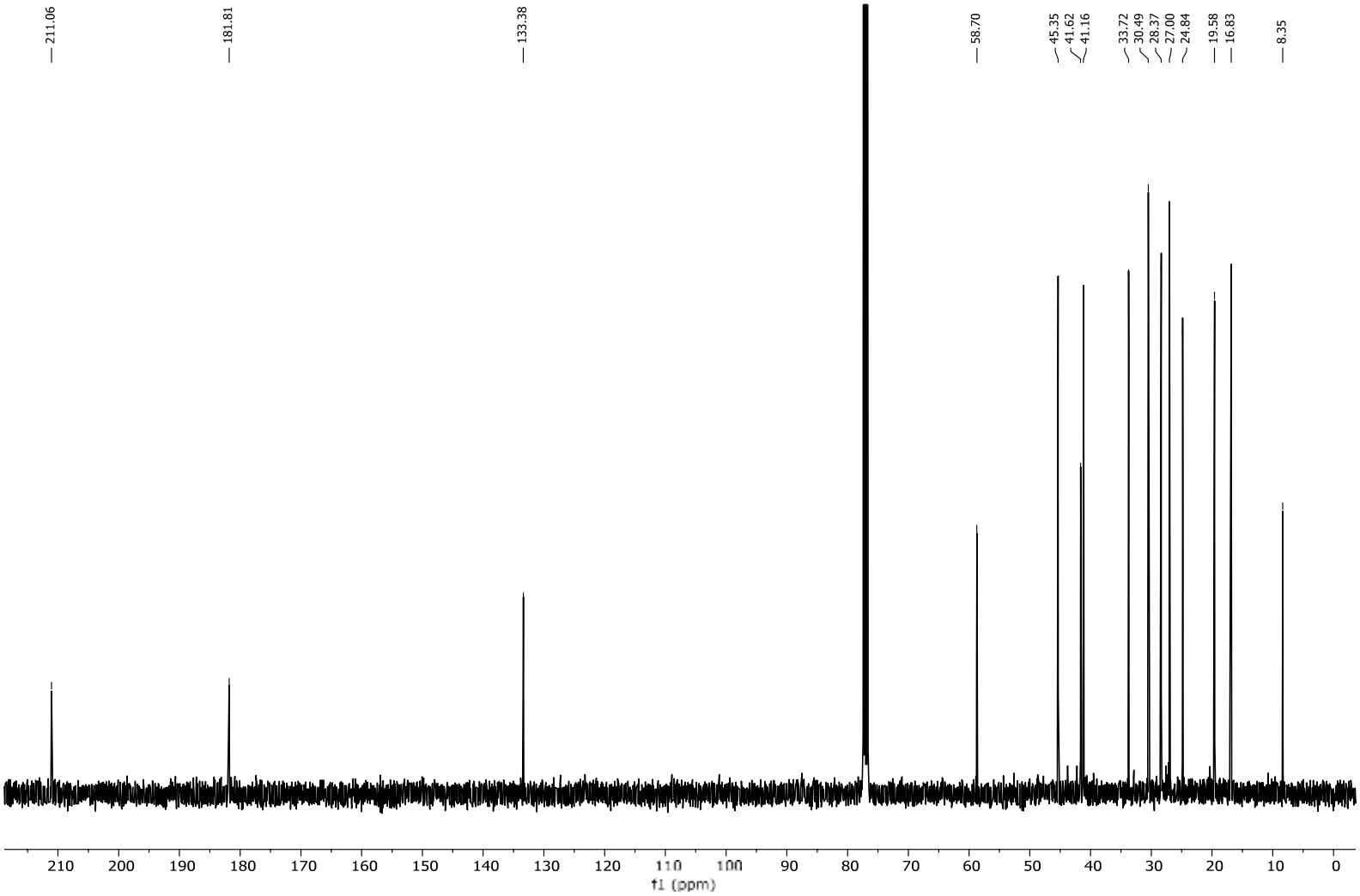
Appendix 4: The IR Spectrum of **113**.



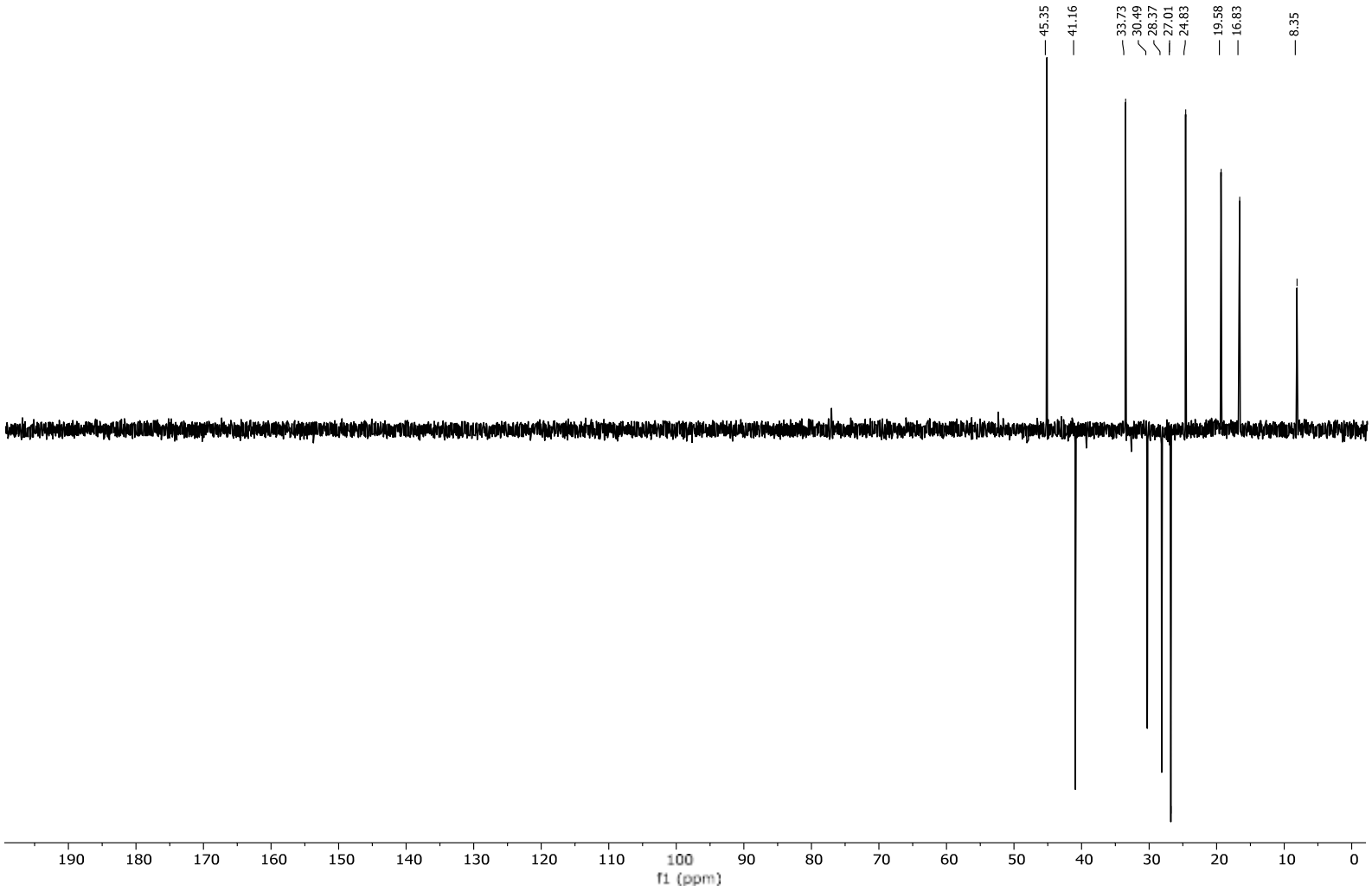
Appendix 5: The ^{1}H-NMR Spectrum of **12** in $CDCl_3$.



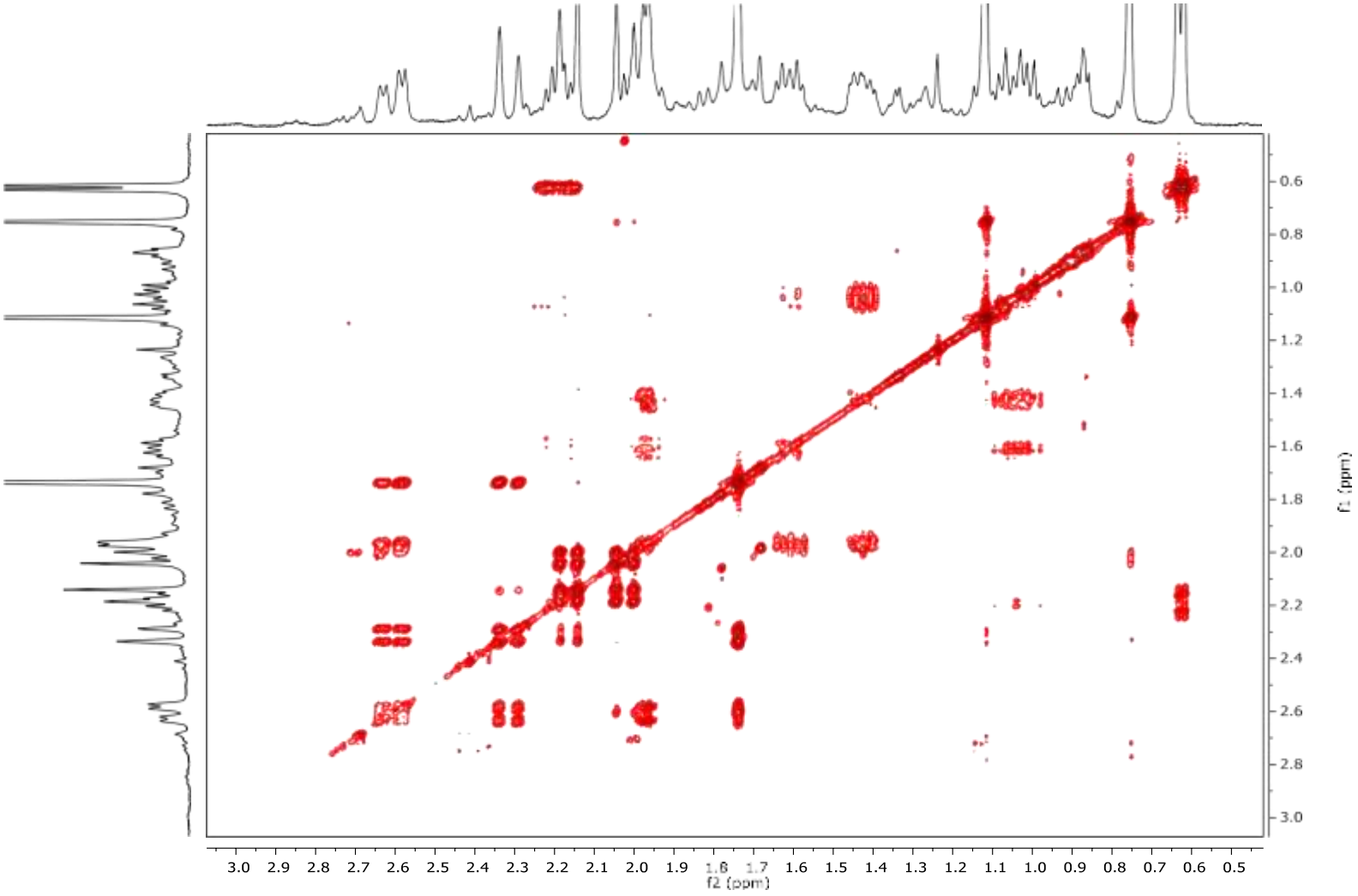
Appendix 6: The ^{13}C-NMR Spectrum of **12** in $CDCl_3$.



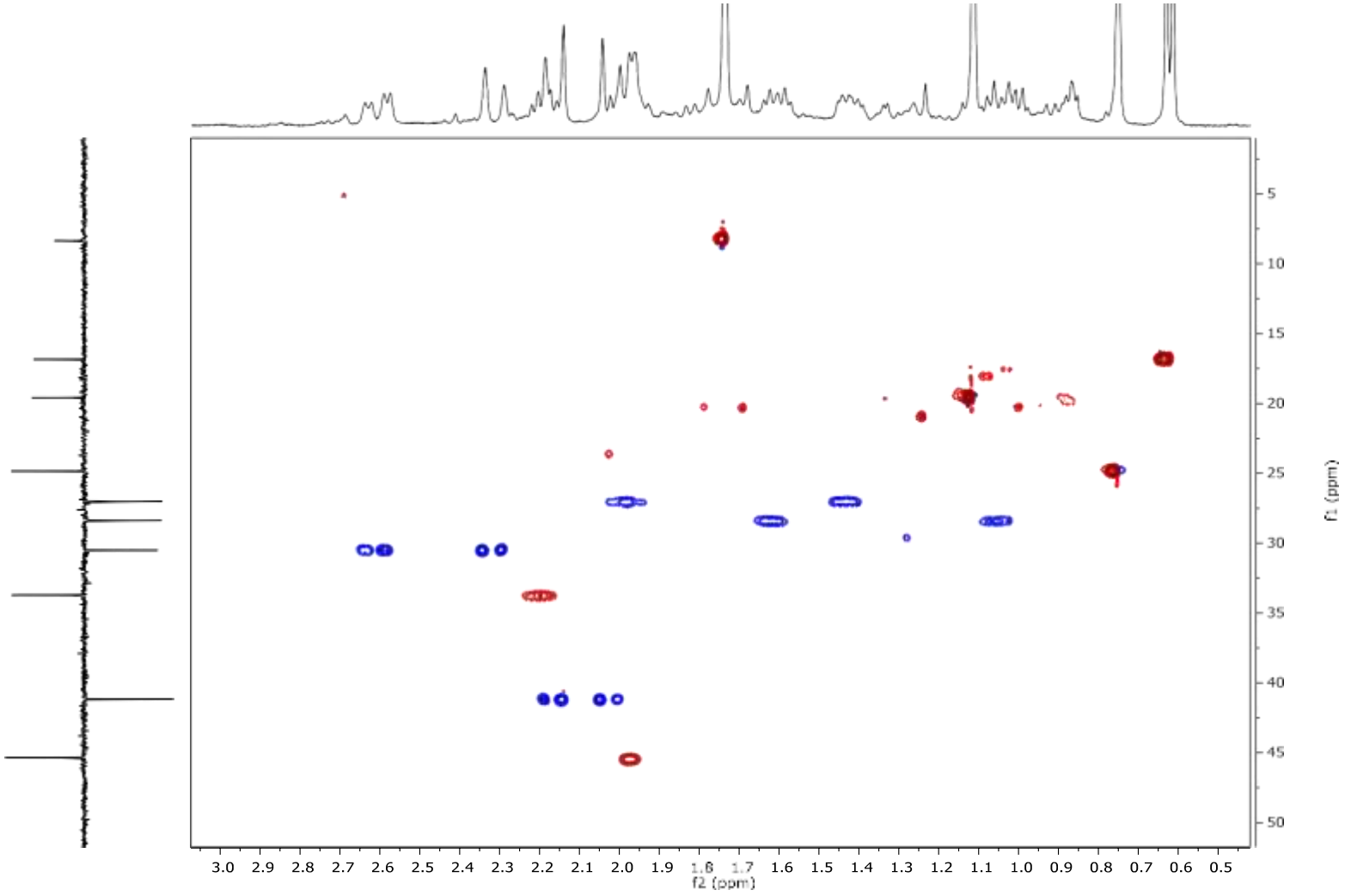
Appendix 7: The DEPT-135 NMR Spectrum of **12** in $CDCl_3$.



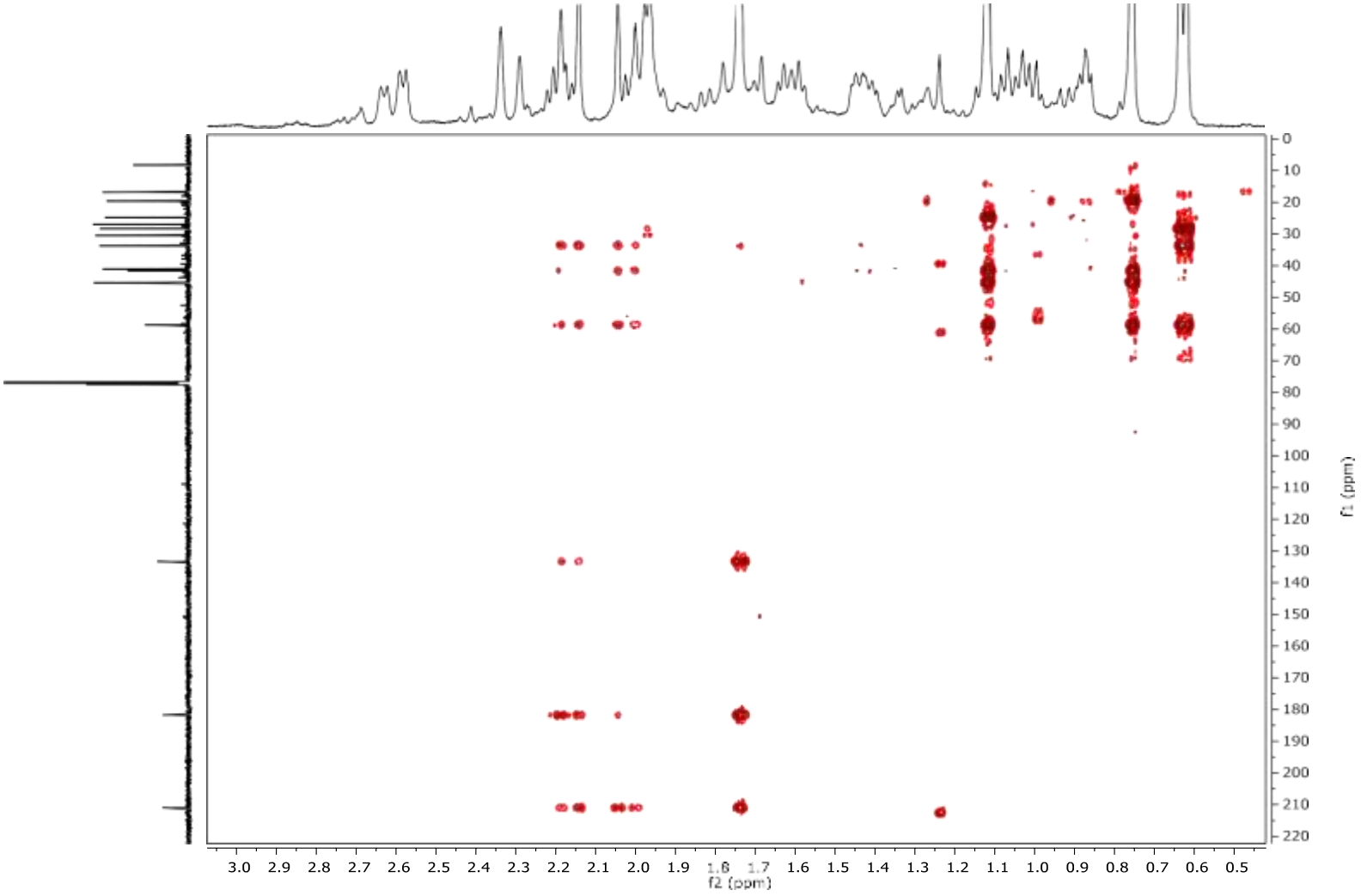
Appendix 8: The ^{1}H–^{1}H COSY Spectrum of **12** in $CDCl_3$.



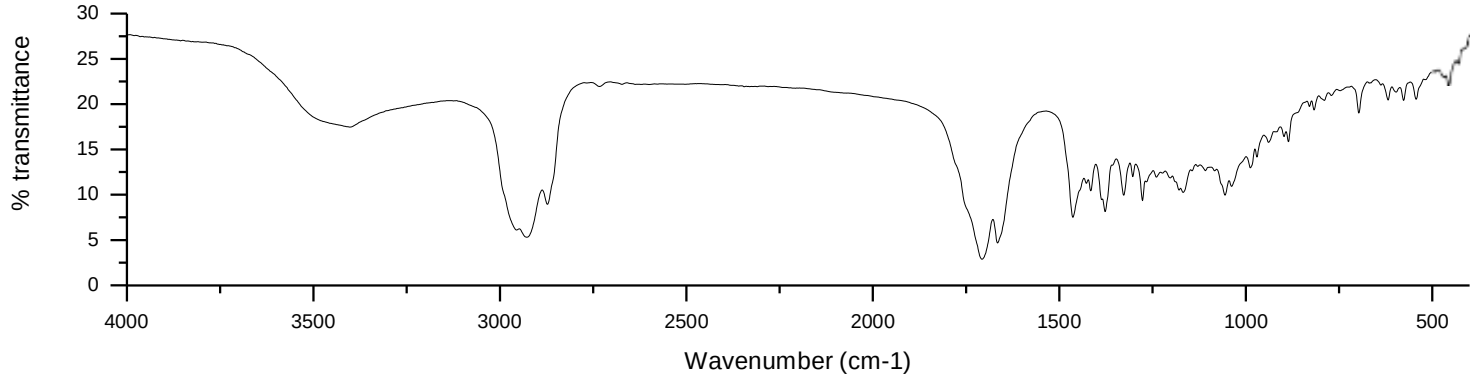
Appendix 9: The HSQC Spectrum of **12** in $CDCl_3$.



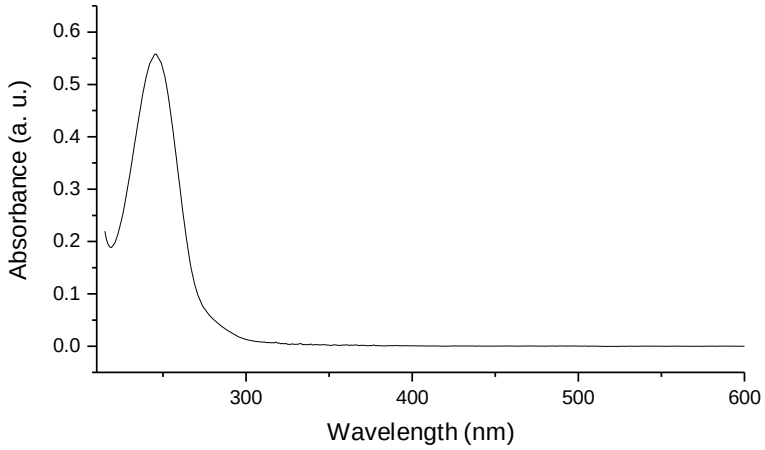
Appendix 10: The HMBC Spectrum of **12** in $CDCl_3$.



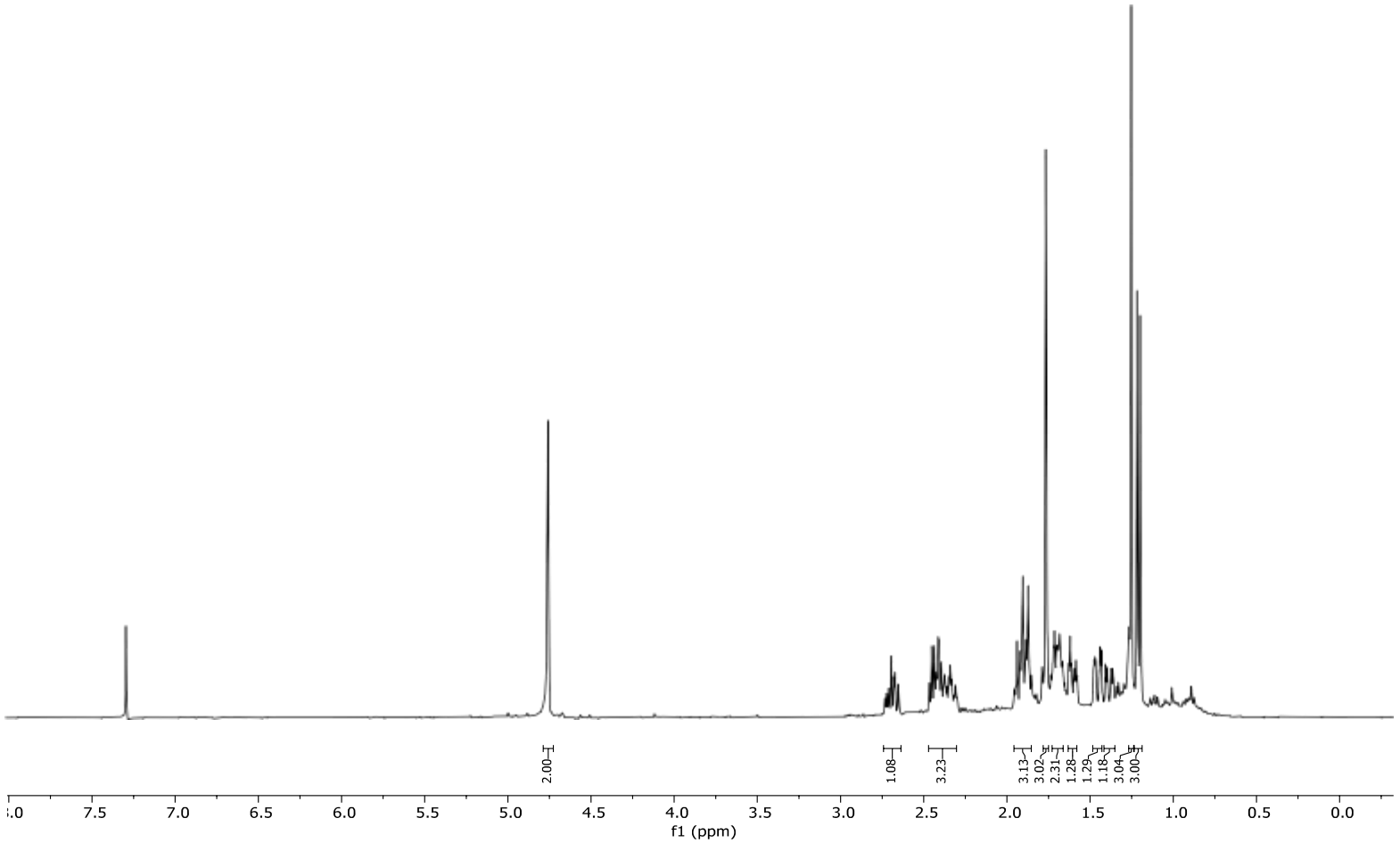
Appendix 11: The IR Spectrum of **12**.



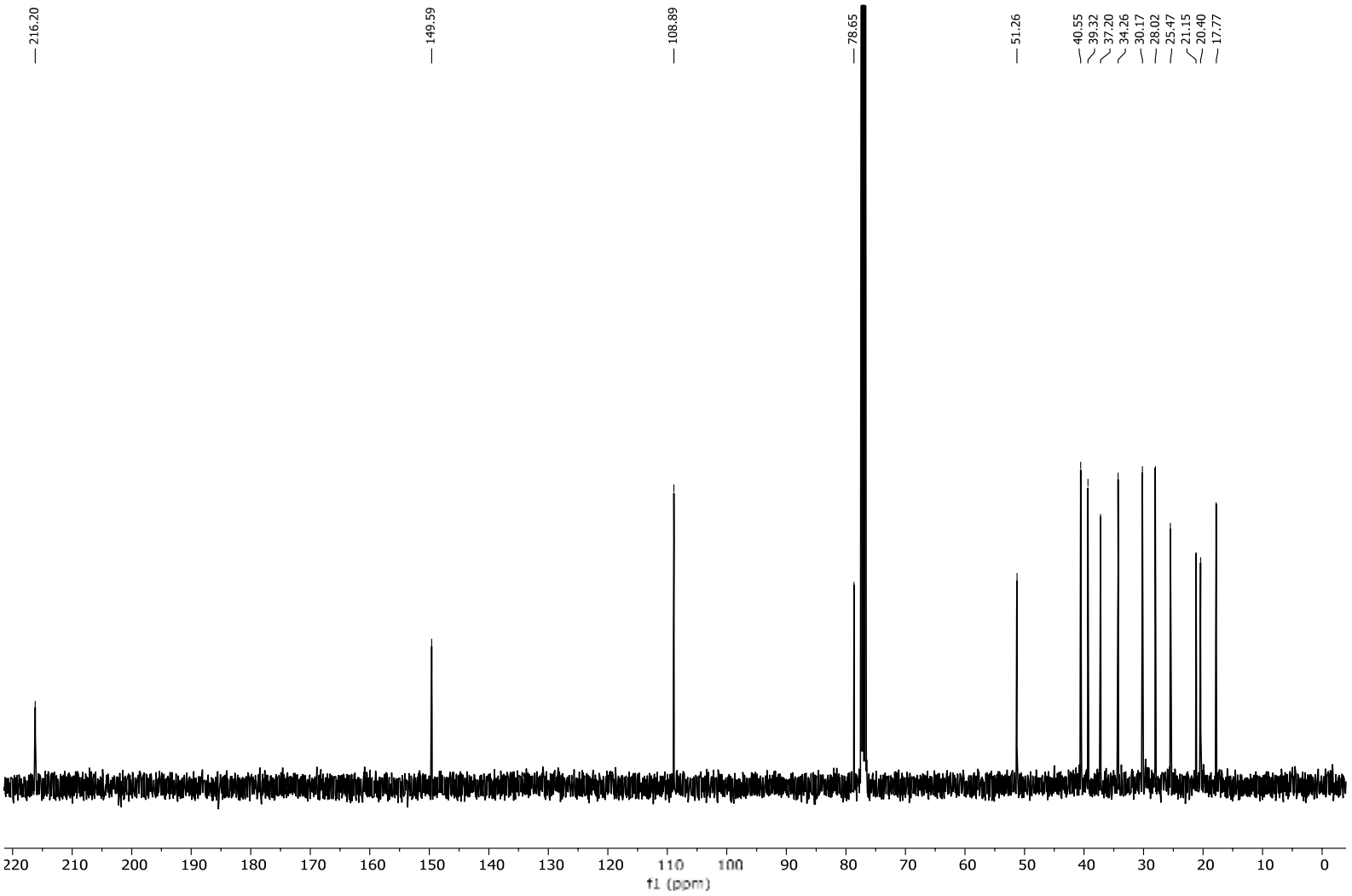
Appendix 12: The UV Spectrum of **12** in Methanol.



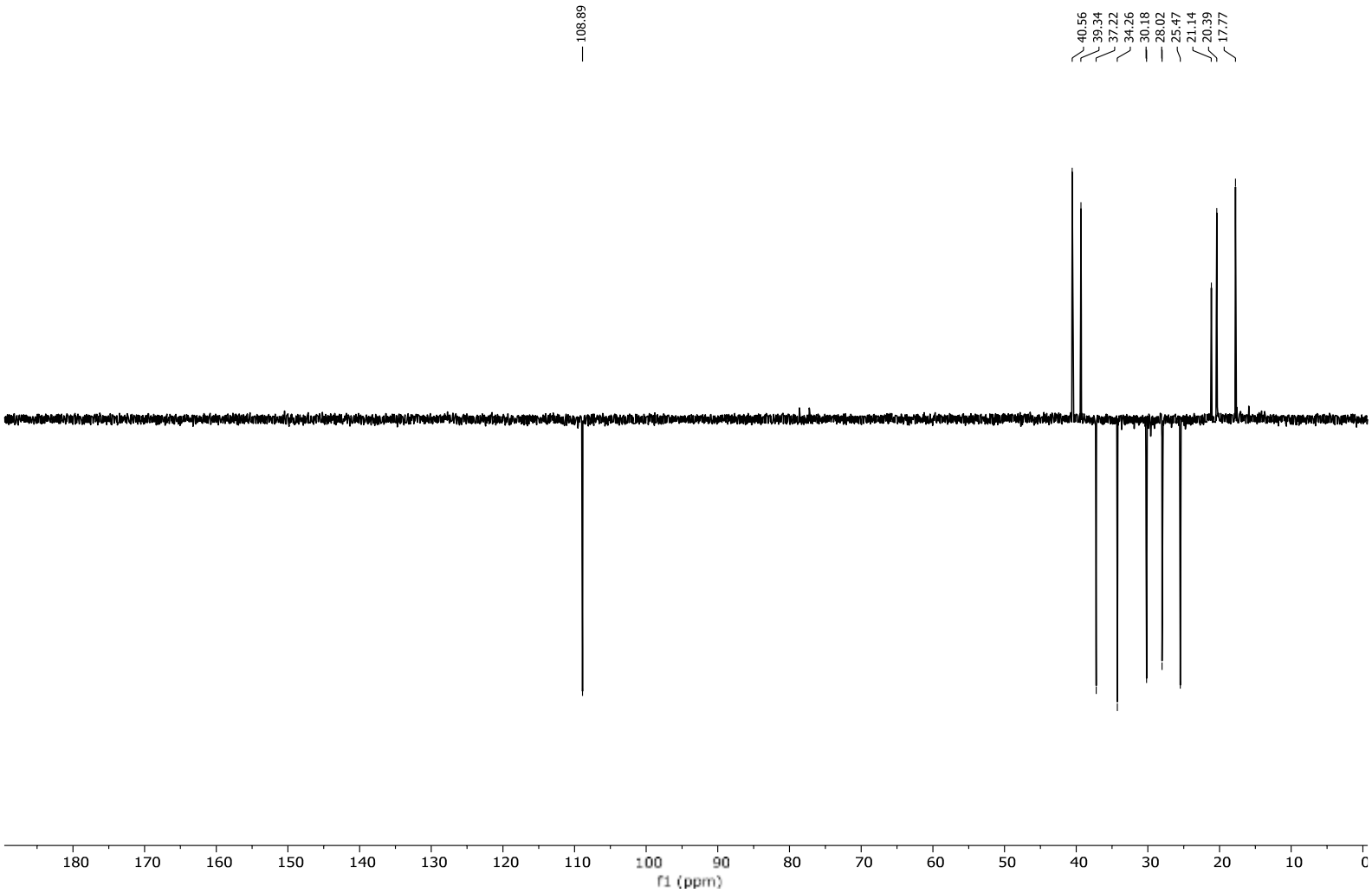
Appendix 13: The ^{1}H-NMR Spectrum of **114** in $CDCl_3$.



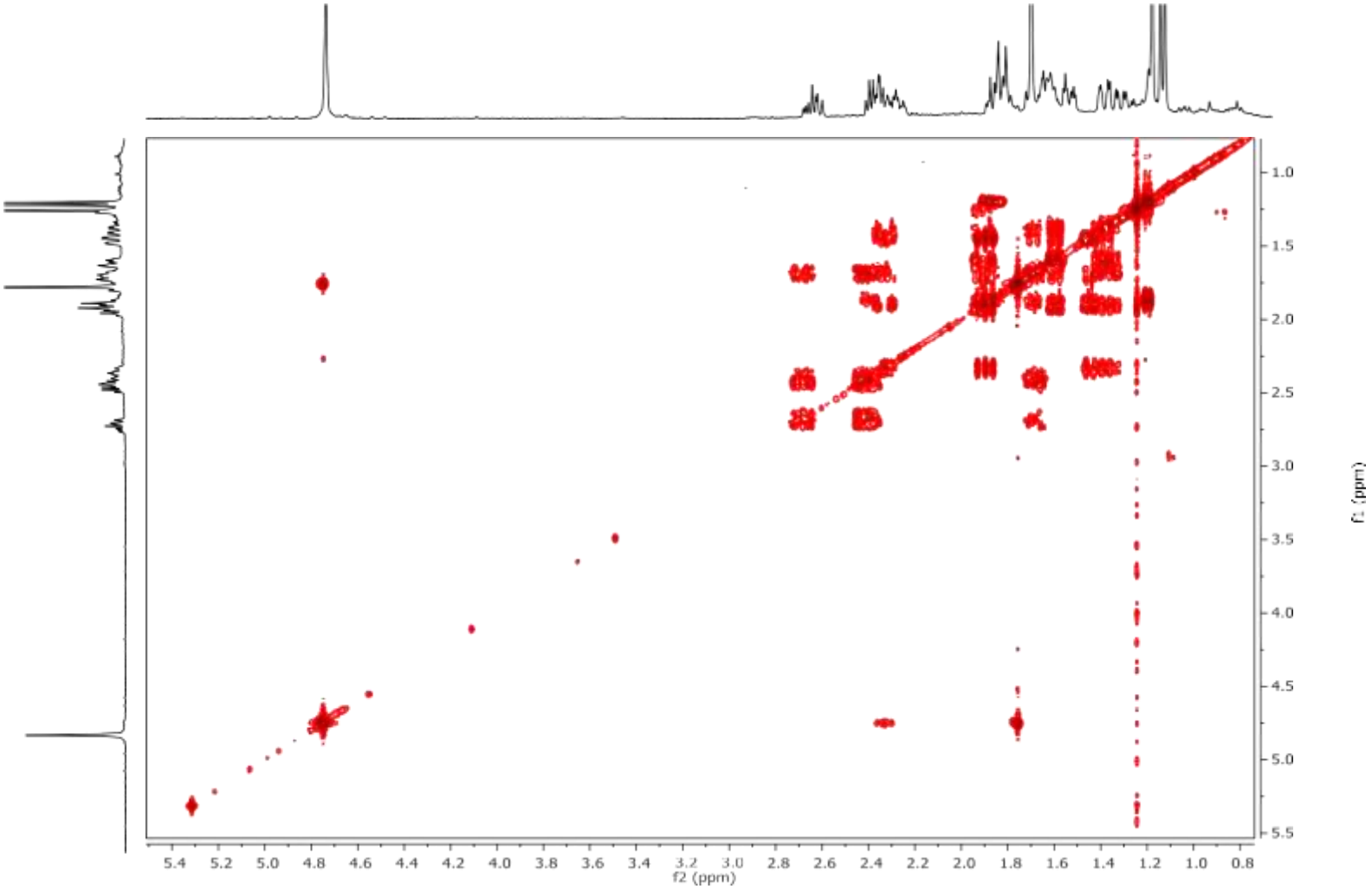
Appendix 14: The ^{13}C-NMR Spectrum of **114** in $CDCl_3$.



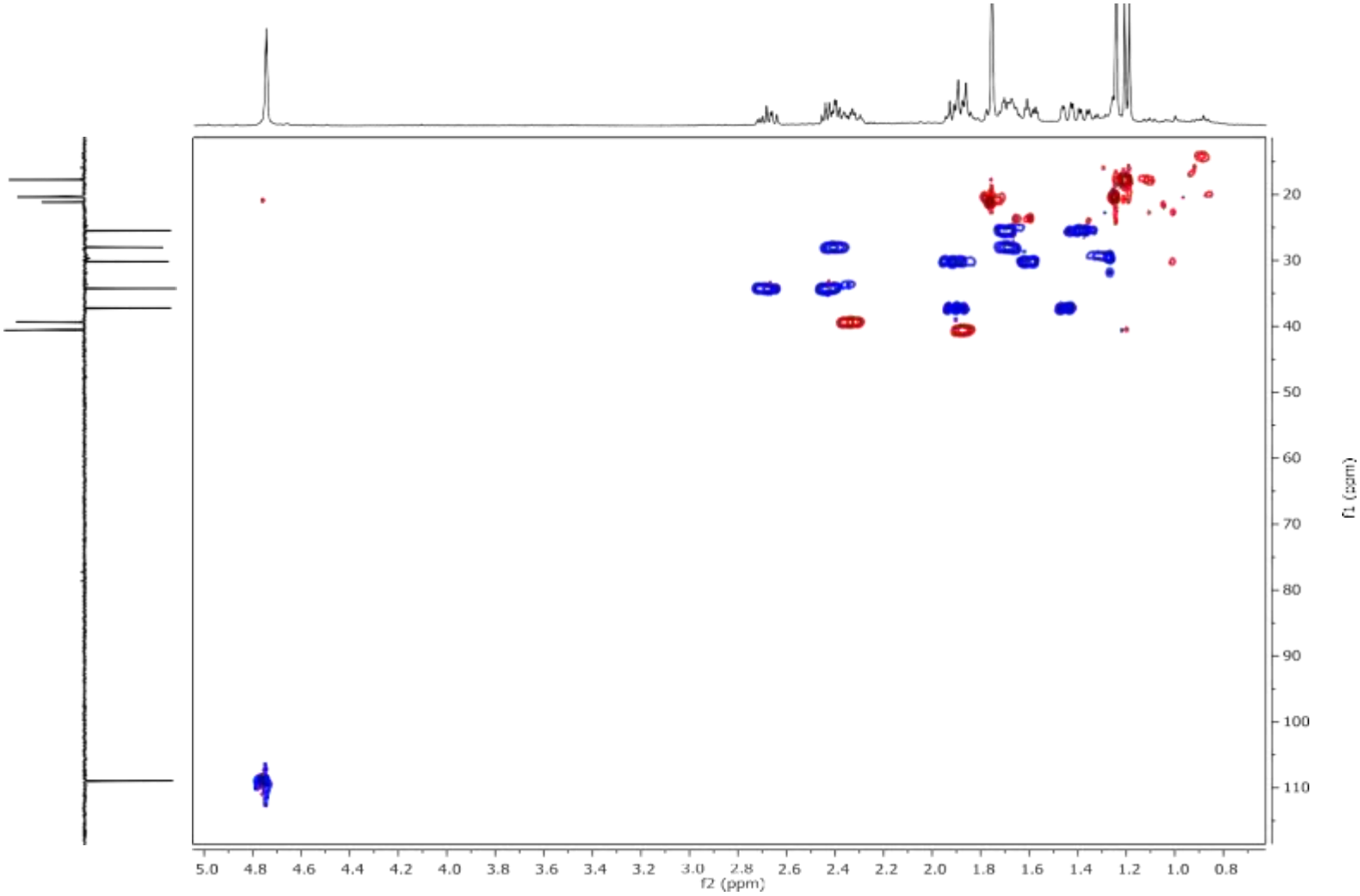
Appendix 15: The DEPT-135 NMR Spectrum of **114** in $CDCl_3$.



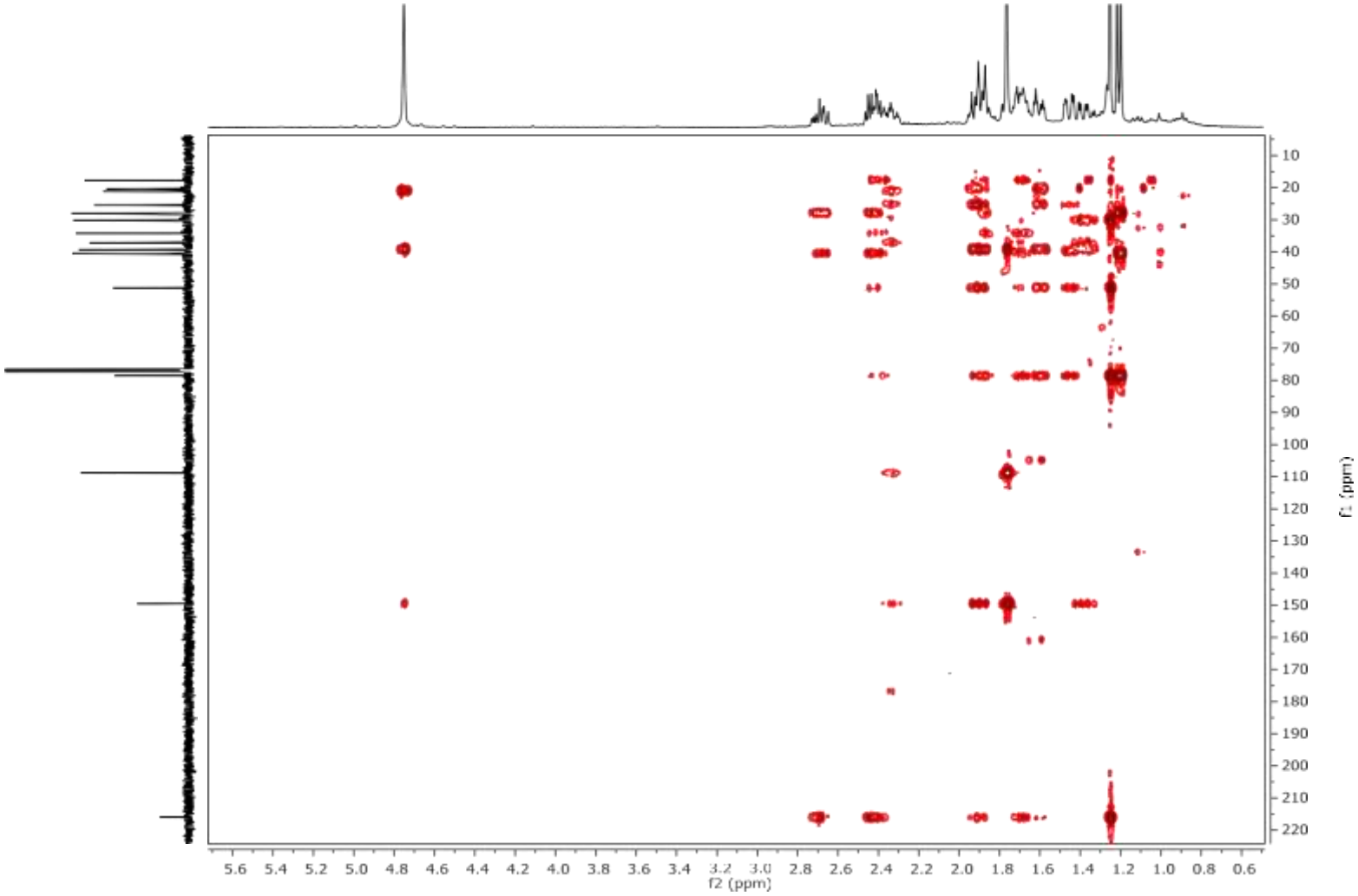
Appendix 16: The ^{1}H–^{1}H COSY Spectrum of **114** in $CDCl_3$.



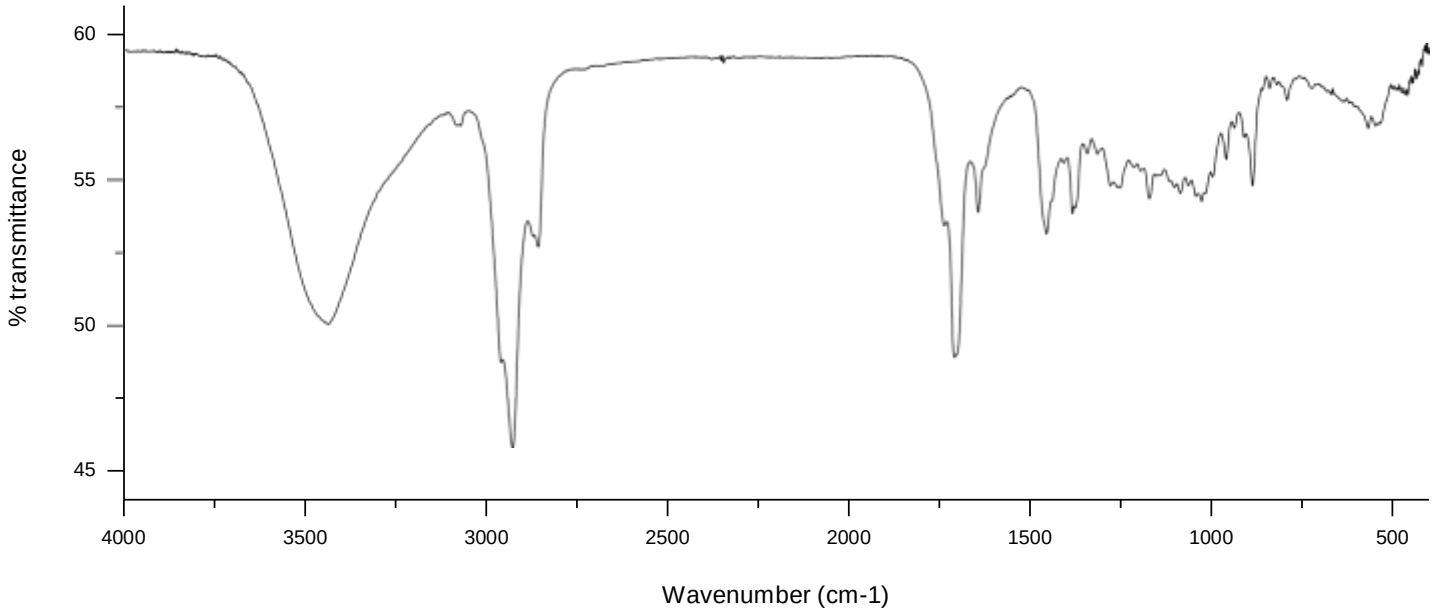
Appendix 17: The HSQC Spectrum of **114** in $CDCl_3$.



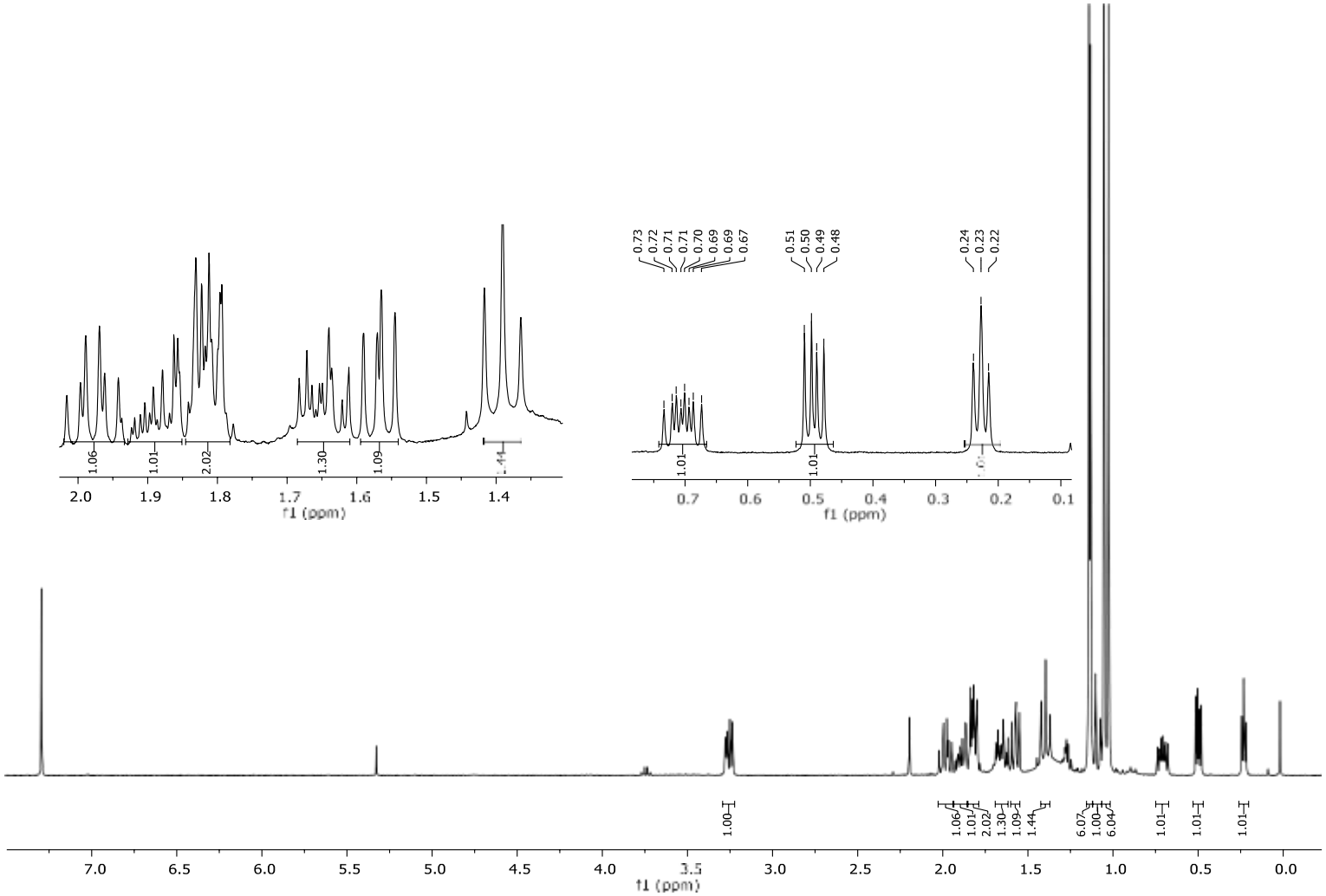
Appendix 18: The HMBC Spectrum of **114** in $CDCl_3$.



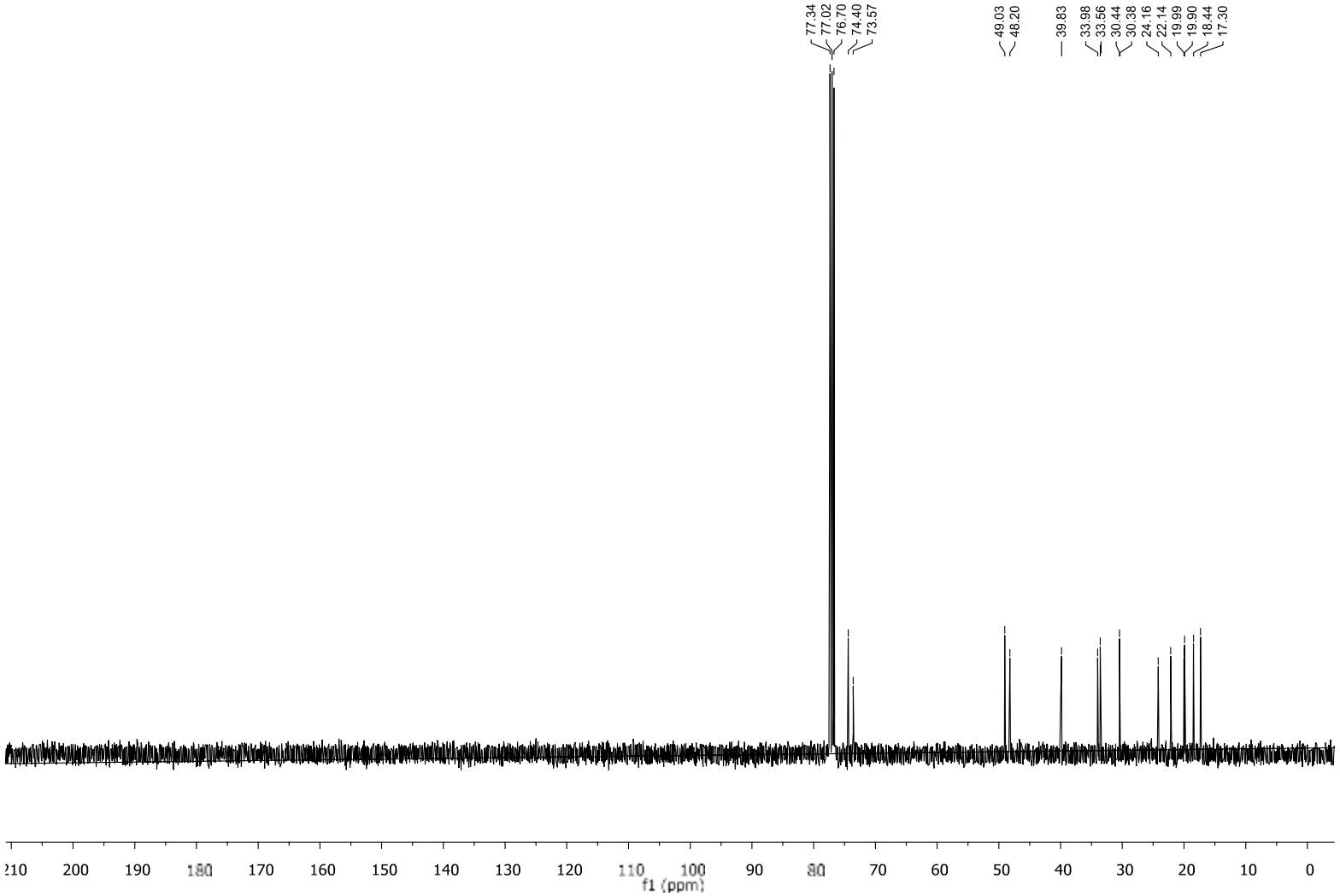
Appendix 19: The IR Spectrum of **114**.



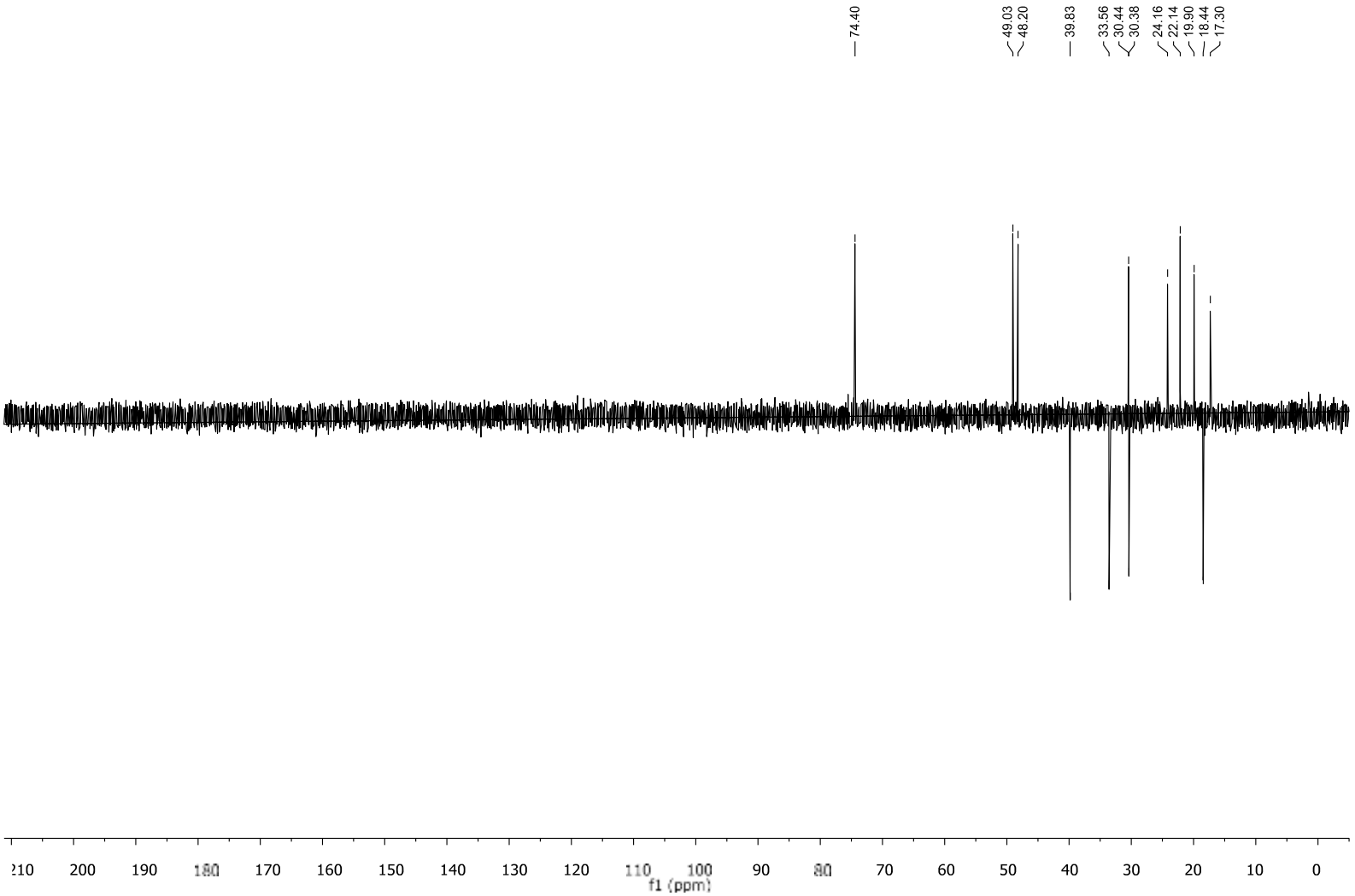
Appendix 20: The ^{1}H-NMR Spectrum of **115** in $CDCl_3$.



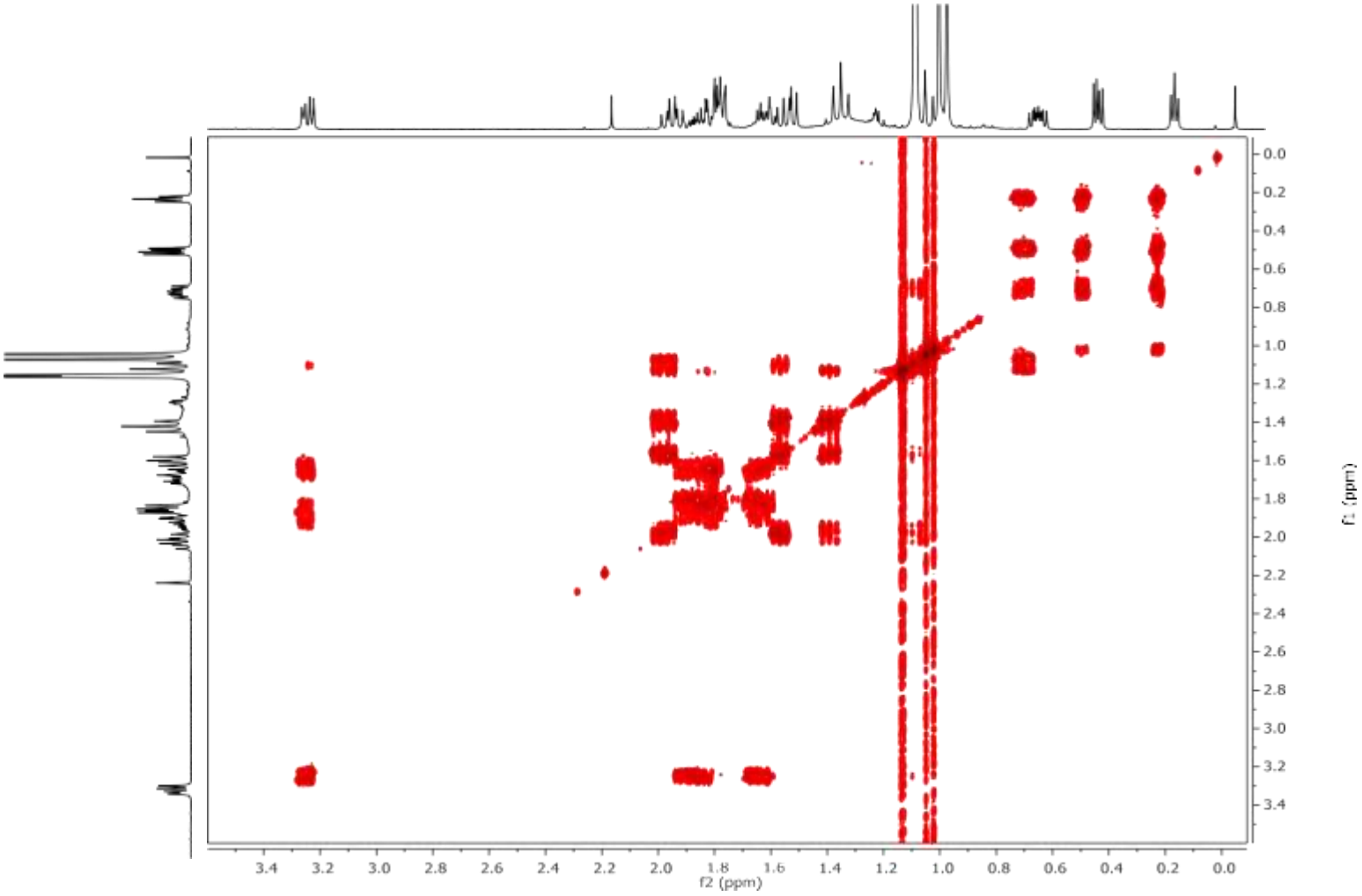
Appendix 21: The ^{13}C-NMR Spectrum of **115** in $CDCl_3$.



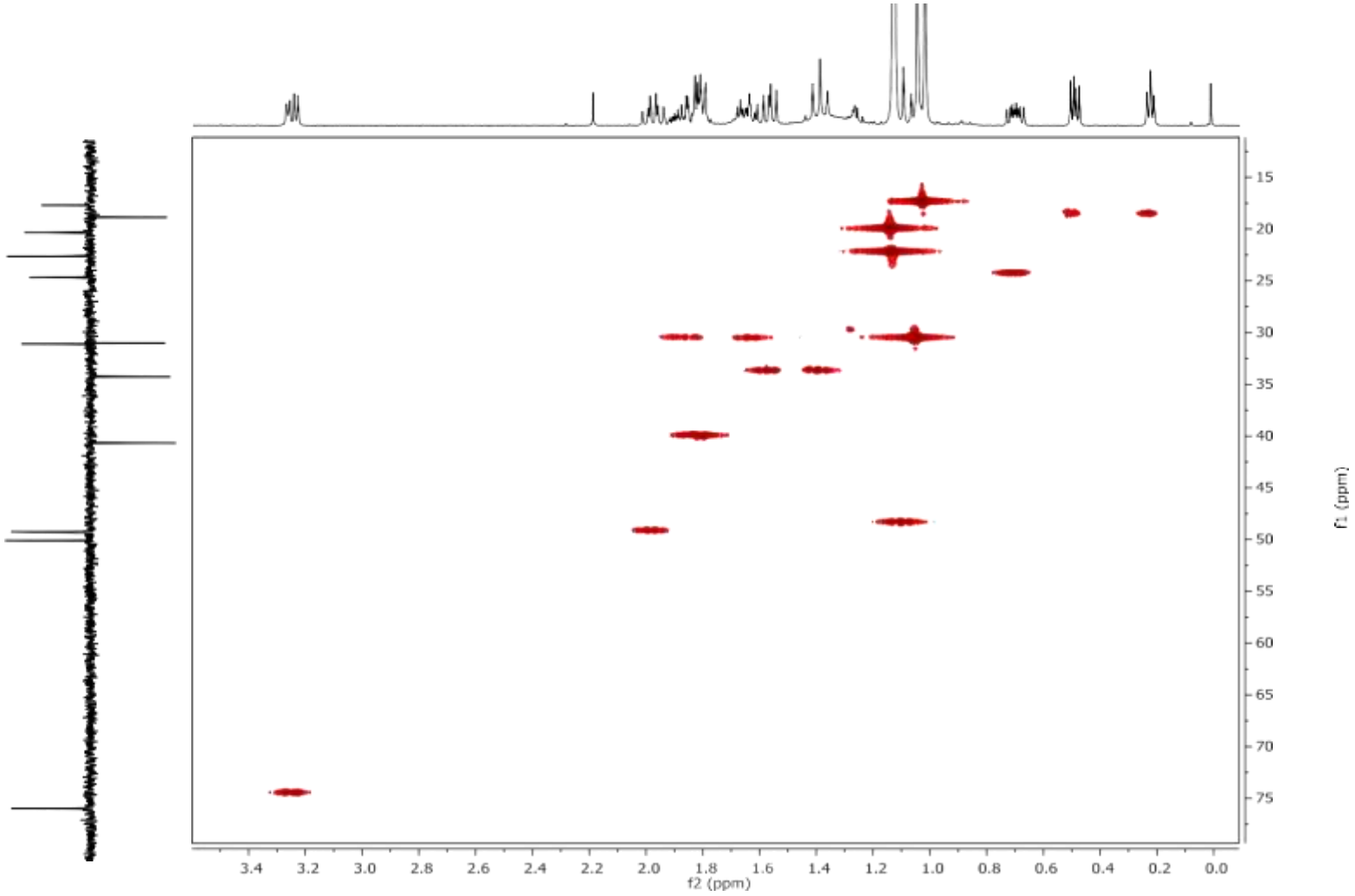
Appendix 22: The DEPT-135 NMR Spectrum of **115** in $CDCl_3$.



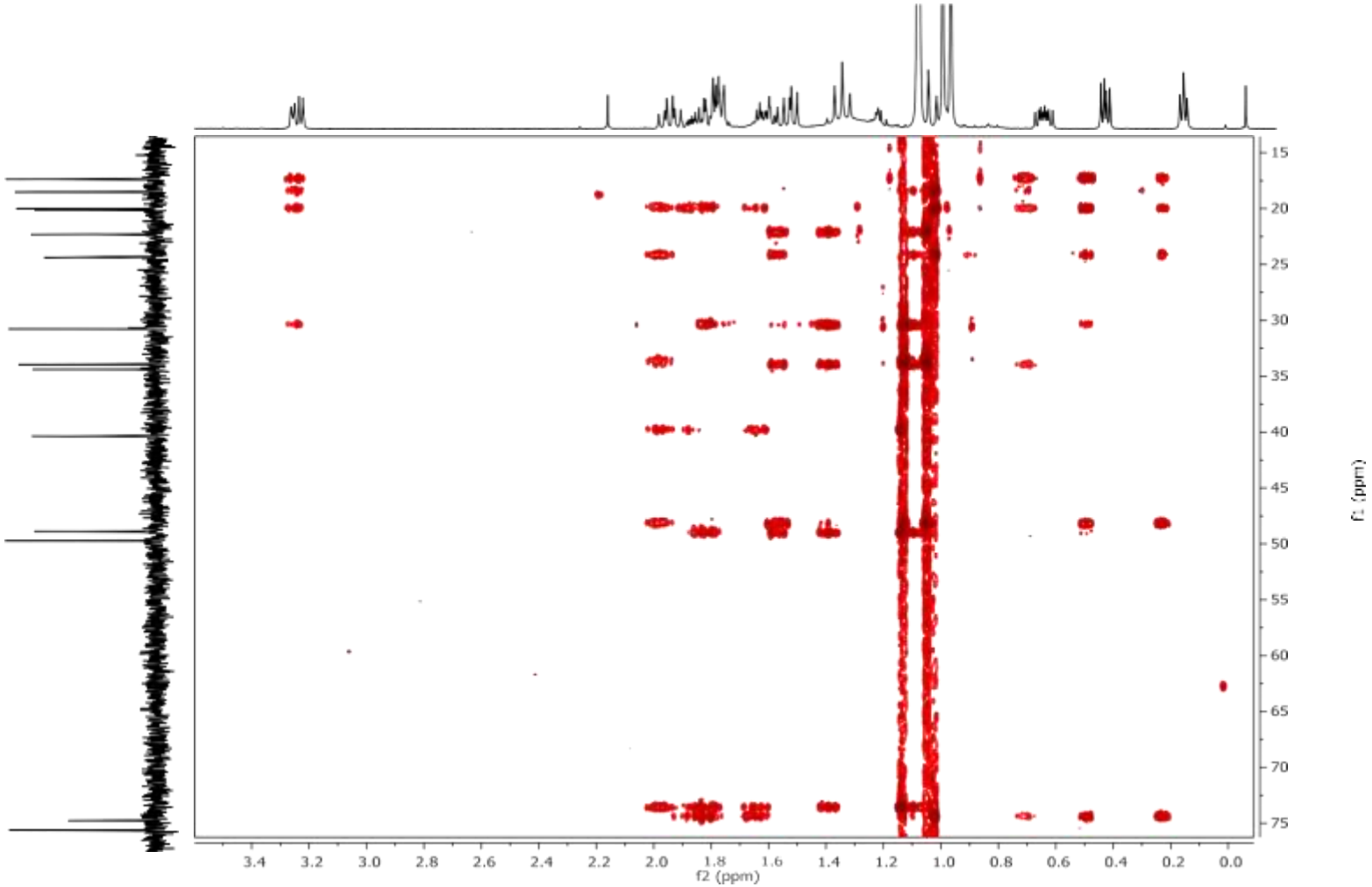
Appendix 23: The ^{1}H–^{1}H COSY Spectrum of **115** in $CDCl_3$.



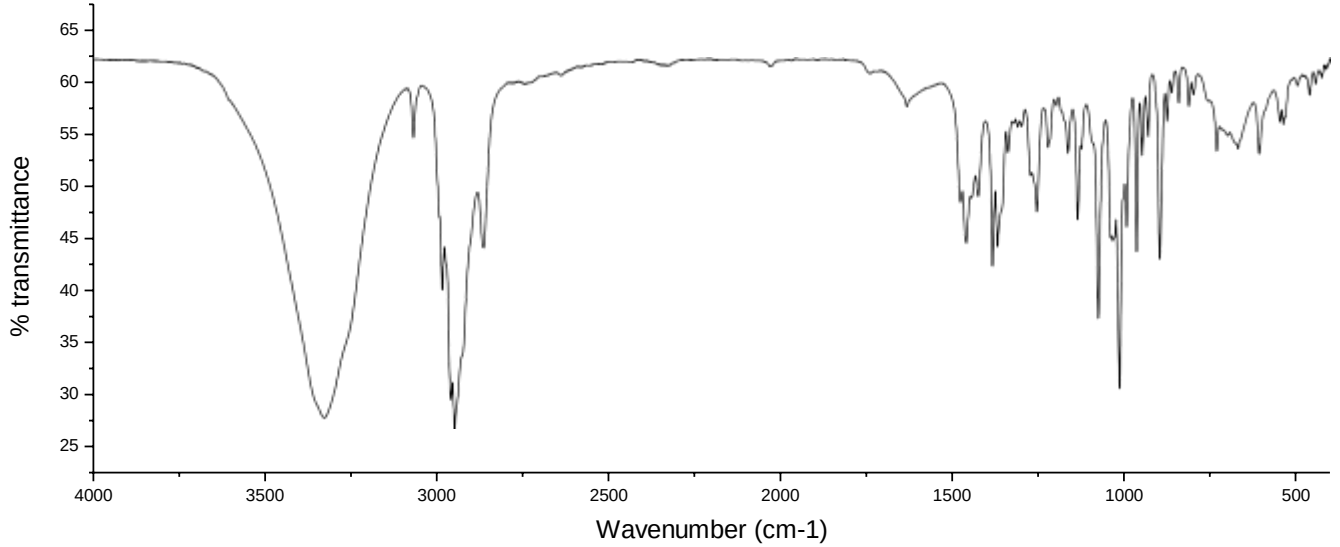
Appendix 24: The HSQC Spectrum of **115** in $CDCl_3$.



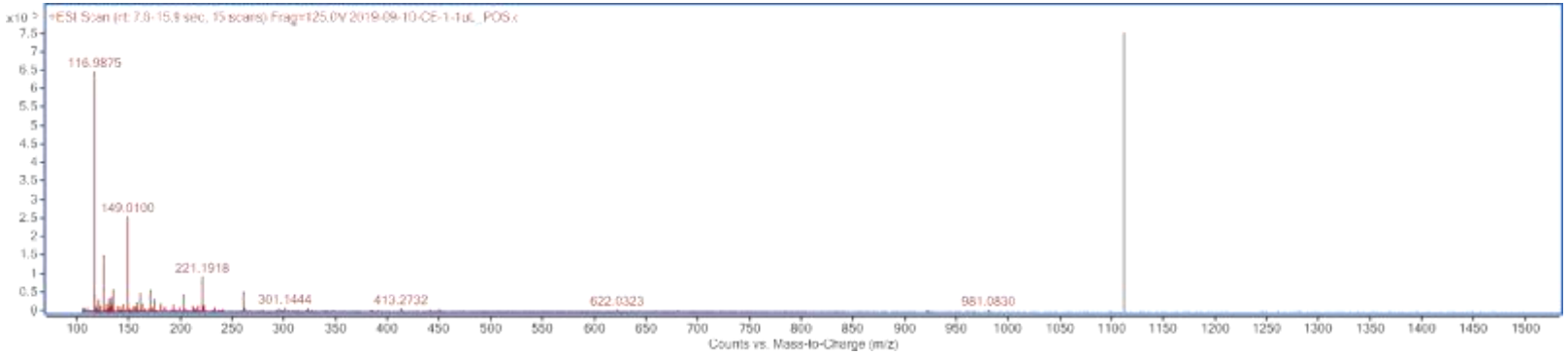
Appendix 25: The HMBC Spectrum of **115** in $CDCl_3$.

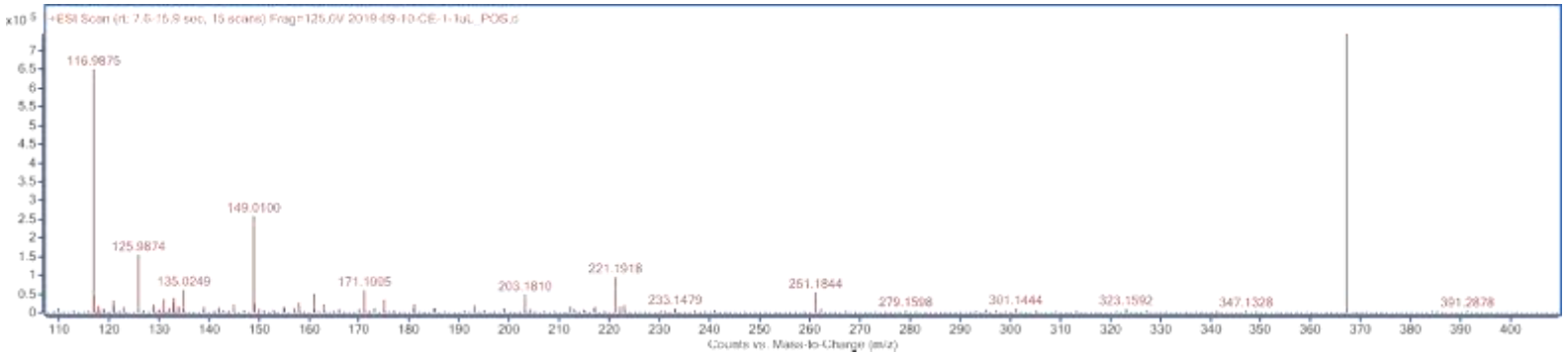


Appendix 26: The IR Spectrum of **115**.

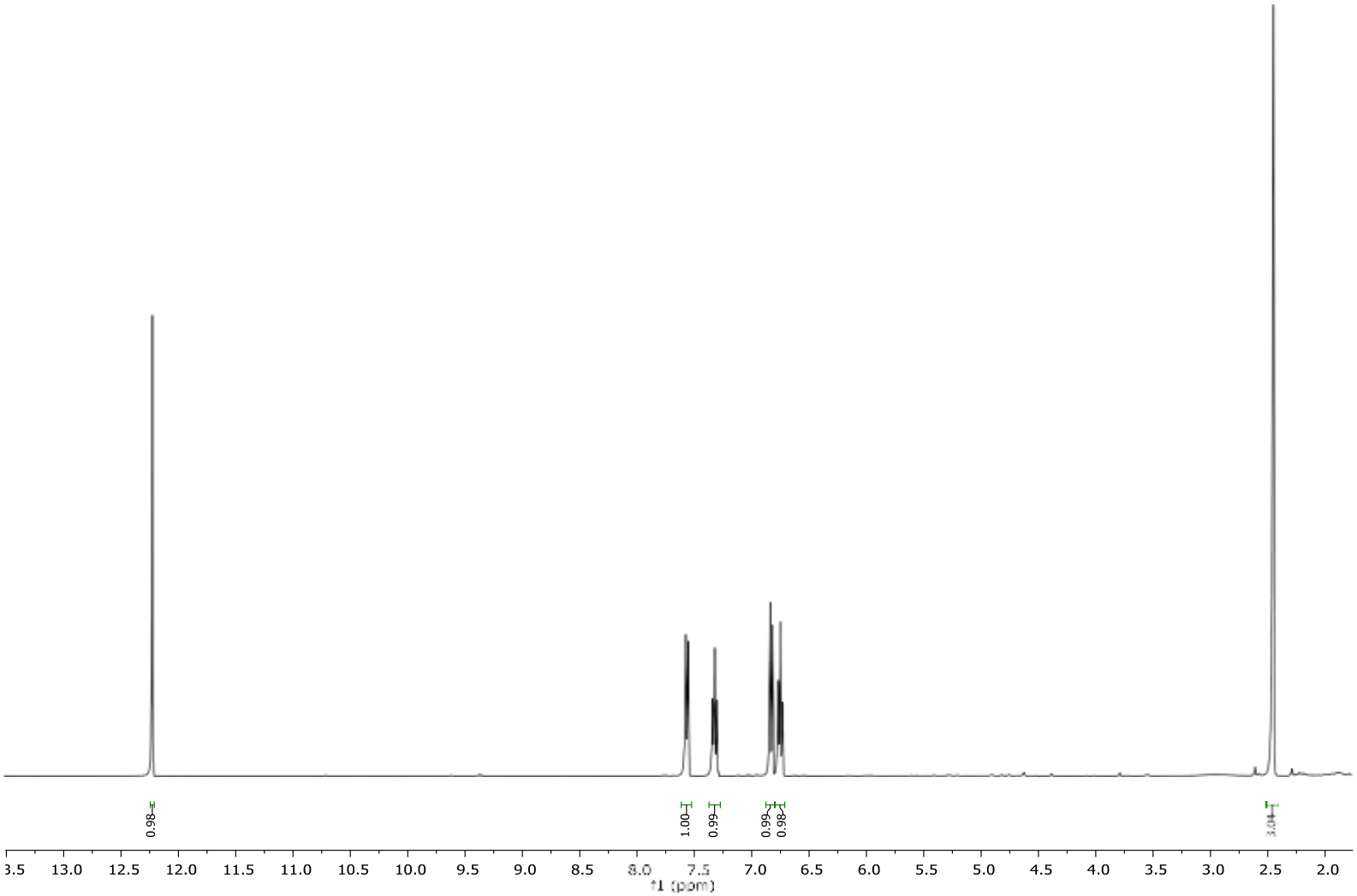


Appendix 27: The HRESIMS of Compound **115**.

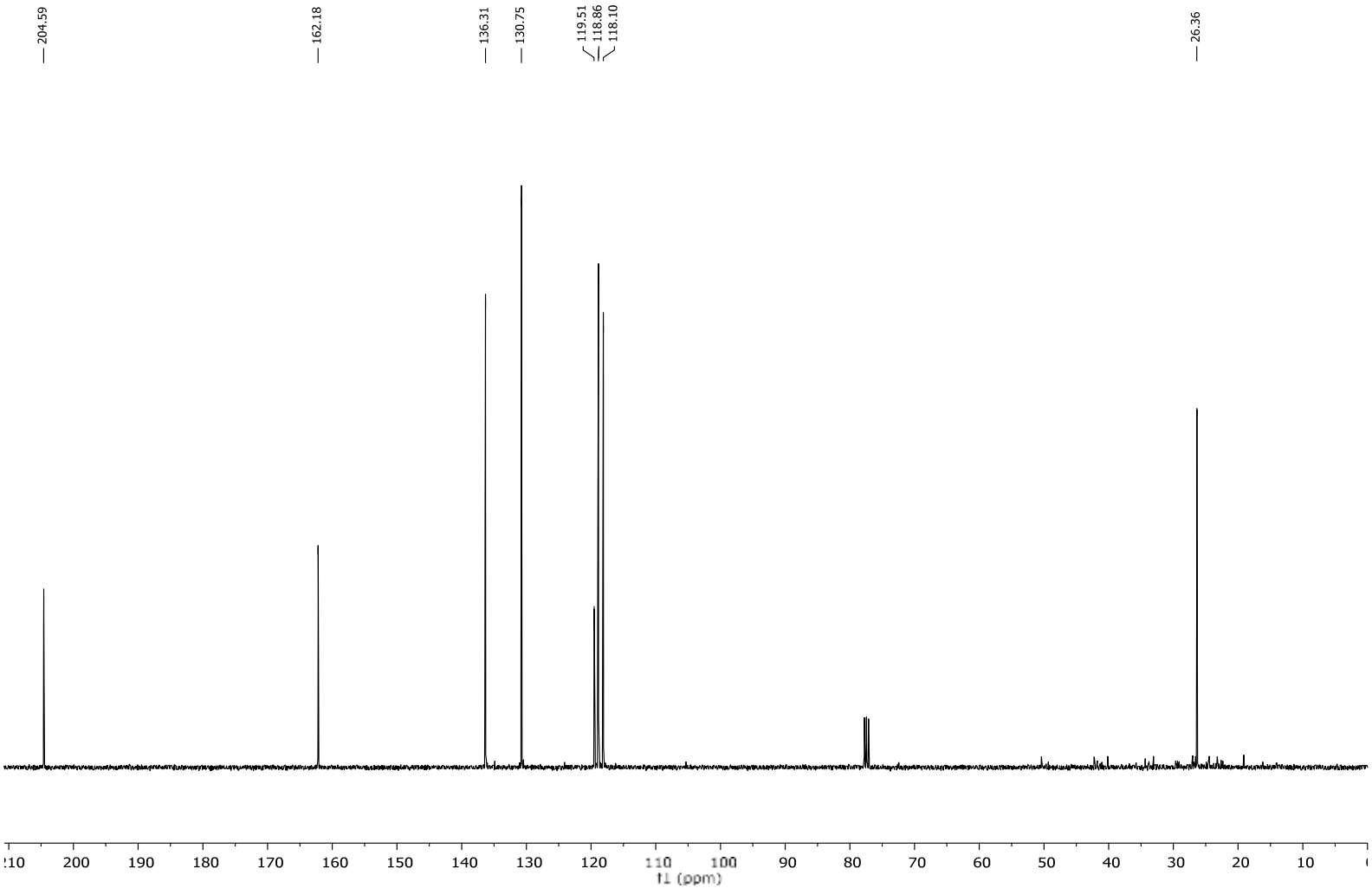




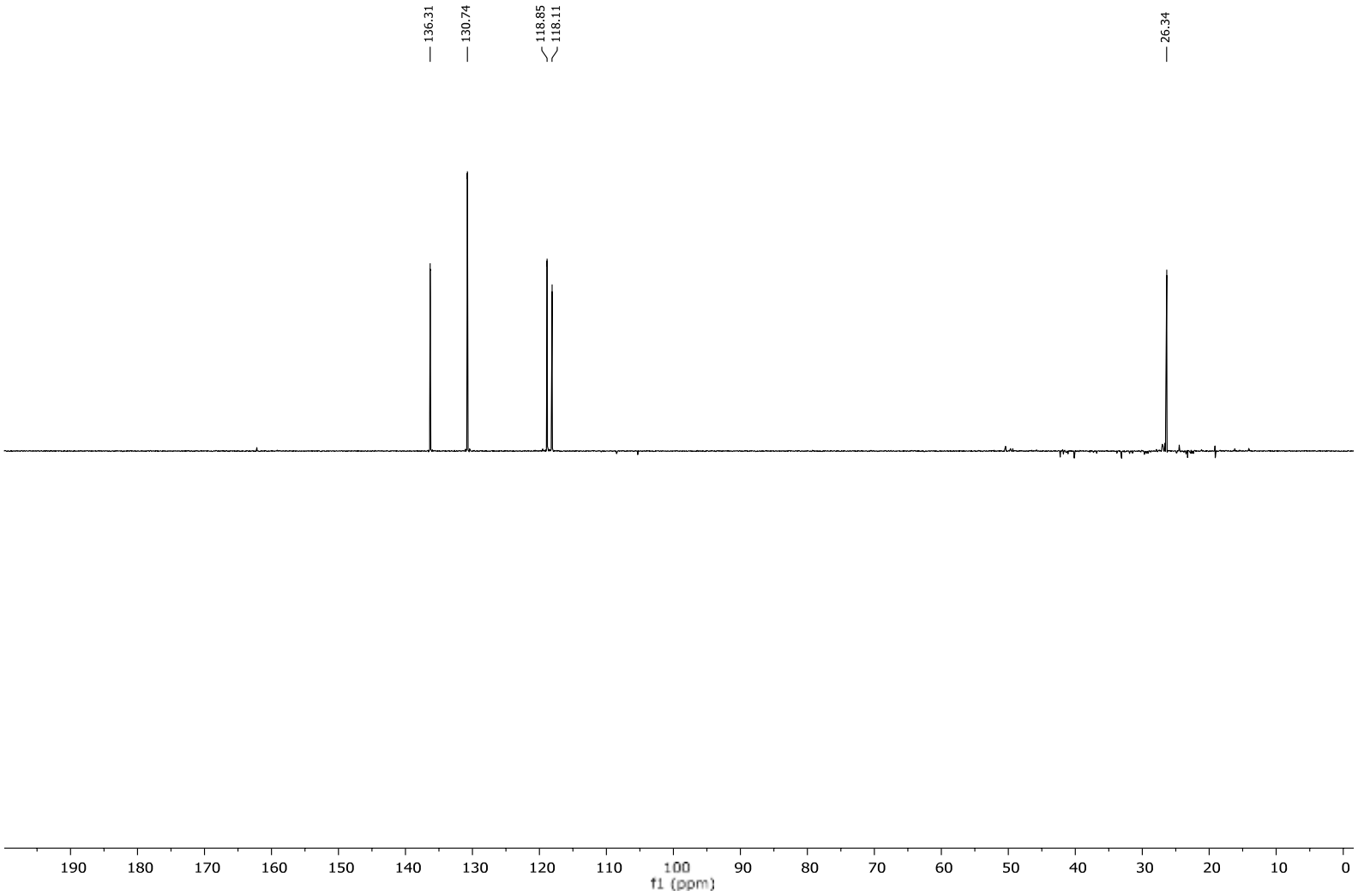
Appendix 28: The ^{1}H-NMR Spectrum of **16** in $CDCl_3$.



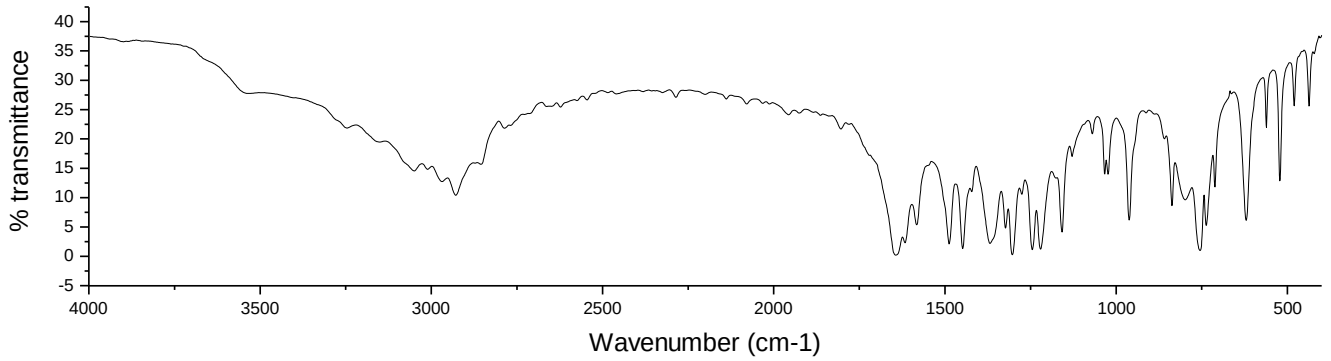
Appendix 29: The ^{13}C-NMR Spectrum of **16** in $CDCl_3$.



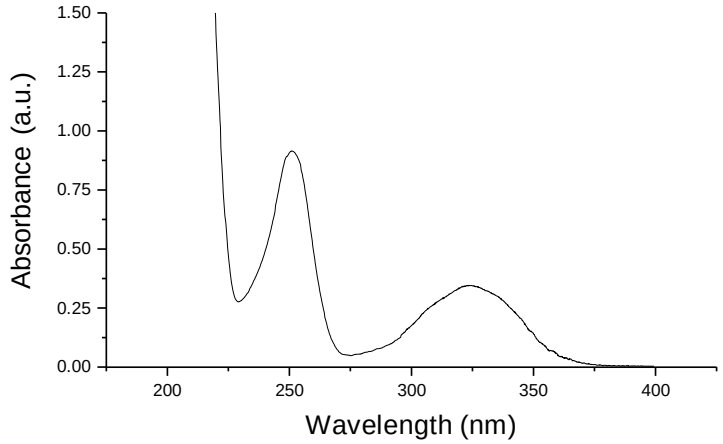
Appendix 30: The DEPT-135 NMR Spectrum of **16** in $CDCl_3$.



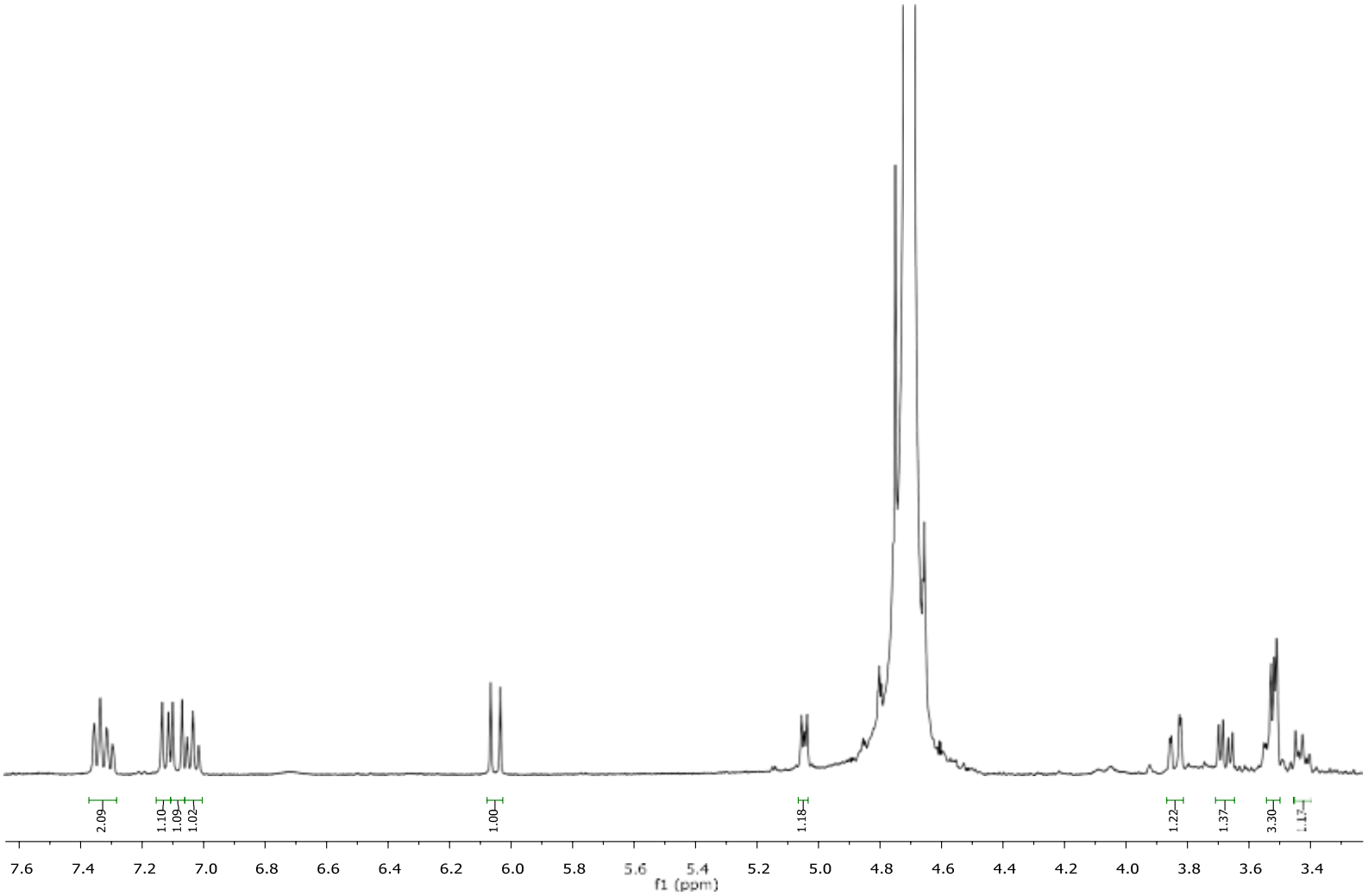
Appendix 31: The IR Spectrum of **16**.



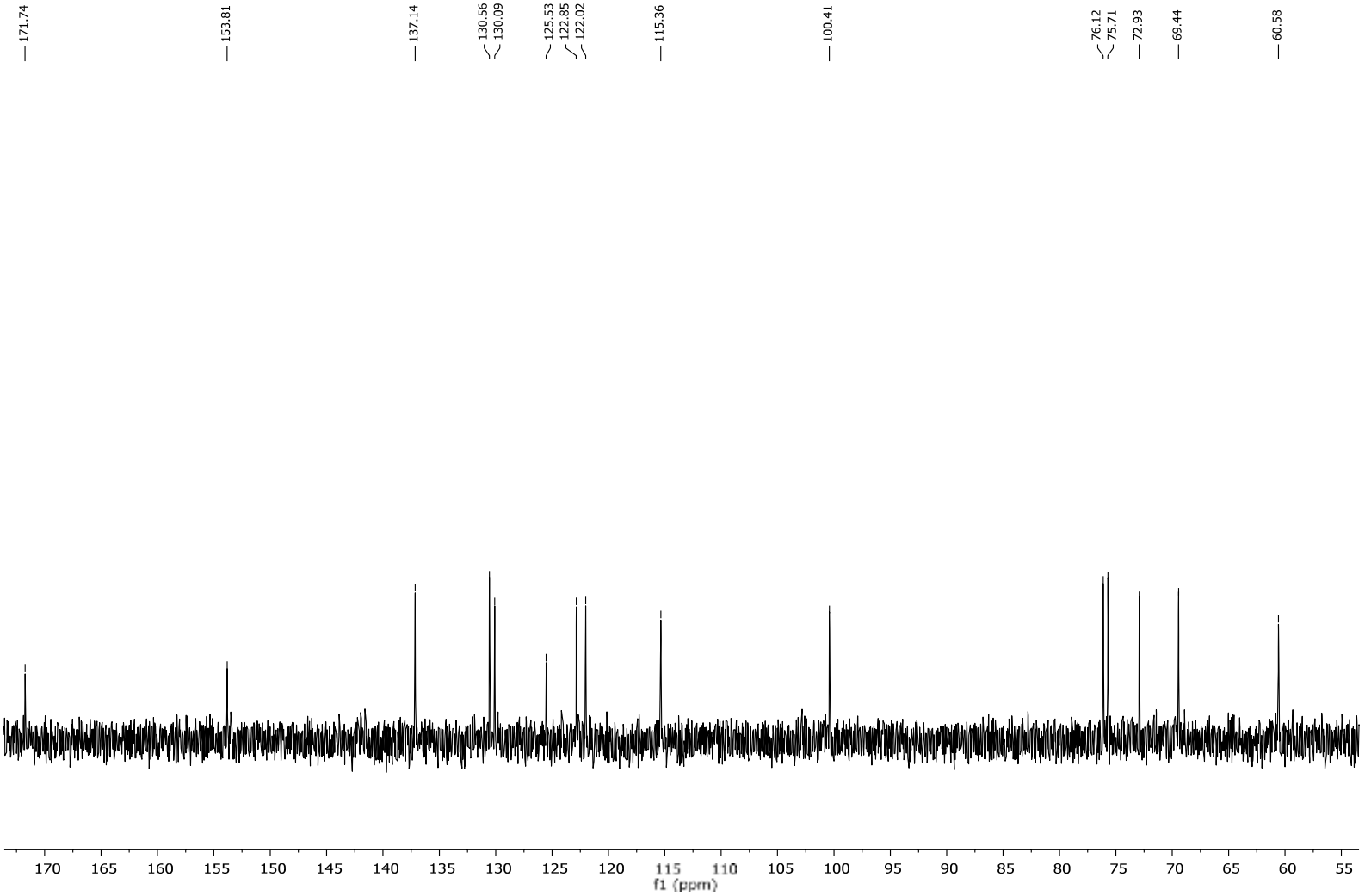
Appendix 32: The UV Spectrum of **16** in Methanol.



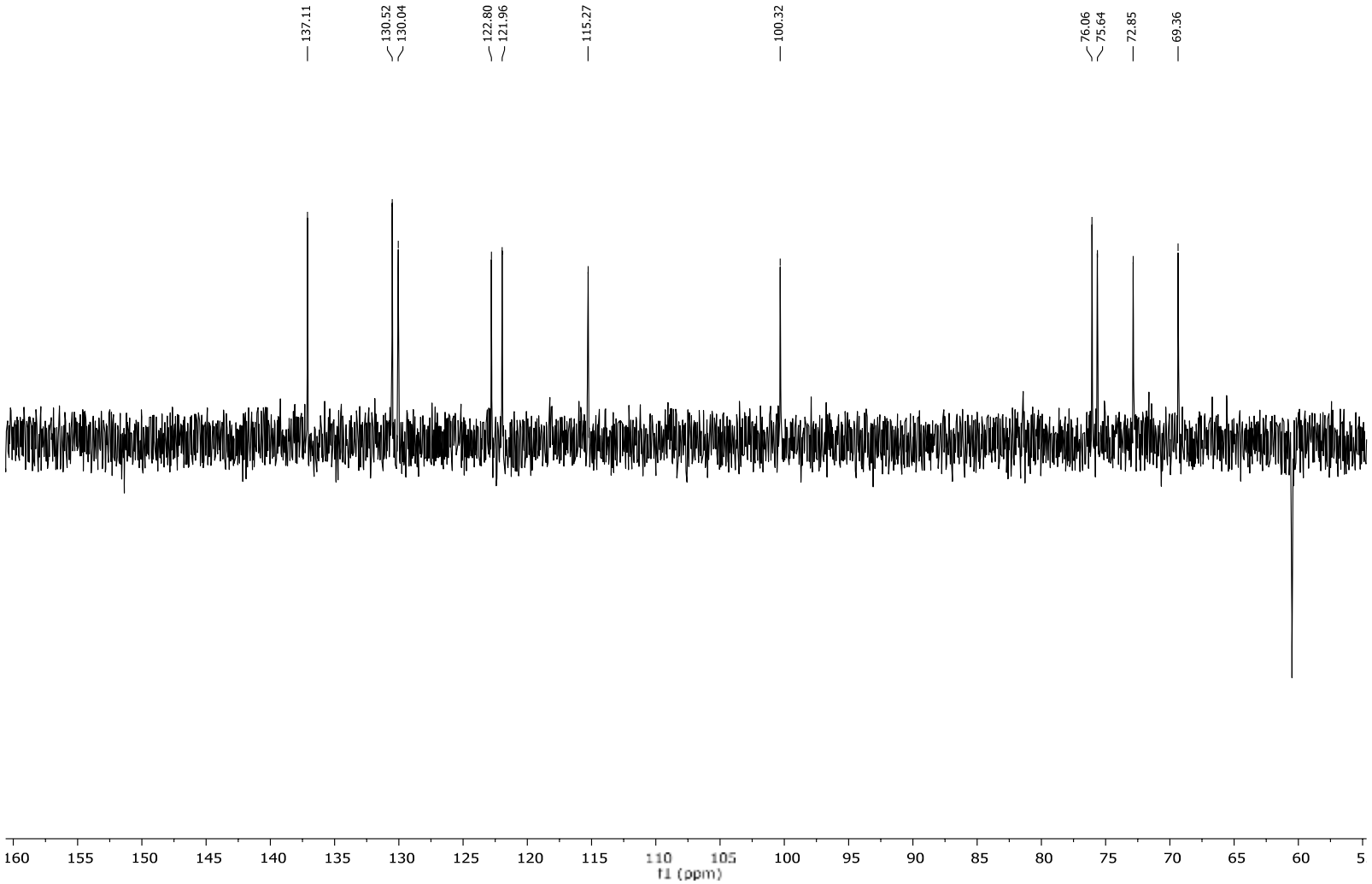
Appendix 33: The ^{1}H-NMR Spectrum of **116** in D_2O.



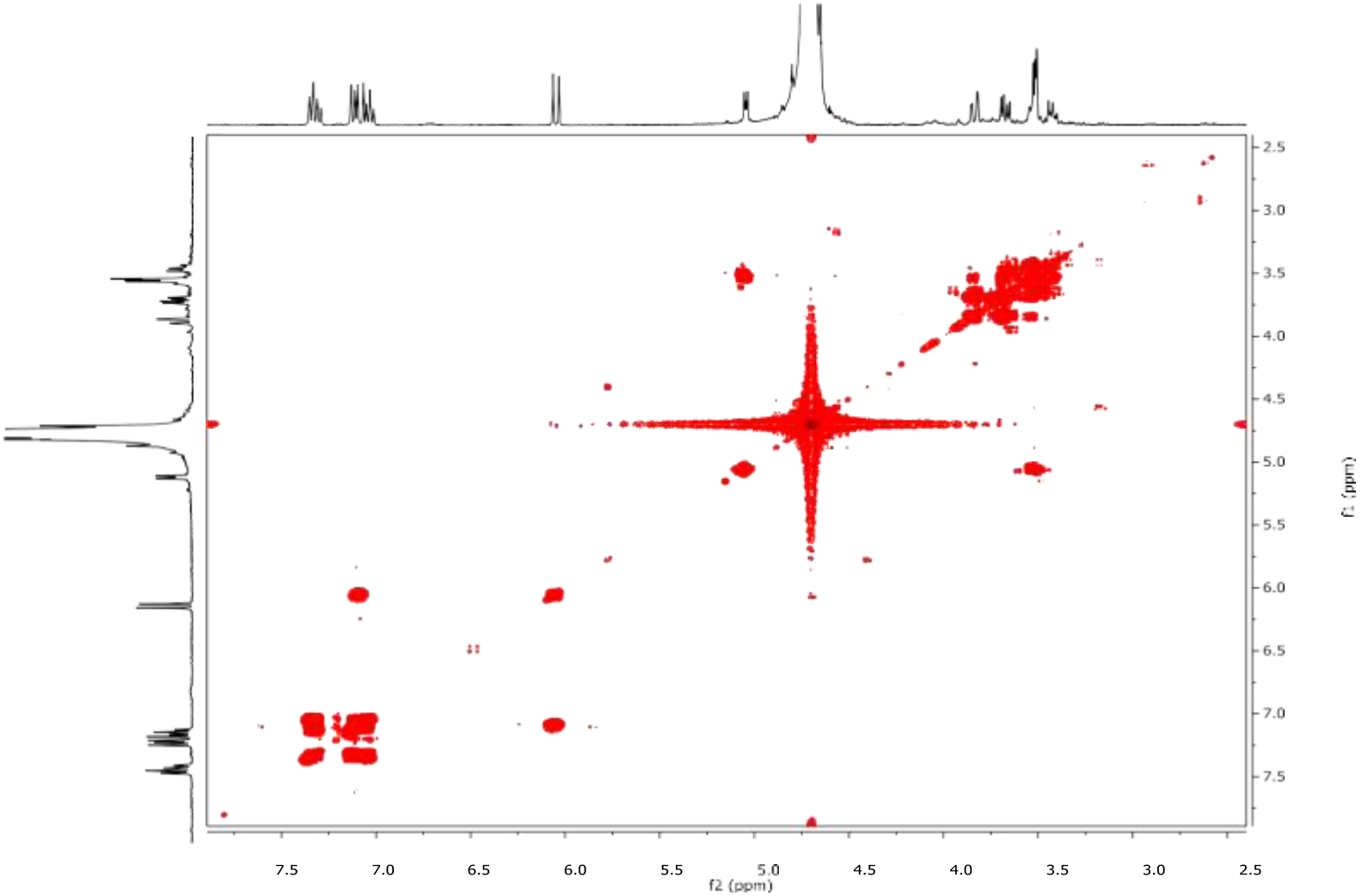
Appendix 34: The ^{13}C-NMR Spectrum of **116** in D_2O.



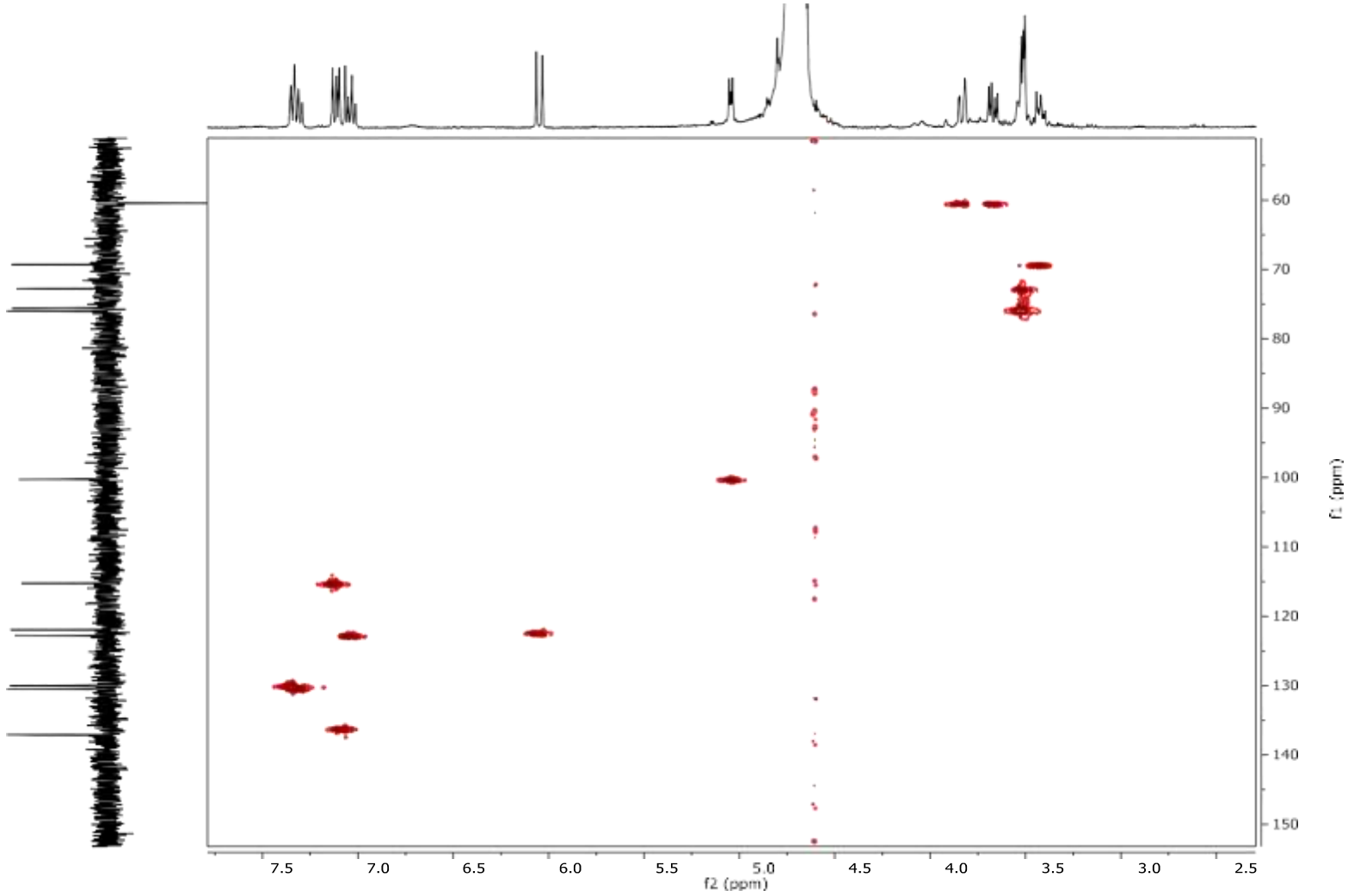
Appendix 35: The DEPT-135 NMR Spectrum of **116** in D_2O.



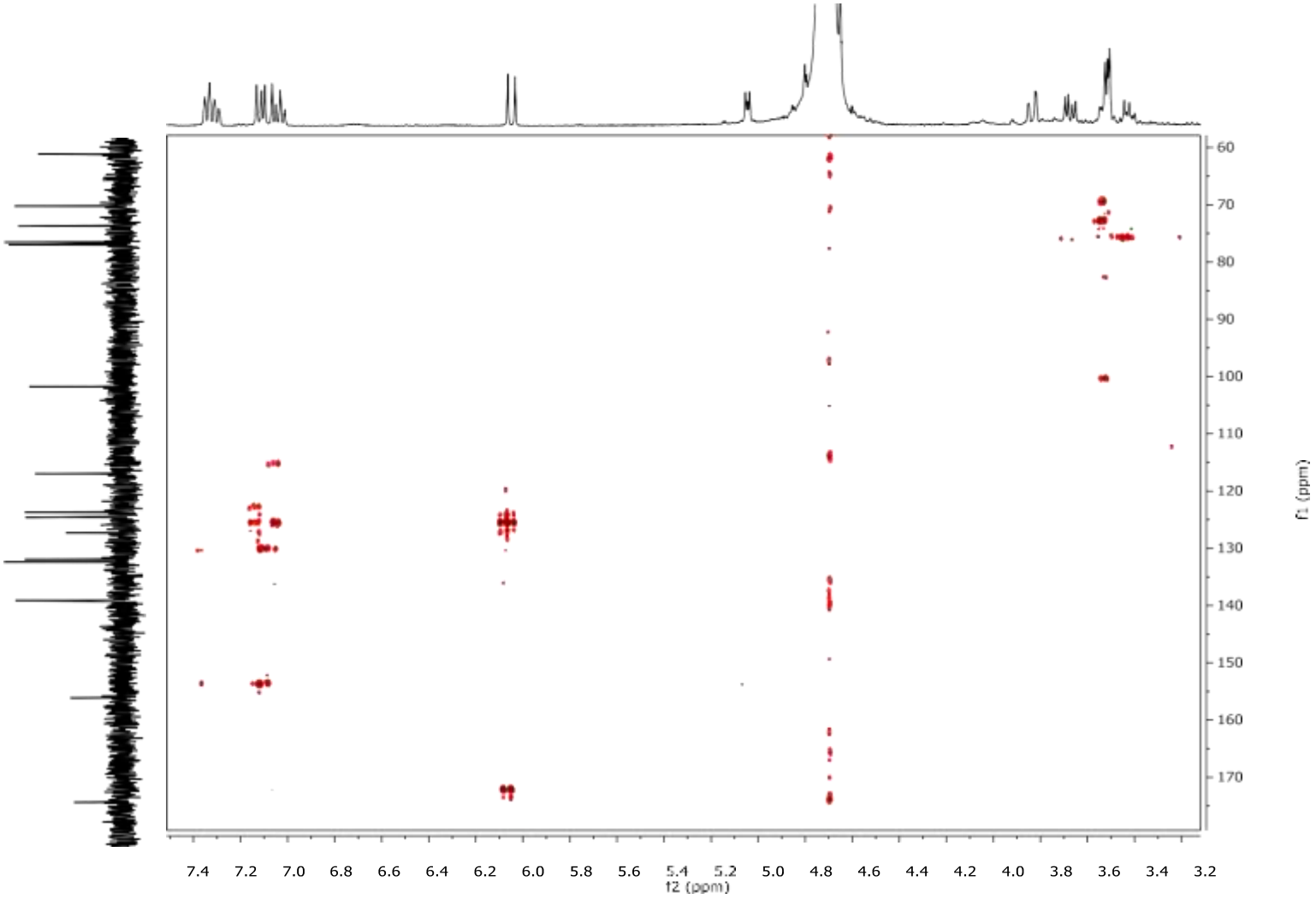
Appendix 36: The ^{1}H–^{1}H COSY Spectrum of **116** in D_2O.



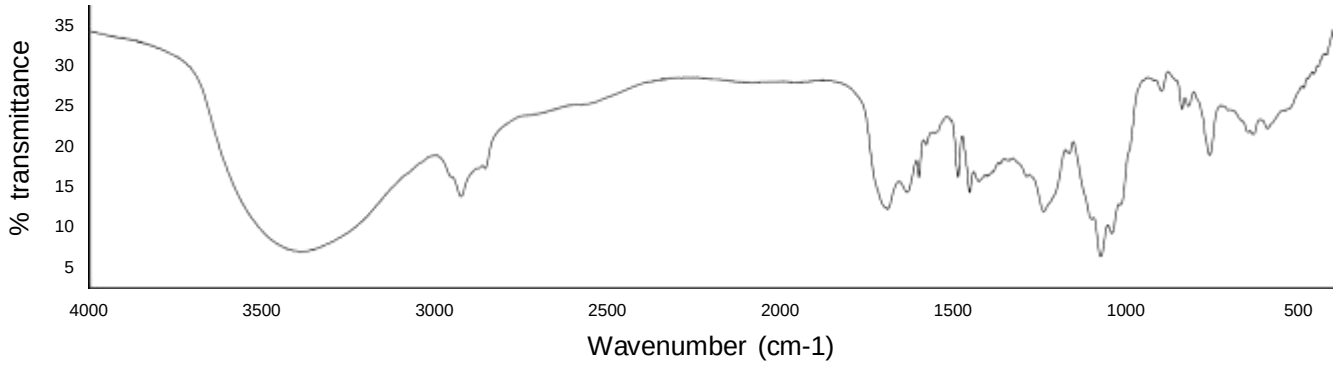
Appendix 37: The HSQC Spectrum of **116** in D_2O.



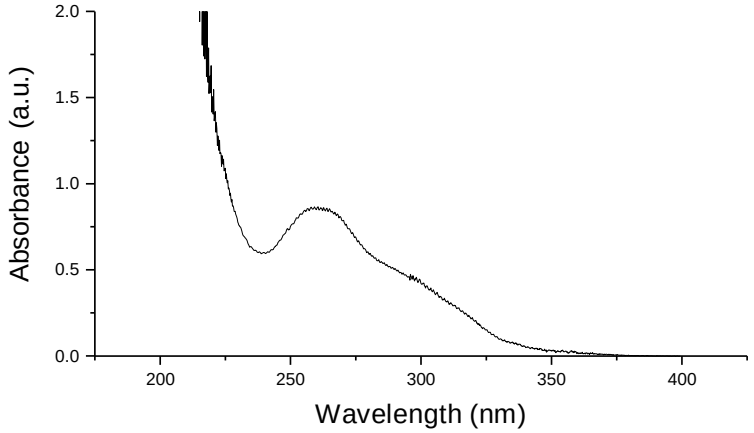
Appendix 38: The HMBC Spectrum of **116** in D_2O.



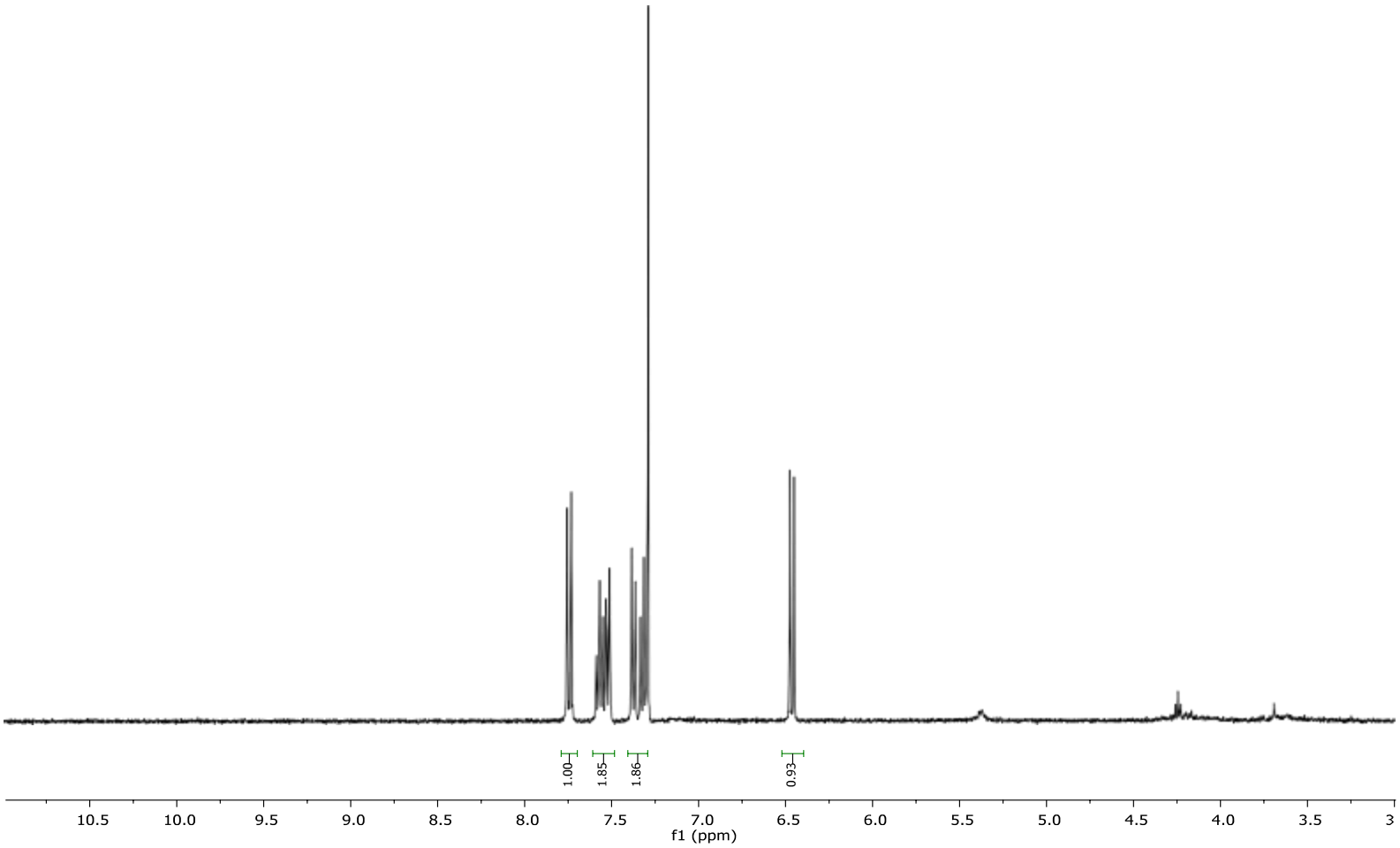
Appendix 39: The IR Spectrum of **116**.



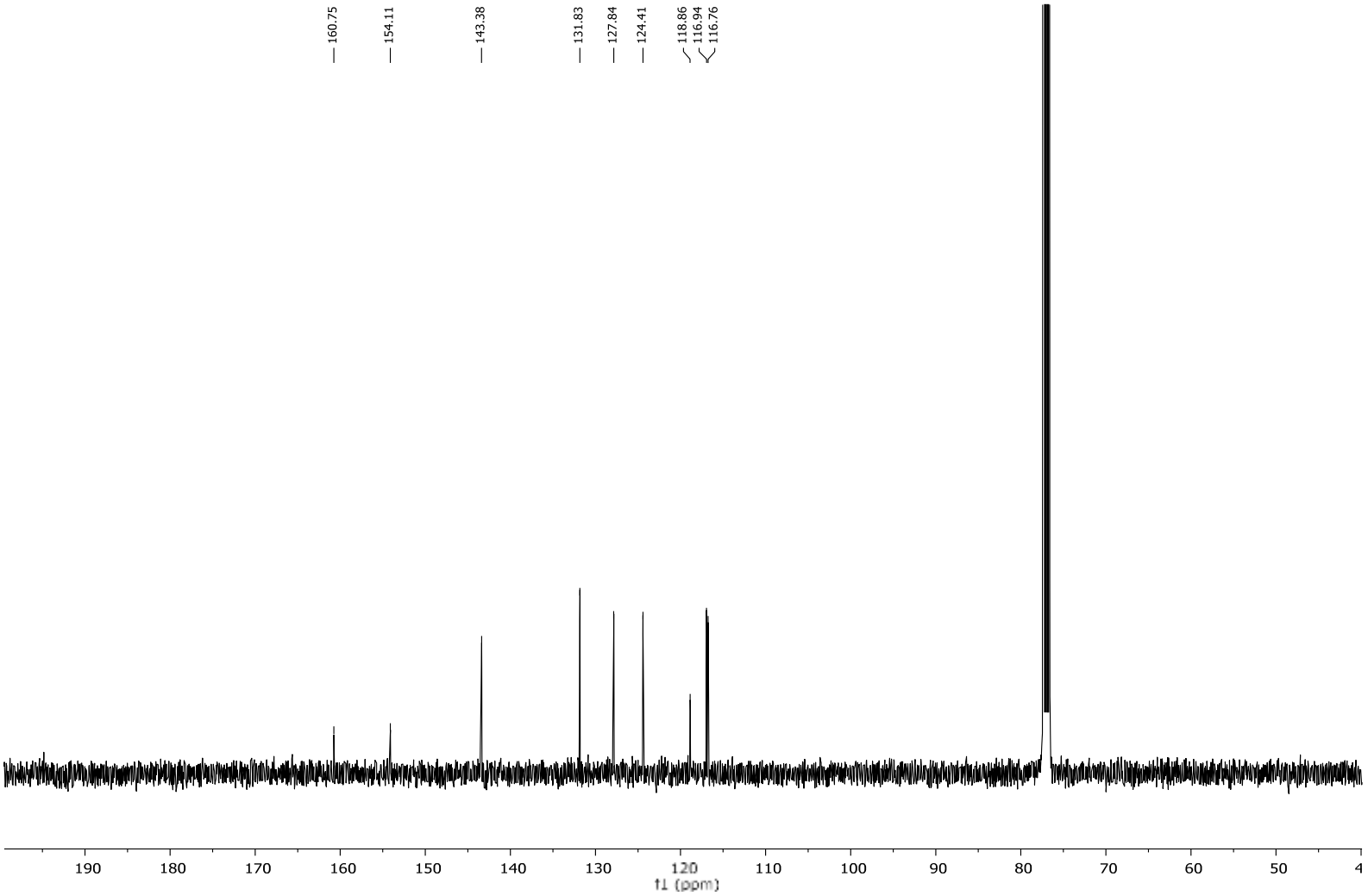
Appendix 40: The UV Spectrum of **116** in Methanol.



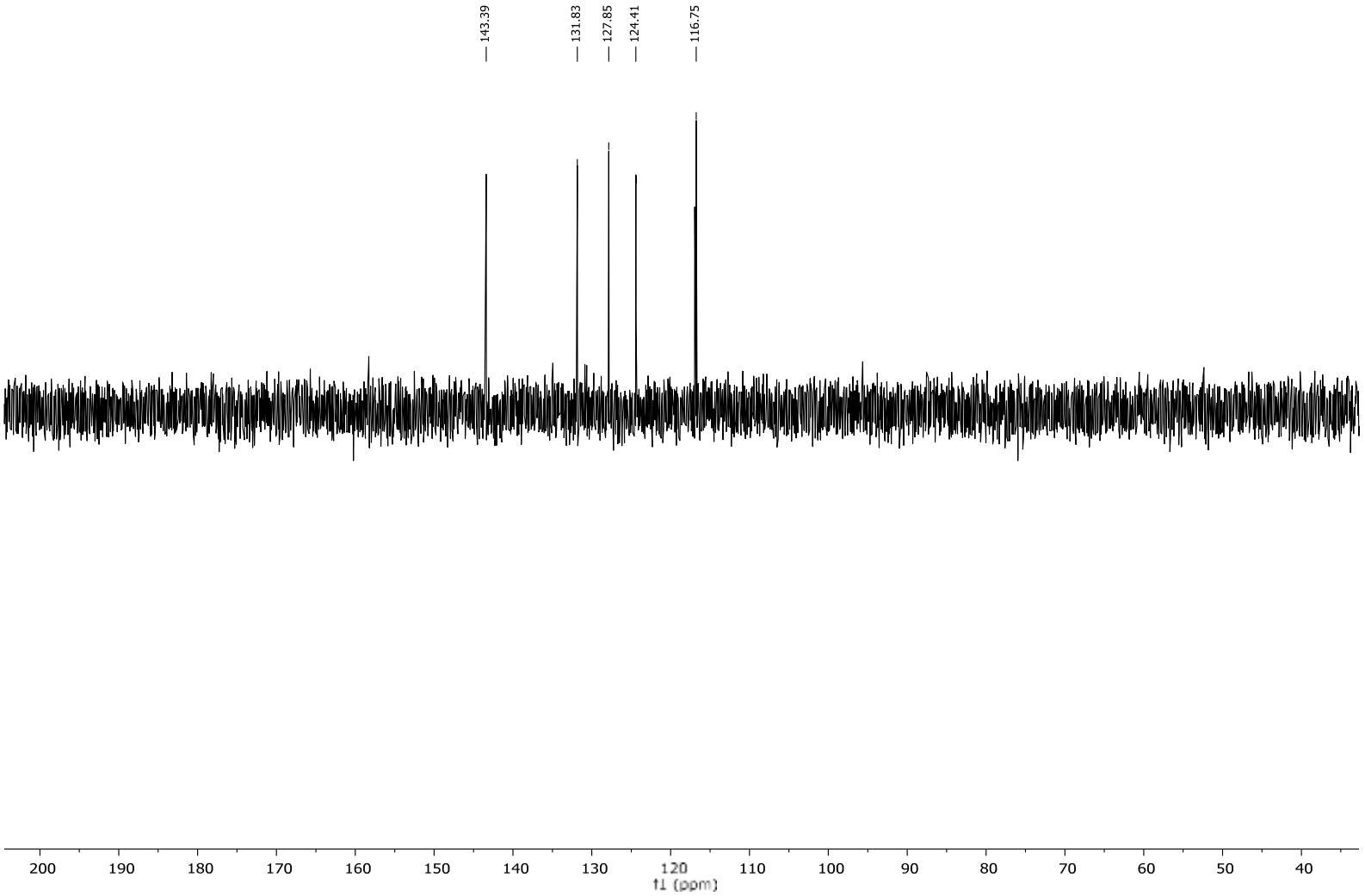
Appendix 41: The ^{1}H-NMR Spectrum of **65** in $CDCl_3$.



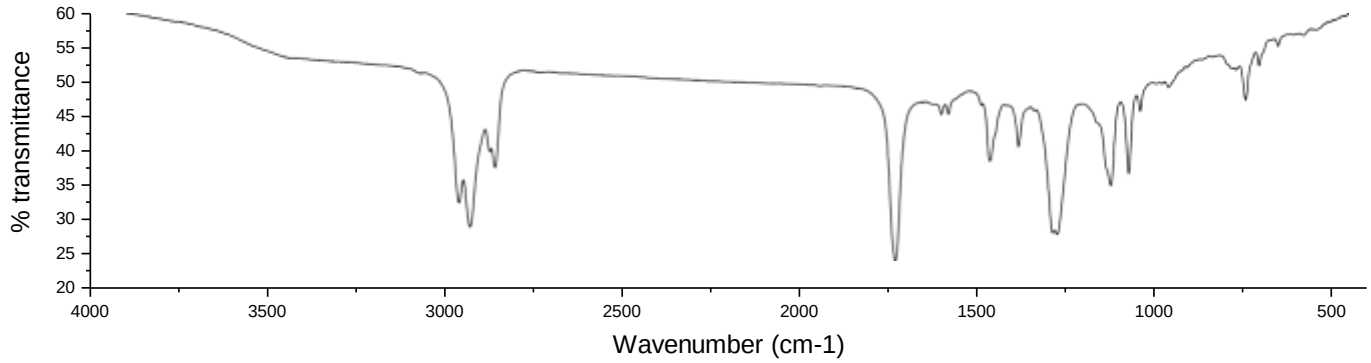
Appendix 42: The ^{13}C-NMR Spectrum of **65** in $CDCl_3$.



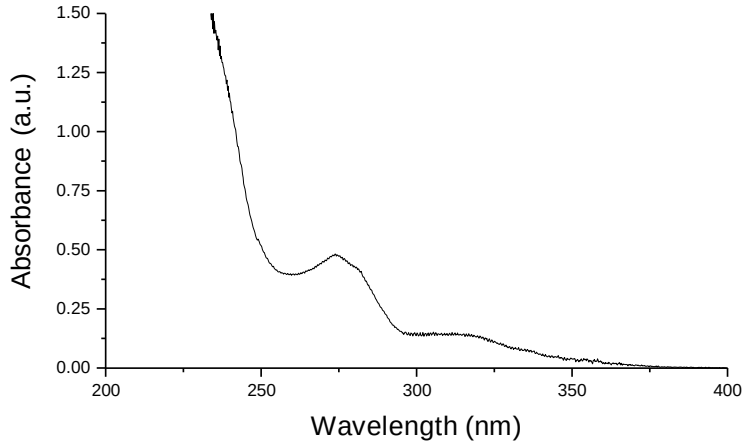
Appendix 43: The DEPT-135 NMR Spectrum of **65** in $CDCl_3$.



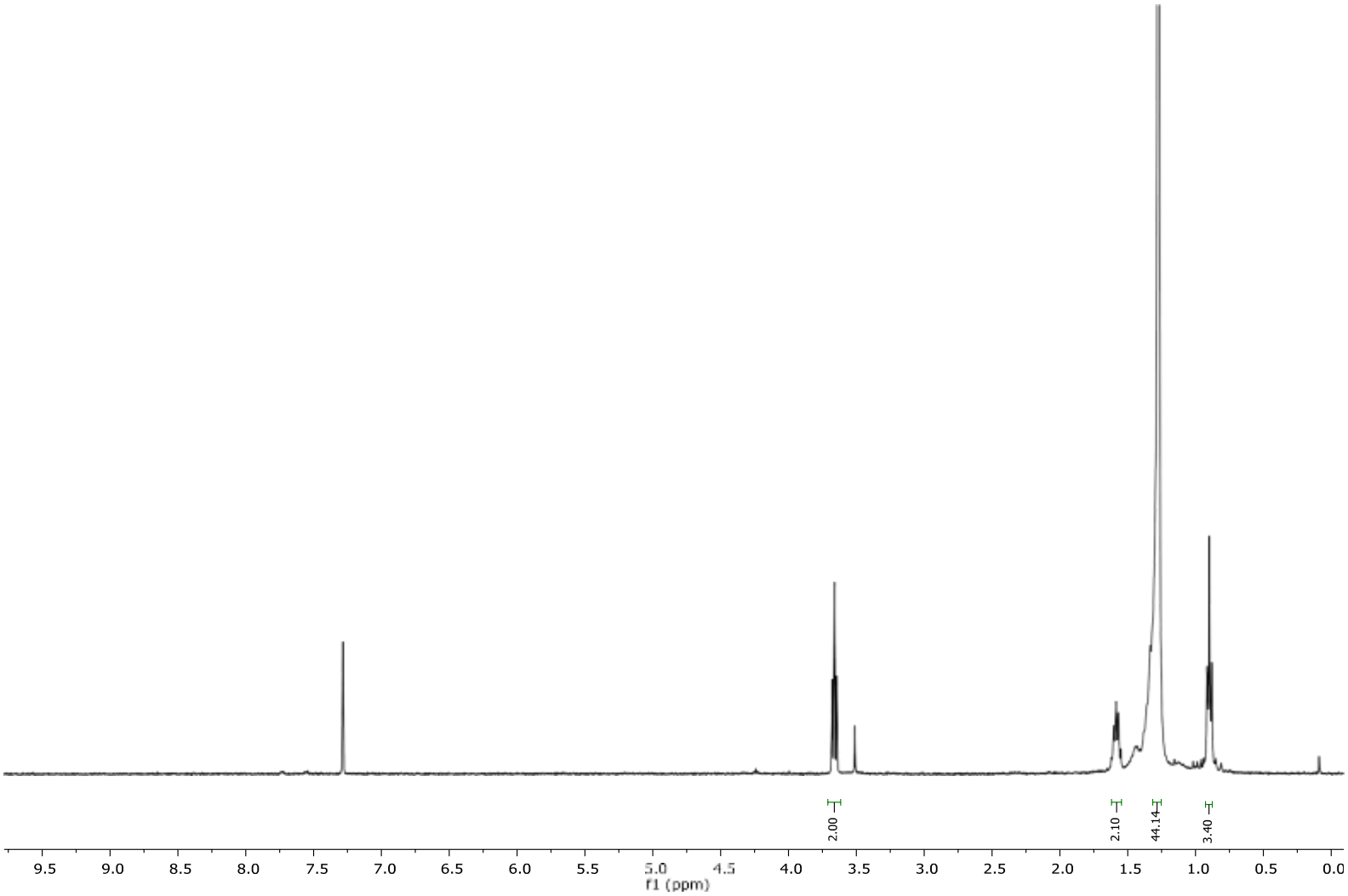
Appendix 44: The IR Spectrum of **65**.



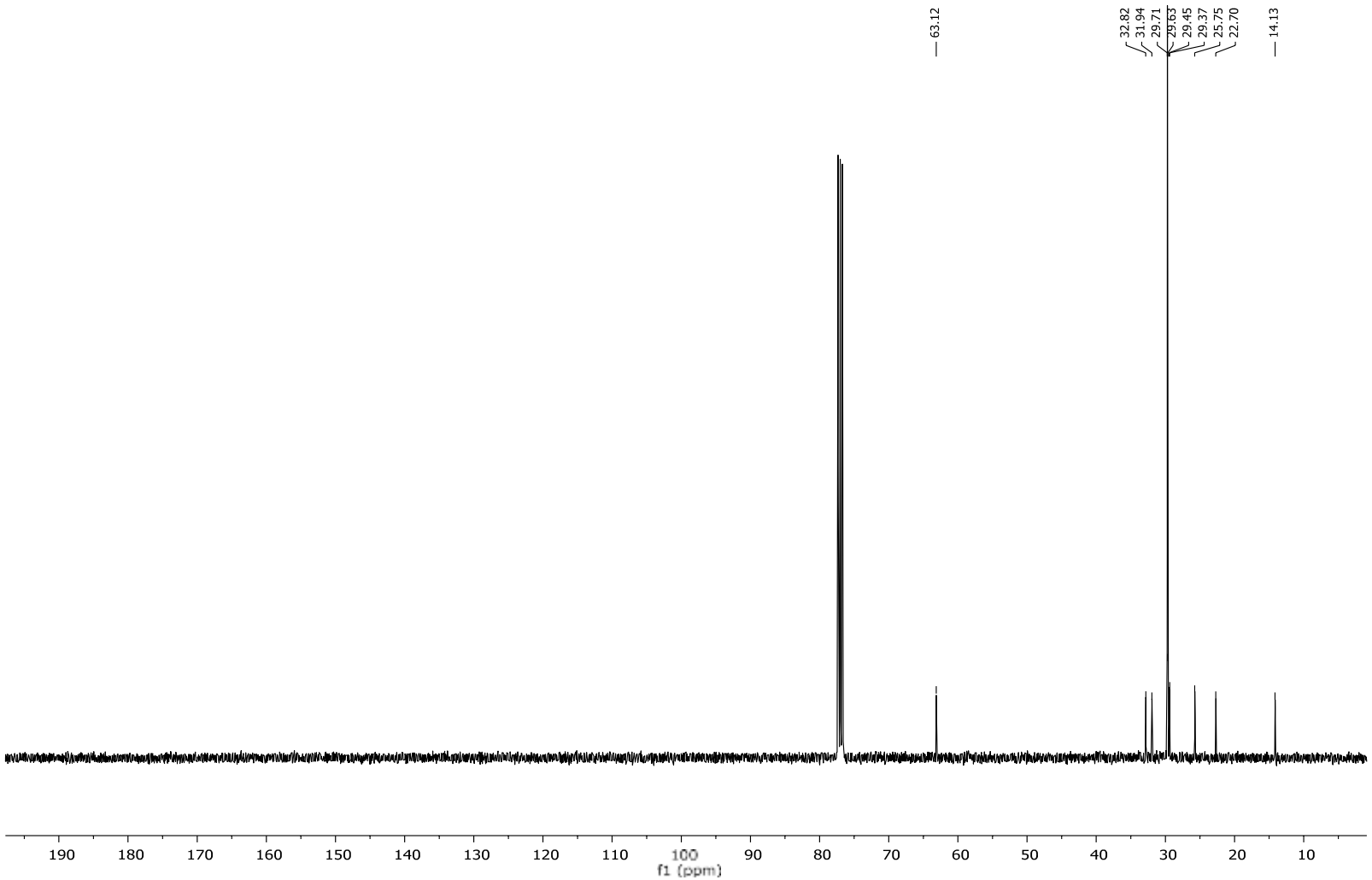
Appendix 45: The UV Spectrum of **65** in Methanol



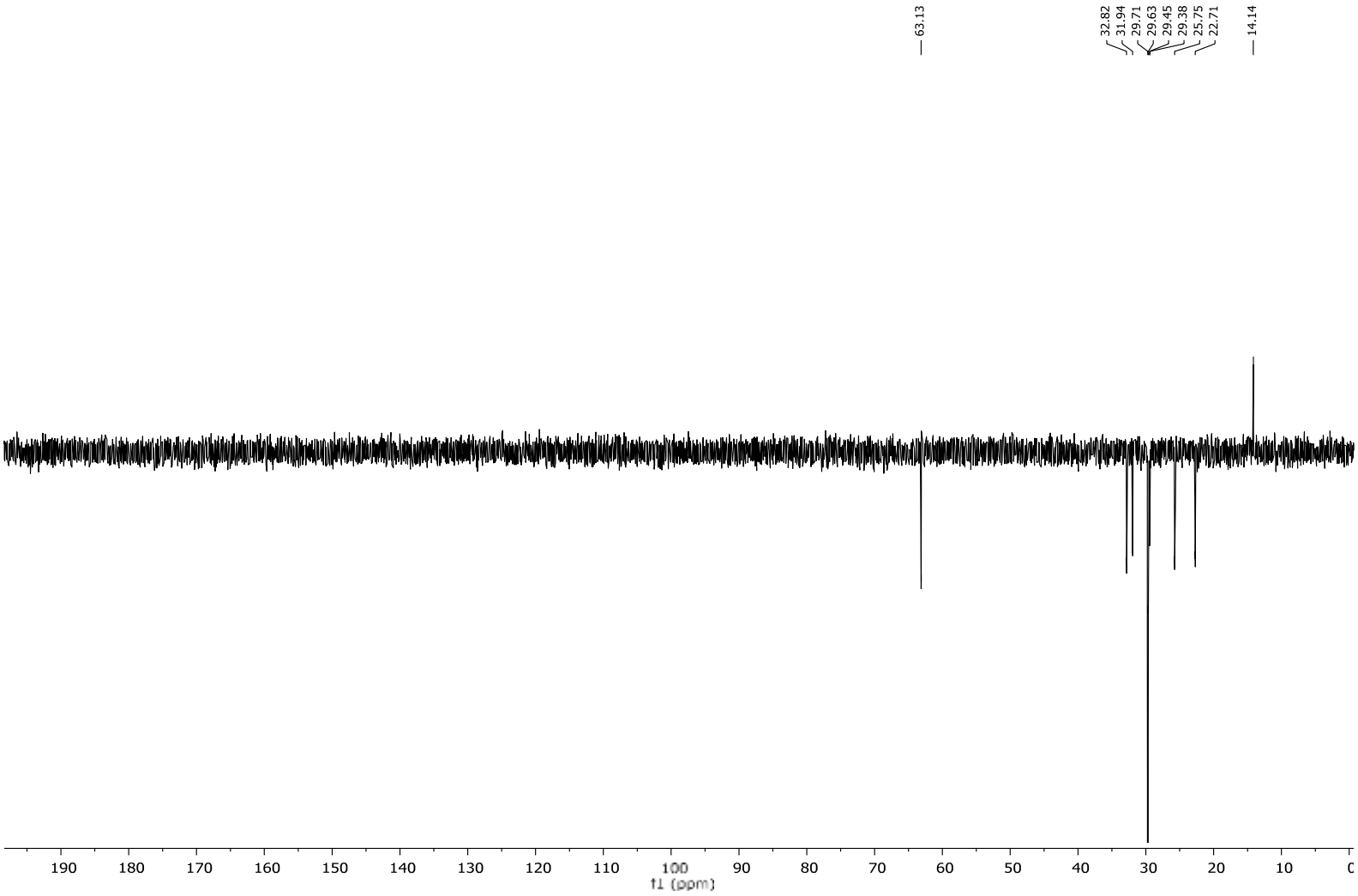
Appendix 46: The ^{1}H-NMR Spectrum of **119** in $CDCl_3$.



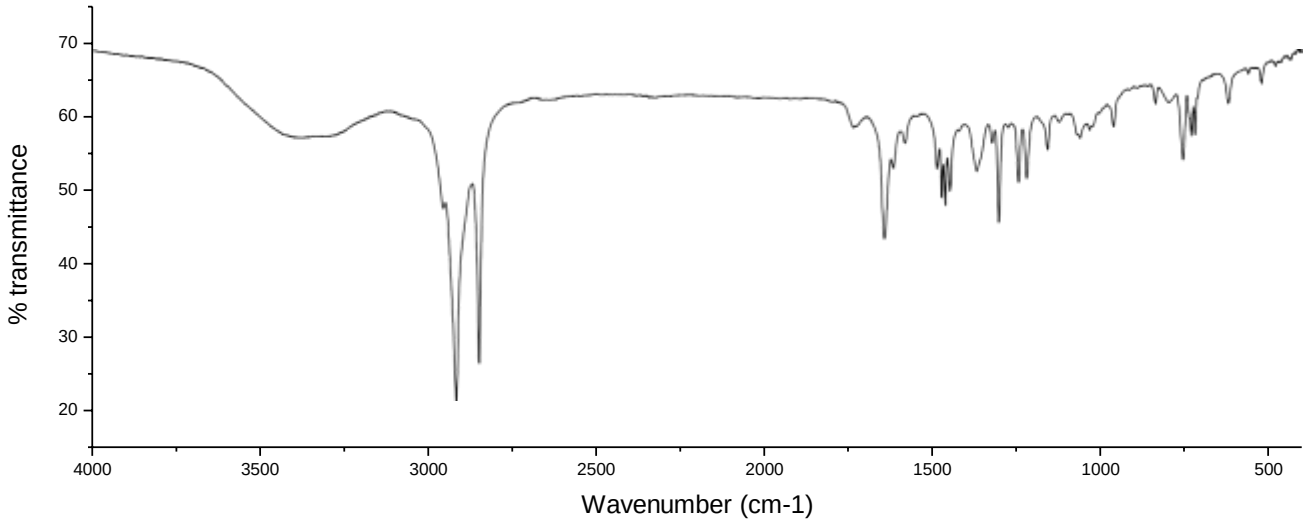
Appendix 47: The ^{13}C-NMR Spectrum of **119** in $CDCl_3$.



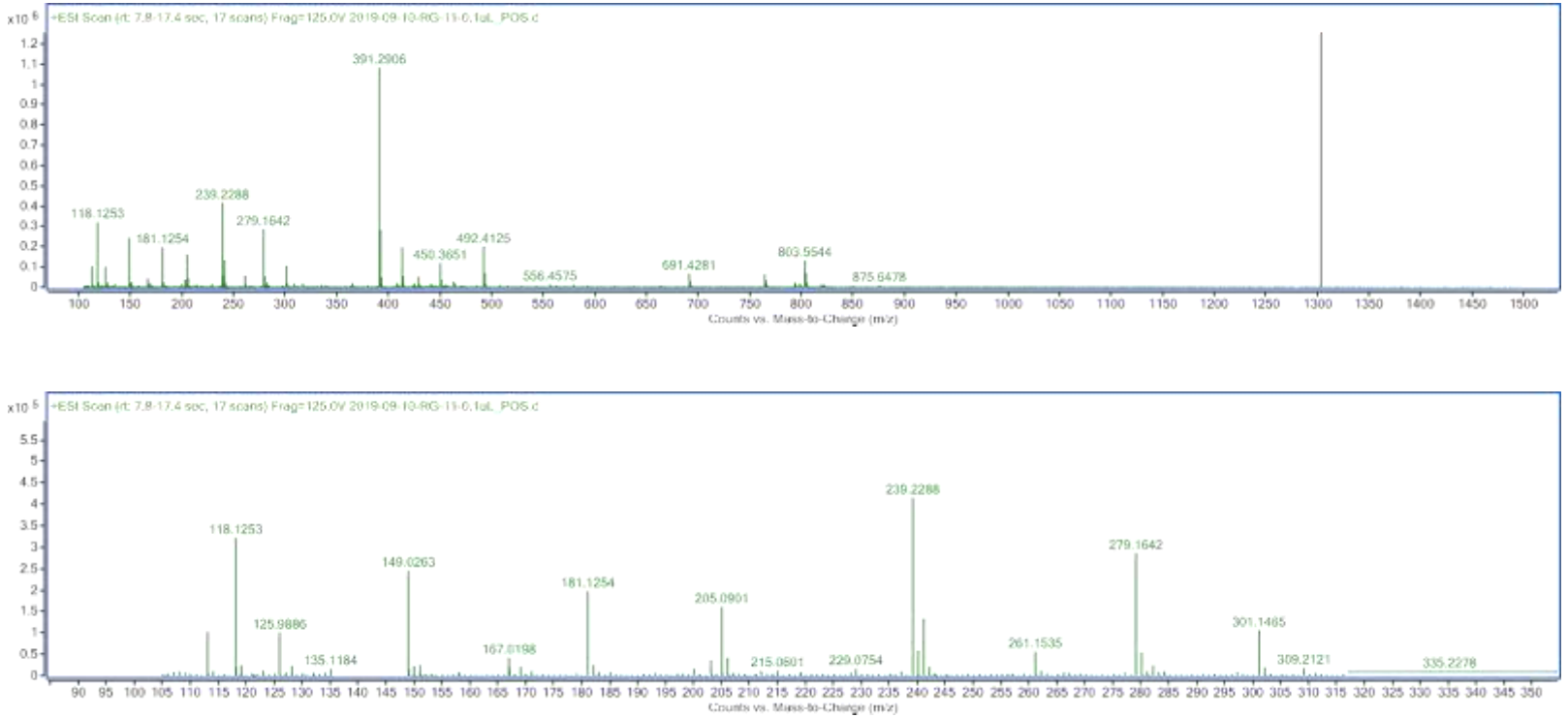
Appendix 48: The DEPT-135 NMR Spectrum of **119** in $CDCl_3$.



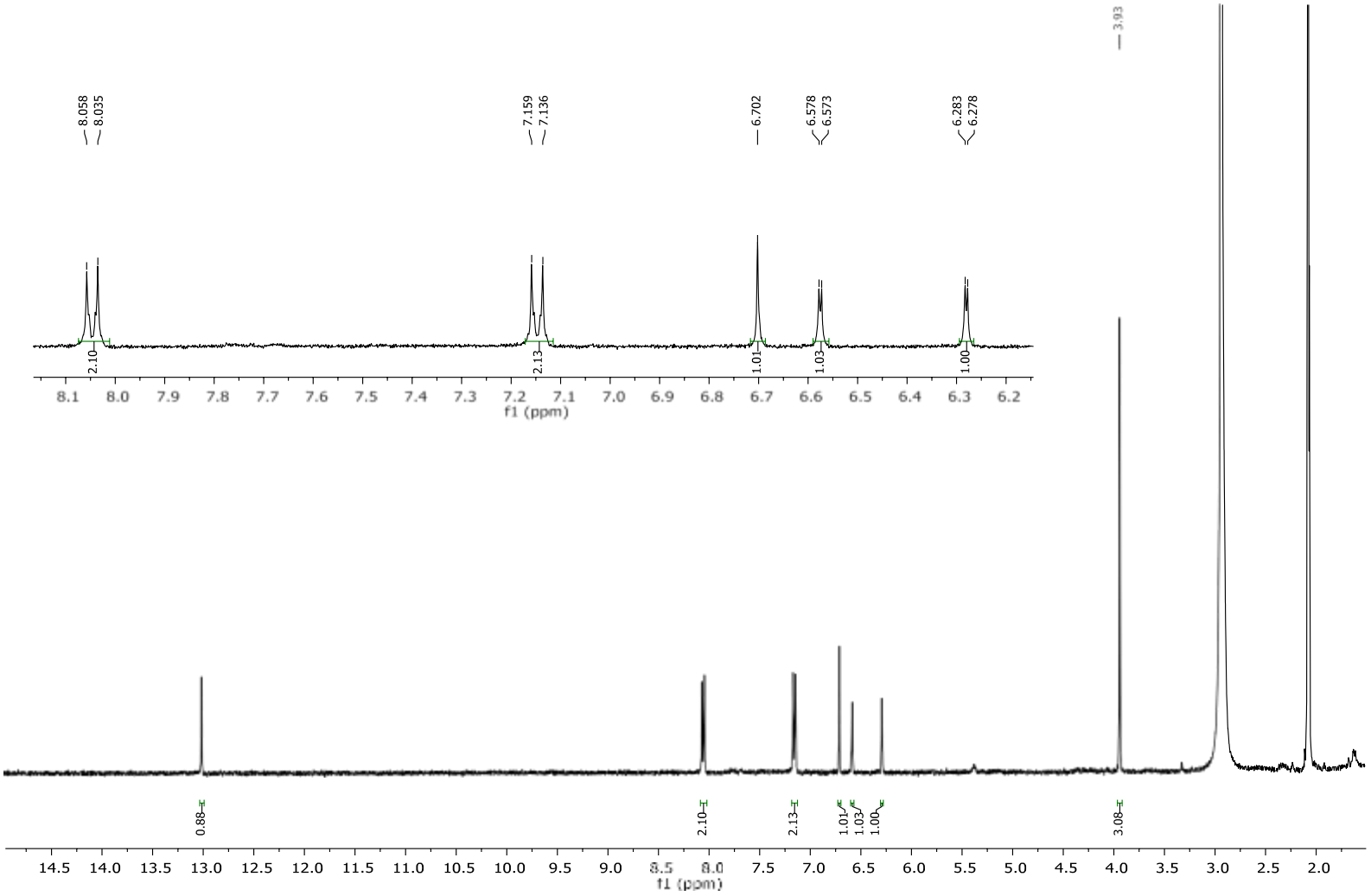
Appendix 49: The IR Spectrum of **119**.



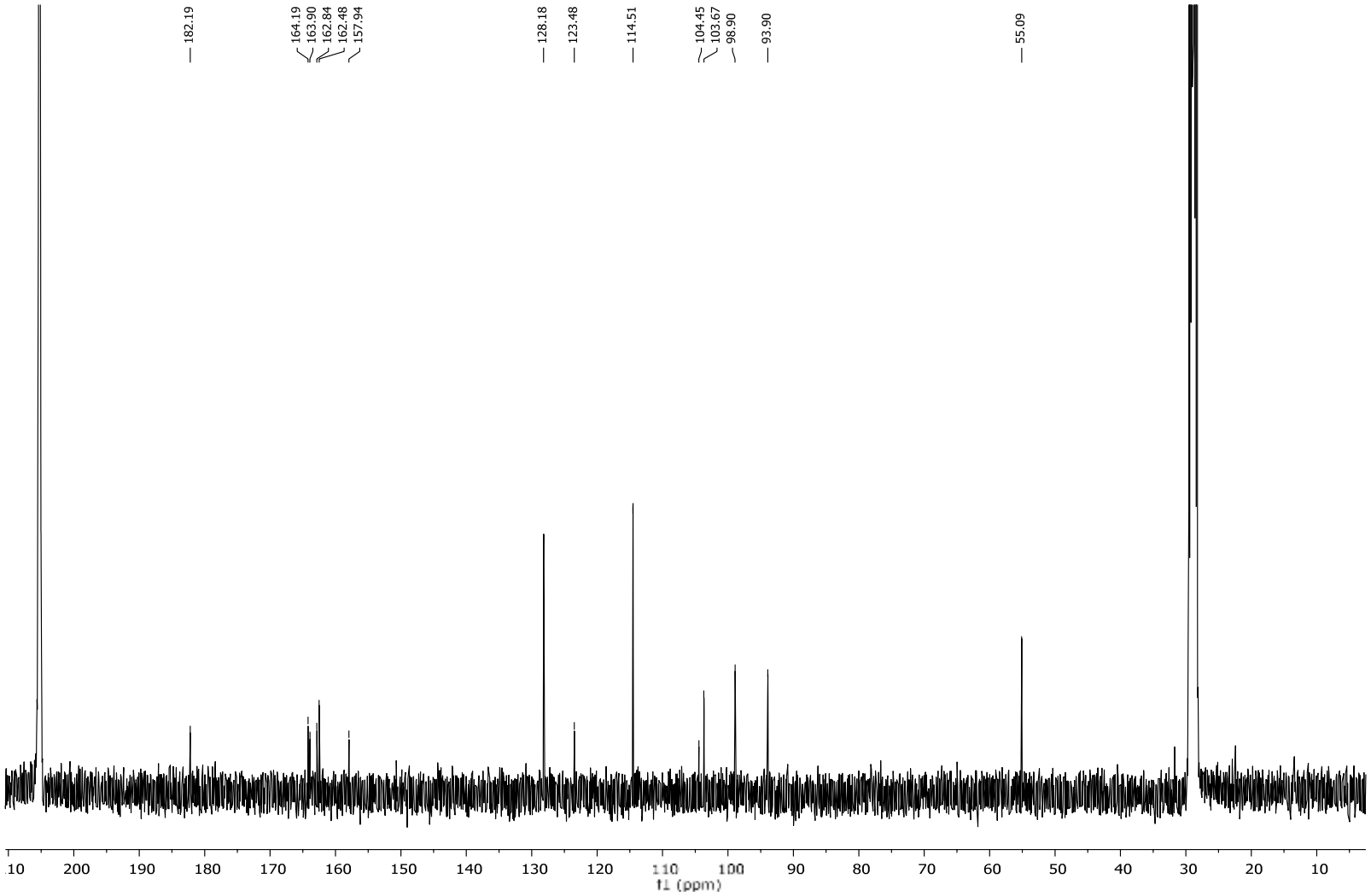
Appendix 50: The HRESIMS of Compound **119**.



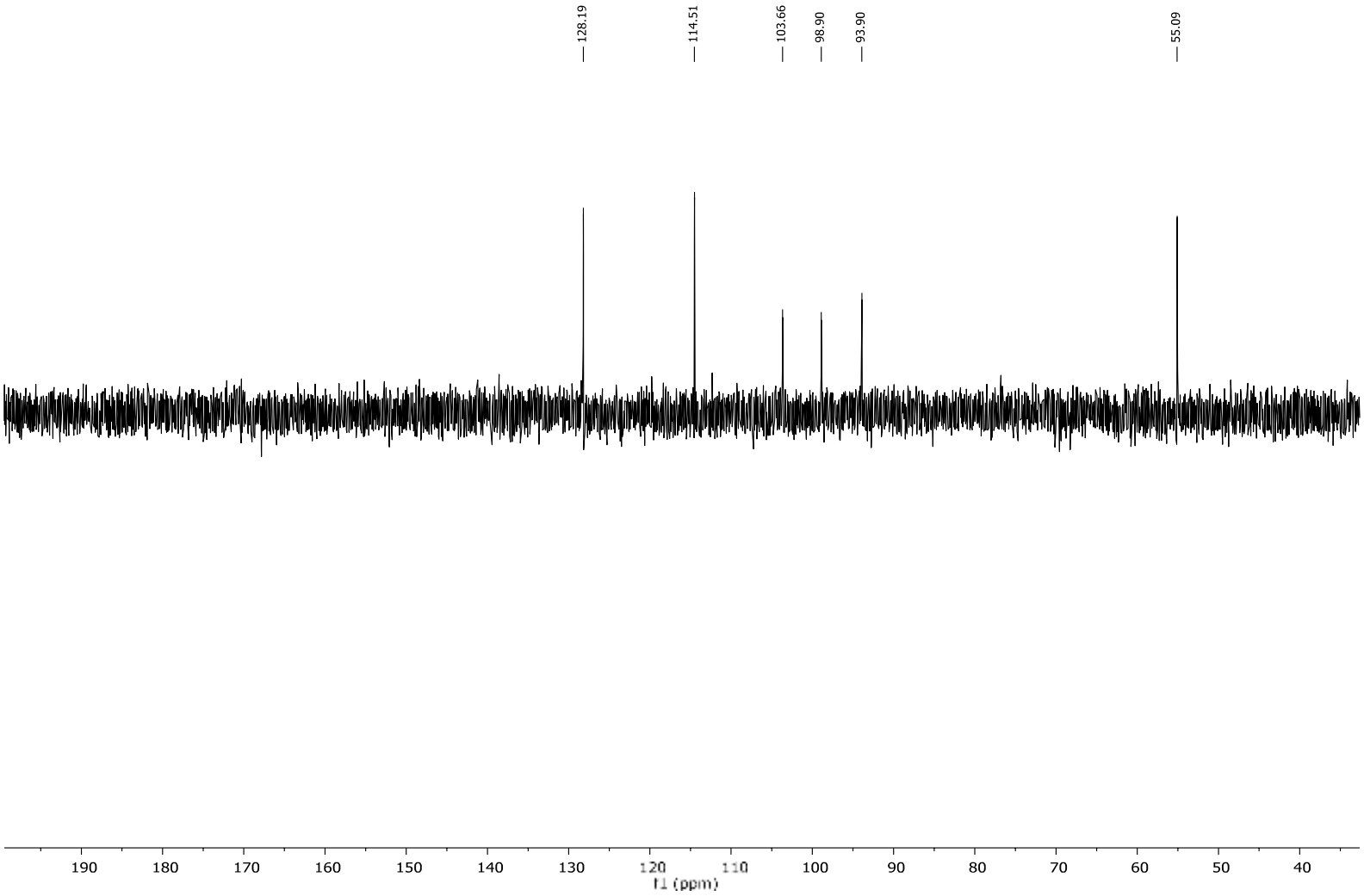
Appendix 51: The ^{1}H-NMR Spectrum of **120** in Acetone-d_6.



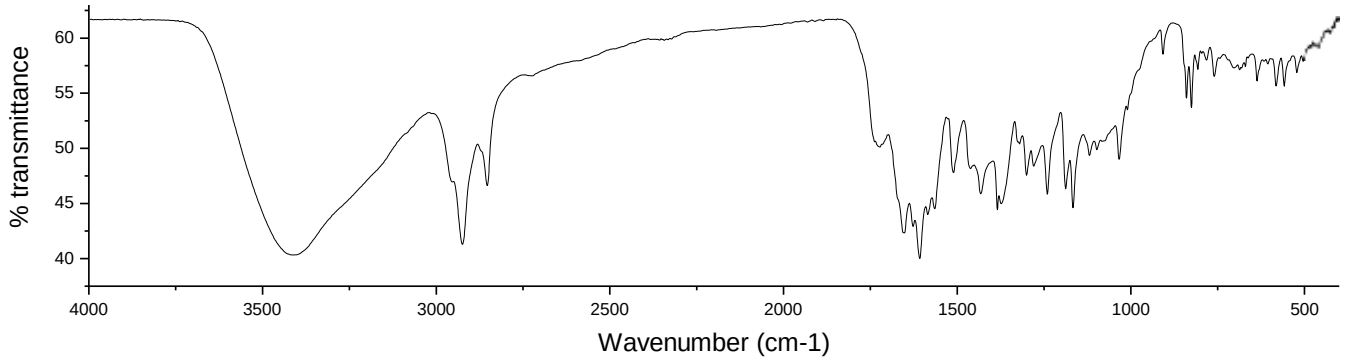
Appendix 52: The ^{13}C-NMR Spectrum of **120** in Acetone-d_6.



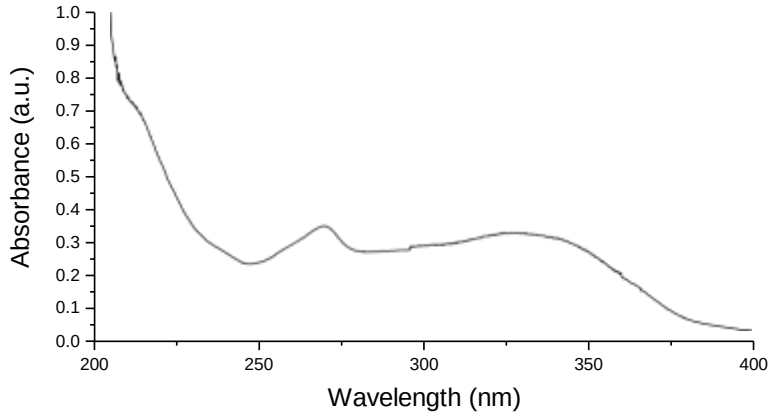
Appendix 53: The DEPT-135 NMR Spectrum of **120** in Acetone-d_6.



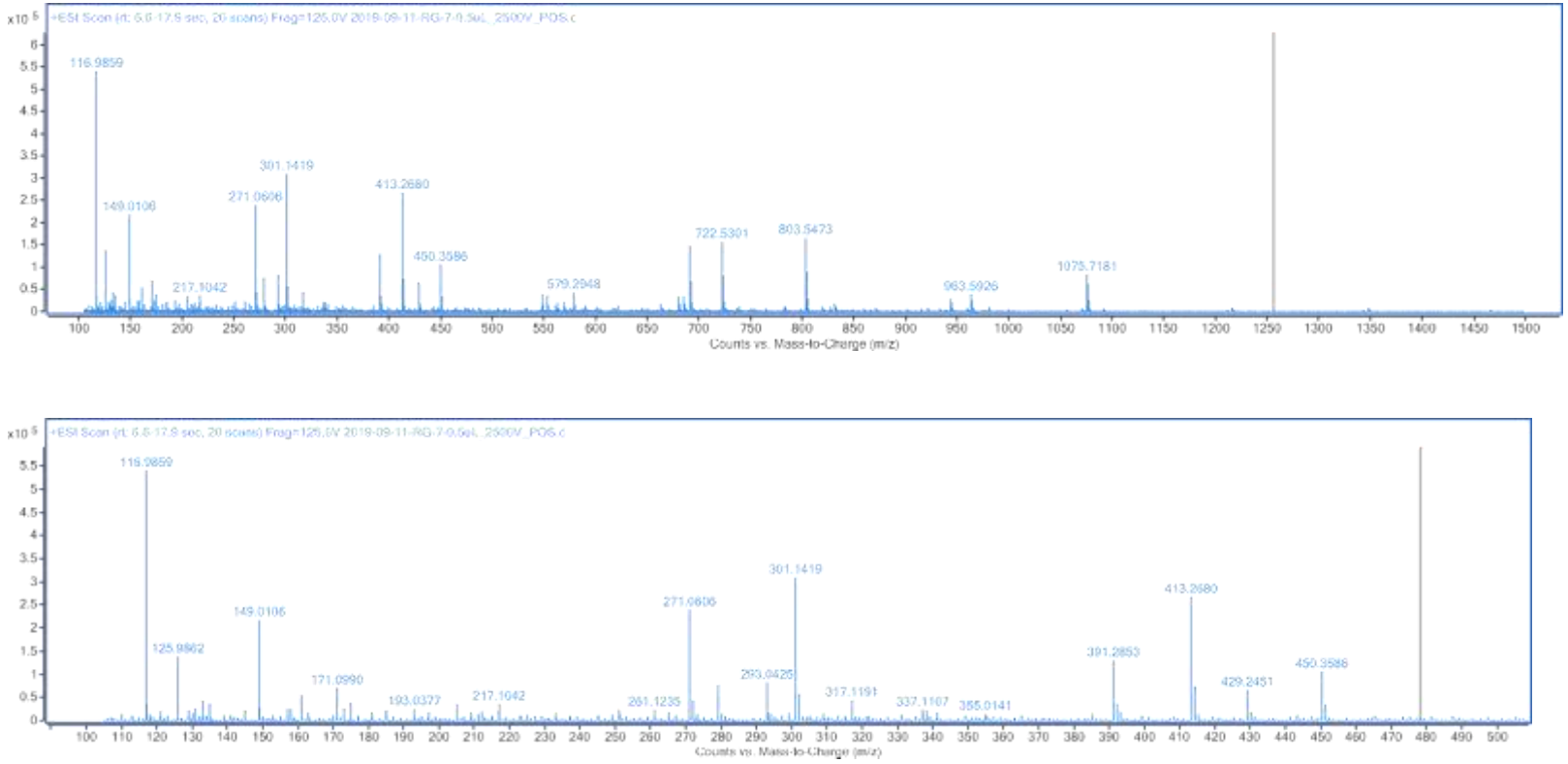
Appendix 54: The IR Spectrum of **120**.



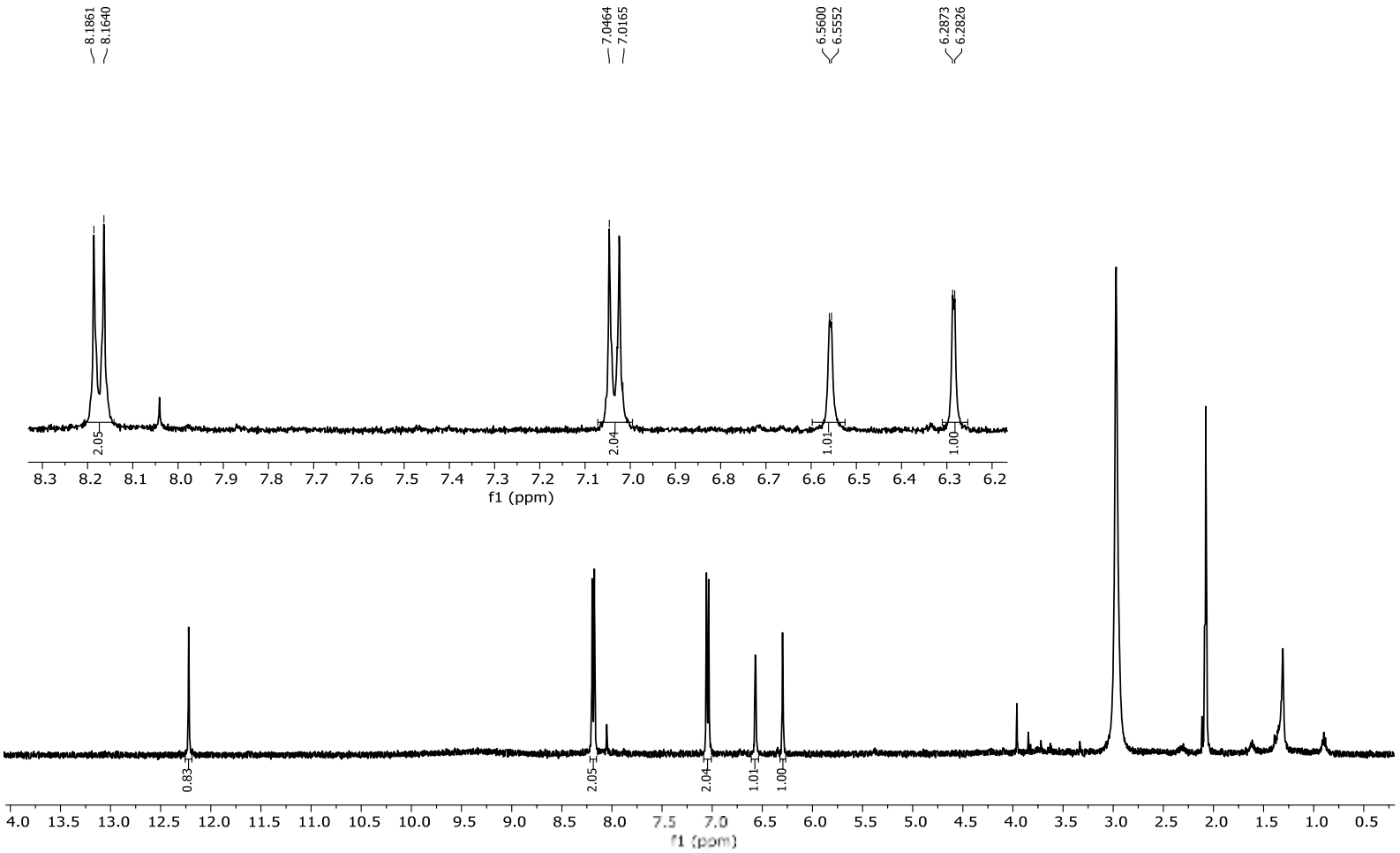
Appendix 55: The UV Spectrum of **120** in Methanol.



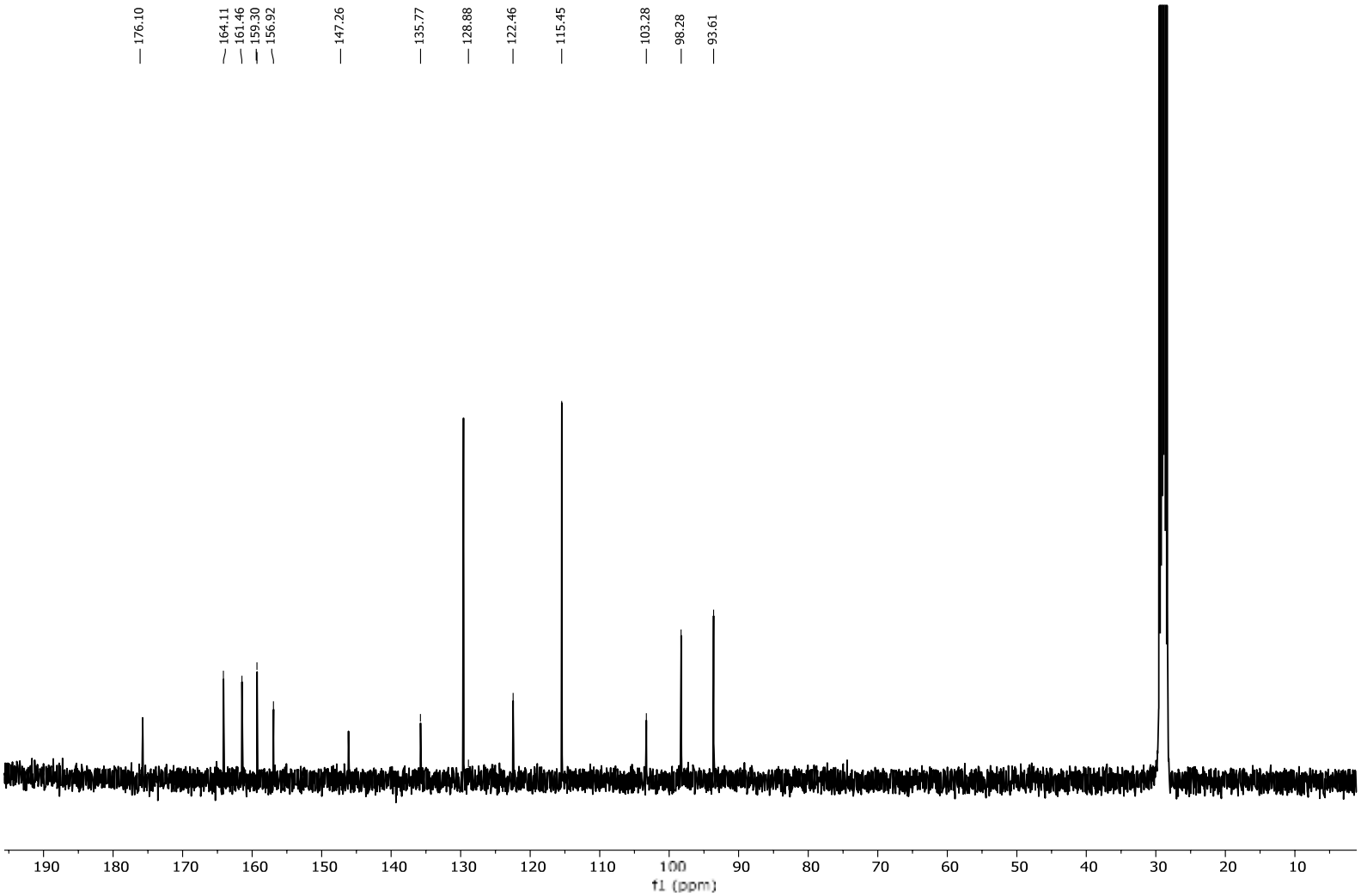
Appendix 56: The HRESIMS of Compound **120**.



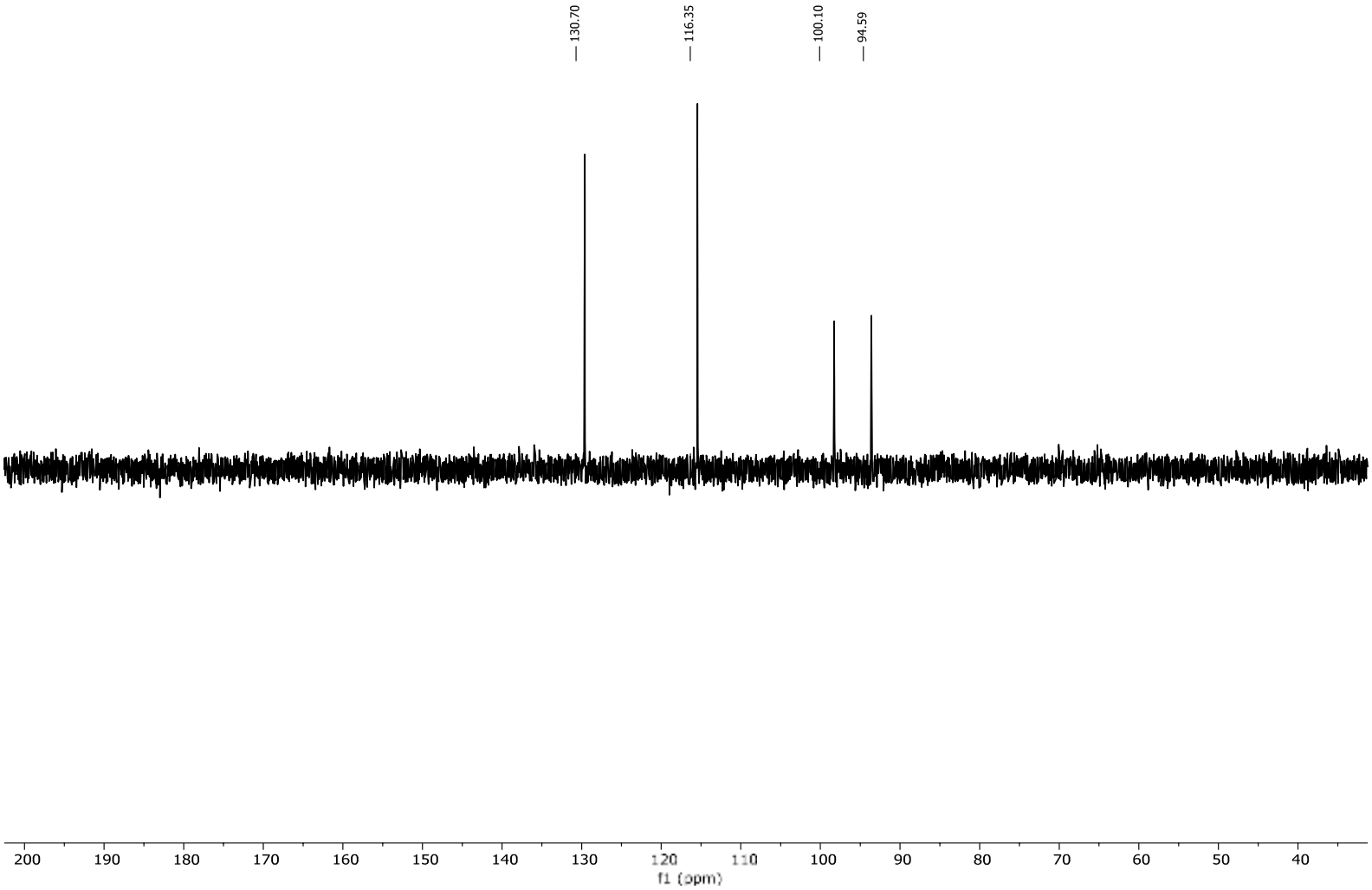
Appendix 57: The ^{1}H-NMR Spectrum of **38** in Acetone-d_6.



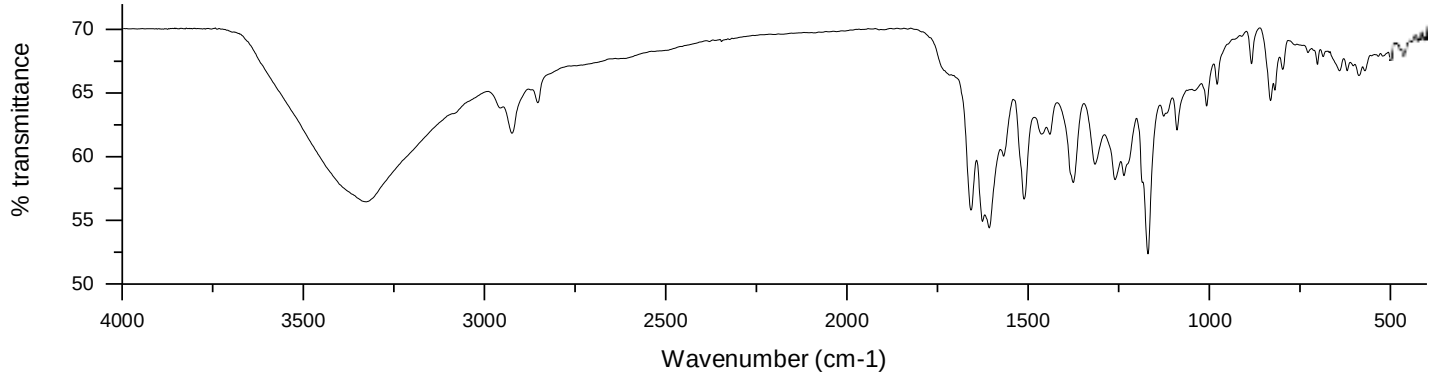
Appendix 58: The ^{13}C-NMR Spectrum of **38** in Acetone-d_6.



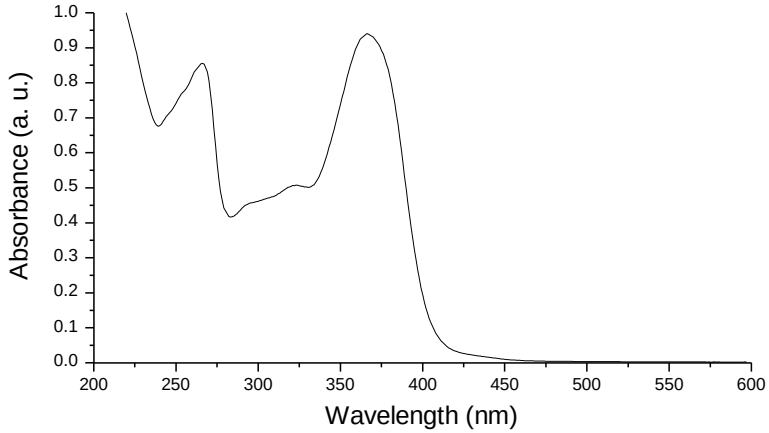
Appendix 59: The DEPT-135 NMR Spectrum of **38** in Acetone-d_6.



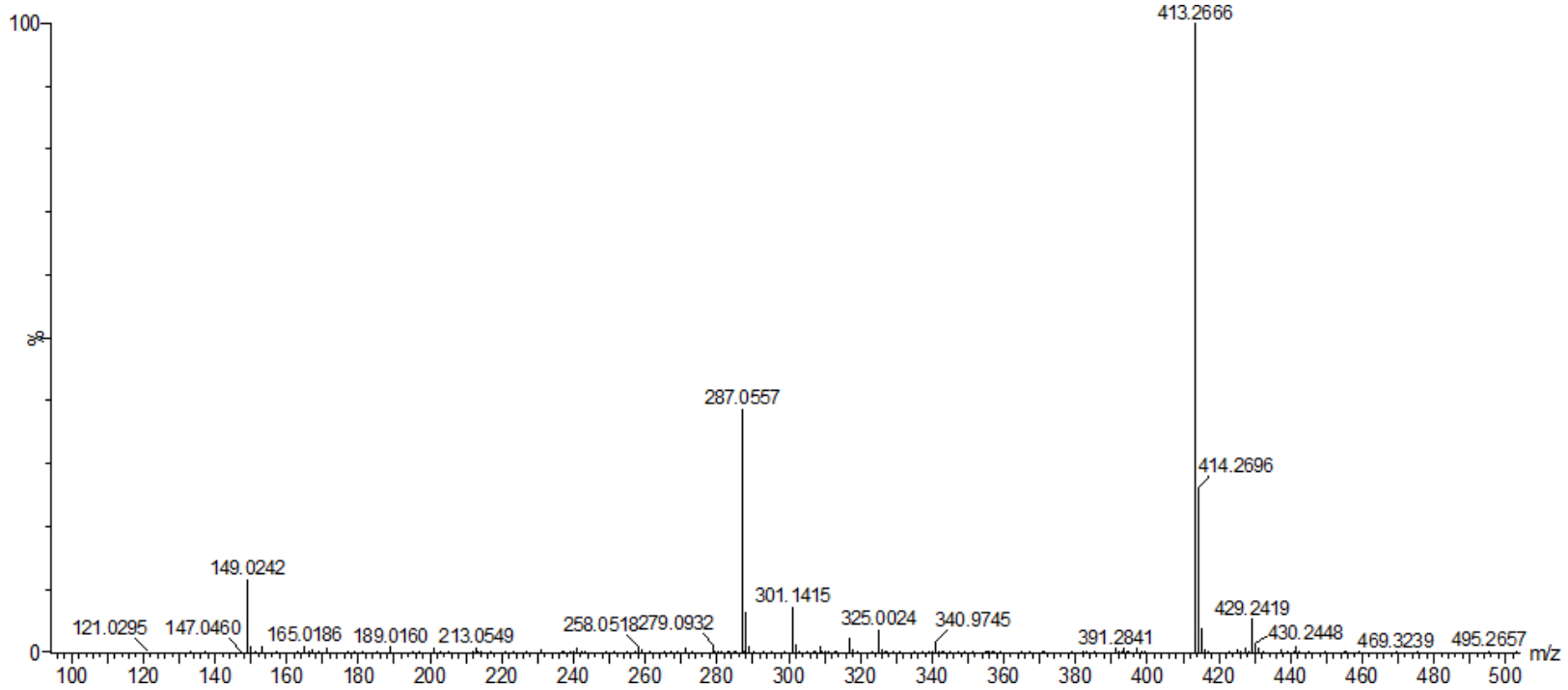
Appendix 60: The IR Spectrum of **38**.



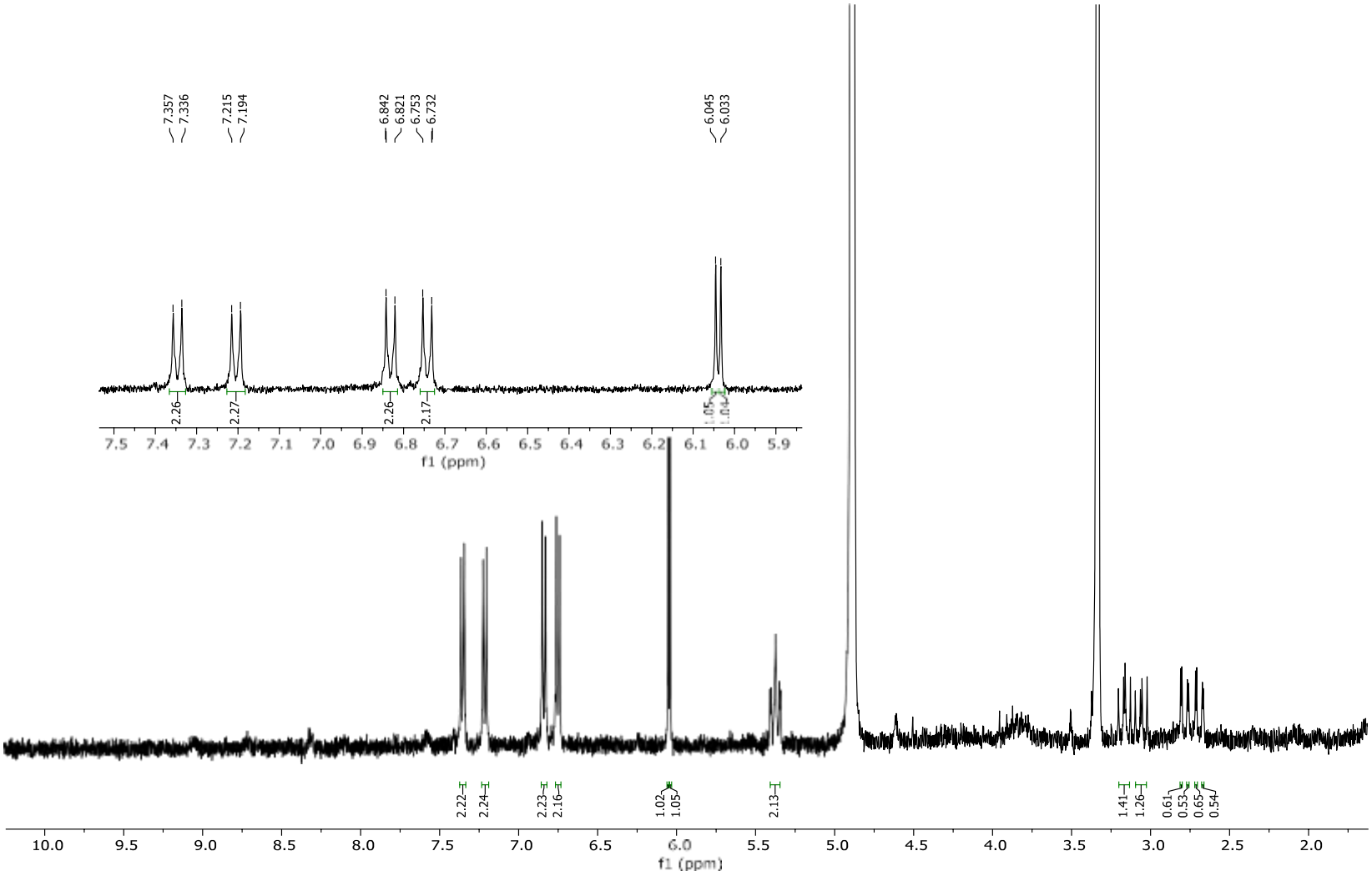
Appendix 61: The UV Spectrum of **38** in Methanol.



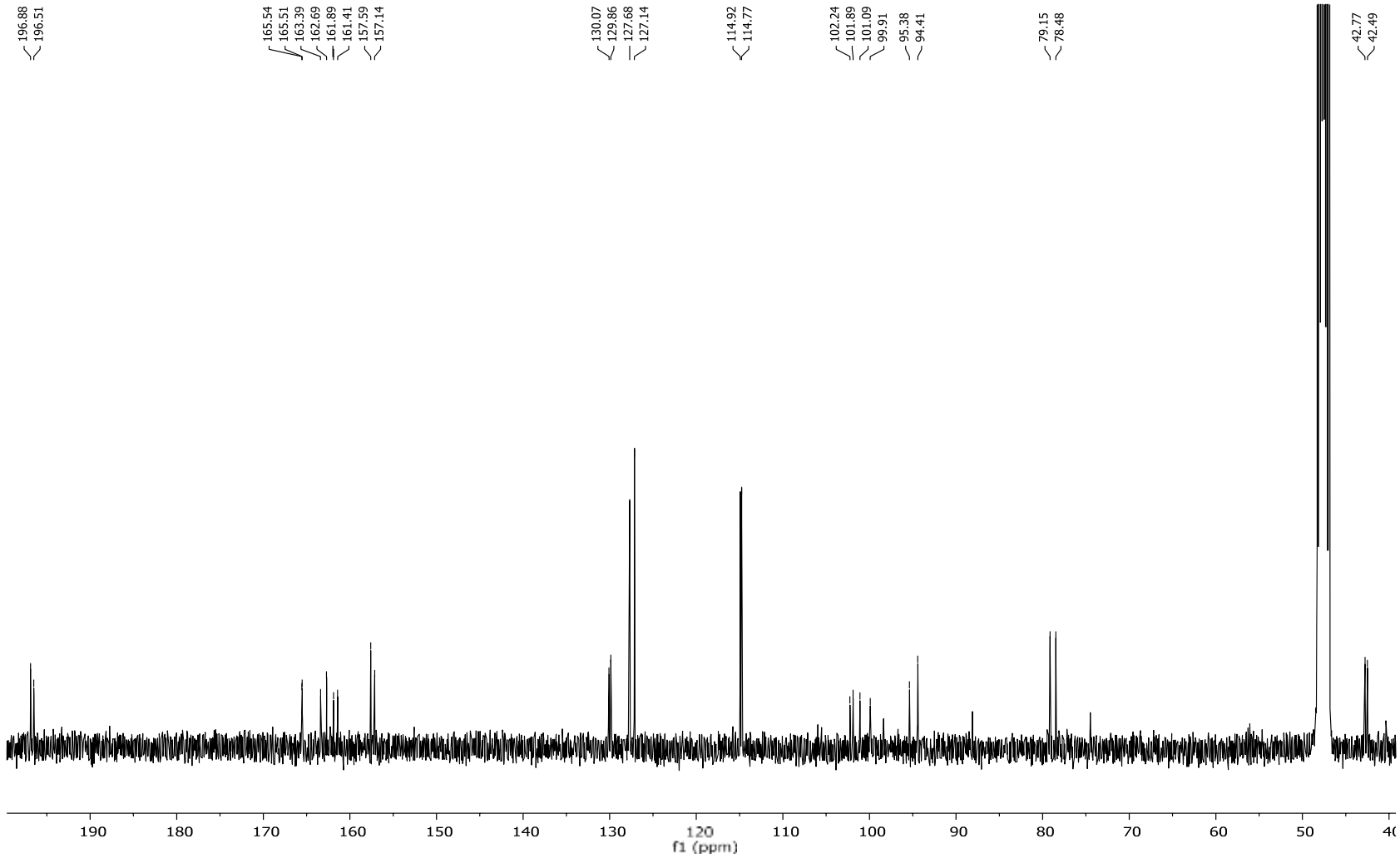
Appendix 62: The HRESIMS of Compound **38**.



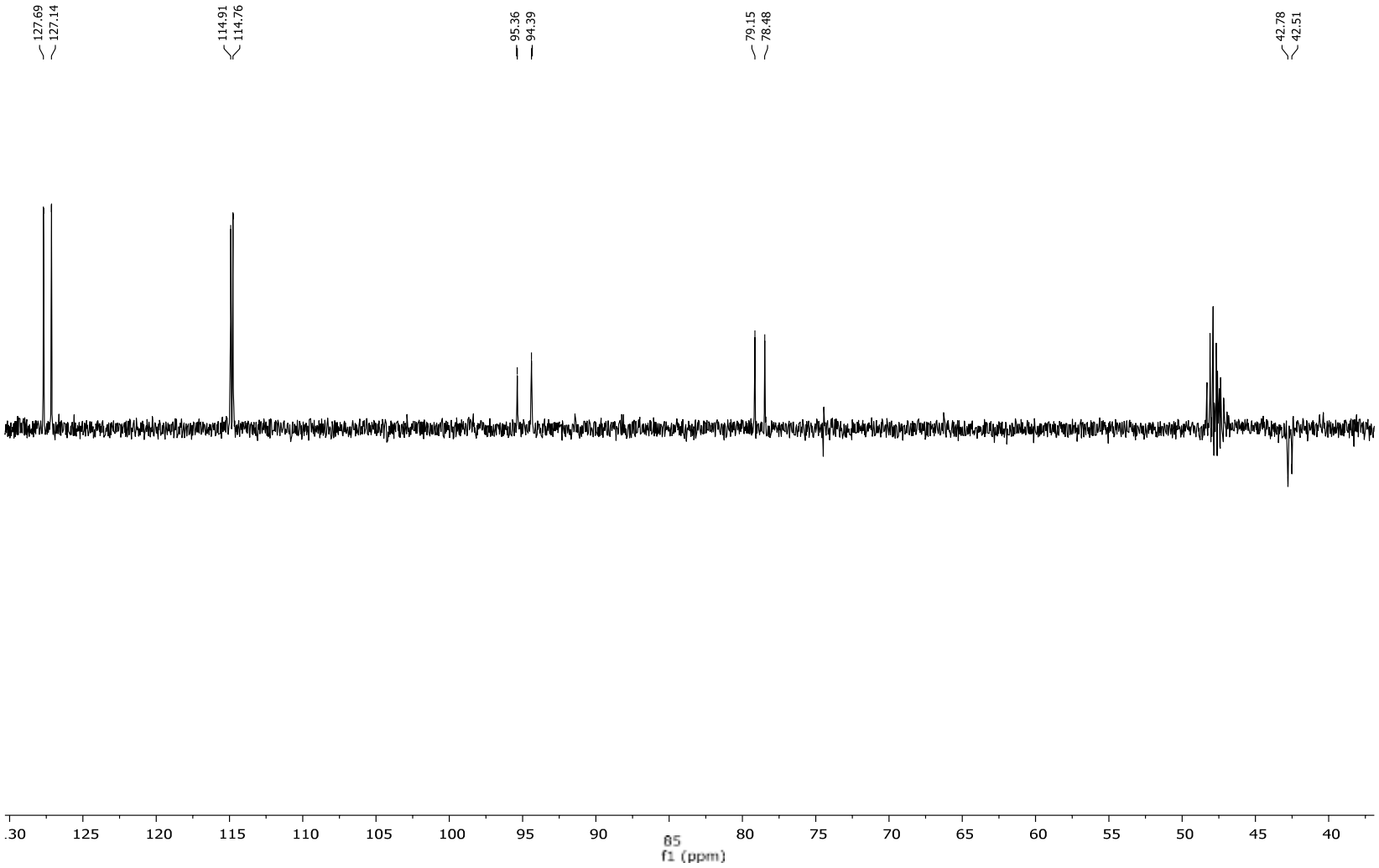
Appendix 63: The ^{1}H-NMR Spectrum of **121** in MeOD-*d*$_4$.



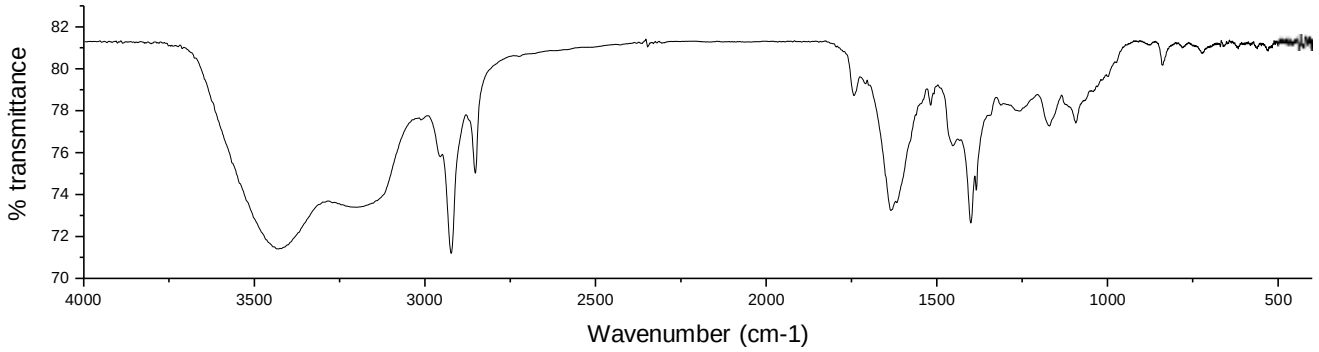
Appendix 64: The ^{13}C-NMR Spectrum of **121** in MeOD-*d*$_4$.



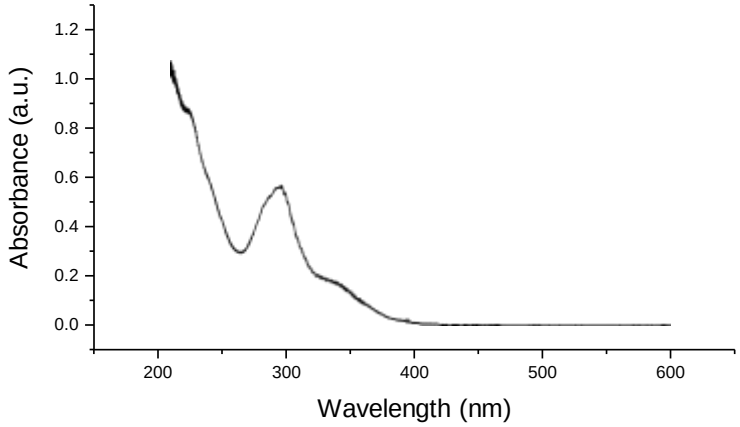
Appendix 65: The DEPT-135 NMR Spectrum of **121** in MeOD-d_4.



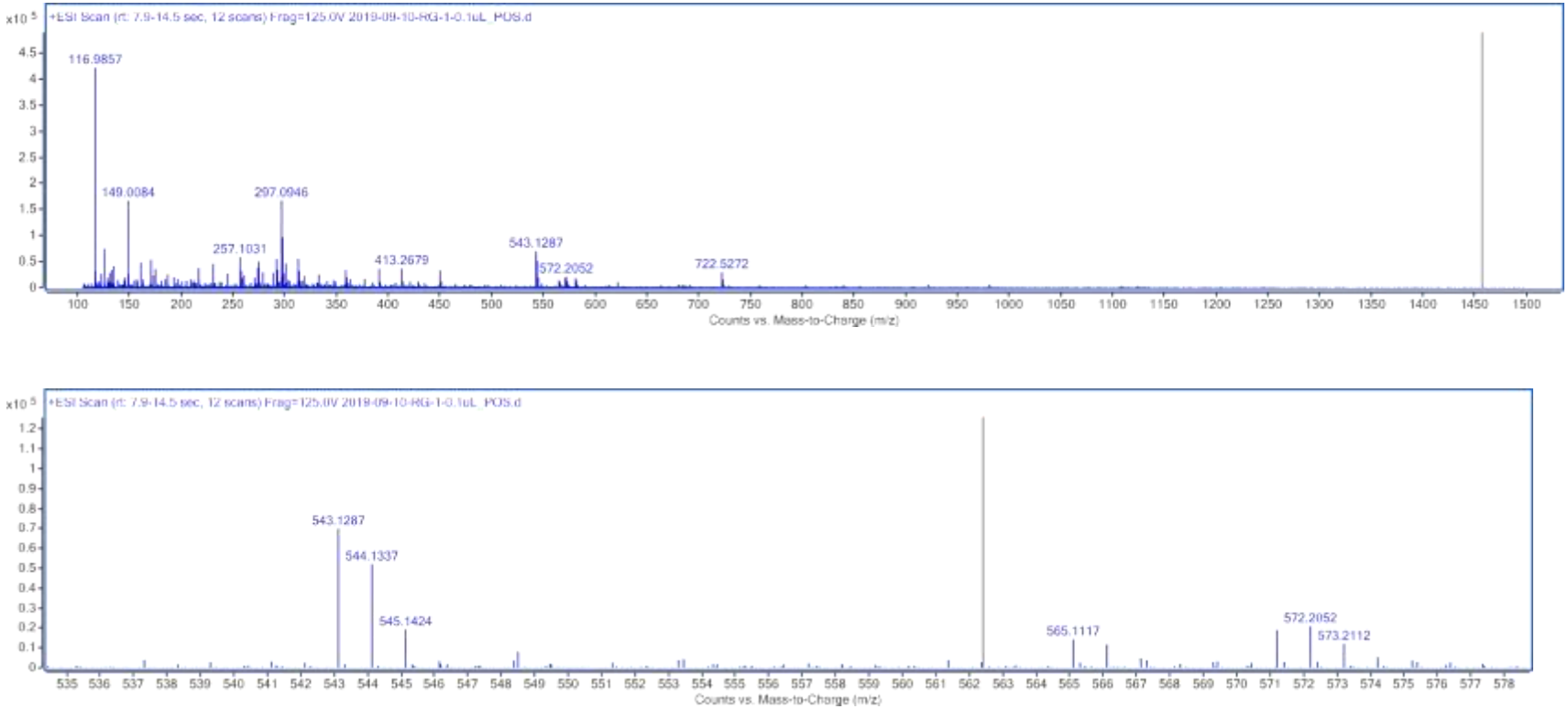
Appendix 66: The IR Spectrum of **121**.



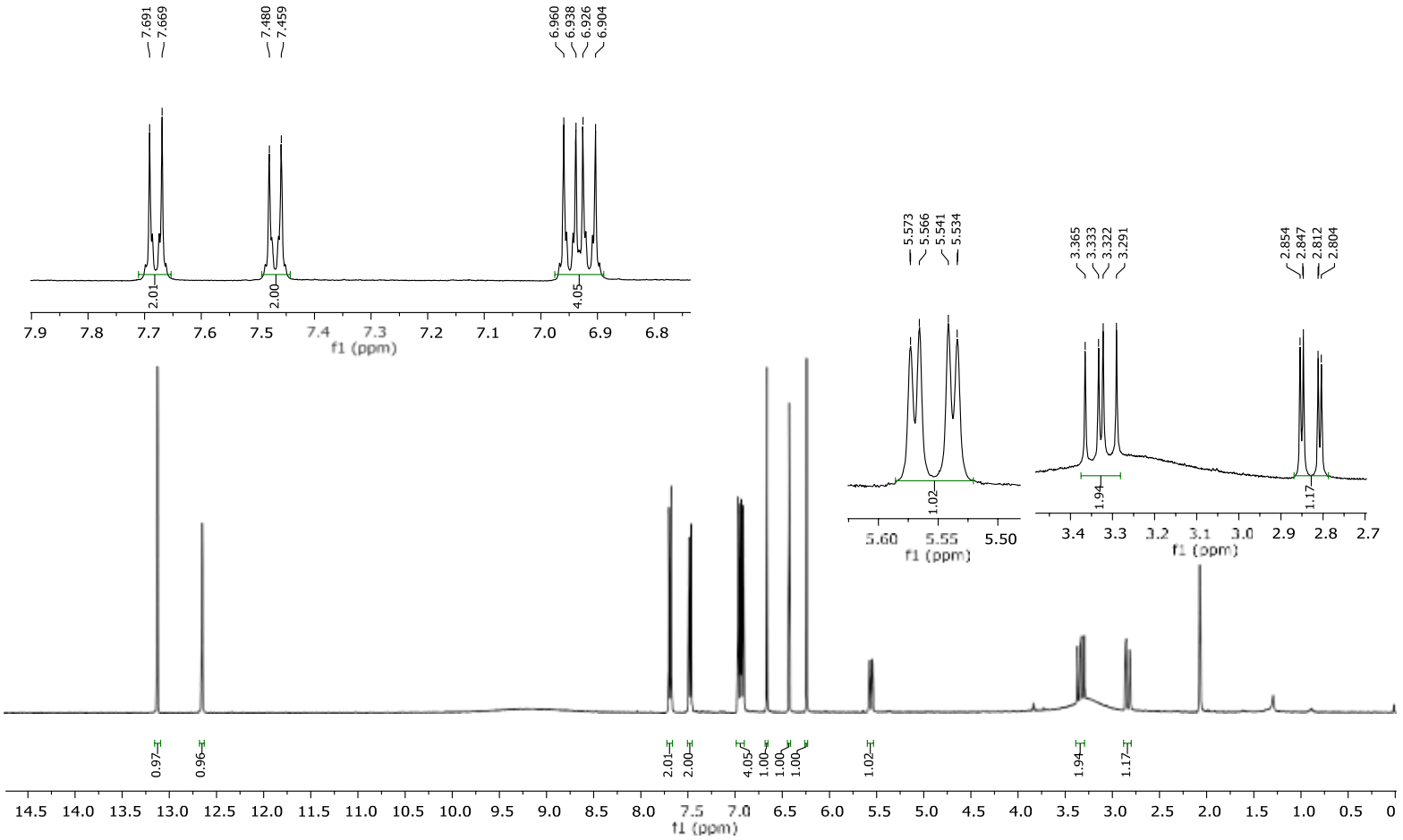
Appendix 67: The UV Spectrum of **121** in Methanol.



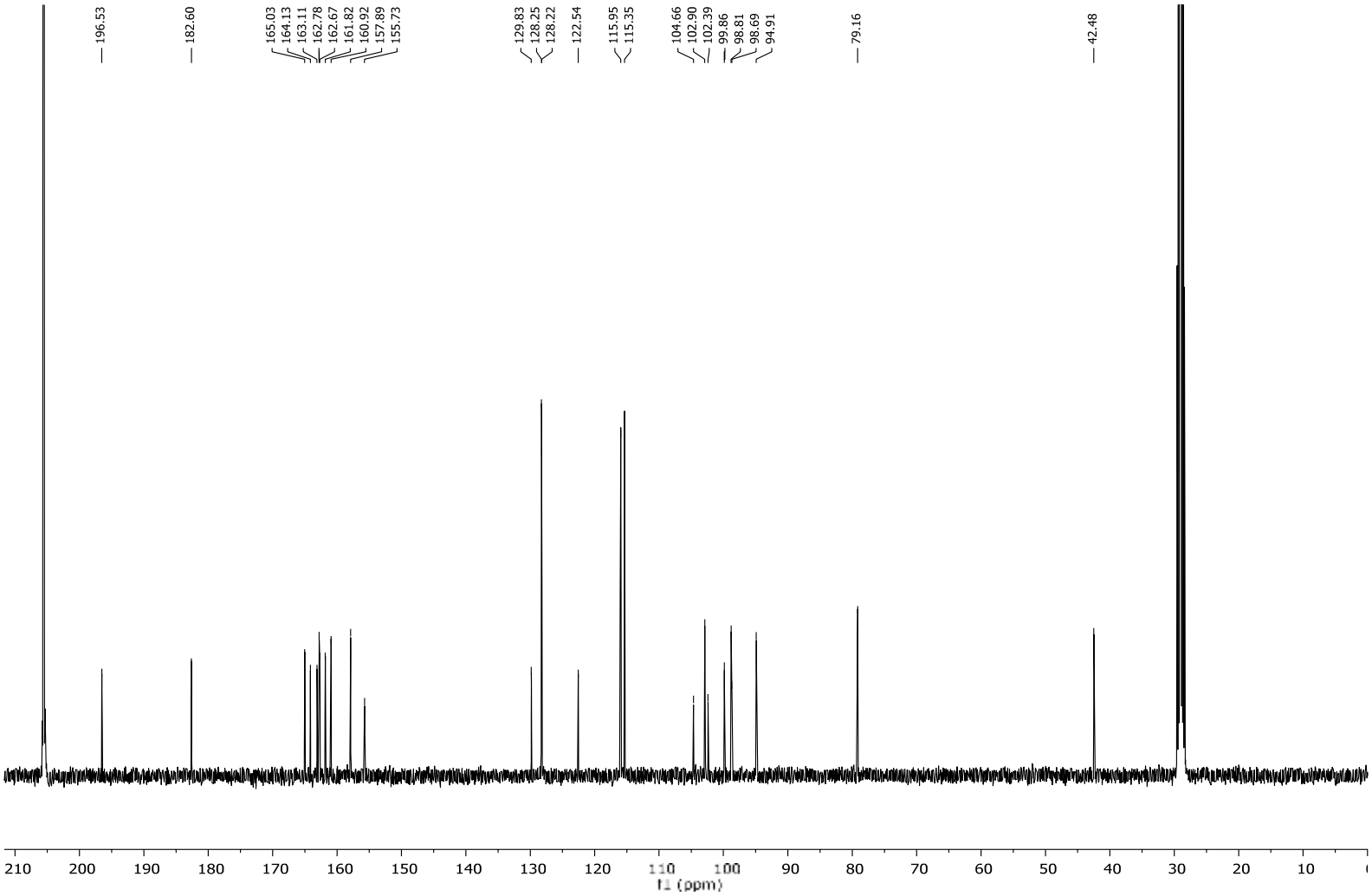
Appendix 68: The HRESIMS of Compound **121**.



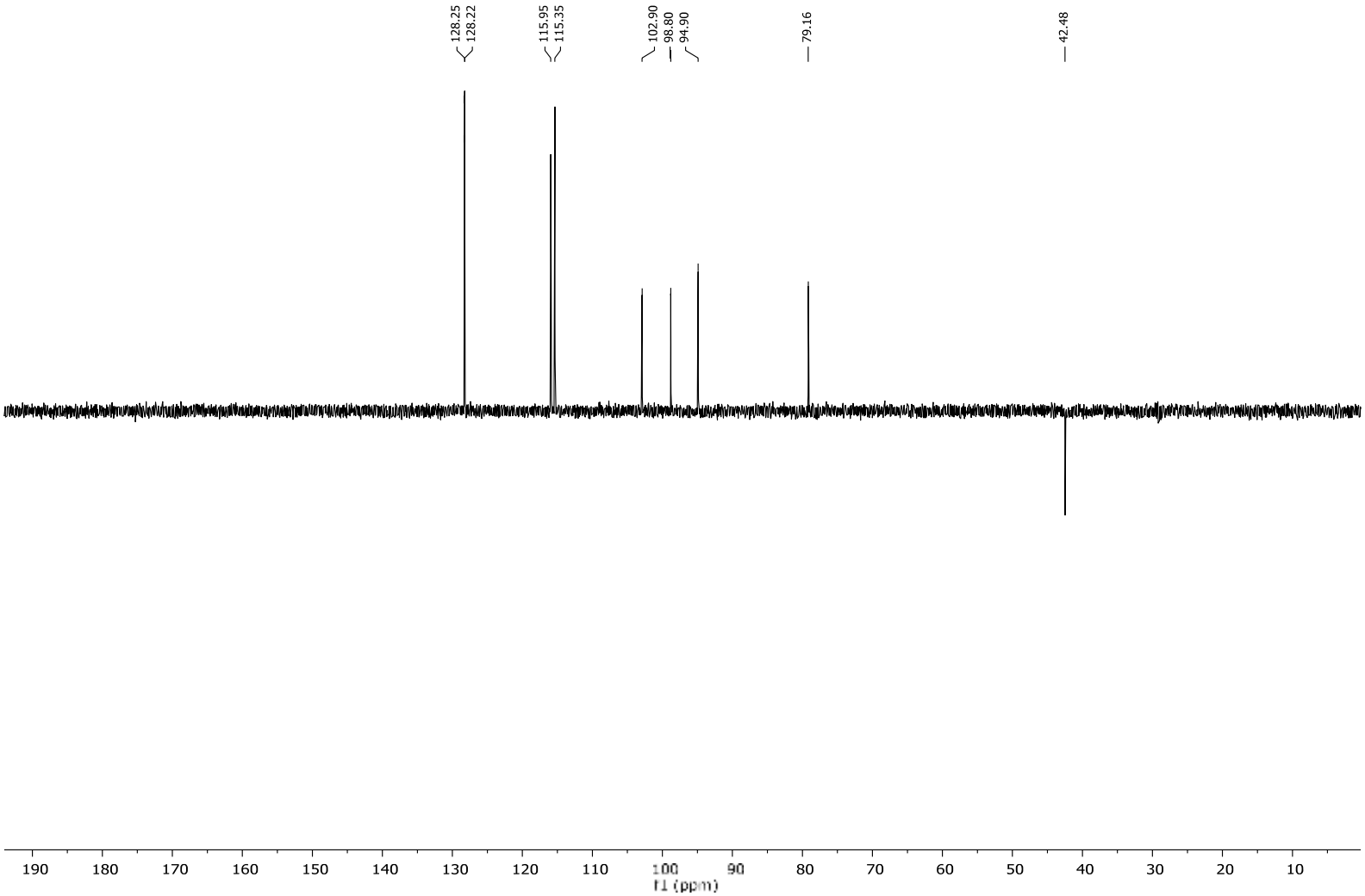
Appendix 69: The ^{1}H-NMR Spectrum of **122** in Acetone-d_6.



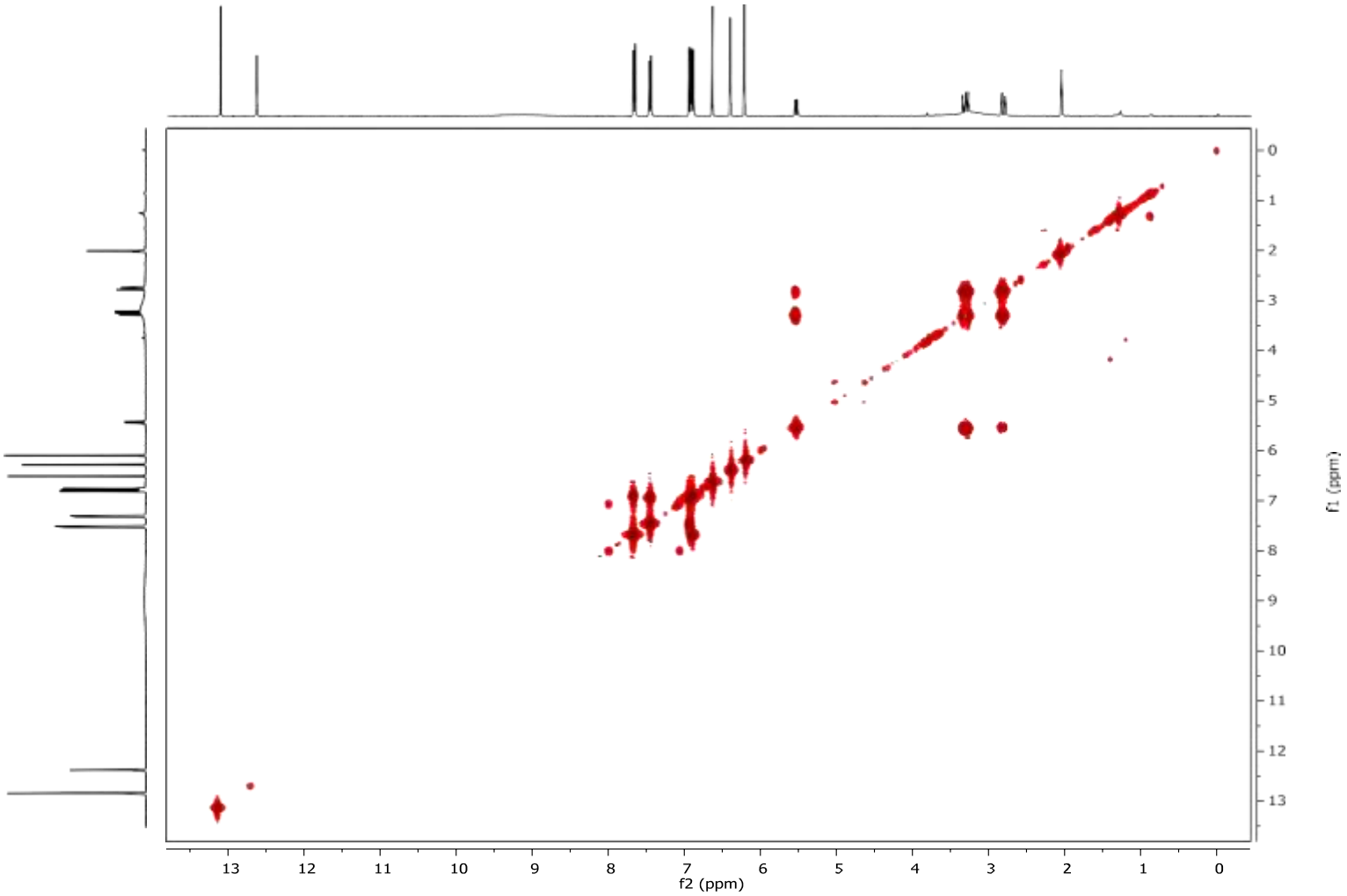
Appendix 70: The ^{13}C-NMR Spectrum of **122** in Acetone-d_6.



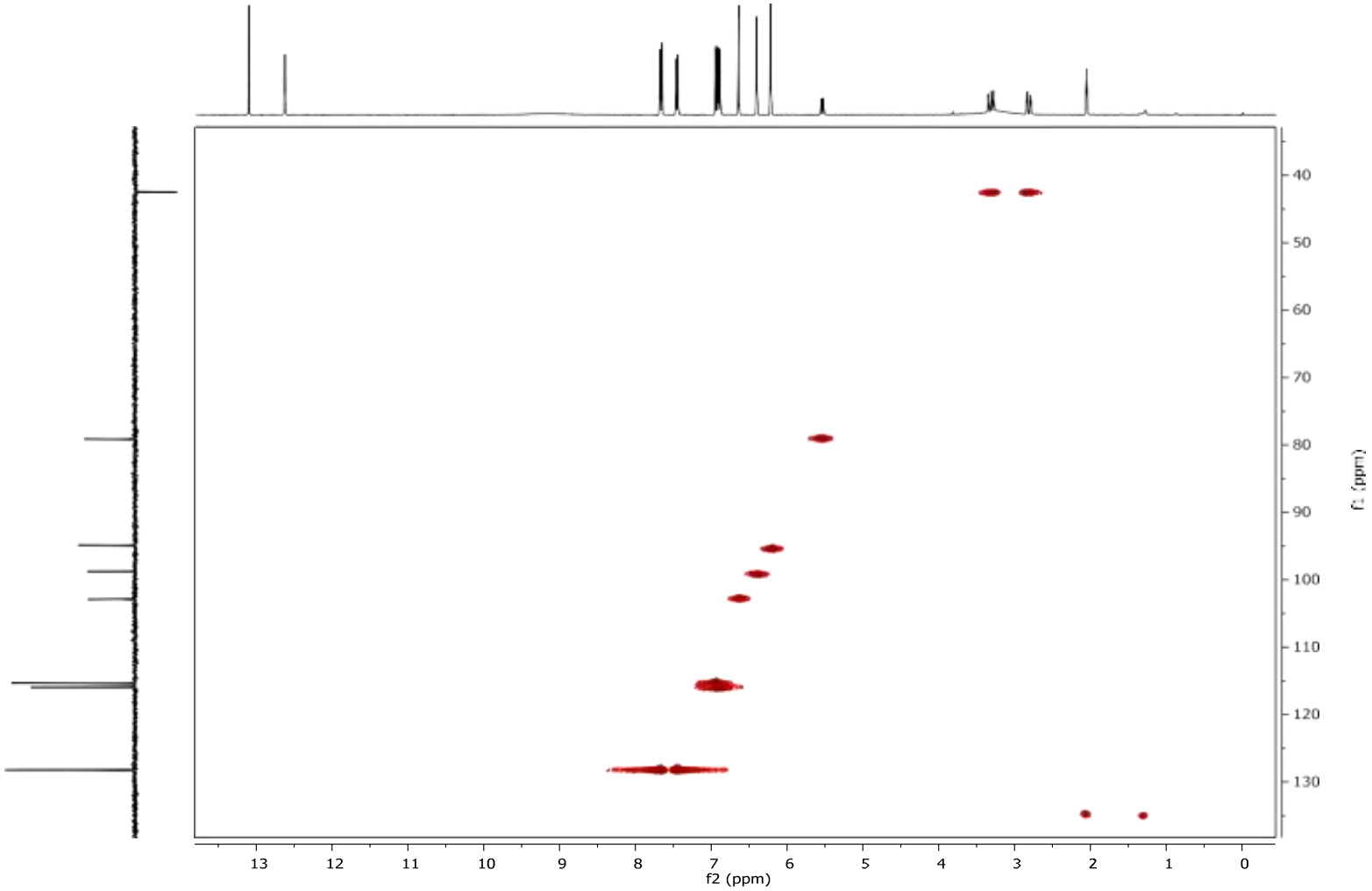
Appendix 71: The DEPT-135 NMR Spectrum of **122** in Acetone-d_6.



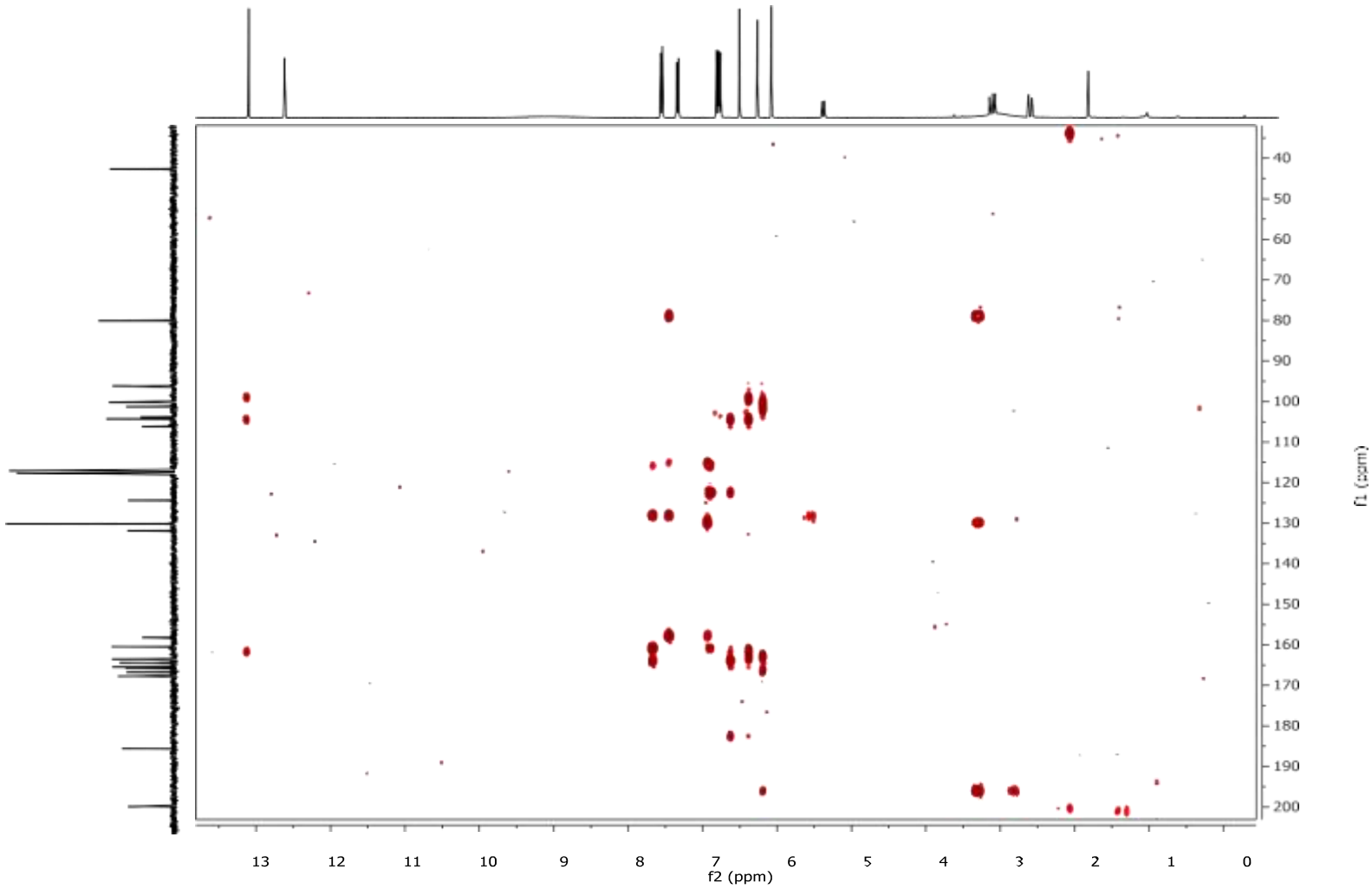
Appendix 72: The ^{1}H–^{1}H COSY Spectrum of **122** in Acetone-d_6.



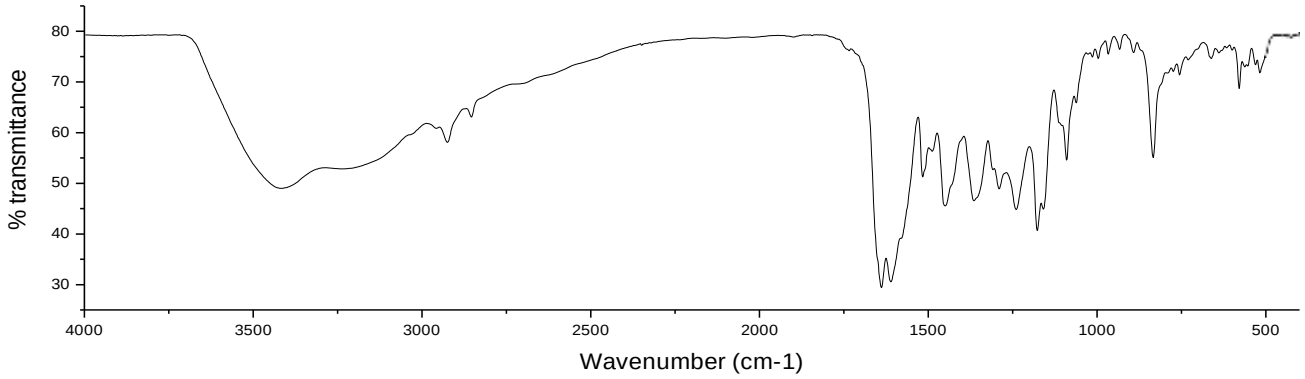
Appendix 73: The HSQC Spectrum of **122** in Acetone-d_6.



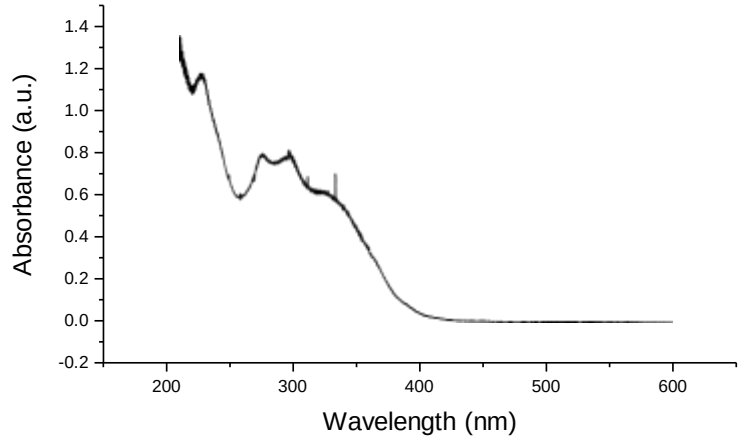
Appendix 74: The HMBC Spectrum of **122** in Acetone-d_6.



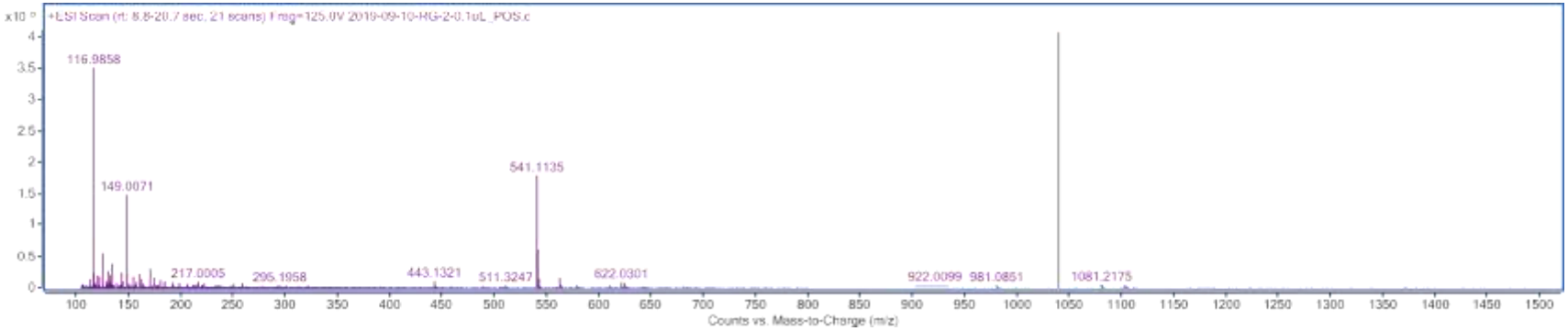
Appendix 75: The IR Spectrum of **122**.

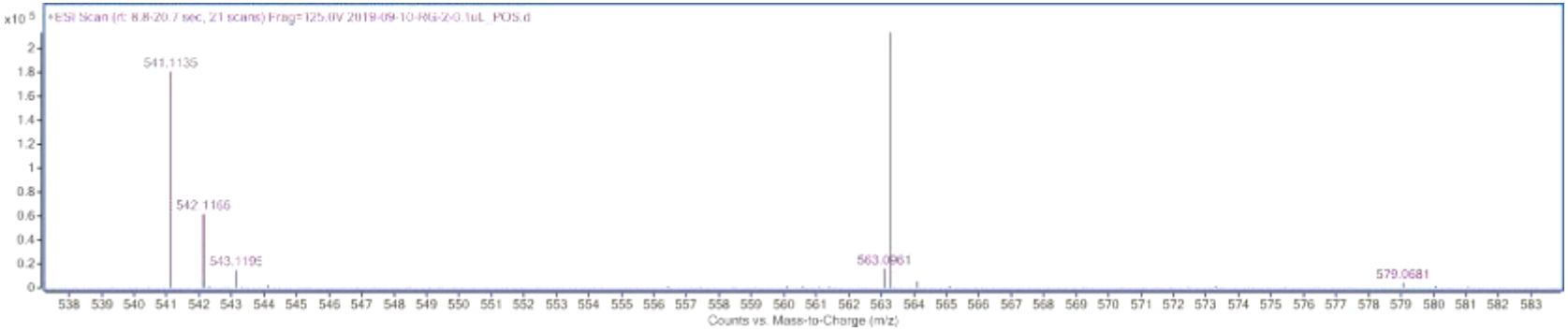


Appendix 76: The UV Spectrum of **122** in Methanol.

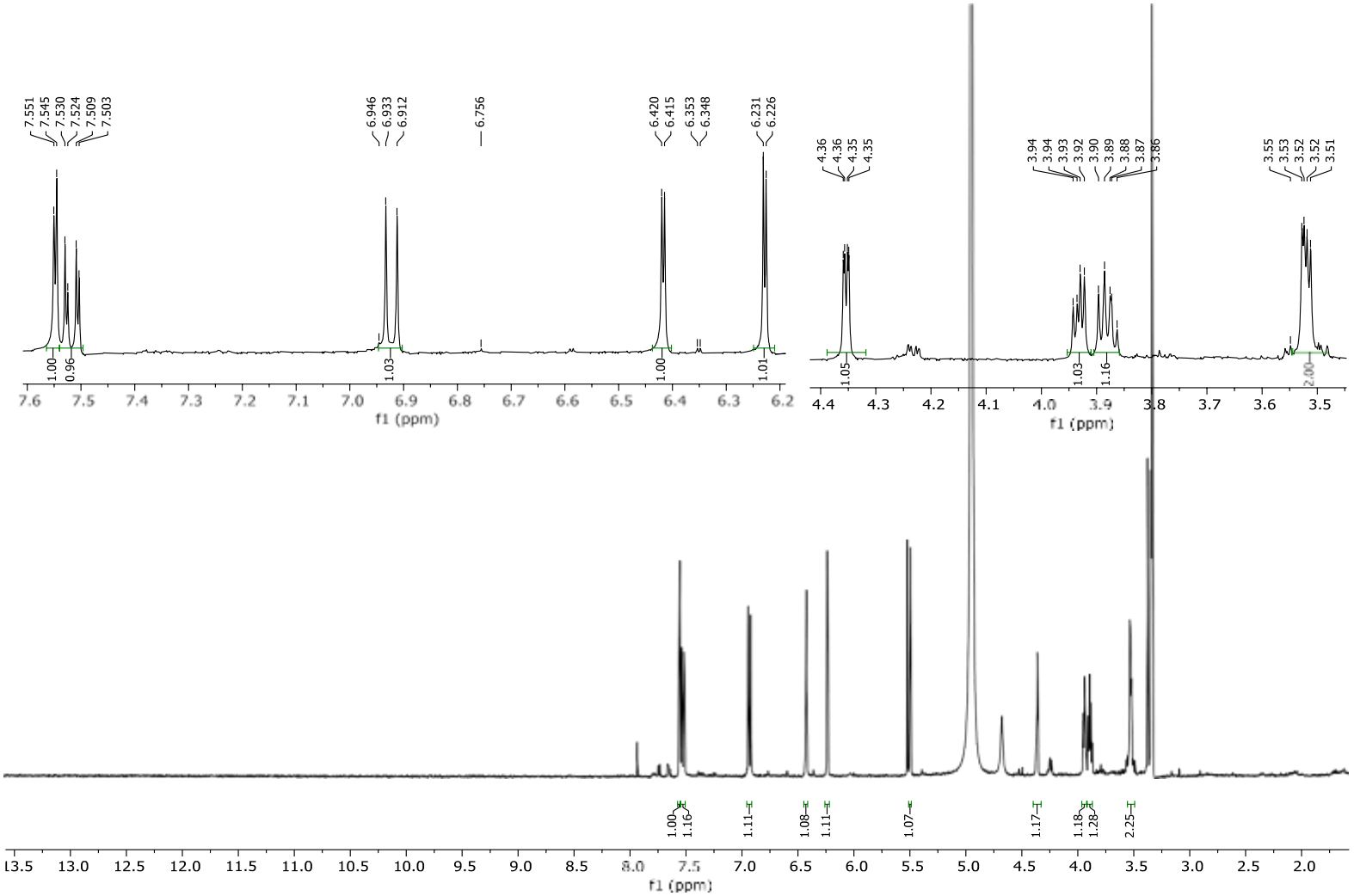


Appendix 77: The HRESIMS of Compound **122**.

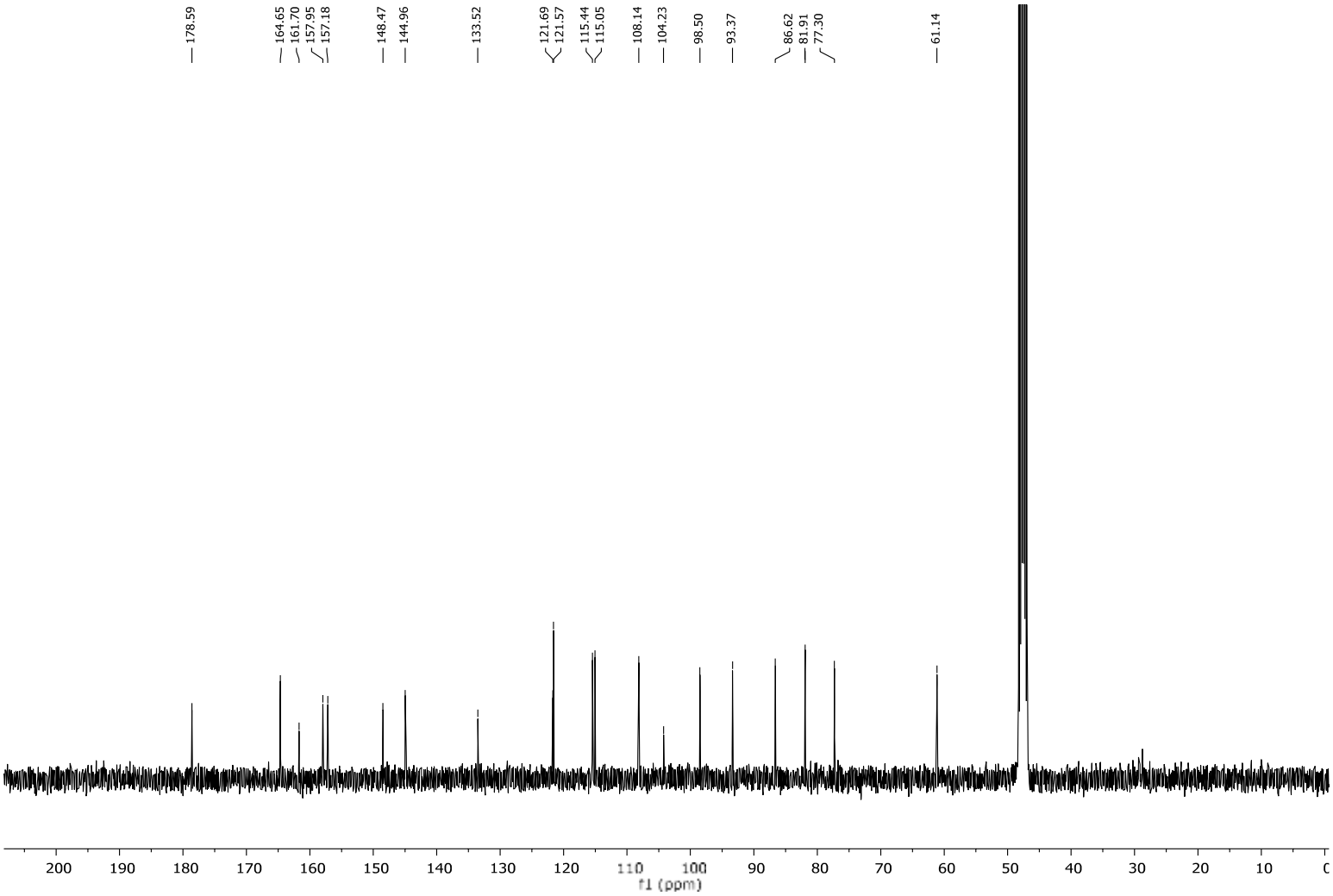




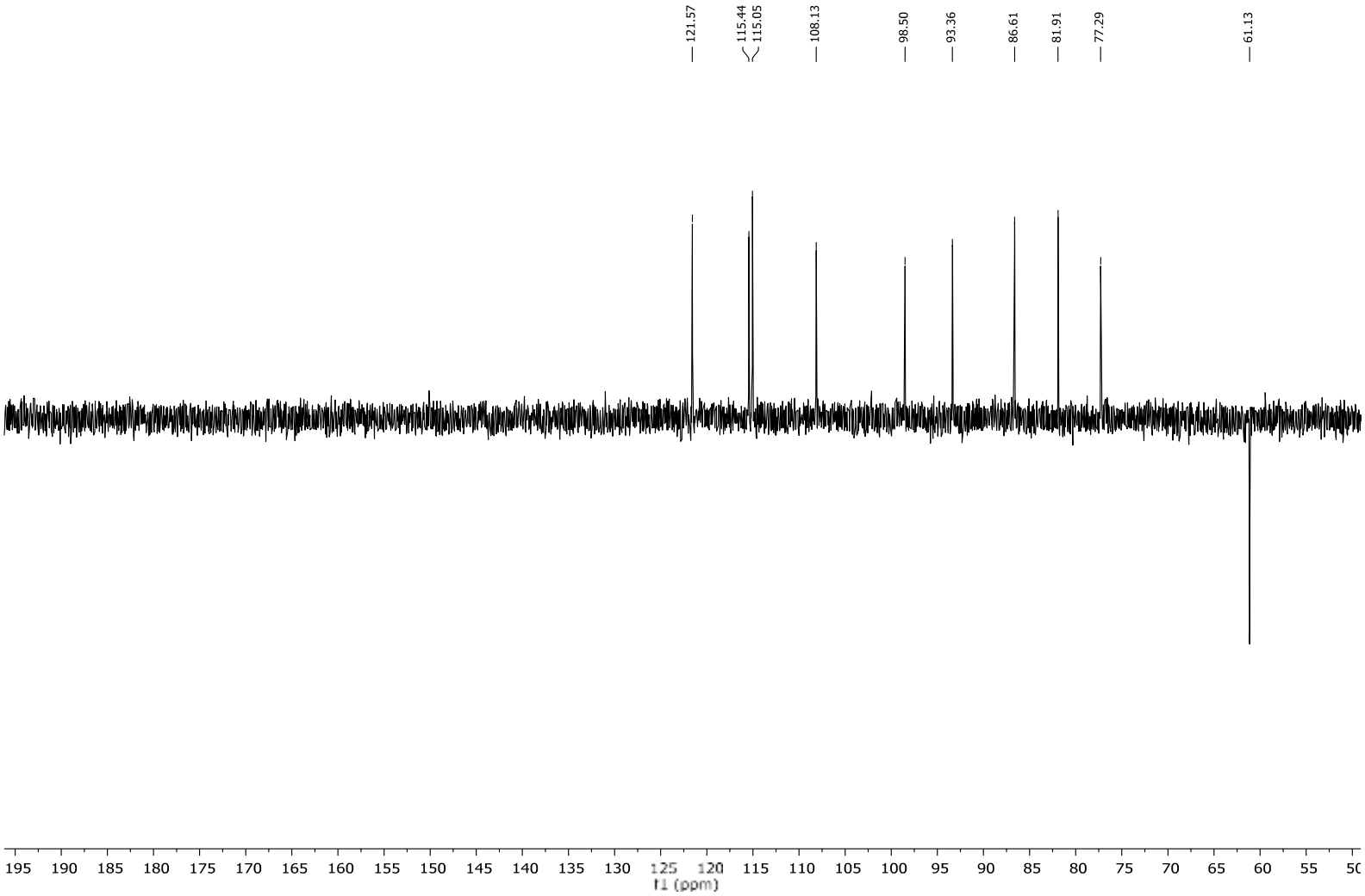
Appendix 78: The ^{1}H-NMR Spectrum of **123** in MeOD-*d*$_4$.



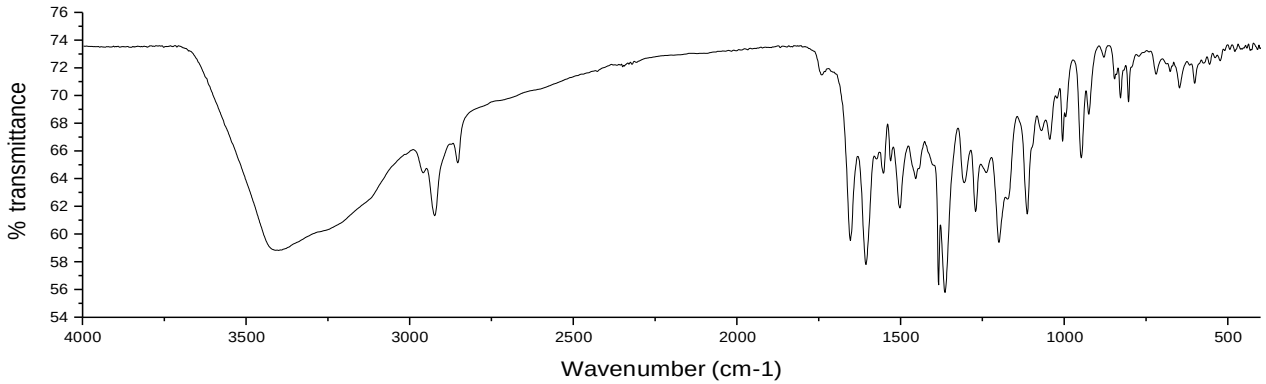
Appendix 79: The ^{13}C-NMR Spectrum of **123** in MeOD-d_4.



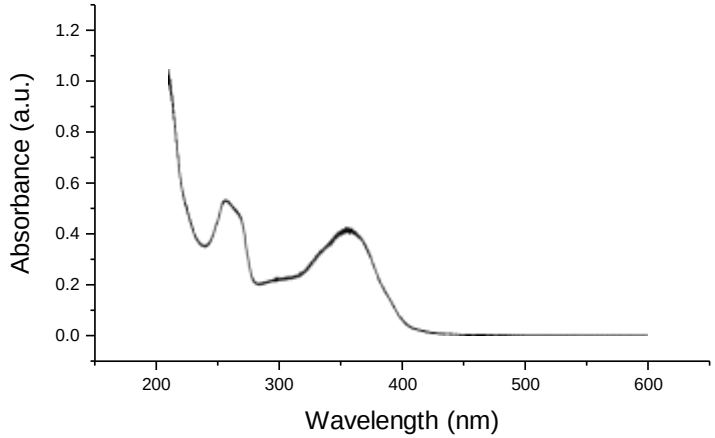
Appendix 80: The DEPT-135 NMR Spectrum of **123** in MeOD-d_4.



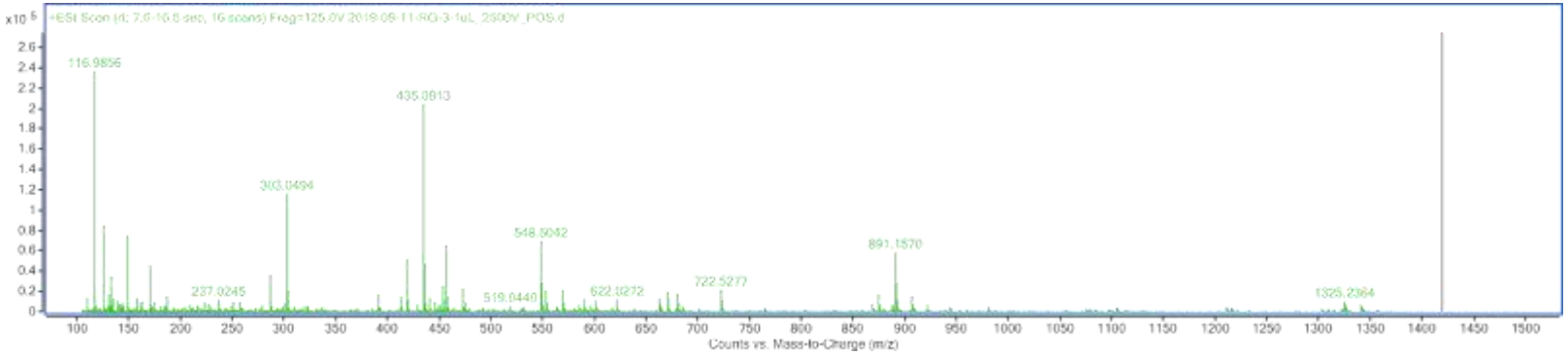
Appendix 81: The IR Spectrum of **123**.

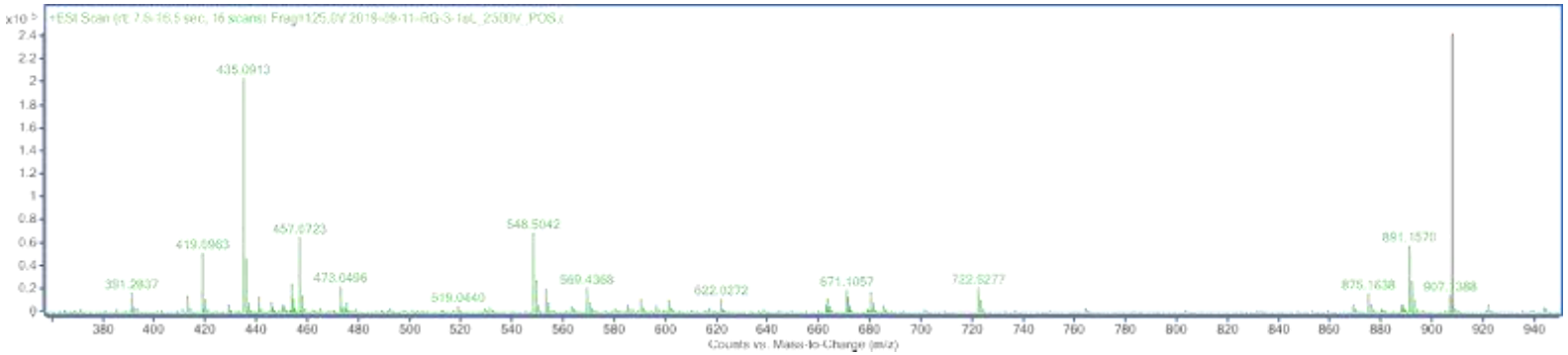


Appendix 82: The UV Spectrum of **123** in Methanol.

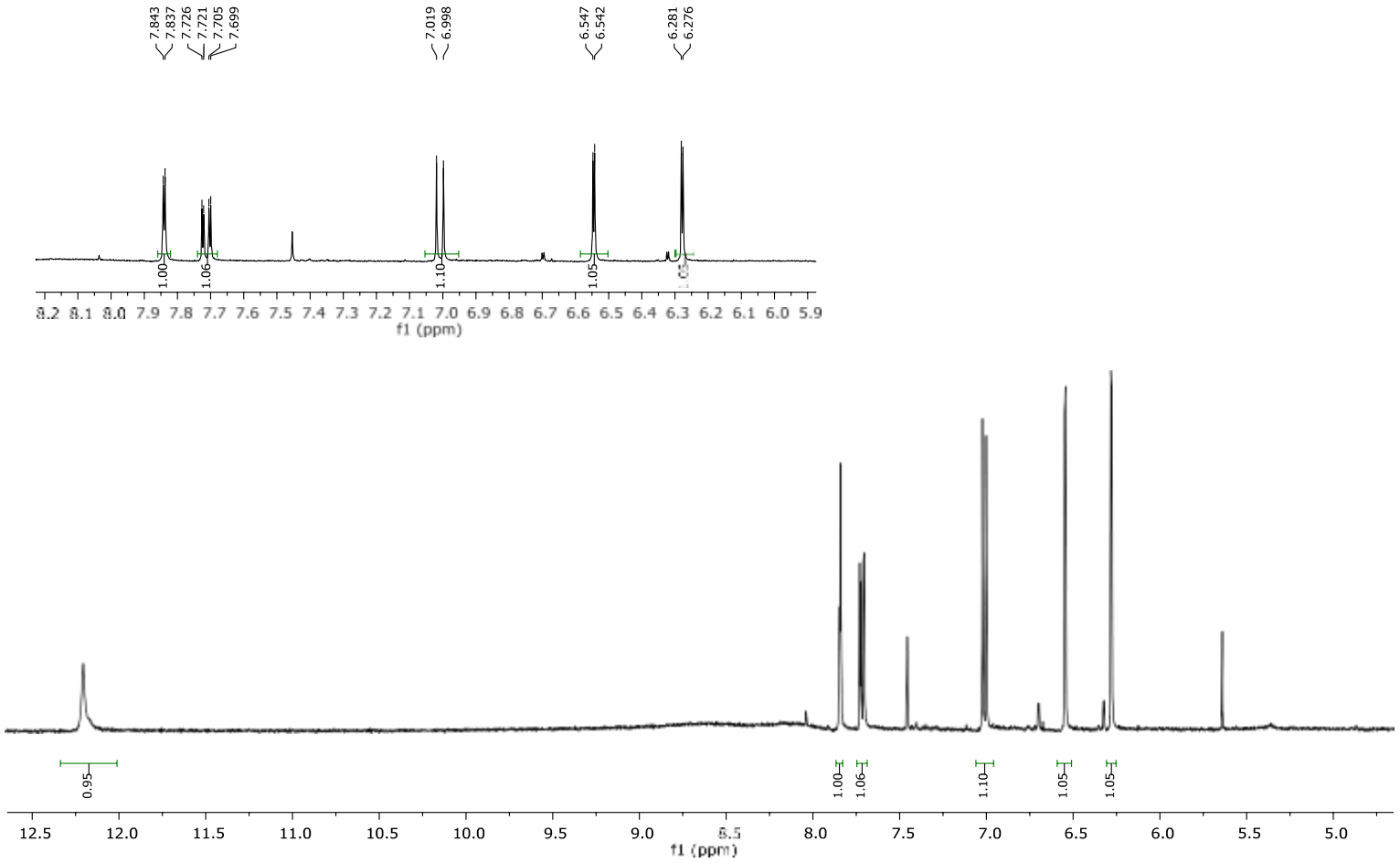


Appendix 83: The HRESIMS of Compound **123**.

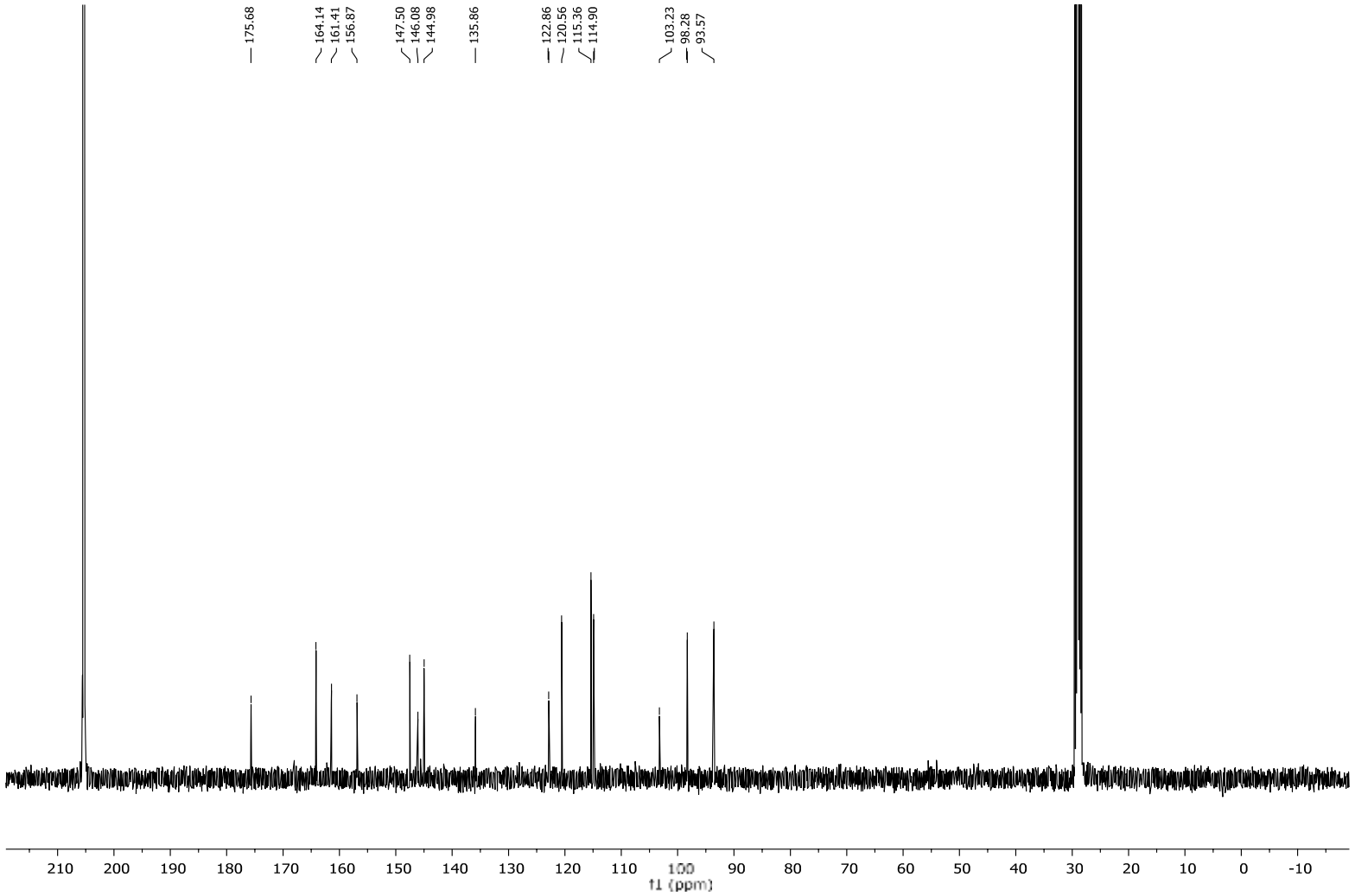




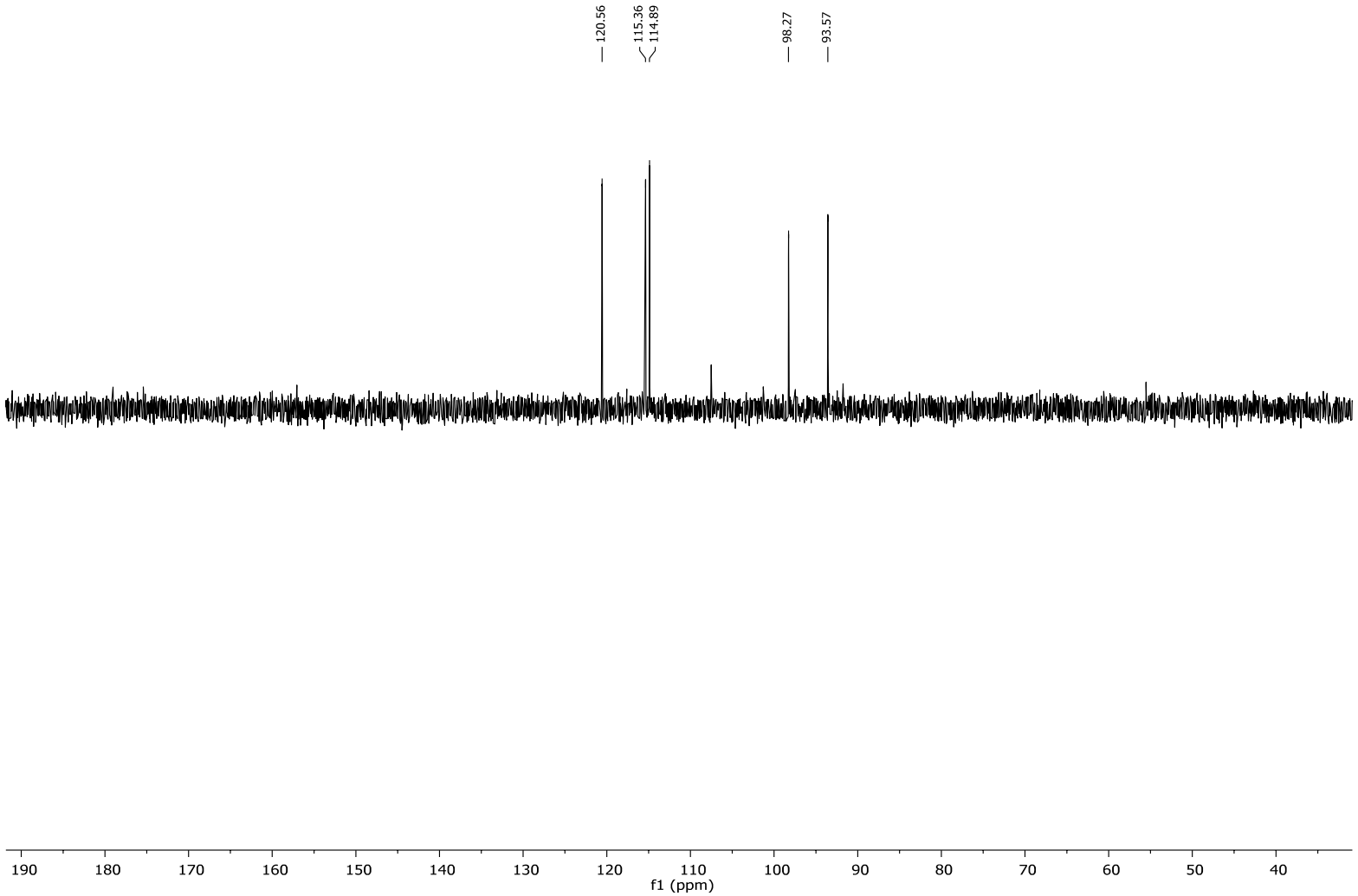
Appendix 84: The ^{1}H-NMR Spectrum of **1** in Acetone-d_6.



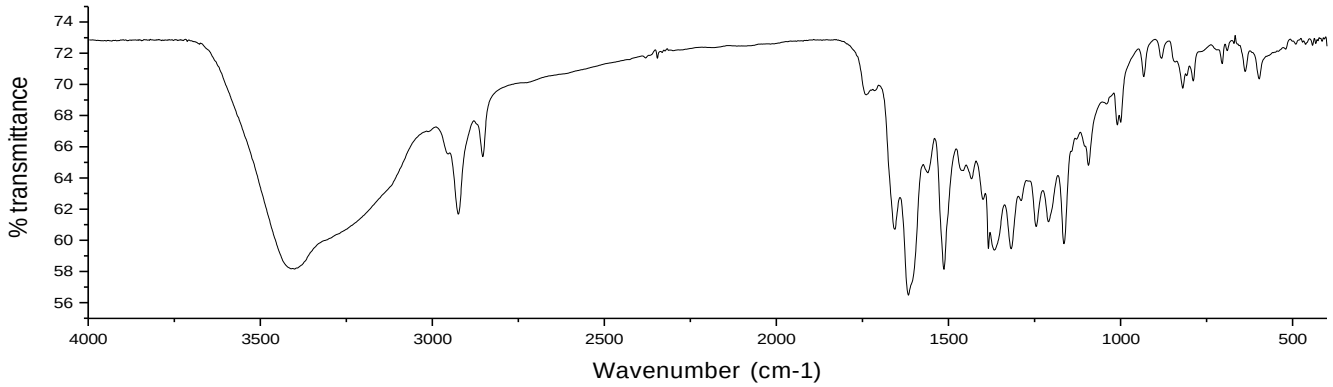
Appendix 85: The ^{13}C-NMR Spectrum of **1** in Acetone-d_6.



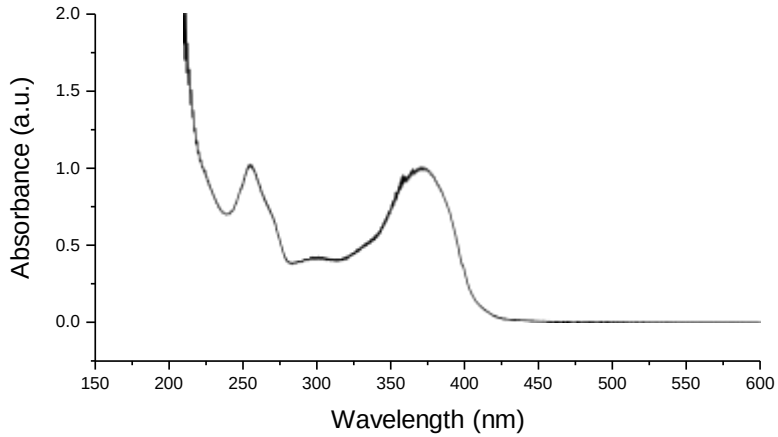
Appendix 86: The DEPT-135 NMR Spectrum of **1** in Acetone-d_6.



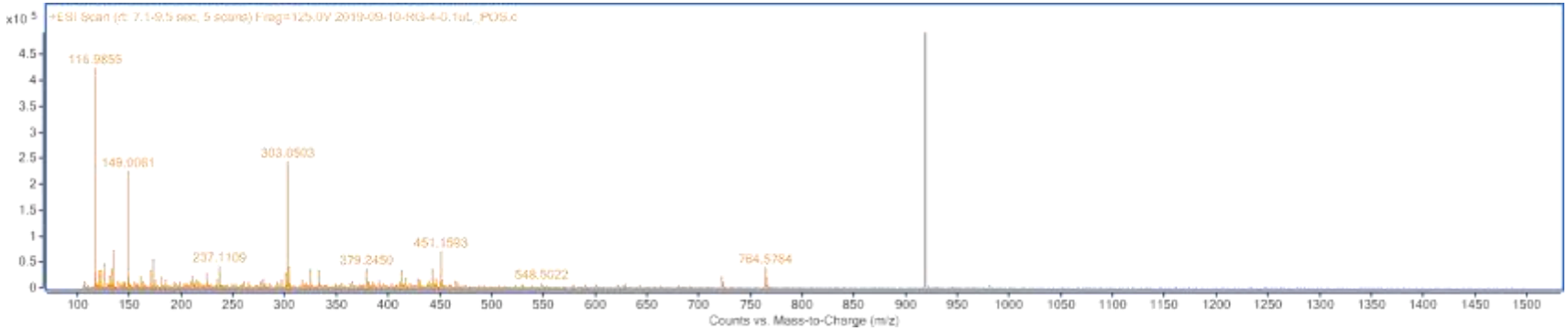
Appendix 87: The IR Spectrum of **1**.

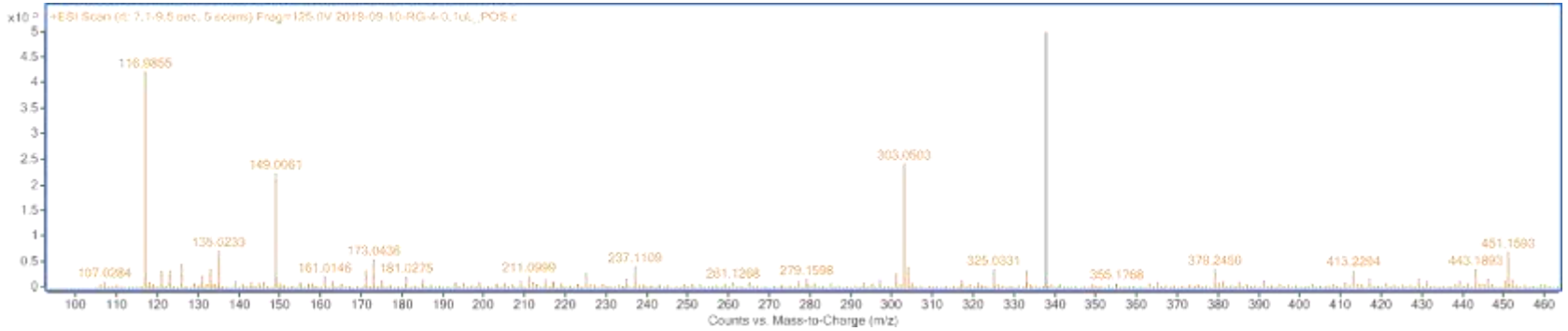


Appendix 88: The UV Spectrum of **1** in Methanol.

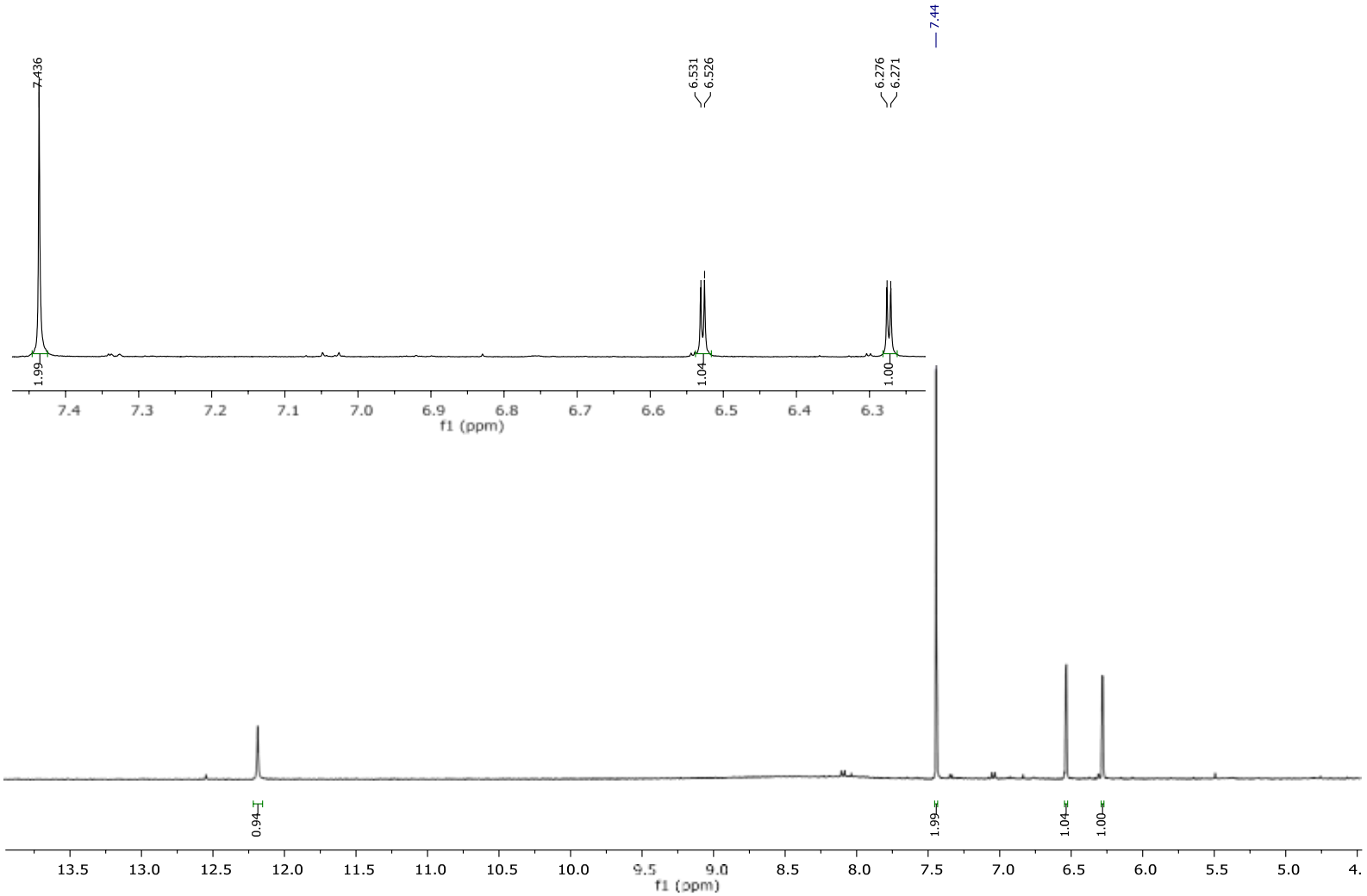


Appendix 89: The HRESIMS of Compound **1**.

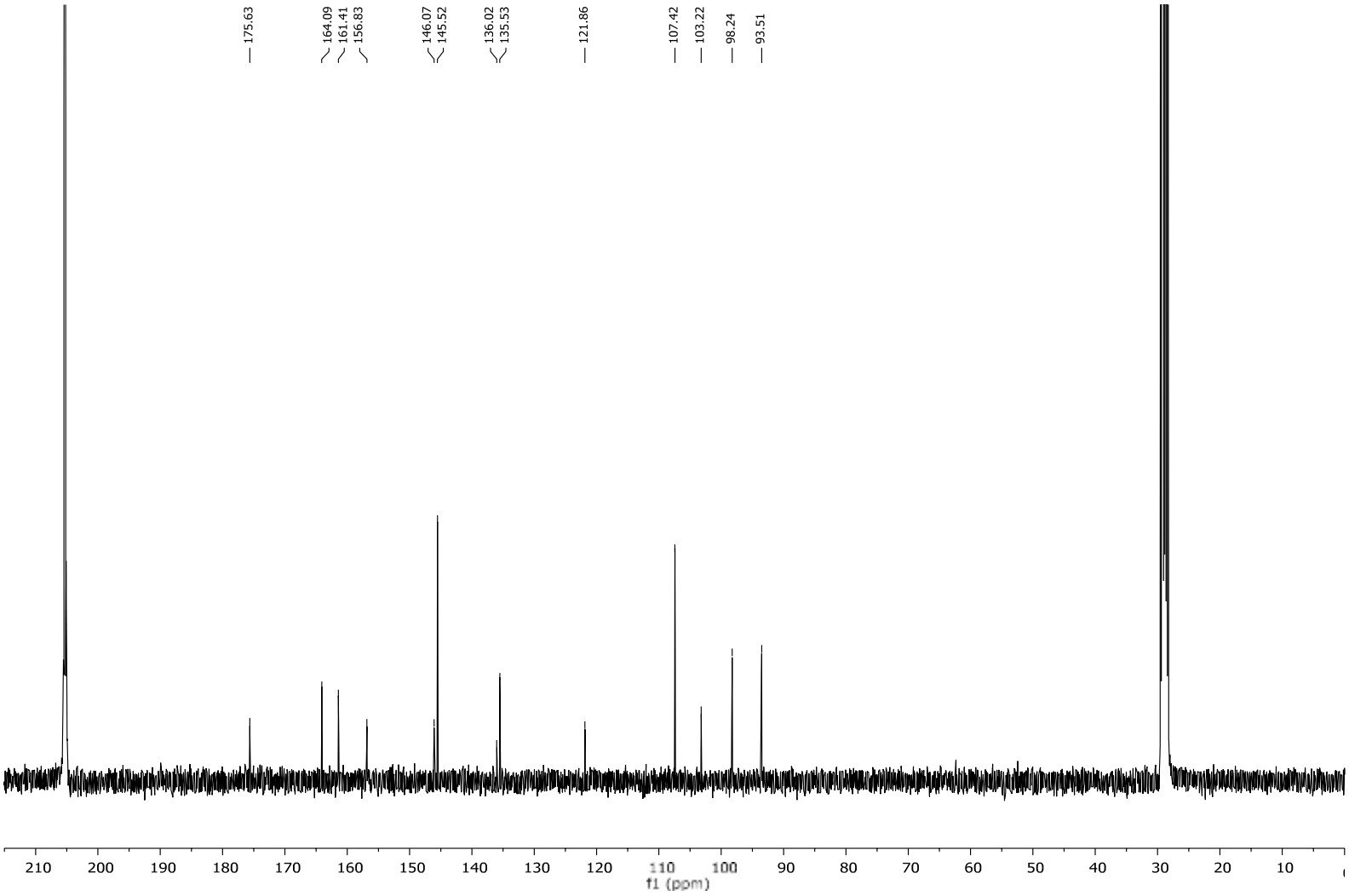




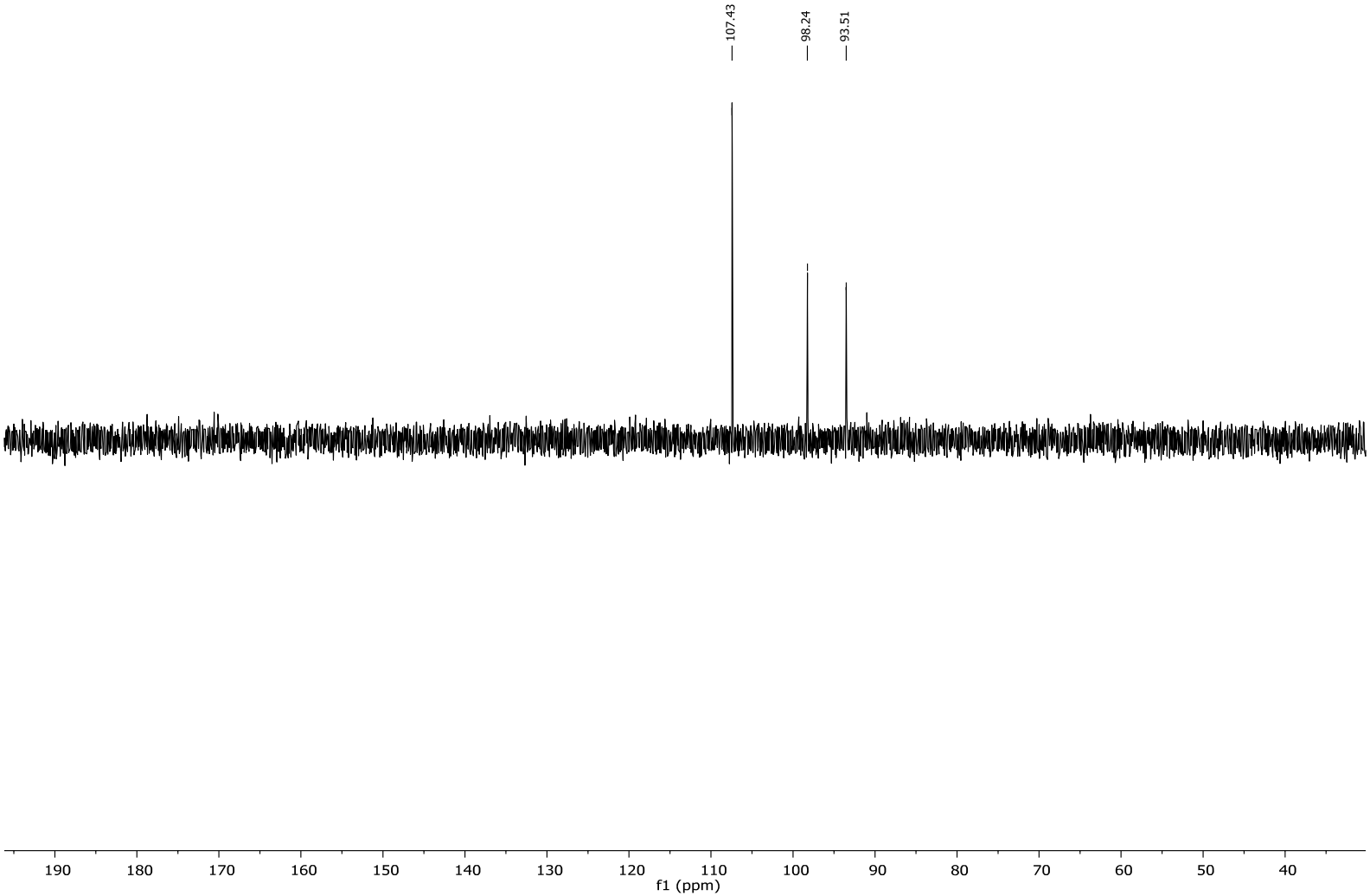
Appendix 90: The ^{1}H-NMR Spectrum of **2** in Acetone-d_6.



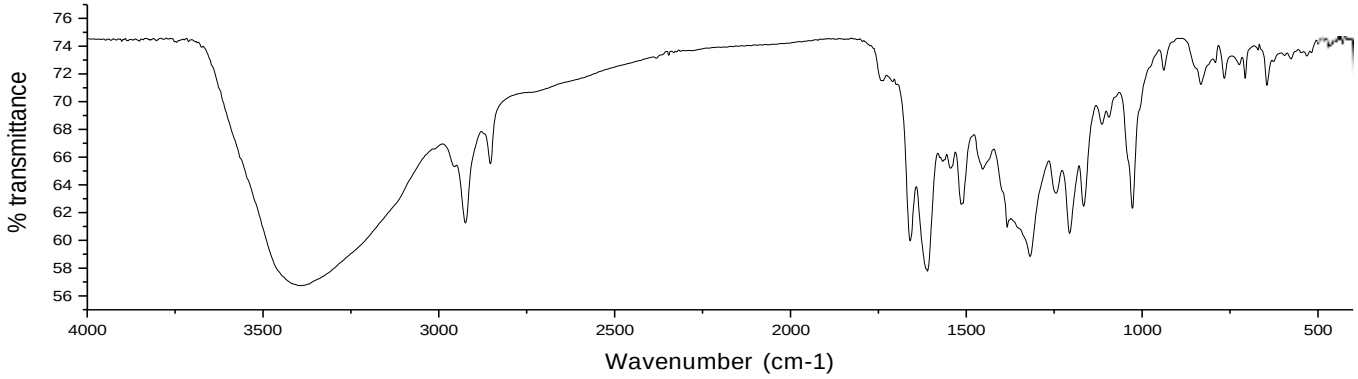
Appendix 91: The ^{13}C-NMR Spectrum of **2** in Acetone-d_6.



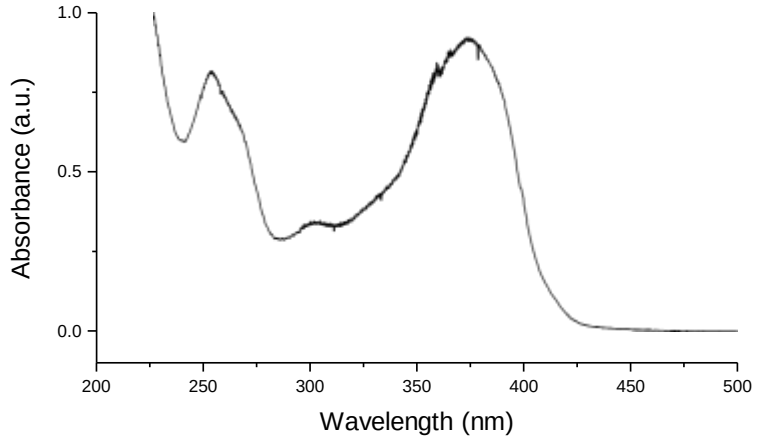
Appendix 92: The DEPT-135 NMR Spectrum of **2** in Acetone-d_6.



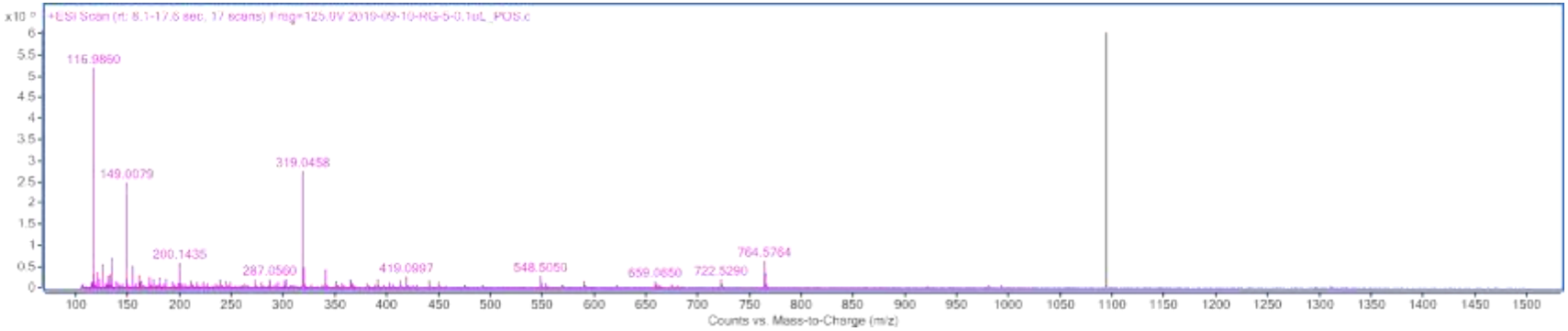
Appendix 93: The IR Spectrum of **2**.

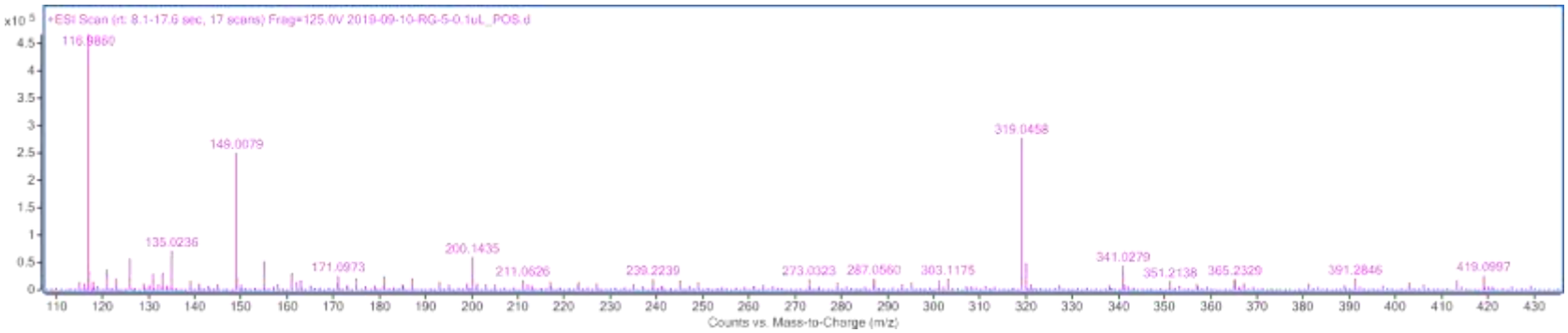


Appendix 94: The UV Spectrum of **2** in Methanol.

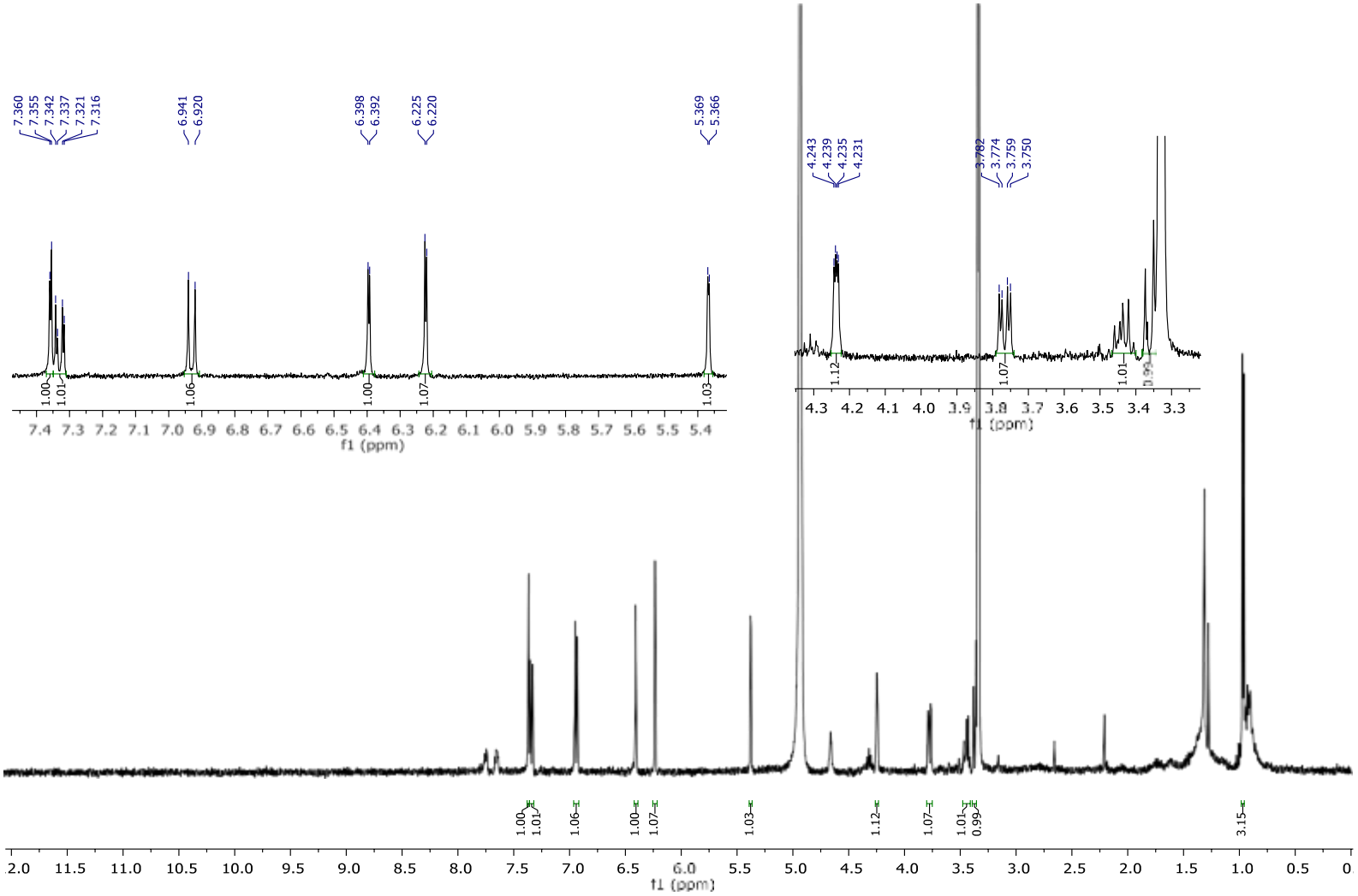


Appendix 95: The HRESIMS of Compound **2**.

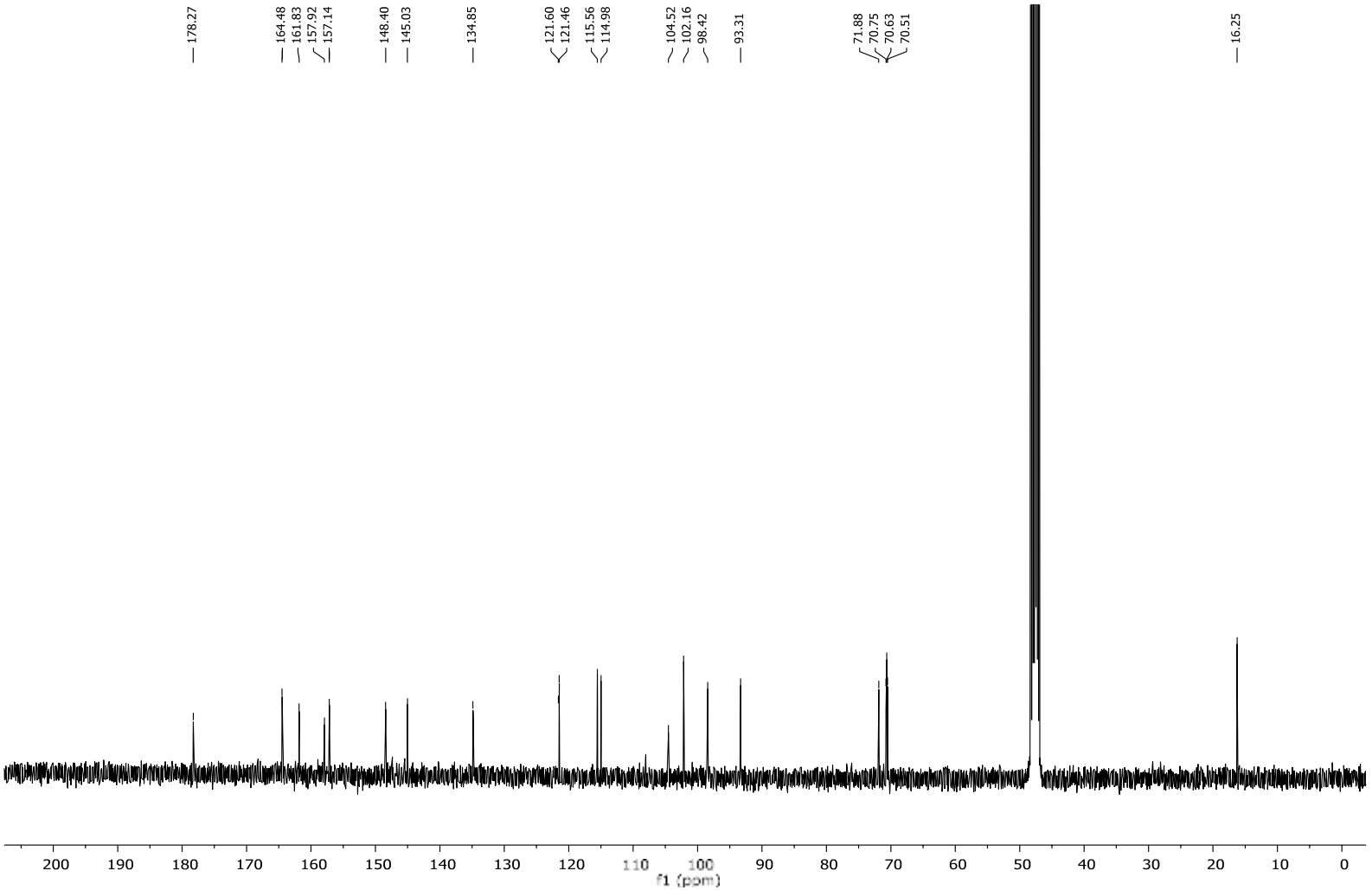




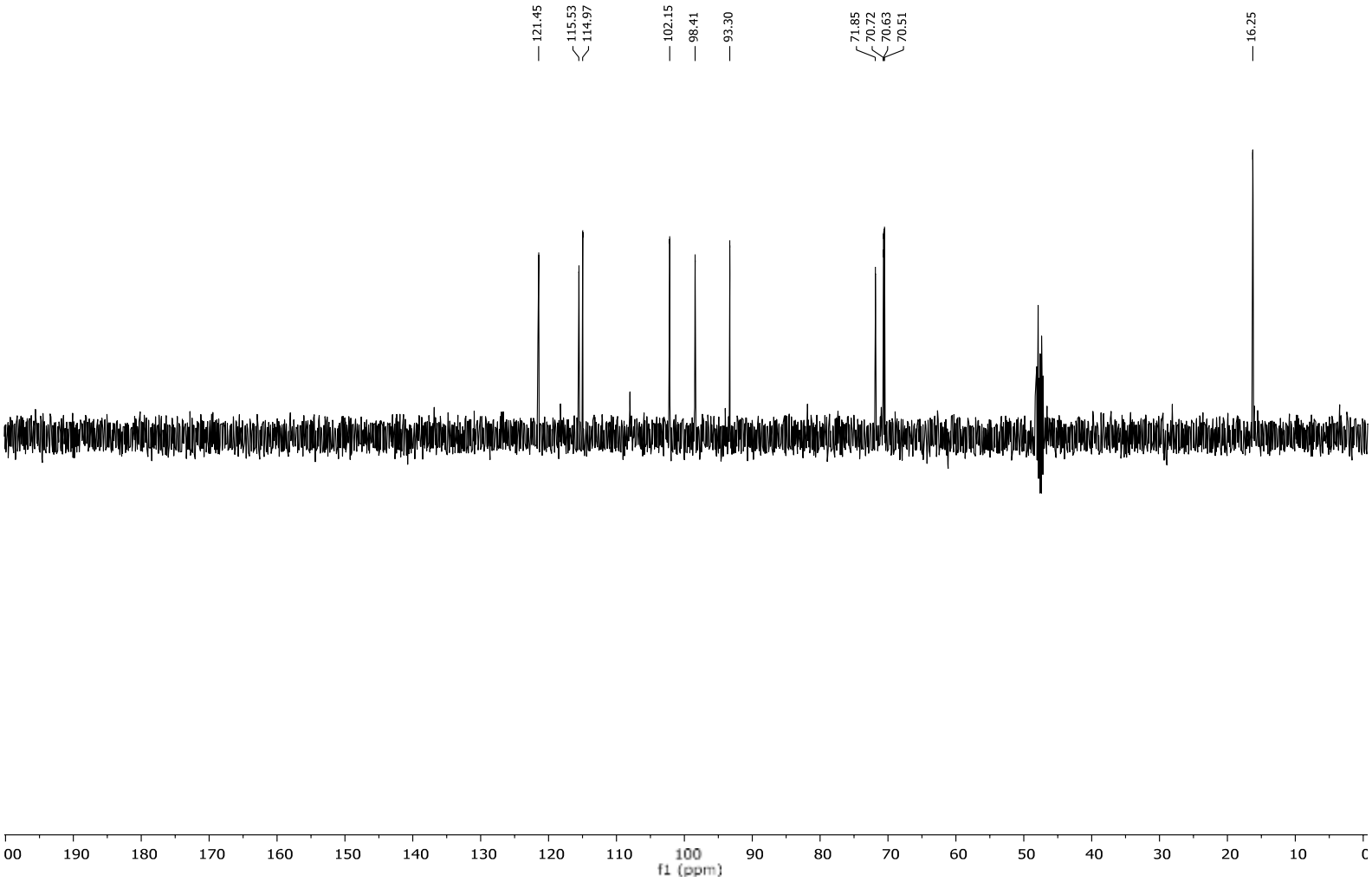
Appendix 96: The ^{1}H-NMR Spectrum of **124** in MeOD-*d*$_4$.



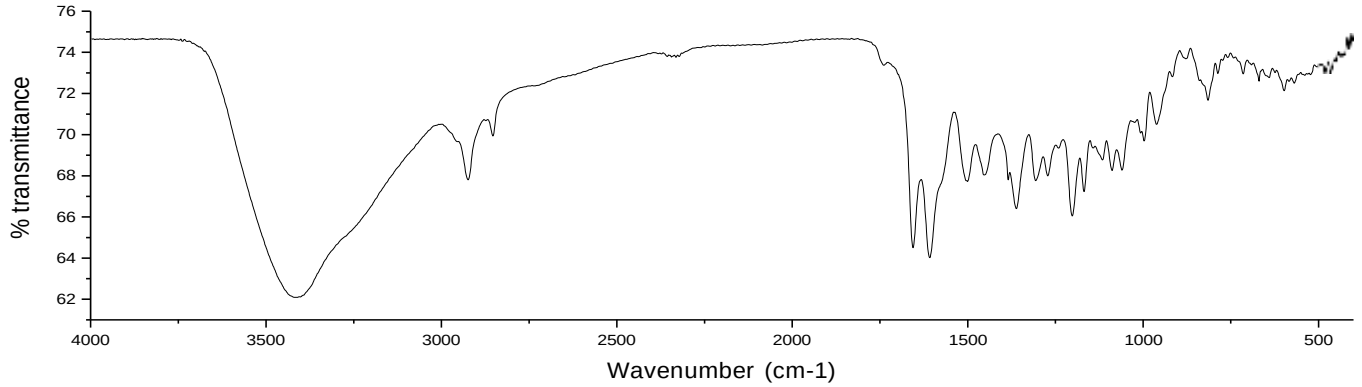
Appendix 97: The ^{13}C-NMR Spectrum of **124** in MeOD-d_4.



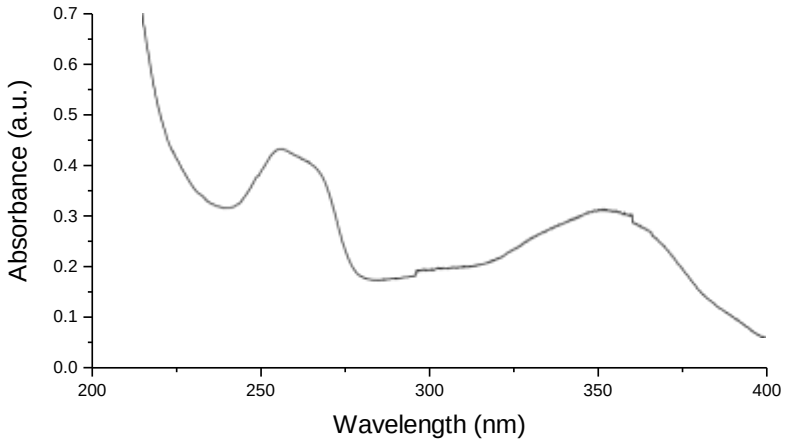
Appendix 98: The DEPT-135 NMR Spectrum of **124** in MeOD-d_4.



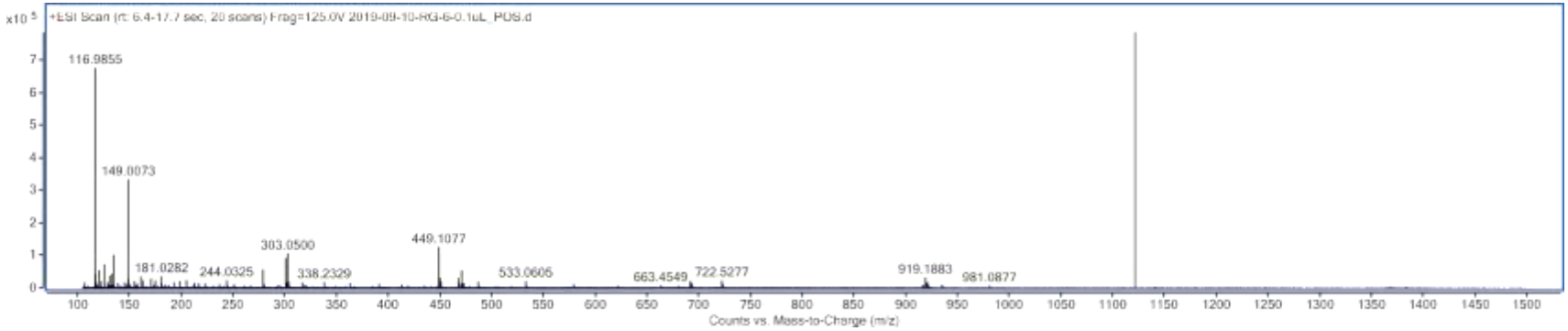
Appendix 99: The IR Spectrum of **124**.

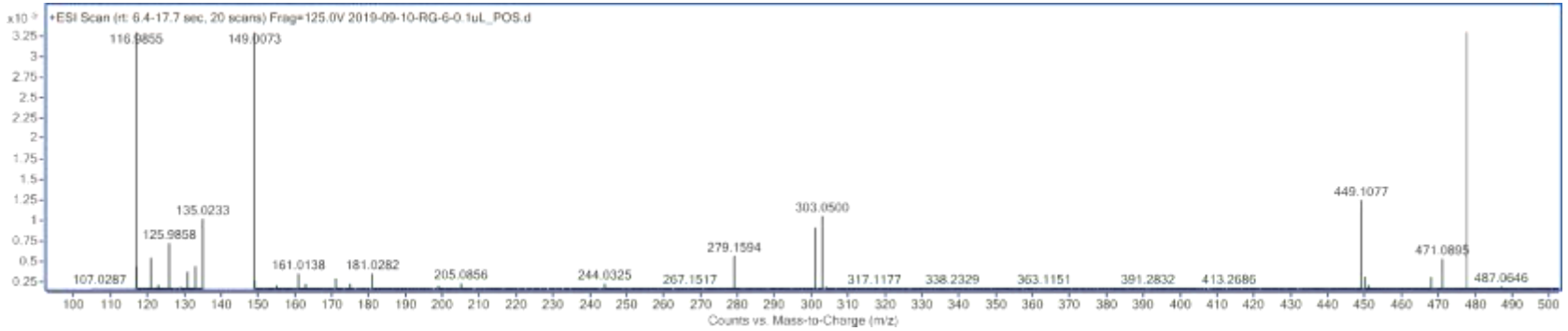


Appendix 100: The UV Spectrum of **124** in Methanol.

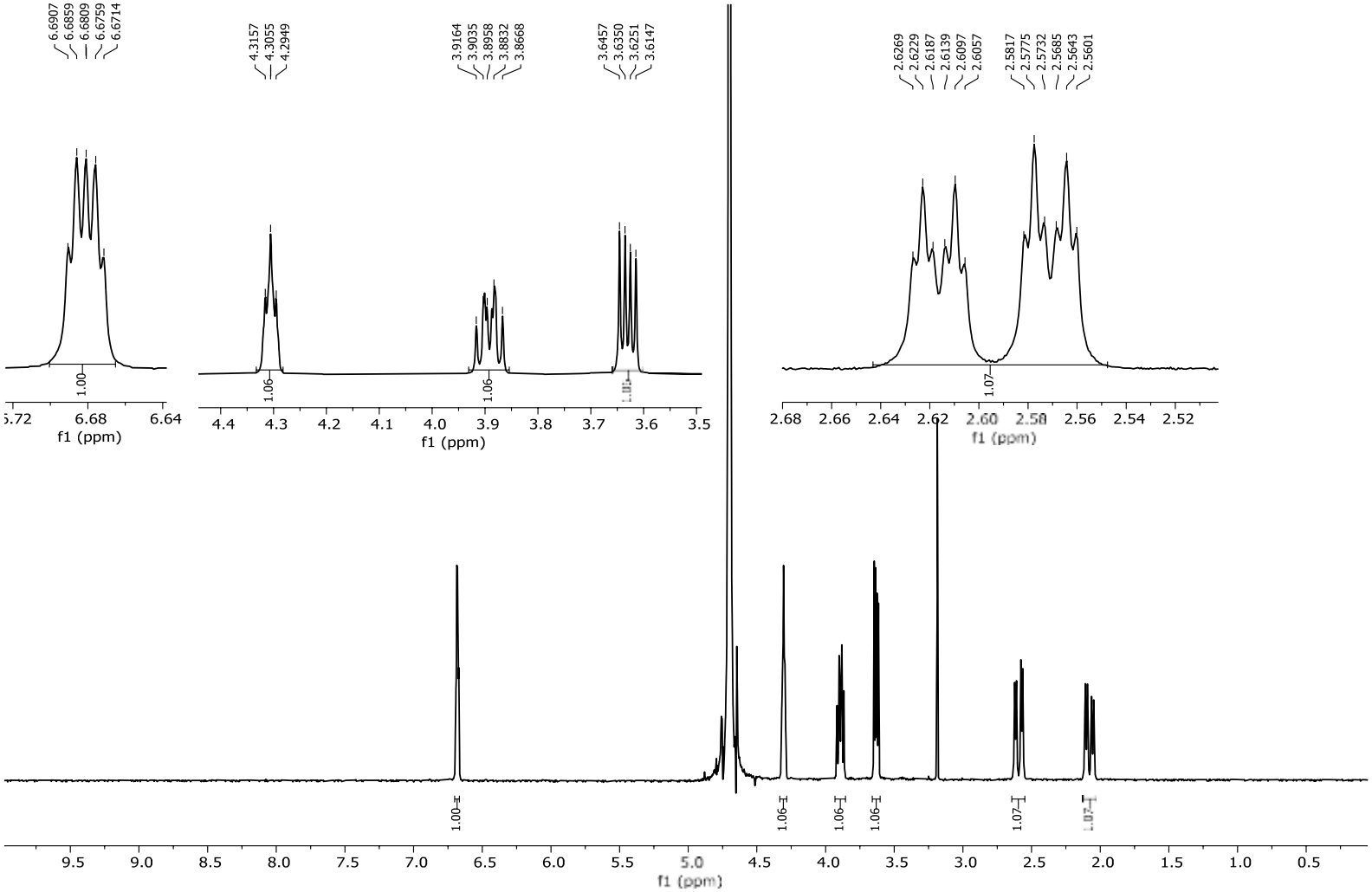


Appendix 101: The HRESIMS of Compound **124**.

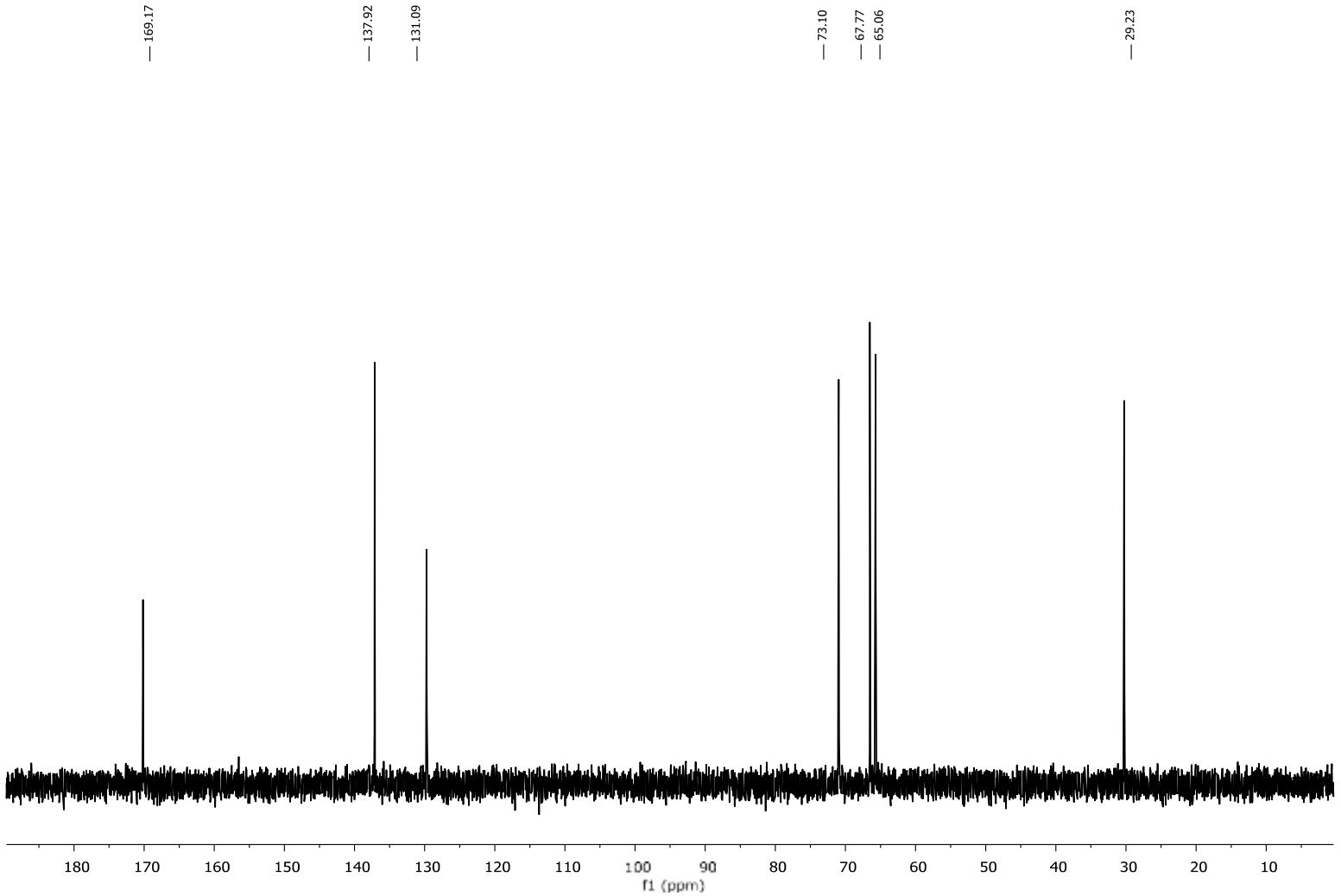




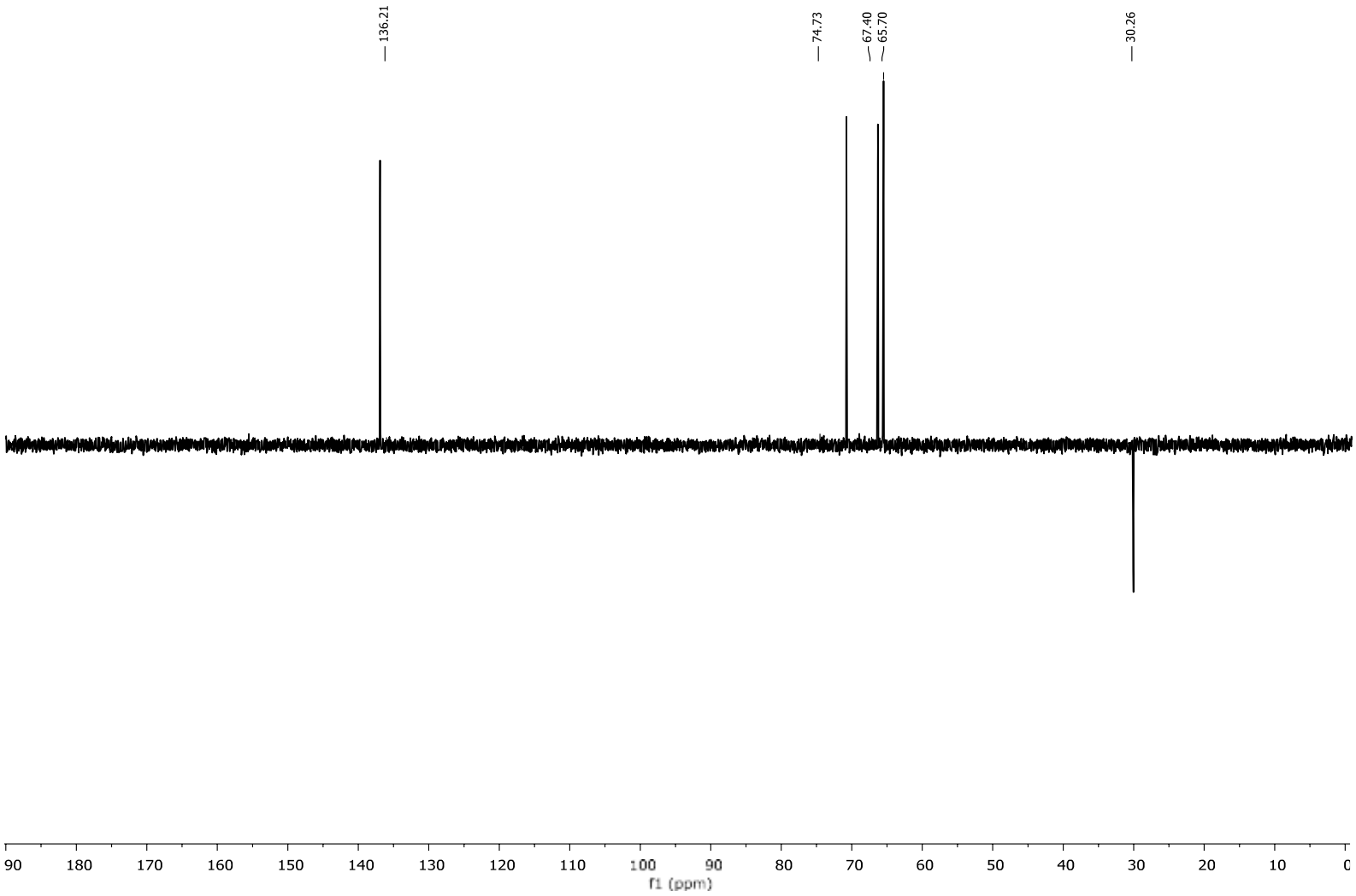
Appendix 102: The ^{1}H-NMR Spectrum of **125** in D_2O.



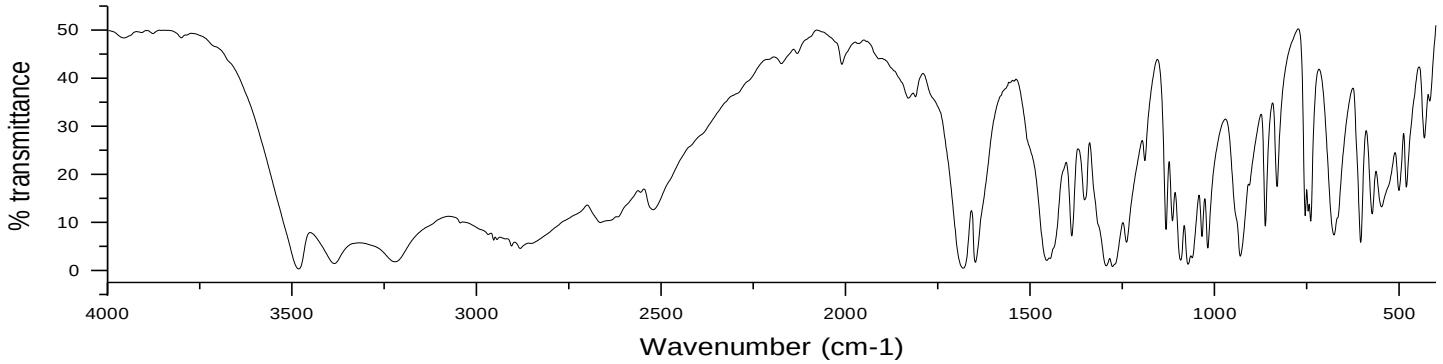
Appendix 103: The ^{13}C-NMR Spectrum of **125** in D_2O.



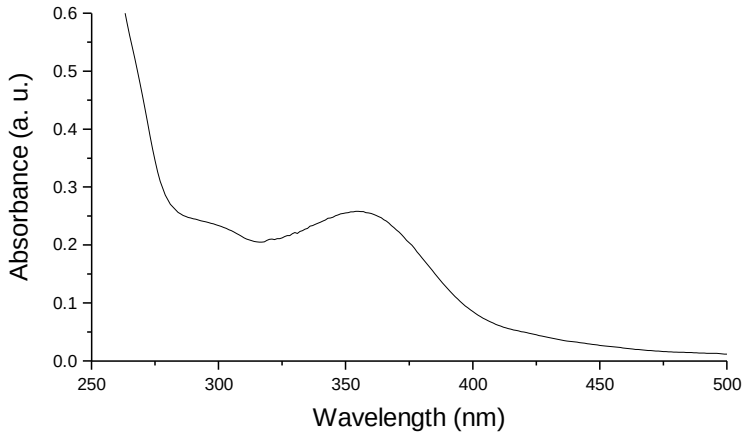
Appendix 104: The DEPT-135 NMR Spectrum of **125** in D_2O.



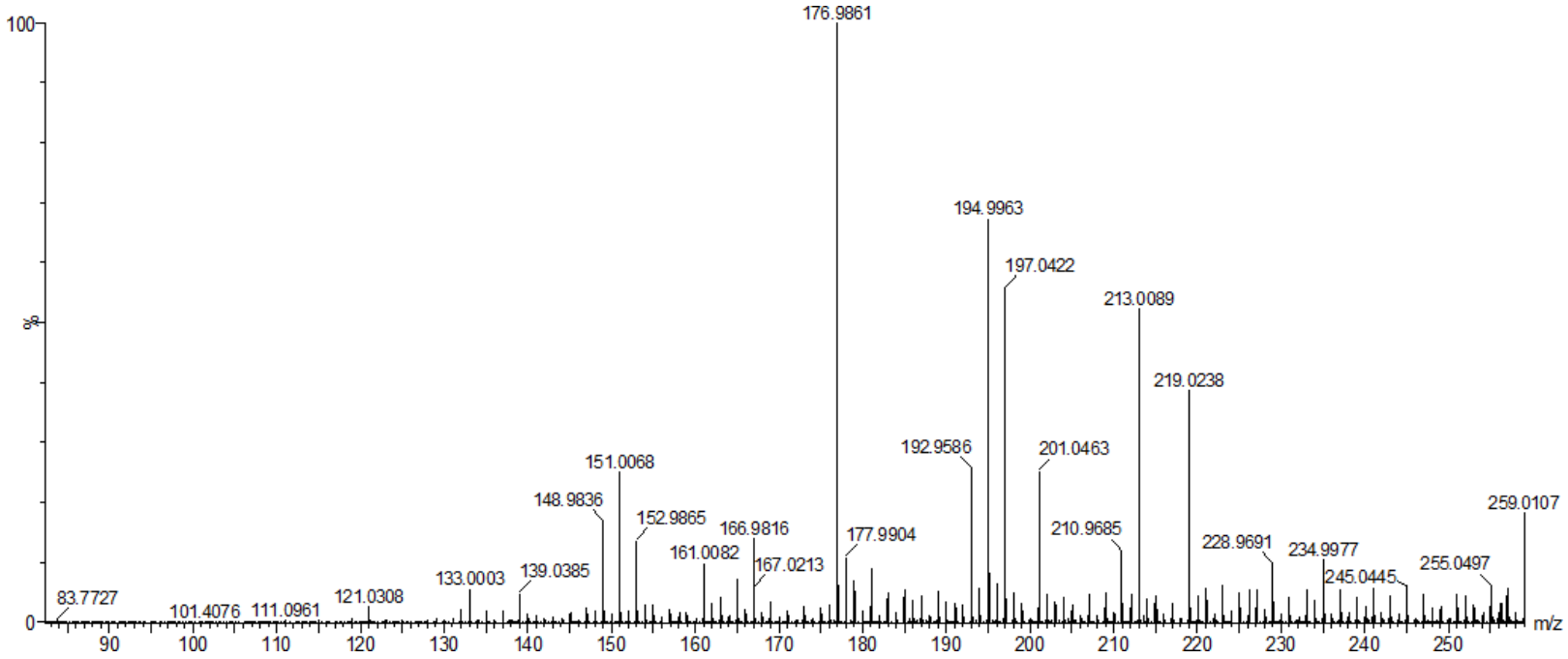
Appendix 105: The IR Spectrum of **125**.



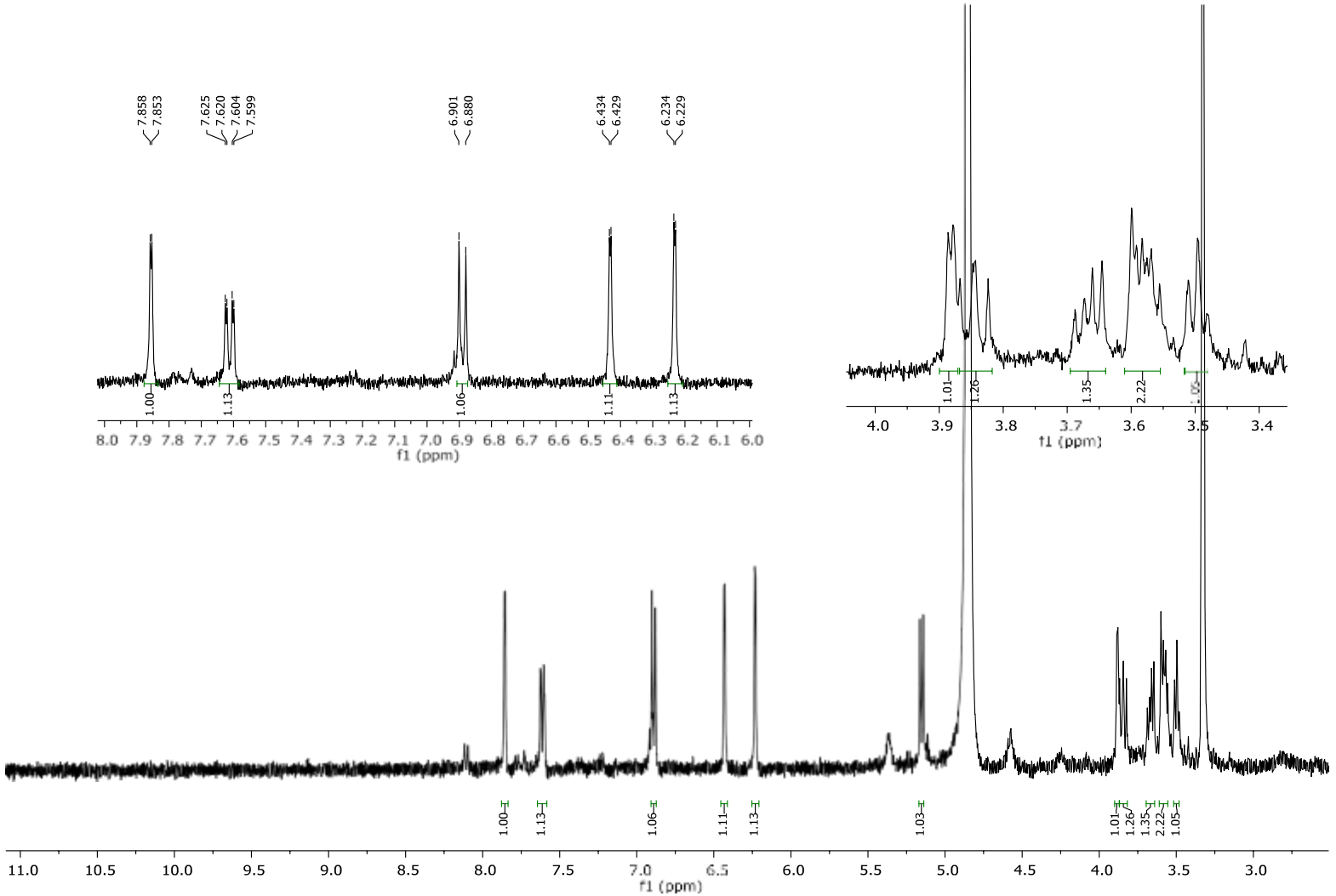
Appendix 106: The UV Spectrum of **125** in Methanol.



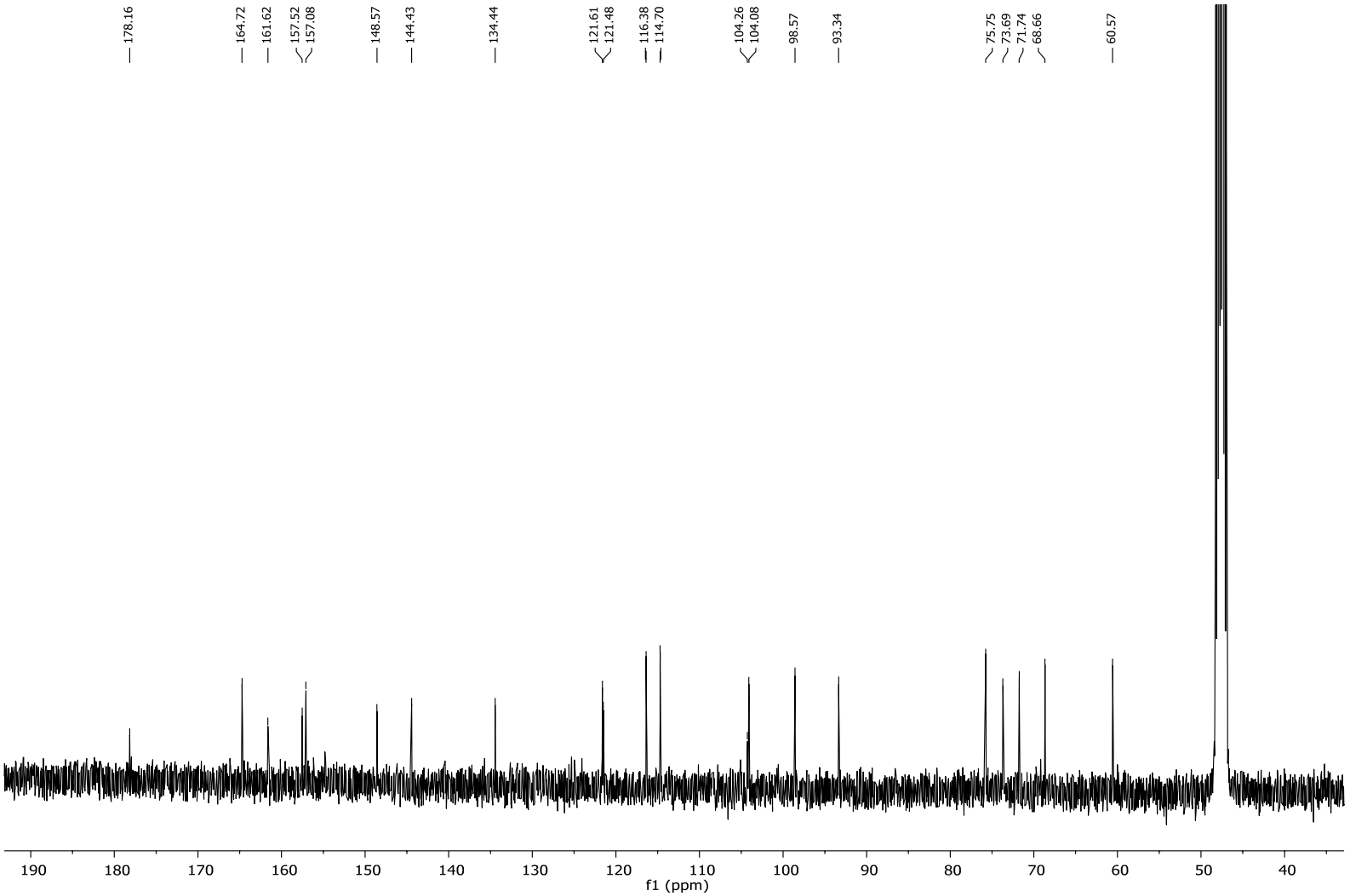
Appendix 107: The HRESIMS of Compound **125**.



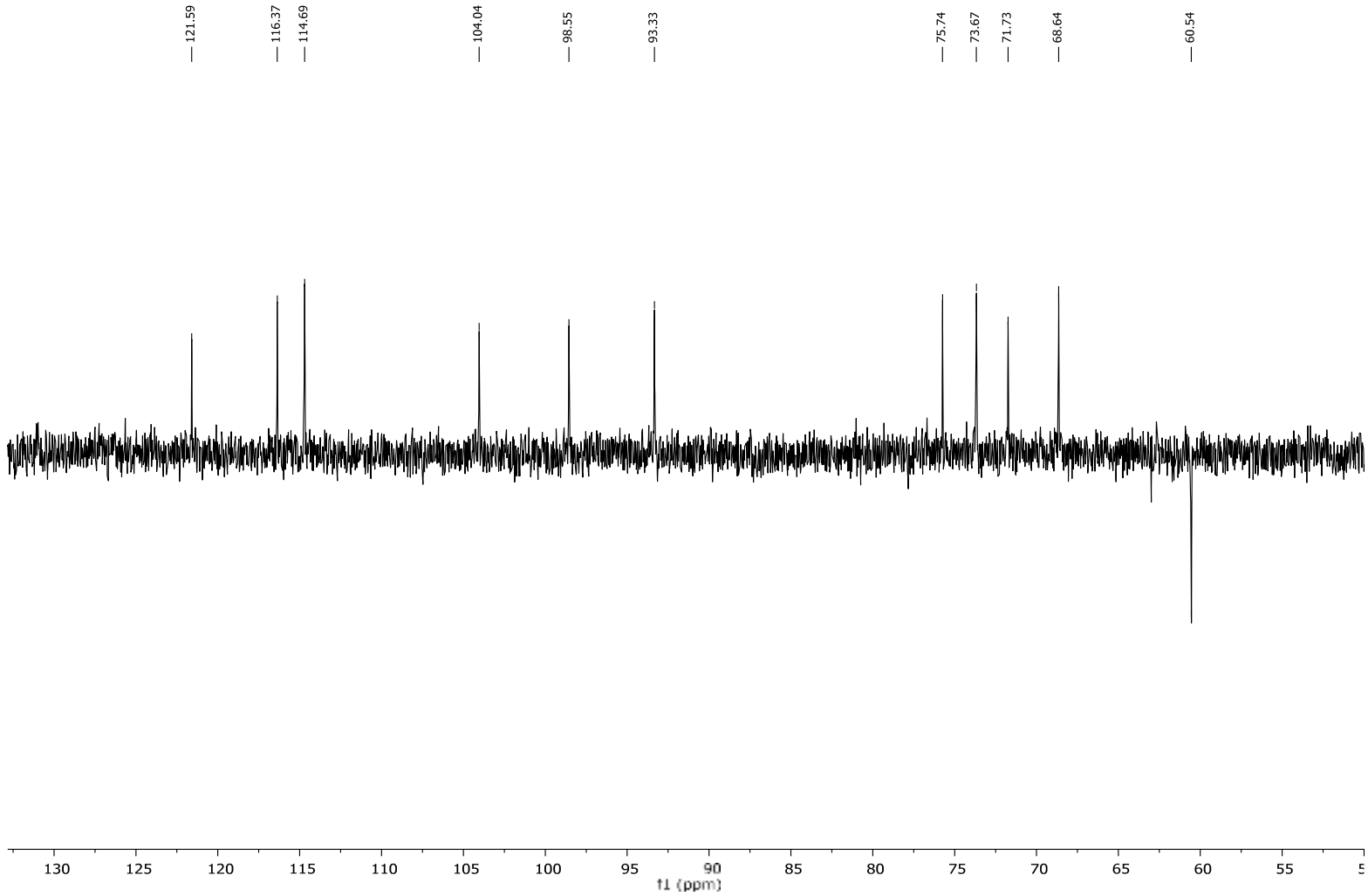
Appendix 108: The ^{1}H-NMR Spectrum of **126** in MeOD-*d*$_4$.



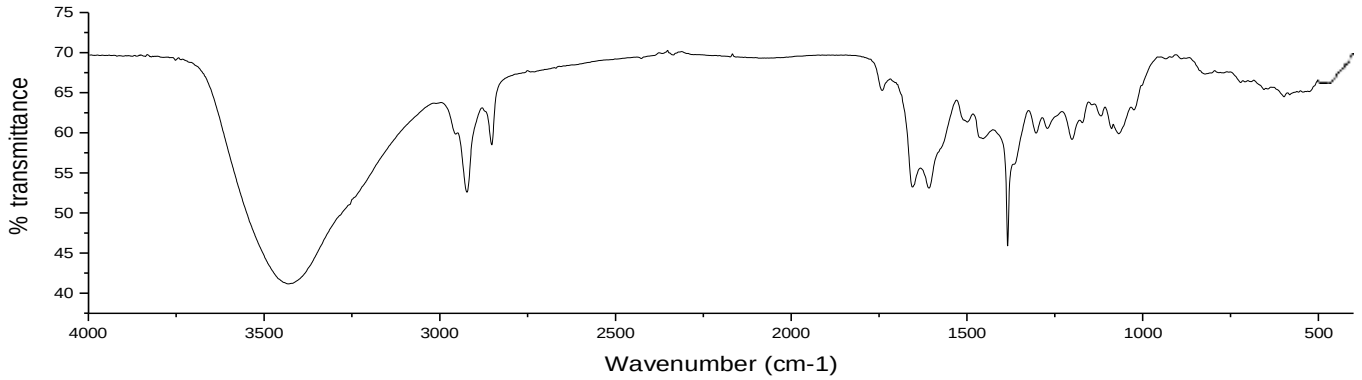
Appendix 109: The ^{13}C-NMR Spectrum of **126** in MeOD-*d*$_4$.



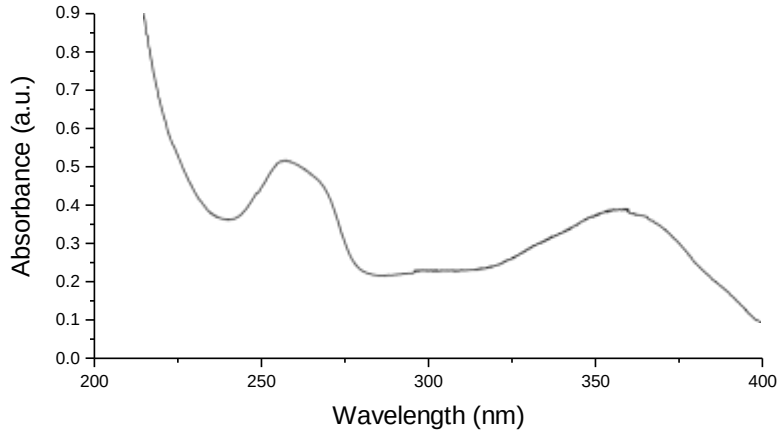
Appendix 110: The DEPT-135 NMR Spectrum of **126** in MeOD-d_4.



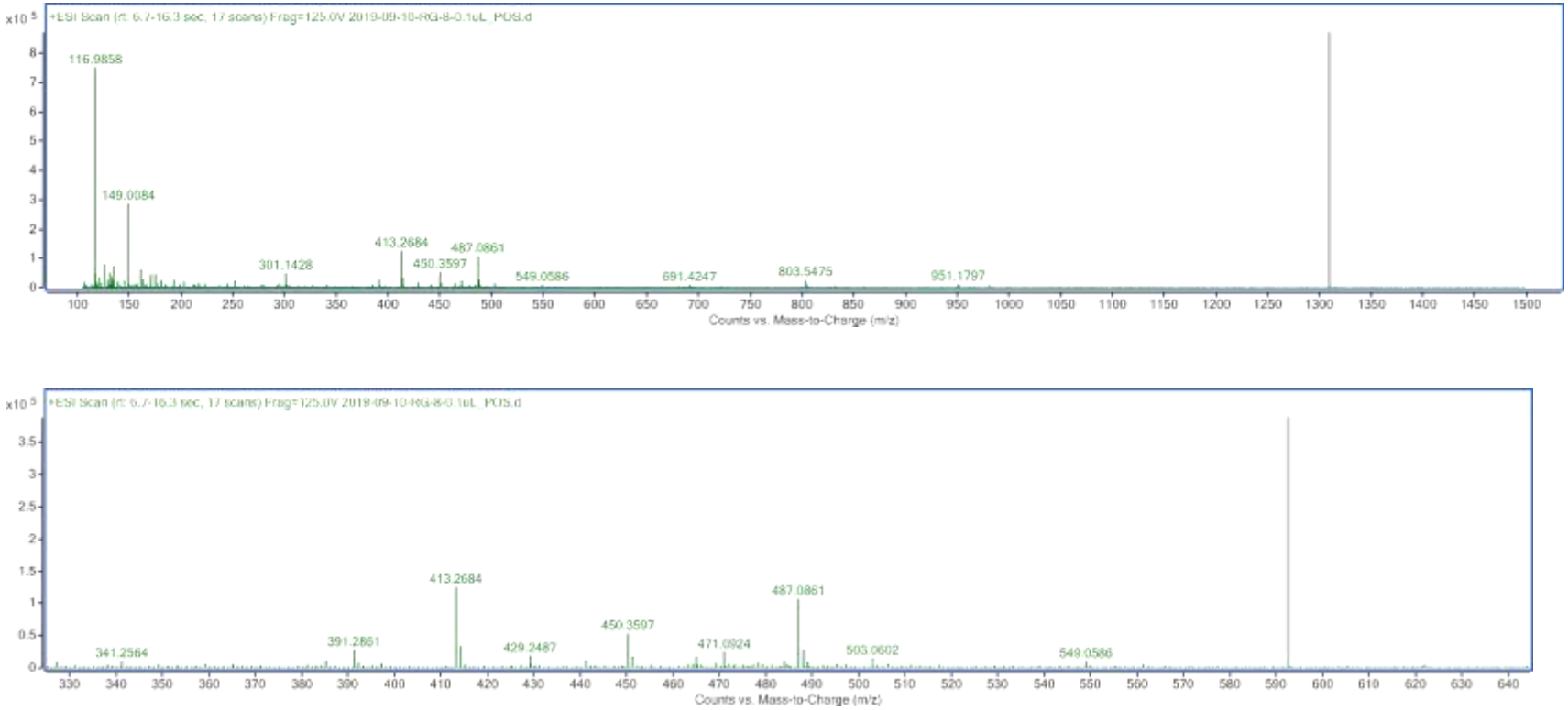
Appendix 111: The IR Spectrum of **126**.



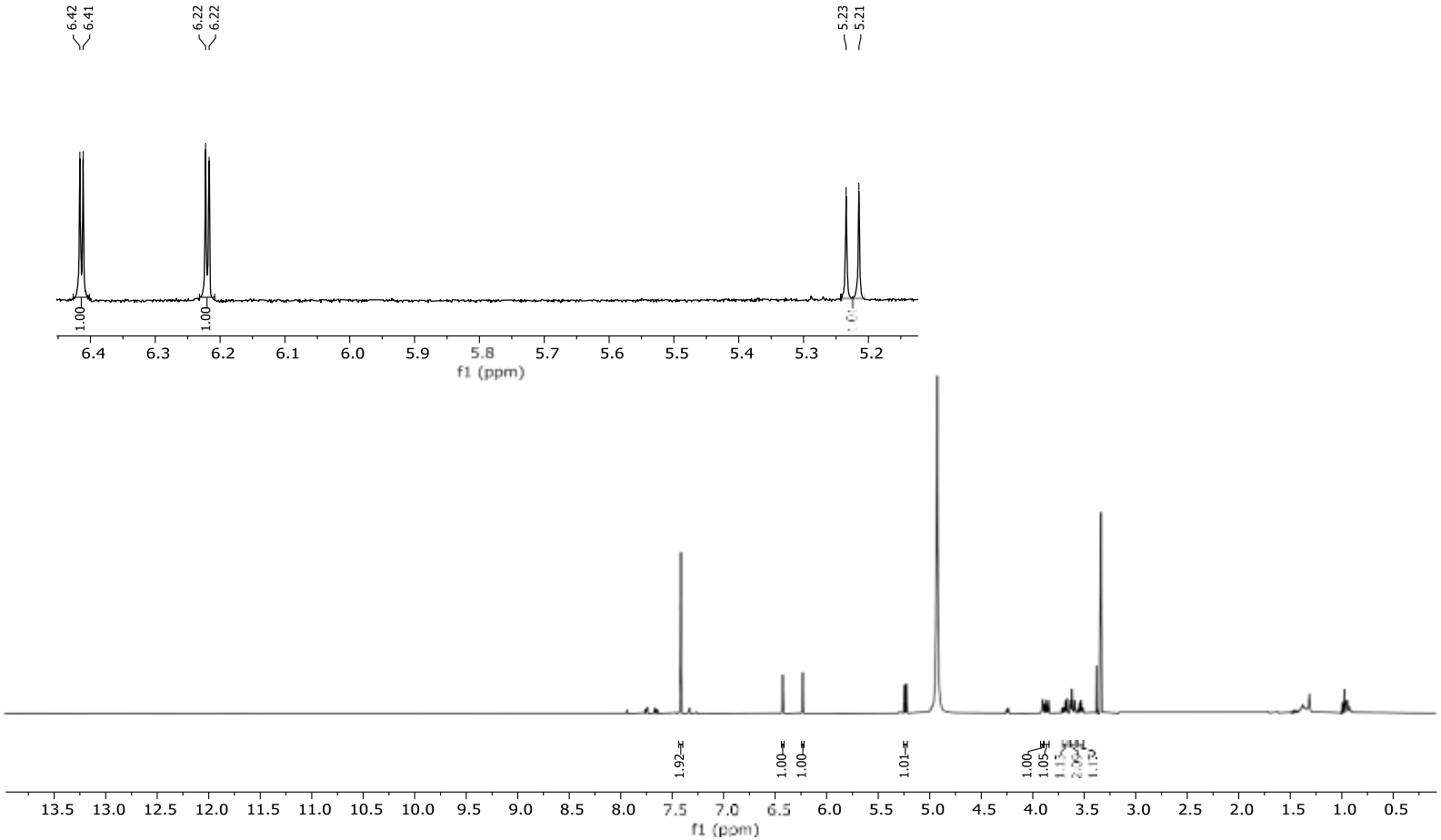
Appendix 112: The UV Spectrum of **126** in Methanol.



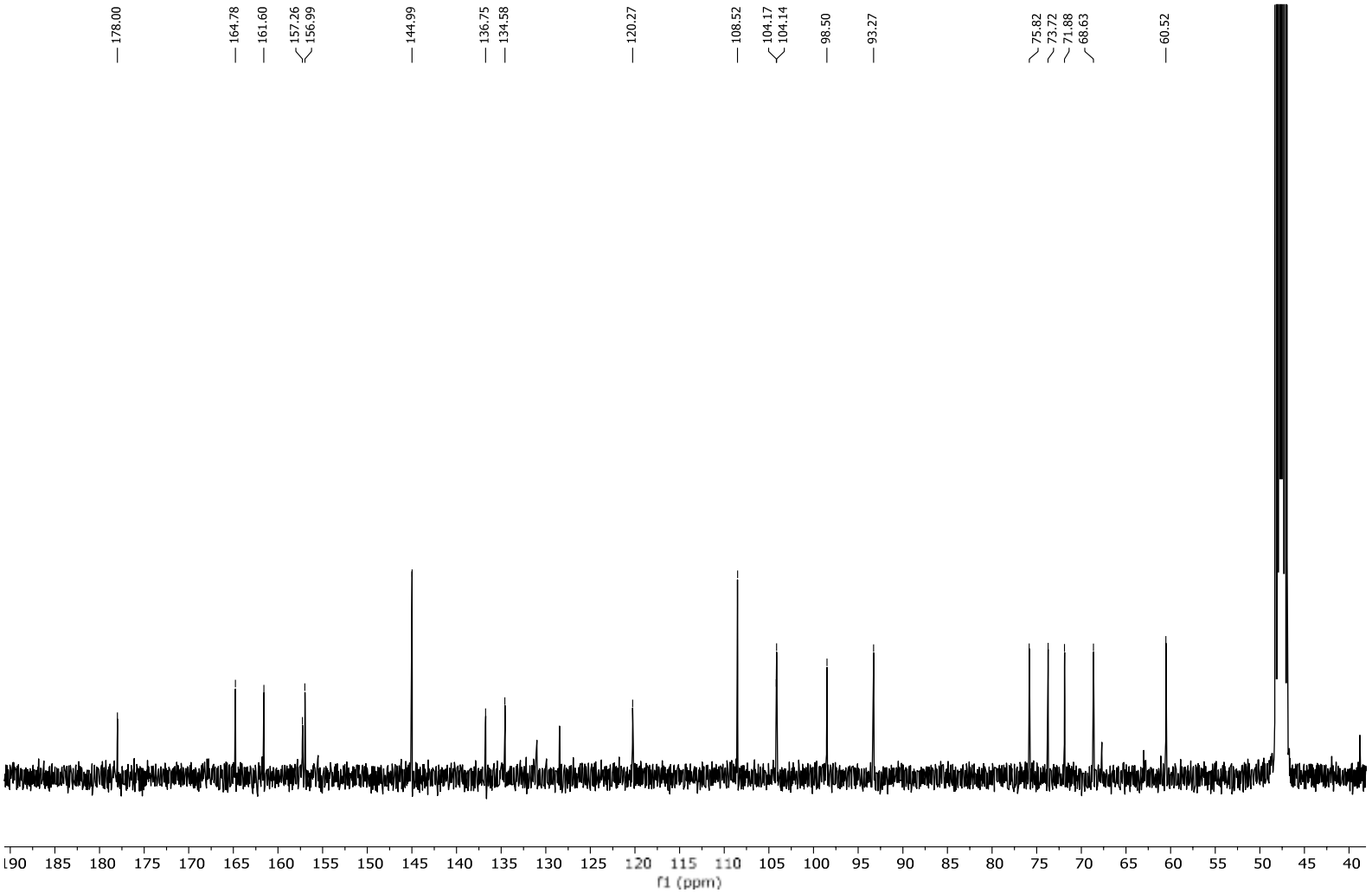
Appendix 113: The HRESIMS of Compound **126**.



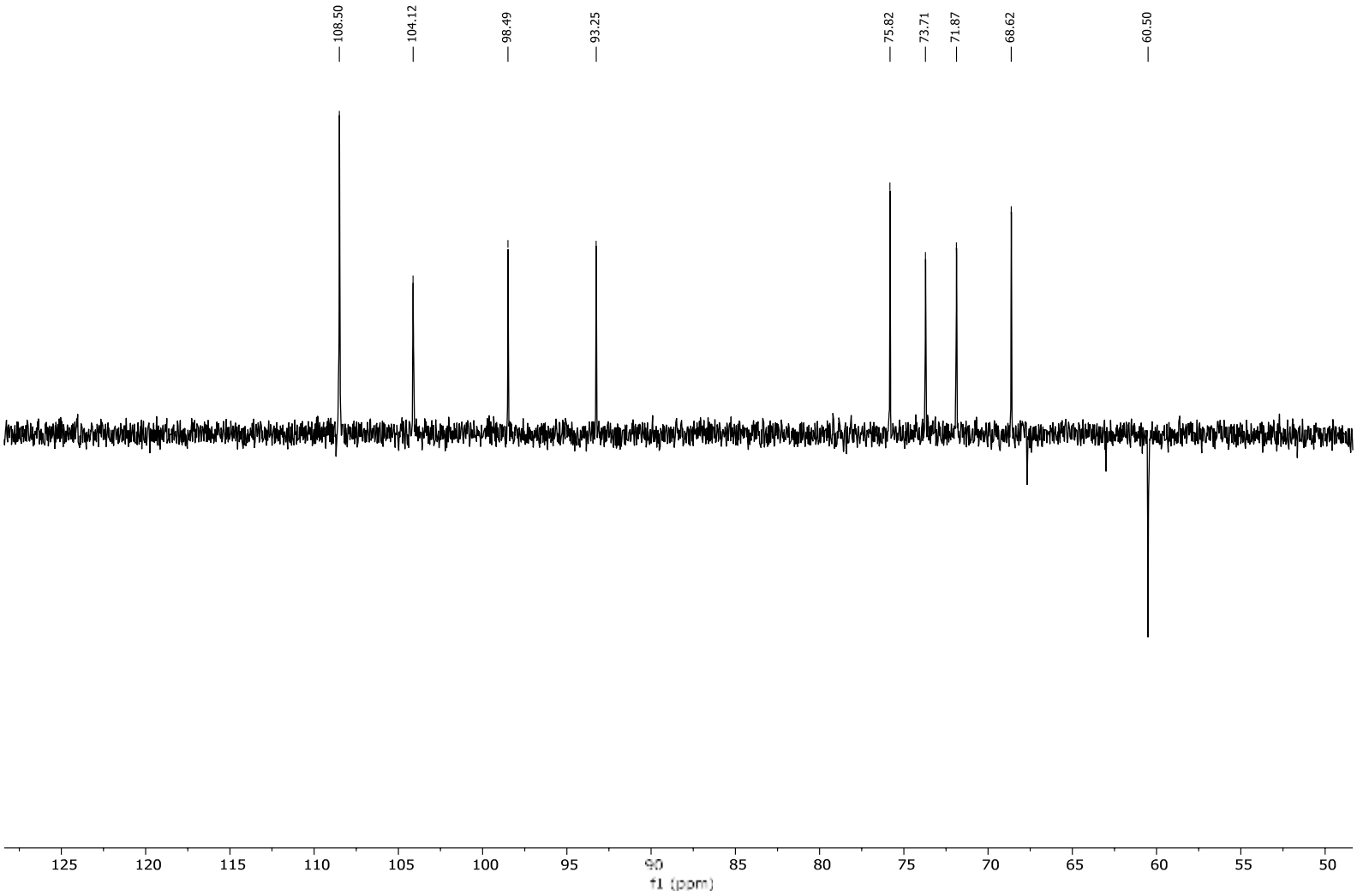
Appendix 114: The ^{1}H-NMR Spectrum of **127** in MeOD-*d*$_4$.



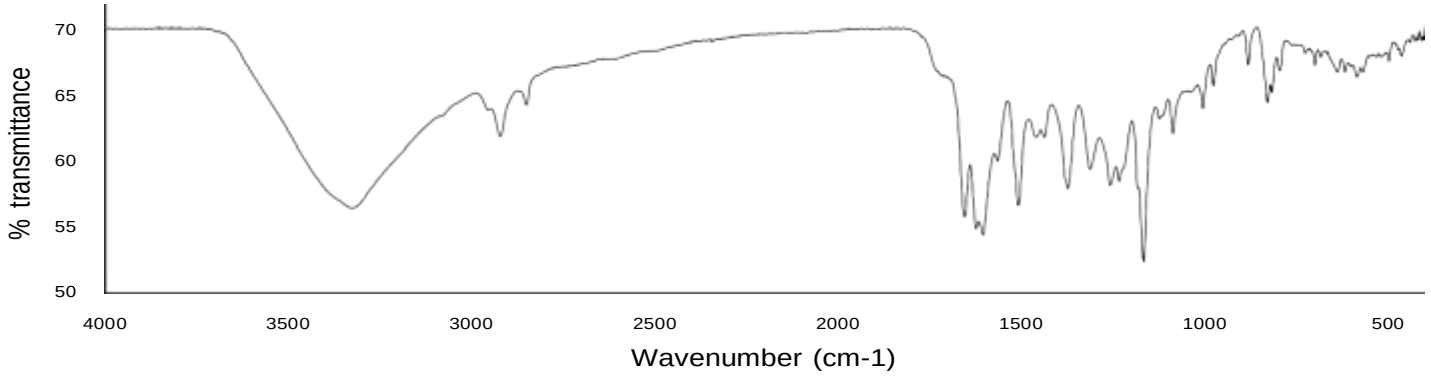
Appendix 115: The ^{13}C-NMR Spectrum of **127** in MeOD-*d*$_4$.



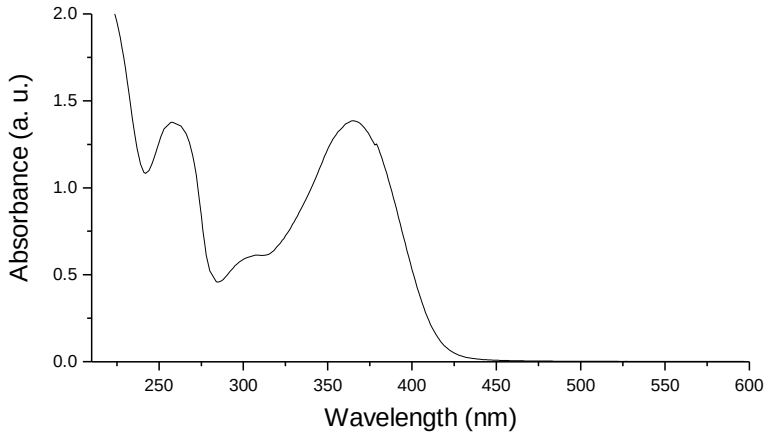
Appendix 116: The DEPT-135 NMR Spectrum of **127** in MeOD-d_4.



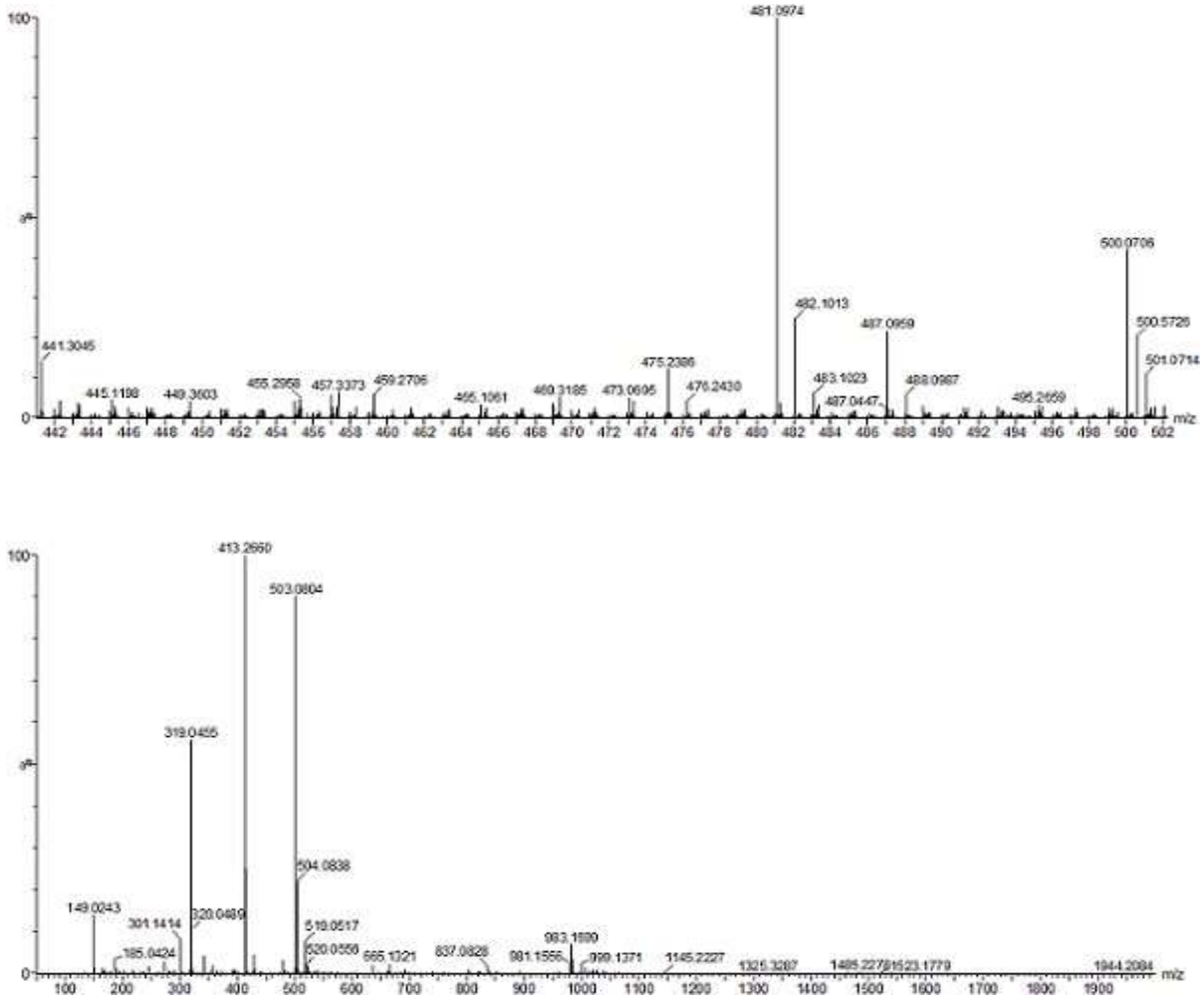
Appendix 117: The IR Spectrum of **127**.



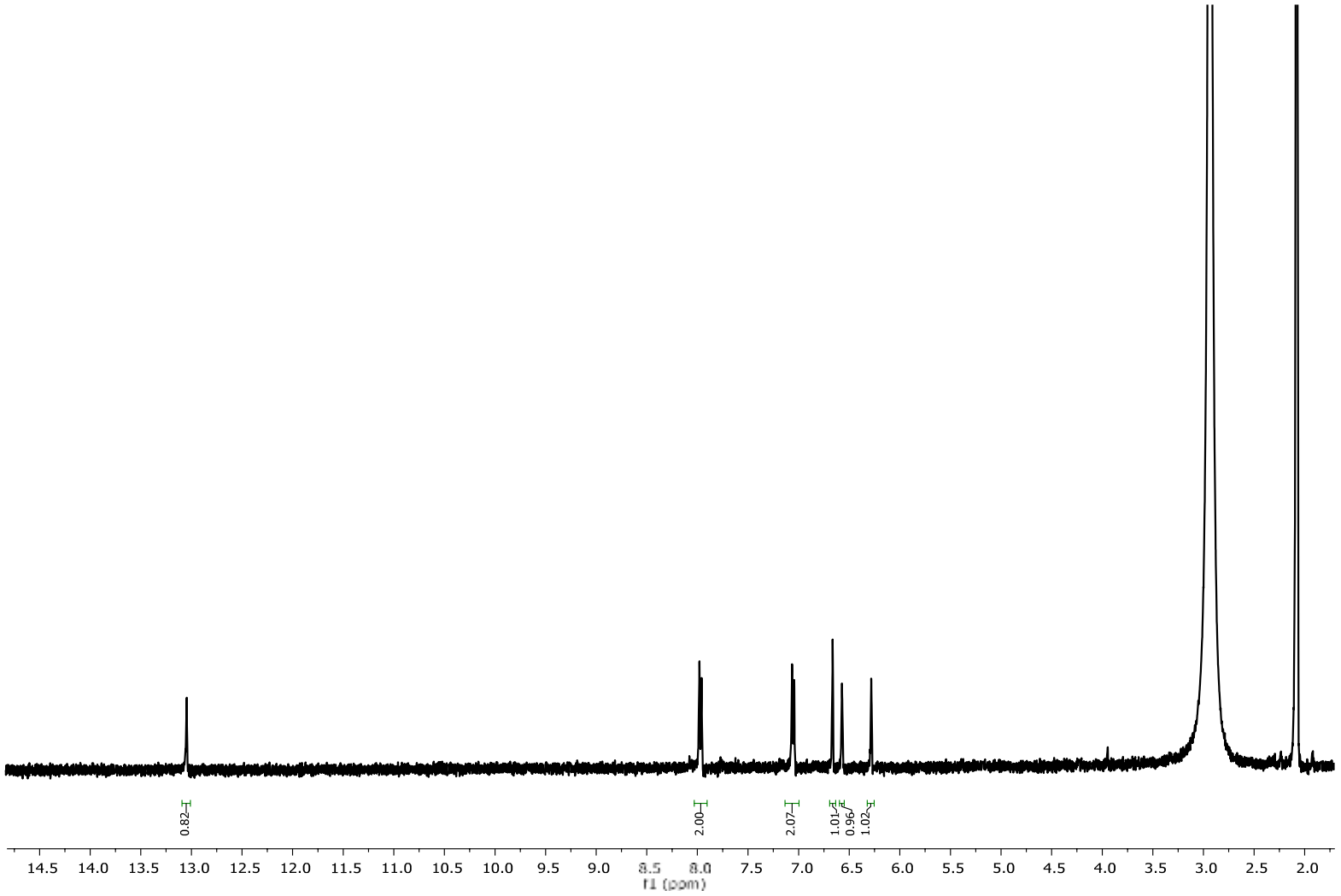
Appendix 118: The UV Spectrum of **127** in Methanol.



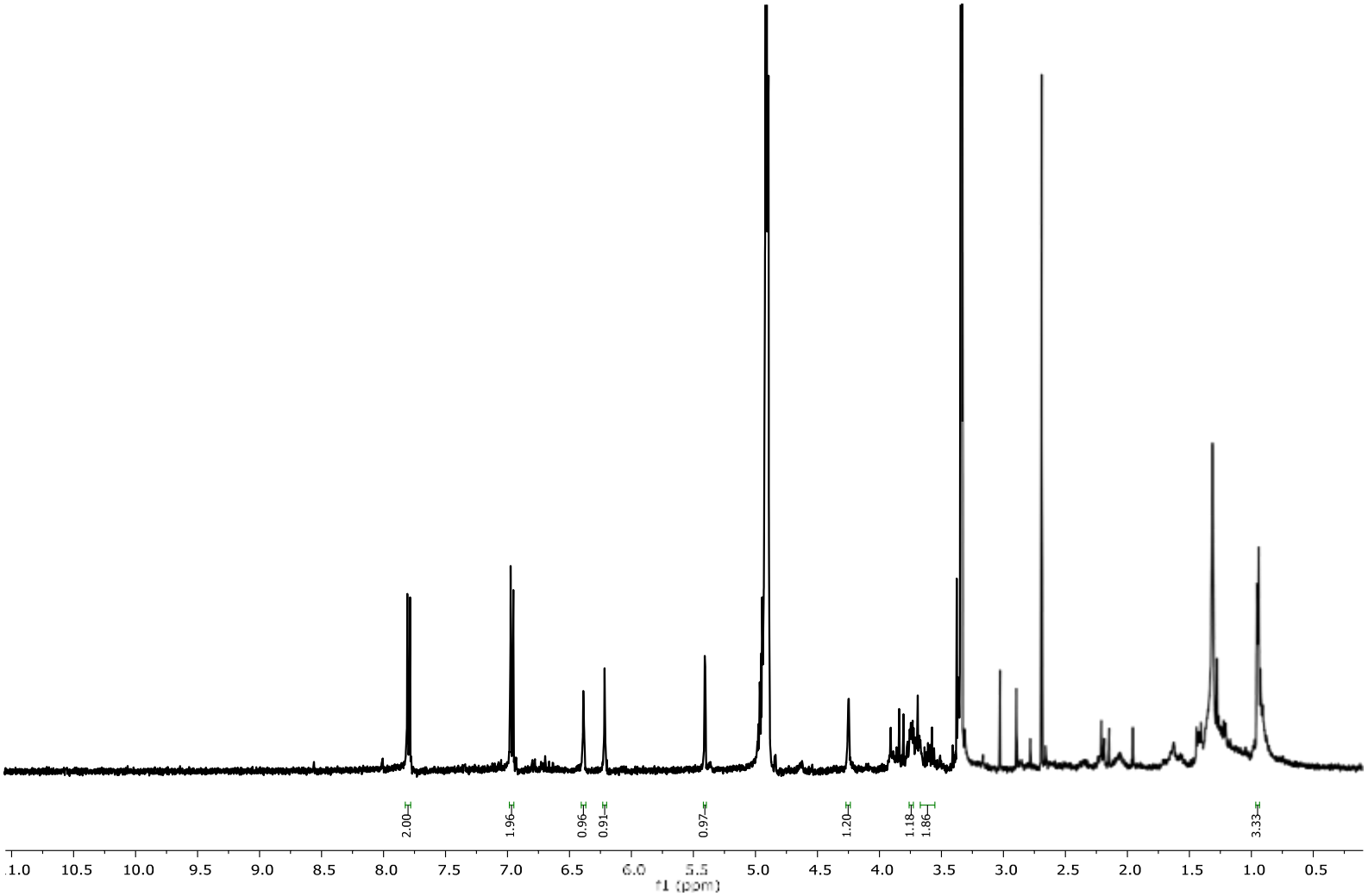
Appendix 119: The HRESIMS of Compound **127**.



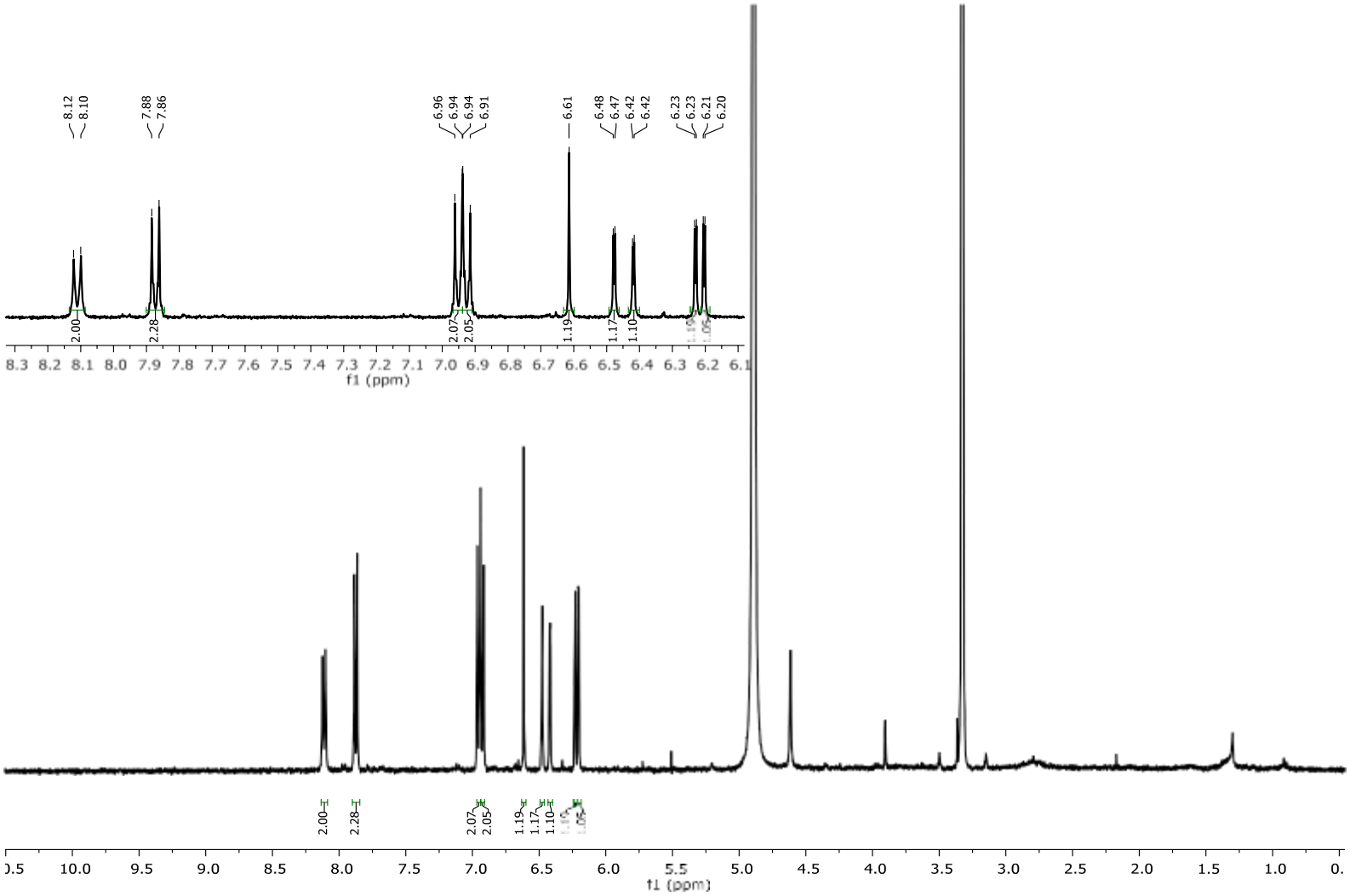
Appendix 120: The ^{1}H-NMR Spectrum of **128** in Acetone-d_6.



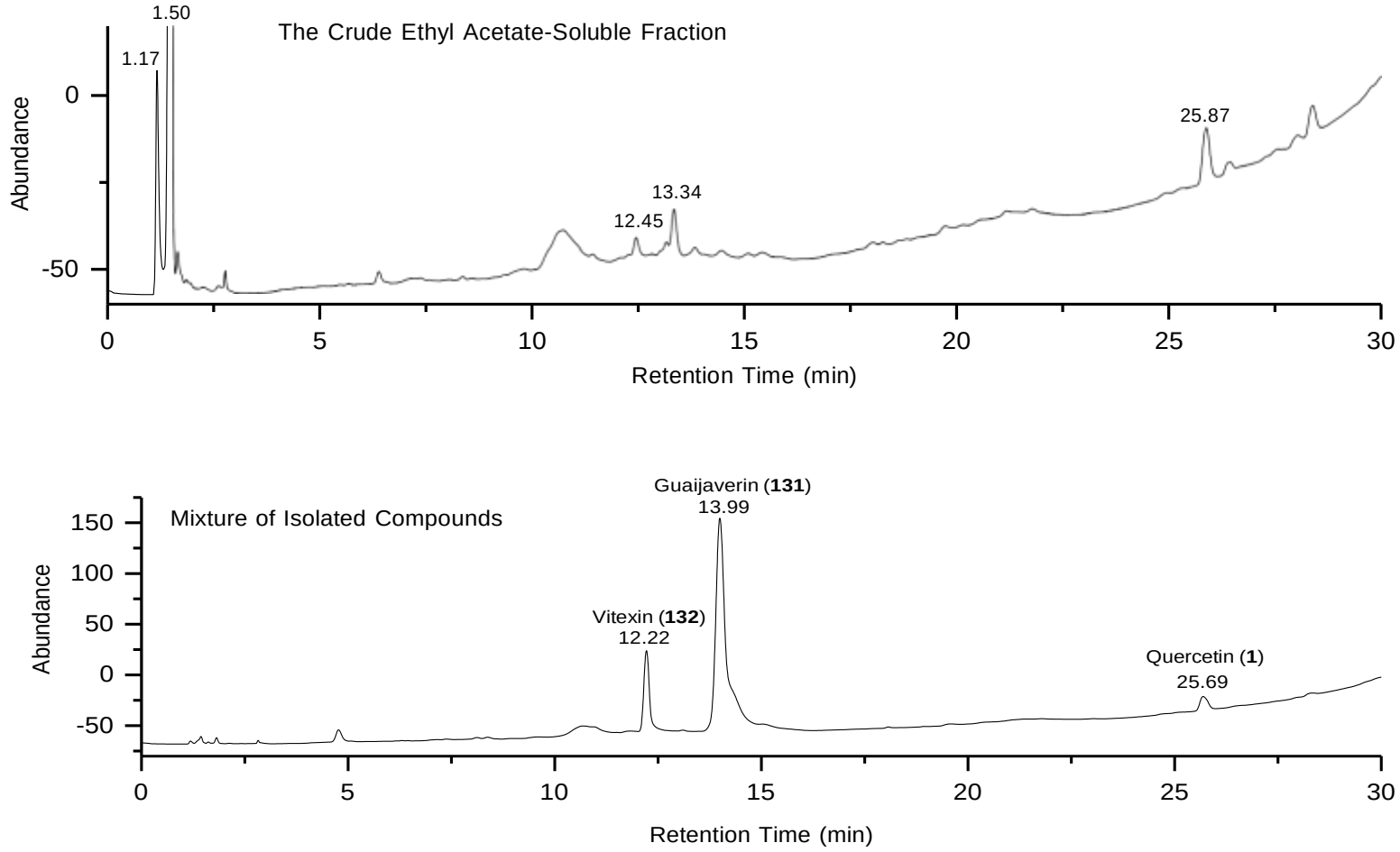
Appendix 121: The ^{1}H-NMR Spectrum of **129** in MeOD-*d*$_4$.



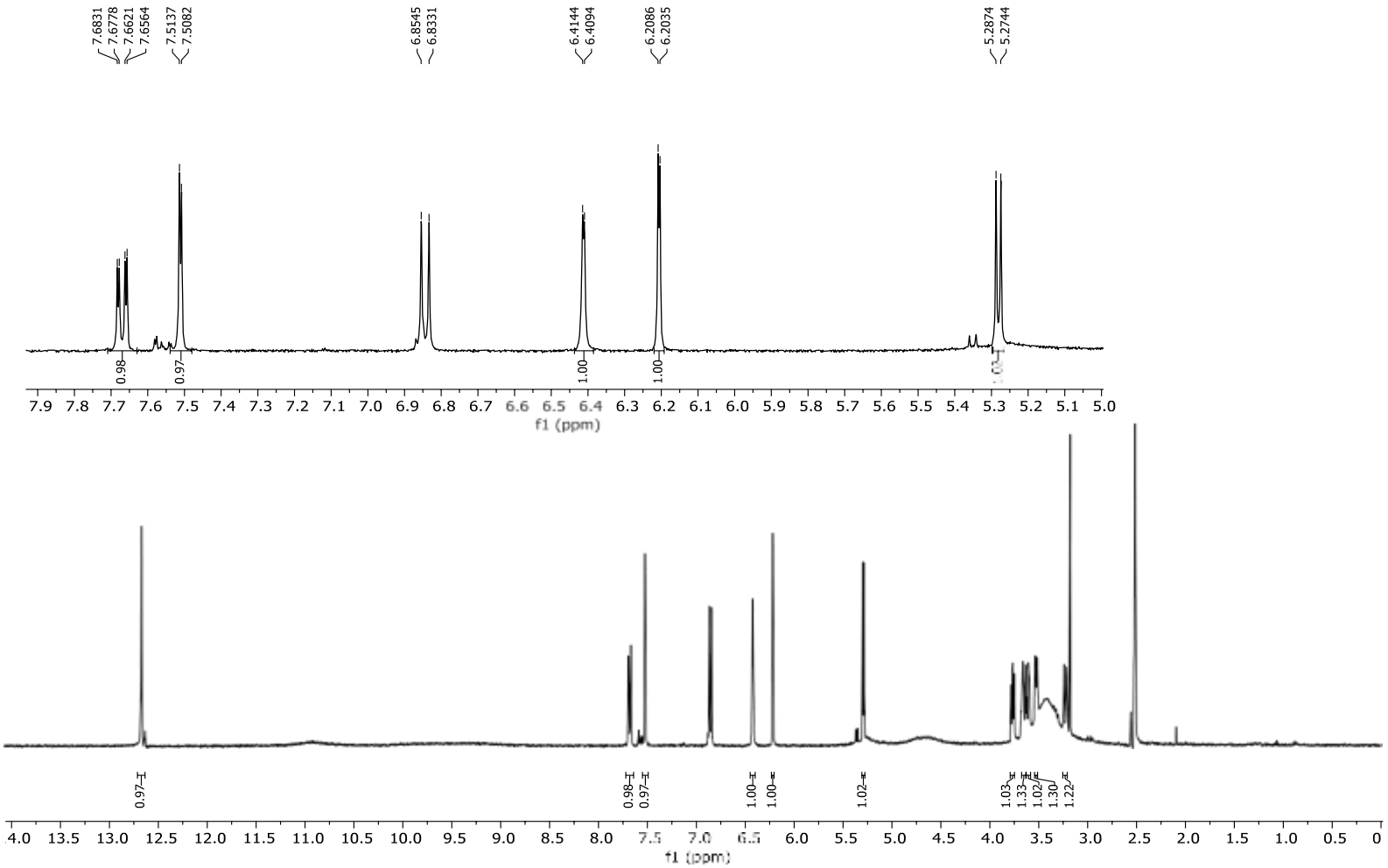
Appendix 122: The ^{1}H-NMR Spectrum of **130** in Acetone-d_6.



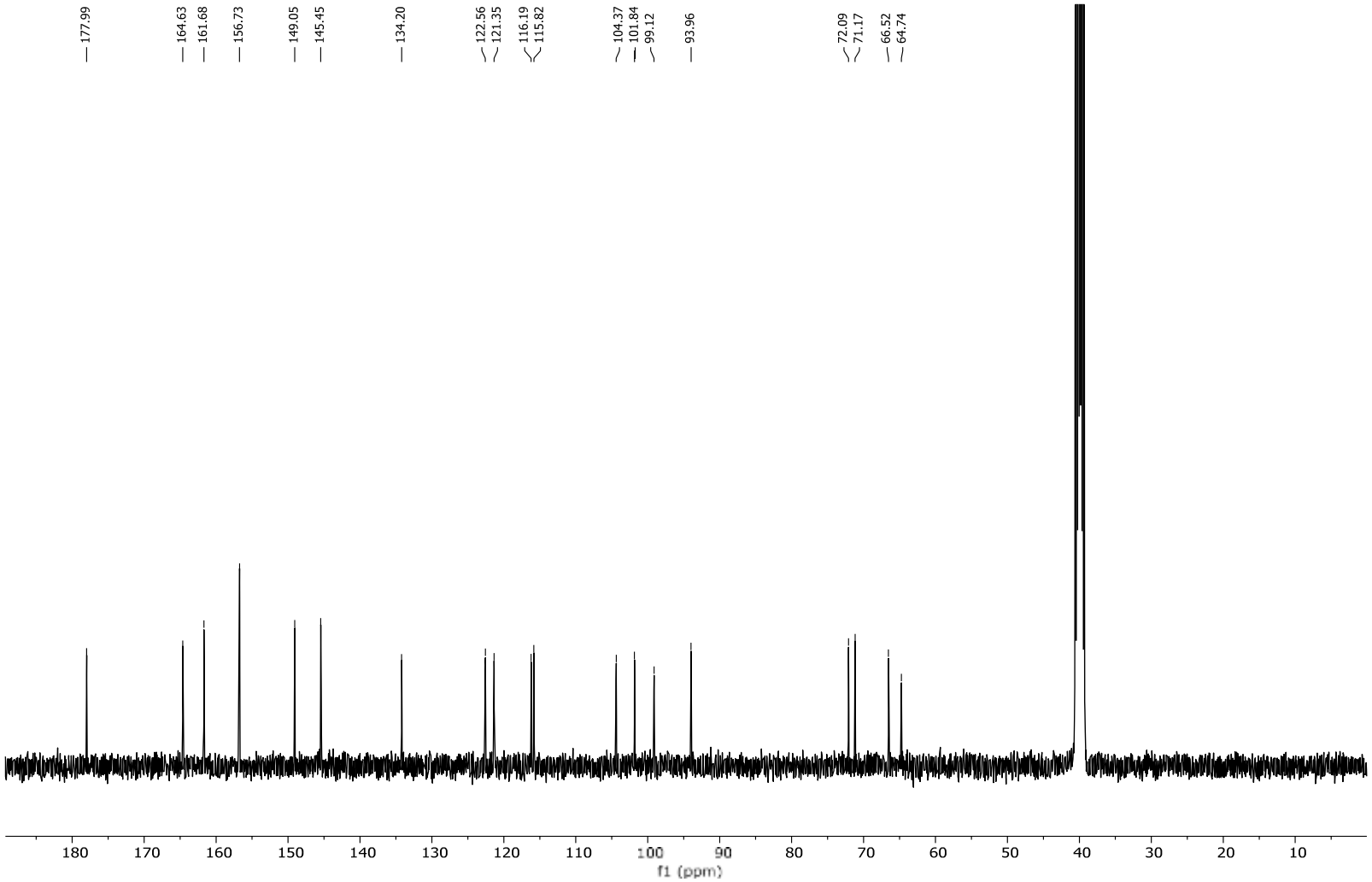
Appendix 123: The HPLC Chromatogram of the Crude Ethyl Acetate-Soluble Fraction of the DCM:MeOH Extract of the Leaves of *R. natalensis* and Compounds Isolated from the Fraction.



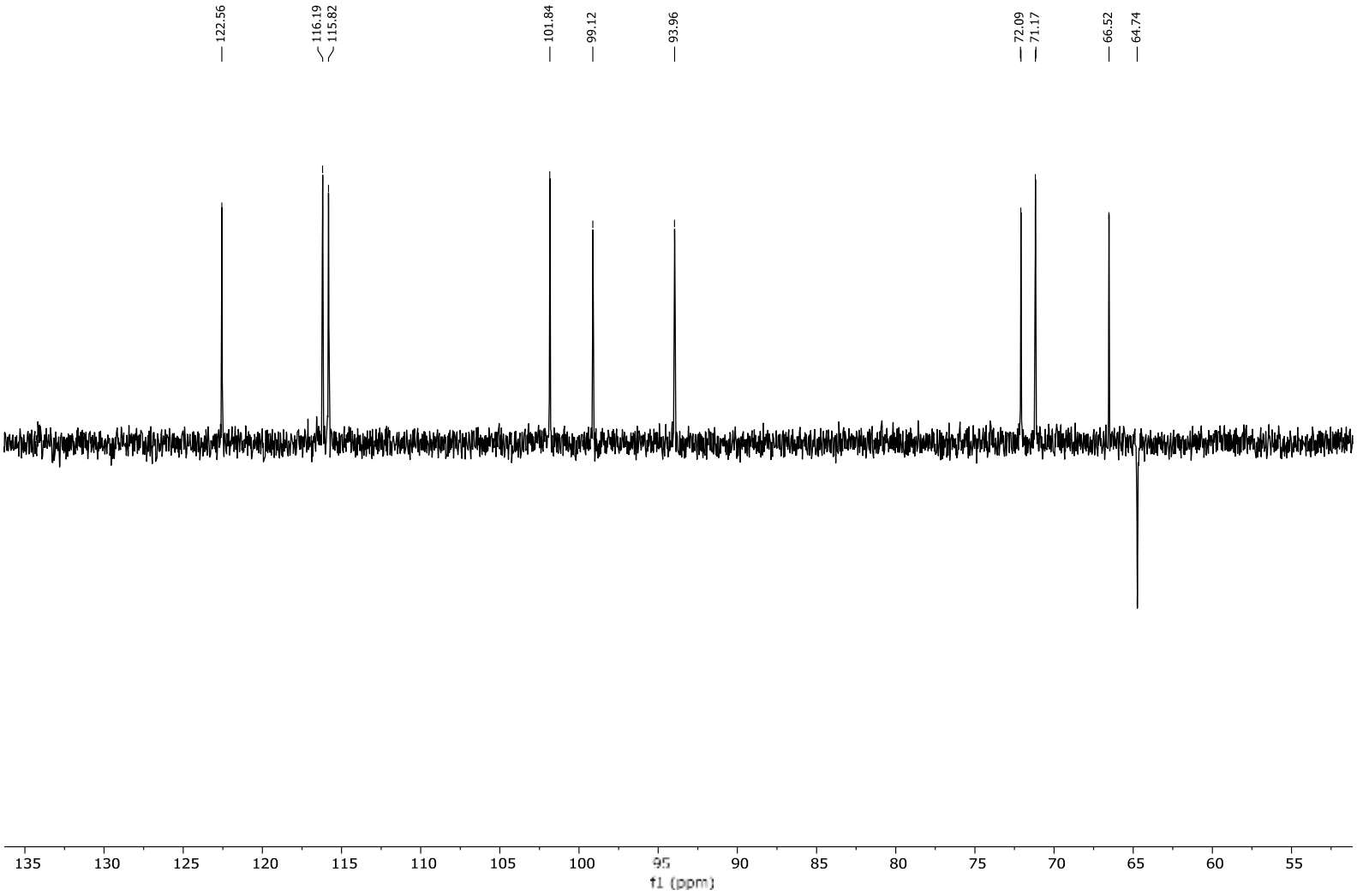
Appendix 124: The ^{1}H-NMR Spectrum of **131** in DMSO-d_6.



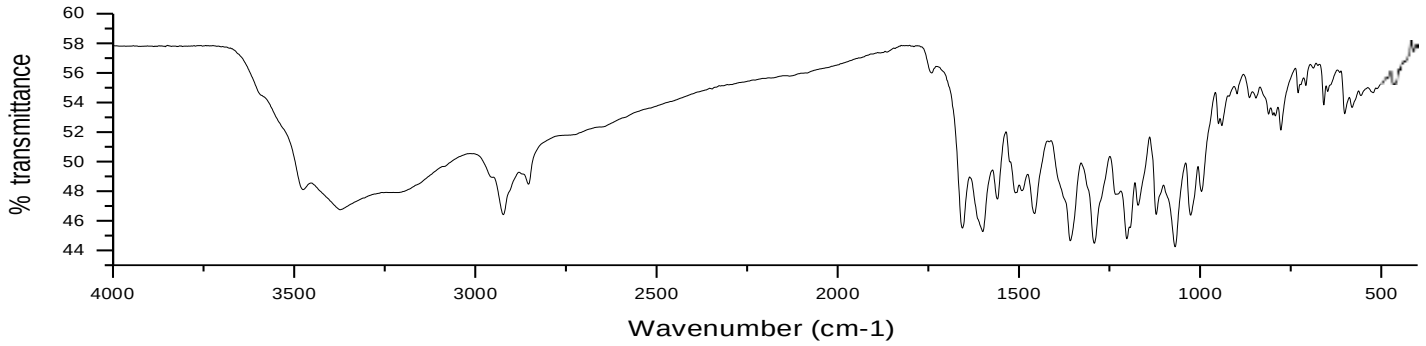
Appendix 125: The ^{13}C-NMR Spectrum of **131** in DMSO-*d*$_6$.



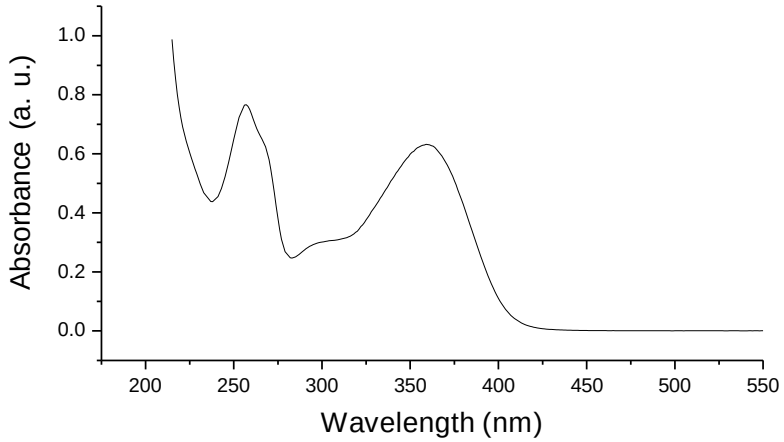
Appendix 126: The DEPT-135 NMR Spectrum of **131** in DMSO-d_6.



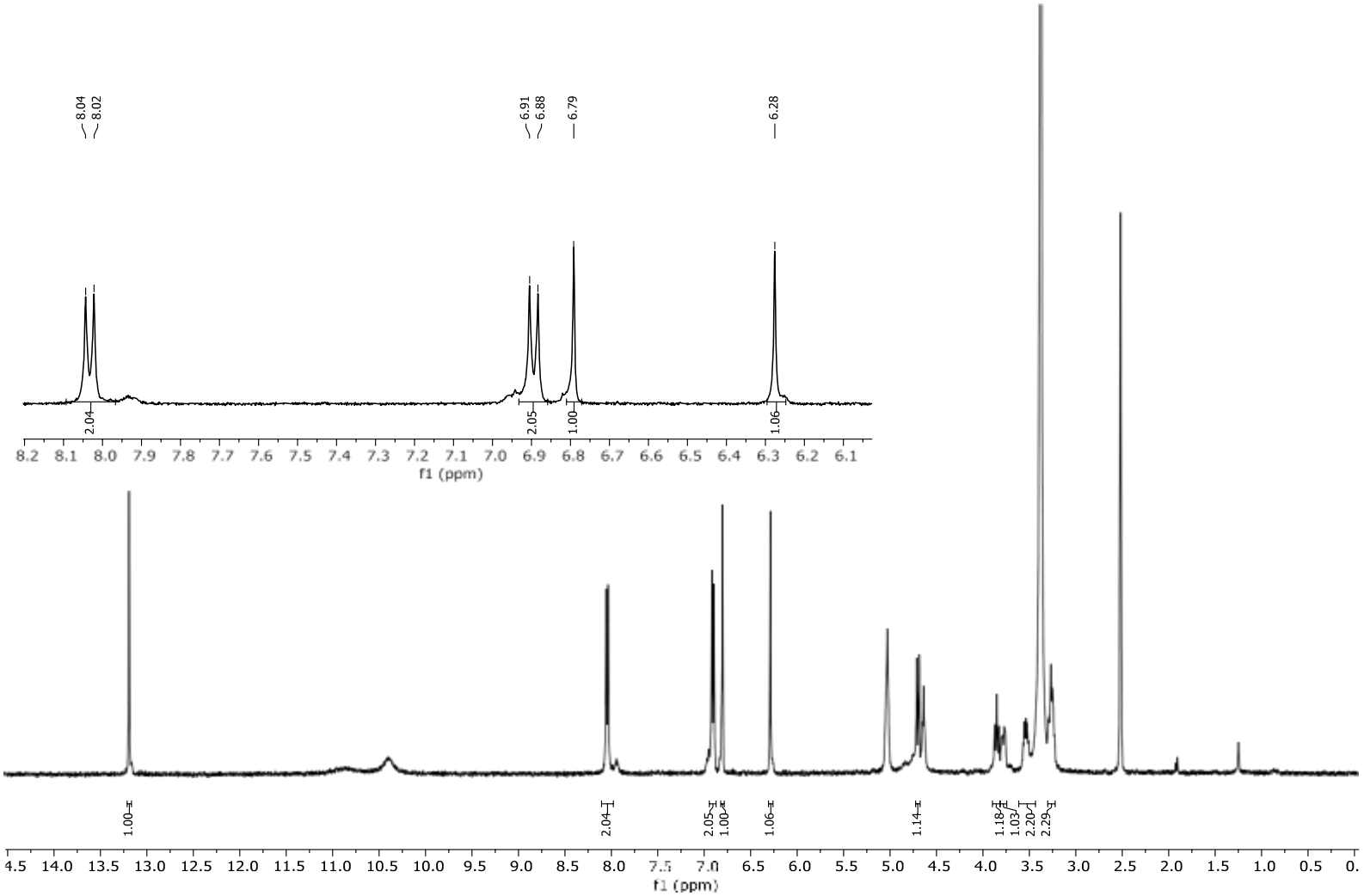
Appendix 127: The IR Spectrum of **131**.



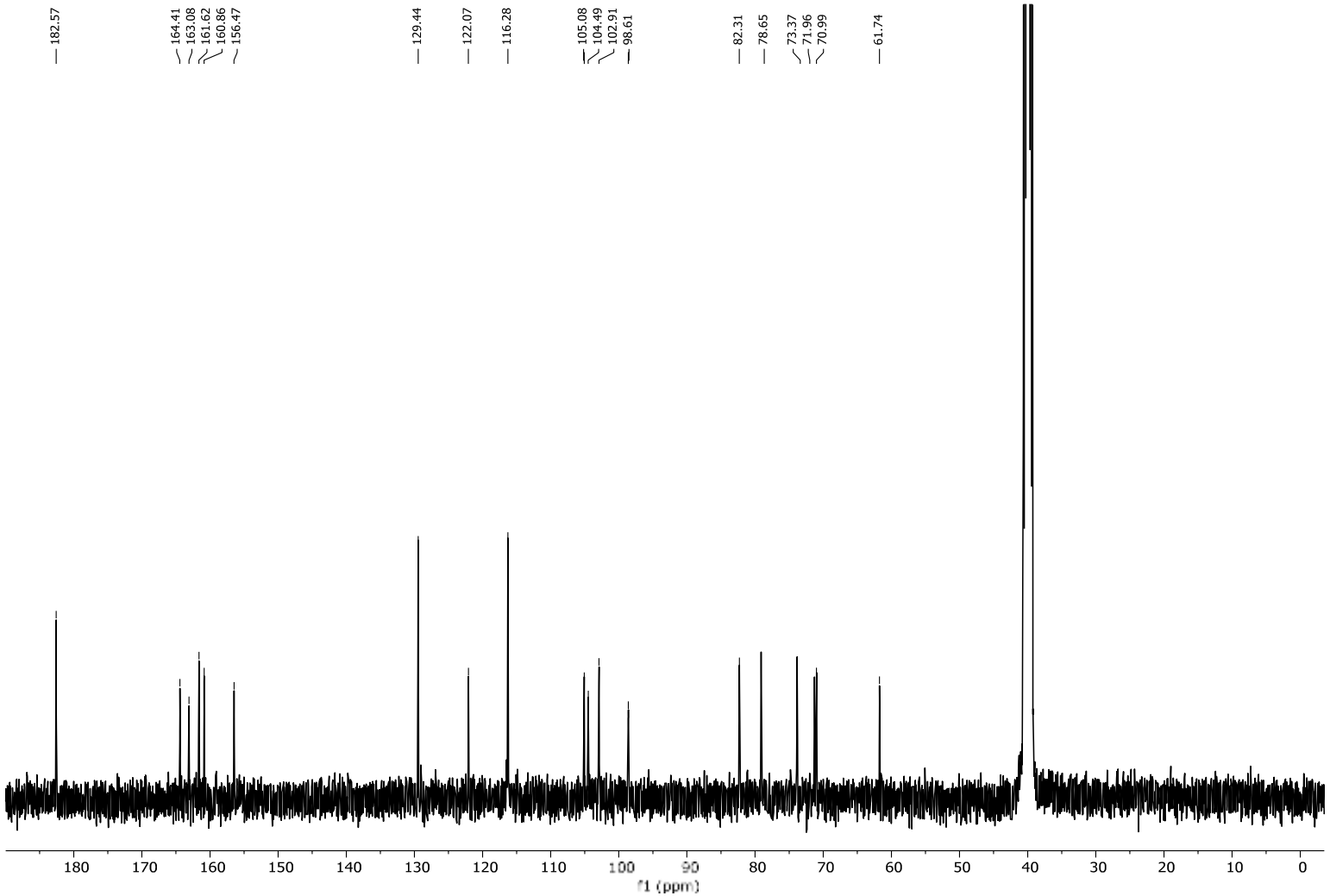
Appendix 128: The UV Spectrum of **131** in Methanol.



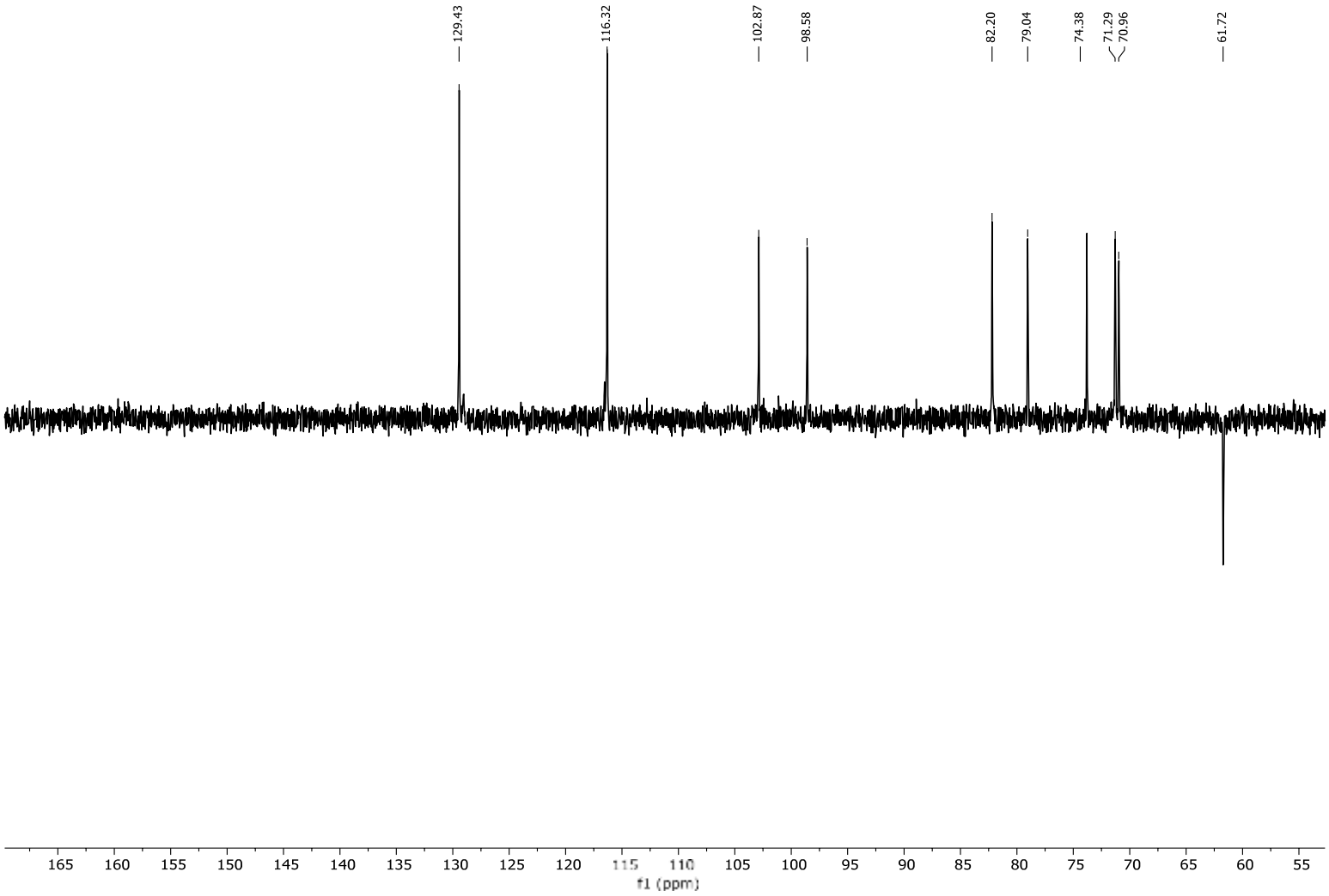
Appendix 129: The ^{1}H-NMR Spectrum of **132** in DMSO-d_6.



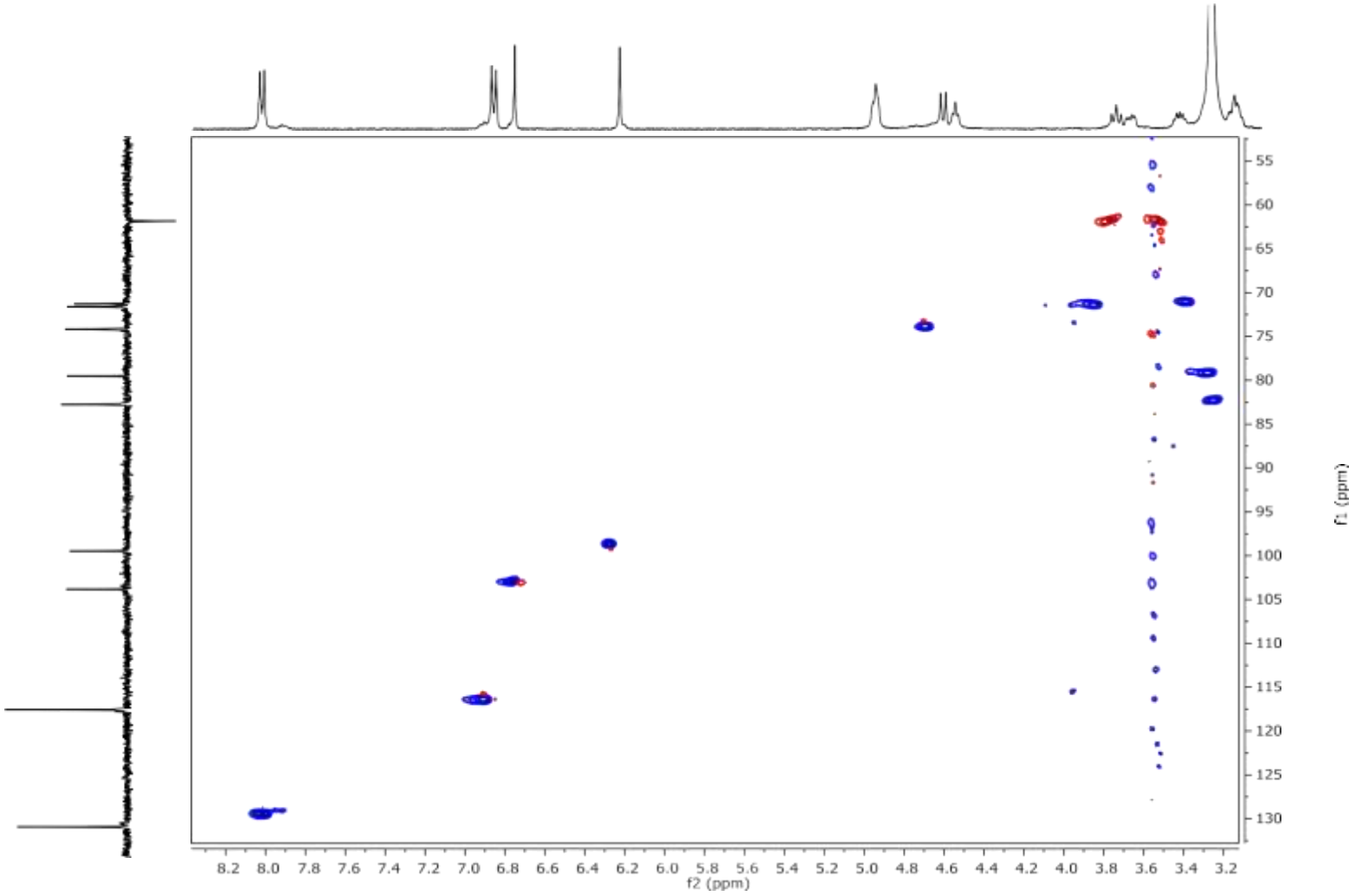
Appendix 130: The ^{13}C-NMR Spectrum of **132** in DMSO-*d*$_6$.



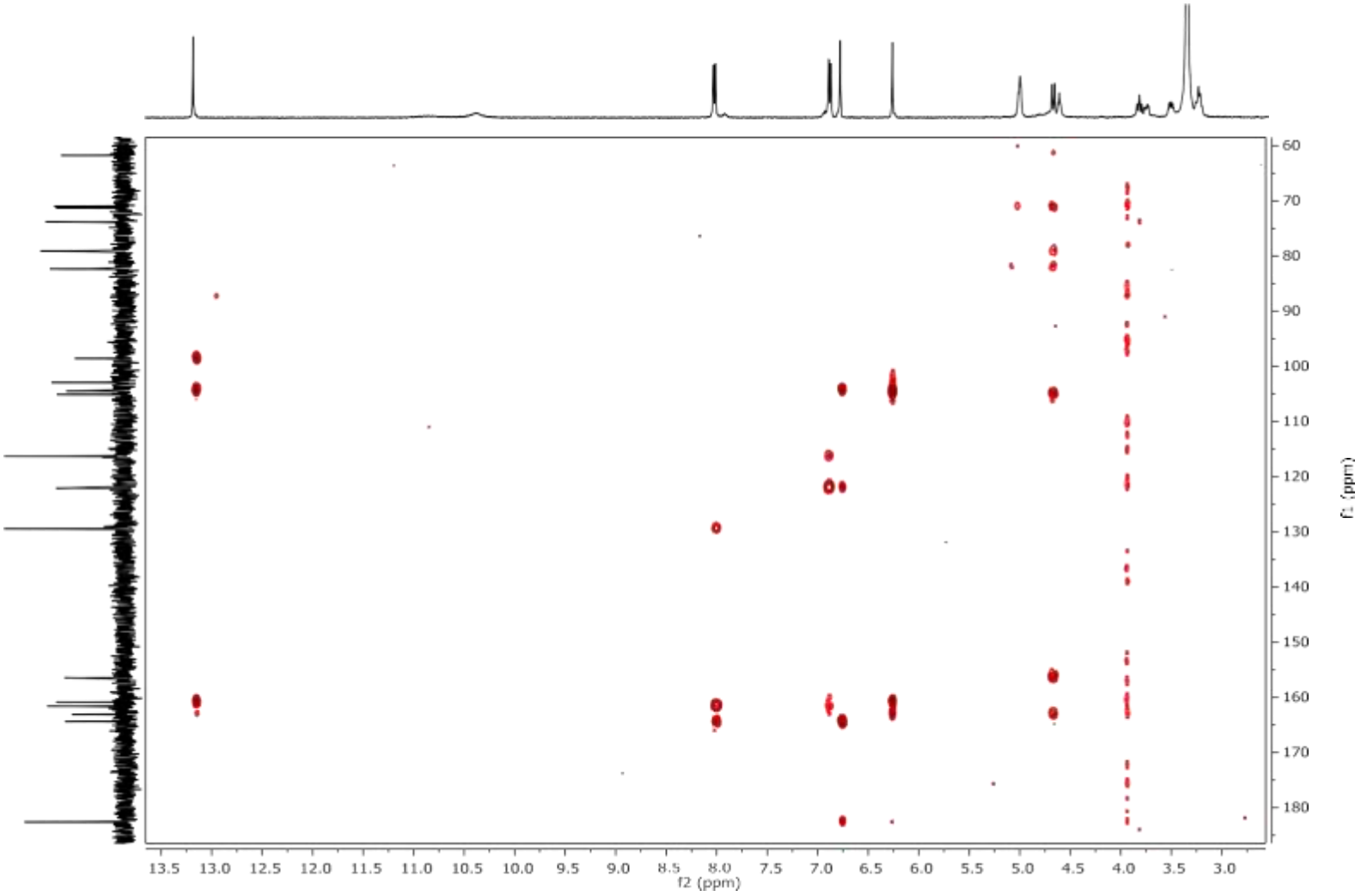
Appendix 131: The DEPT-135 NMR Spectrum of **132** in DMSO-d_6.



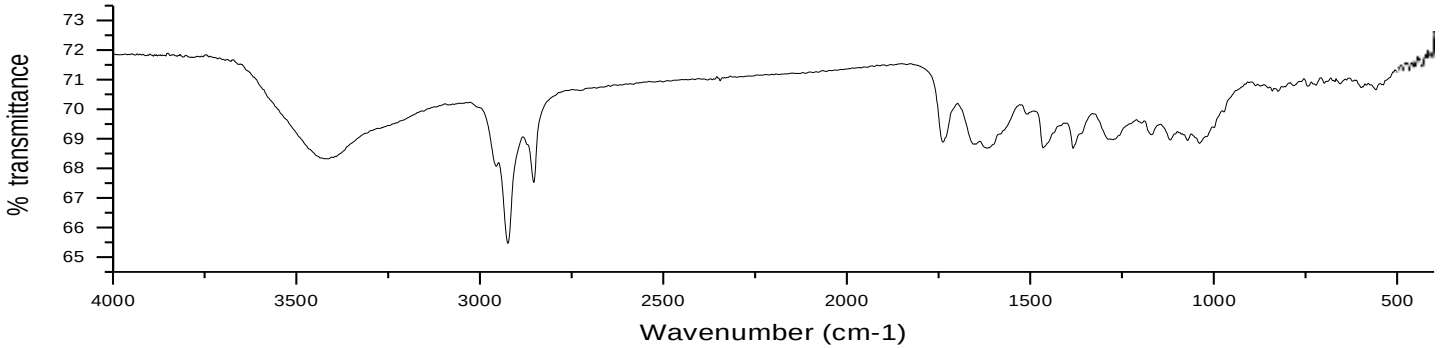
Appendix 132: The HSQC Spectrum of **132** in DMSO-d_6.



Appendix 133: The HMBC Spectrum of **132** in DMSO-d_6.



Appendix 134: The IR Spectrum of **132**.



Appendix 135: The UV Spectrum of **132** in Methanol.

